Karlsruher Institut für Technologie

Uniformly Accurate Methods for Klein–Gordon type Equations

Von der Fakultät für Mathematik des
Karlsruher Instituts für Technologie
zur Erlangung des akademischen Grades eines

Doktors der Naturwissenschaften

genehmigte

Dissertation

von

Simon Baumstark

Datum der Einreichung: 14.06.2018

Tag der mündlichen Prüfung: 12.07.2018

Referentin: JProf. Dr. Katharina Schratz
Koreferent: Prof. Dr. Guido Schneider

Acknowledgement

First of all I would like to express my gratitude to my supervisor JProf. Dr. Katharina Schratz for her support over the last three years. Already during my studies and my master thesis she supported me with useful comments, remarks, advices, and a sympathetic ear. Every time a question occurs she takes time and we had a lot of fruitful discussions. Thank you for the good mentoring and patience for my questions. I am grateful for her confidence in my skills and the outstanding supervision. I am also very grateful that my supervisor gave me the opportunity to visit many excellent summer schools and conferences. I really appreciate working with her.

Thank you to my second supervisor Prof. Dr. Guido Schneider for the suggested corrections and the helpful visits in Stuttgart.

This thesis is also part of the project B1 in the CRC 1173 "Wave phenomena: analysis and numerics". I am thankful for the opportunity to participate in this research program.

Thanks to my (present and former) colleagues of the research group "Scientific Computing" at the Institute for Applied and Numerical Mathematics for the pleasant working environment and the cakes! Furthermore, I want to thank all the colleagues at the CRC for the pleasent collegiality. In particular, I want to thank Patrick Krämer for his helpful feedback and the good collaboration during my time as a master and PhD student. Additionally, thanks to Laura Lindner for being the best office mate.

Thanks to Laura Linder, Anja Link, Julian Baumstark and Patrick Krämer for proof-reading and their suggestions on style issues. In particular, I would like to thank my friends for their support during my studies and my time as a PhD student.

Last but not least I would like to thank my fiancee Anja and my family for their unconditional love and support. This thesis would not have been possible without you!

Abstract

The main contribution of this thesis is the development of a novel class of uniformly accurate methods for Klein–Gordon type equations.
Klein–Gordon type equations in the non-relativistic limit regime, i.e., $c \gg 1$, are numerically very challenging to treat, since the solutions are highly oscillatory in time. Standard Gautschi-type methods suffer from severe time step restrictions as they require a CFL-condition $c^2\tau < 1$ with time step size τ to resolve the oscillations. Within this thesis we overcome this difficulty by introducing limit integrators, which allows us to reduce the highly oscillatory problem to the integration of a non-oscillatory limit system. This procedure allows error bounds of order $\mathcal{O}(c^{-2} + \tau^2)$ without any step size restrictions. Thus, these integrators are very efficient in the regime $c \gg 1$. However, the limit integrators fail for small values of c. In order to derive numerical schemes that work well for small as well as for large c, we use the ansatz of *twisted variables*, which allows us to develop uniformly accurate methods with respect to c. In particular, we introduce efficient and robust uniformly accurate exponential-type integrators for the Klein–Gordon equation which resolve the solution in the relativistic regime as well as in the highly oscillatory non-relativistic regime without any step size restriction. In contrast to previous works, we do not employ any asymptotic nor multiscale expansion of the solution. Compared to classical methods our new schemes allow us to reduce the regularity assumptions as they converge under the same regularity assumptions required for the integration of the corresponding nonlinear Schrödinger limit system. In addition, the newly derived first- and second-order exponential-type integrators converge to the classical Lie and Strang splitting schemes for the nonlinear Schrödinger limit system.
Moreover, we present uniformly accurate schemes for the Klein–Gordon–Schrödinger system which are also based on the ansatz of twisted variables. Again, our first- and second-order exponential-type integrators are asymptotically consistent, in the sense of asymptotically converging to the corresponding limit integrator of the decoupled free Schrödinger limit system.
In contrast to the classical Klein–Gordon equation and the Klein–Gordon–Schrödinger system the ansatz of twisted variables cannot be applied to the Klein–Gordon–Zakharov system straight forwardly, due to a loss of derivative in the system. Nevertheless, we construct and analyze a novel class of integrators which are uniformly accurate. Moreover, the introduced scheme is asymptotically consistent and approximates the solutions of the corresponding Zakharov limit system in the high-plasma frequency limit.
For all uniformly accurate integrators we establish rigorous error estimates and underline their uniform convergence property numerically.

Contents

CHAPTER 1

Introduction

1.1 The Numerical Challenge of Highly Oscillatory Problems

Ordinary and partial differential equations play a fundamental role in modeling physical processes in science. However, only a few of these equations can be solved exactly and a solution can be written down explicitly. For the remaining equations we have to derive numerical schemes in order to compute approximations to the solution. For a long time scientists developed and constructed numerical schemes for different types of equations. However, very often, standard numerical methods are not suitable for all differential equations in the same way. In particular, if the solution of the underlying equation is highly oscillatory, it becomes very challenging for numerical methods to resolve the oscillations.

Now, let us assume that we have a highly oscillatory function given (see Figure 1.1) and we want to compute an approximation of this function numerically.

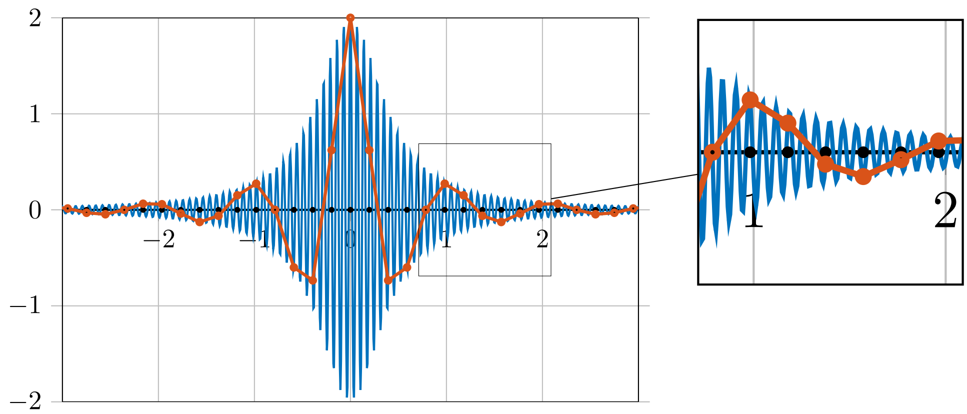

Figure 1.1: Plot of a highly oscillatory function in blue. Grid points of the discretization in black. Approximation in red.

Therefore, we have to discretize the interval into a finite number of points. At these grid points we compute approximations of the function values. Afterwards we construct our numerical solution by interpolating between the approximated values. Figure 1.1 shows an example where the approximation fails completely even though we approximate the function values exactly. We can improve the approximation by introducing a finer grid. However, this is more costly with respect to memory and computational time, which is important to avoid in numerical analysis.

If we have information about the highly oscillatory structure, in a mathematical sense, we try to filter out these oscillations (see e.g., [23, 64–67]). Thereafter, we can split the highly oscillatory solution into a highly oscillatory part and a slowly varying function, called envelope (see Figure 1.2).

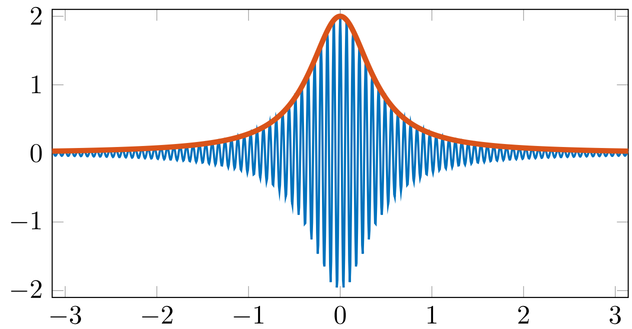

Figure 1.2: Plot of a highly oscillatory function in blue and its envelope in red.

Let us consider a simple example of a highly oscillatory ordinary differential equation, the so-called harmonic oscillator (see Figure 1.3). For more details on harmonic oscillators we refer to [63, 71]. Mathematically, the harmonic oscillator is described by the following ordinary differential equation

$$y''(t) = -\omega^2 y(t), \qquad y(0) = -1, \qquad y'(0) = 0, \qquad \omega \in \mathbb{R}, \tag{1.1}$$

where $y(0)$ describes the initial location and $y'(0)$ the initial velocity of the mass attached to the spring (see Figure 1.3).

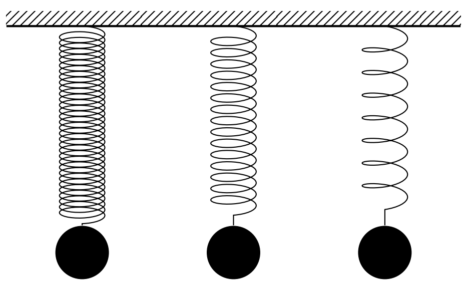

Figure 1.3: Figure of three springs with different stiffness. From left to right the stiffness of the spring decreases. A soft spring corresponds to a small value of ω and a stiff spring corresponds to a large value of ω. Soft and stiff springs cause slowly varying and highly oscillatory solutions of the harmonic oscillator, respectively.

The solution $y(t)$ is slowly varying for small values of ω and highly oscillatory for $\omega \gg 1$ (see Figure 1.4). Physically small values of ω describe a soft spring and large ω describe a stiff spring. The exact solution of (1.1) reads

$$y(t) = -\cos(\omega t).$$

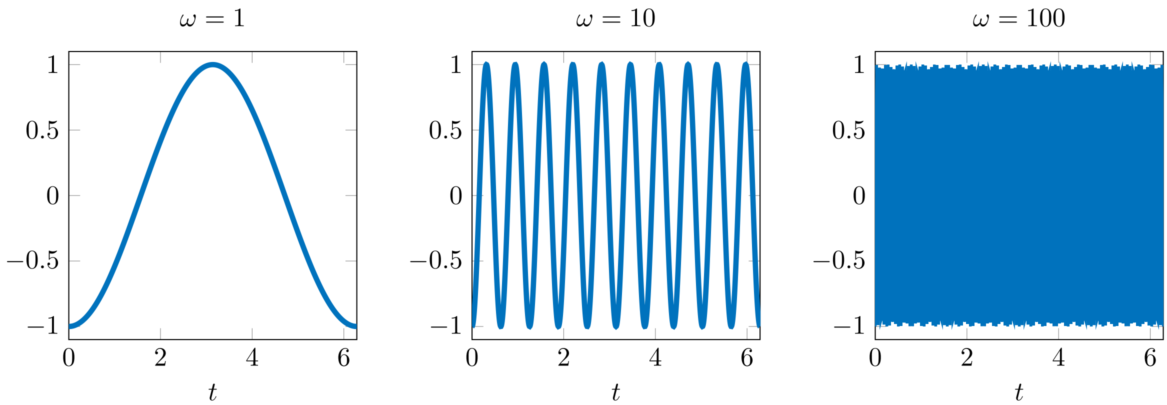

Figure 1.4: Plot of the exact solution of the harmonic oscillator for different values of ω.

Now, we apply standard numerical methods to solve the equation (1.1) in order to see how they perform. We set $\omega = 10$ and discretize with N grid points and grid size τ. As we mentioned before it may happen that the discretization is not a good choice to obtain a good approximation of the exact solution, even though the approximation at the grid points is exact (see Figure 1.5).

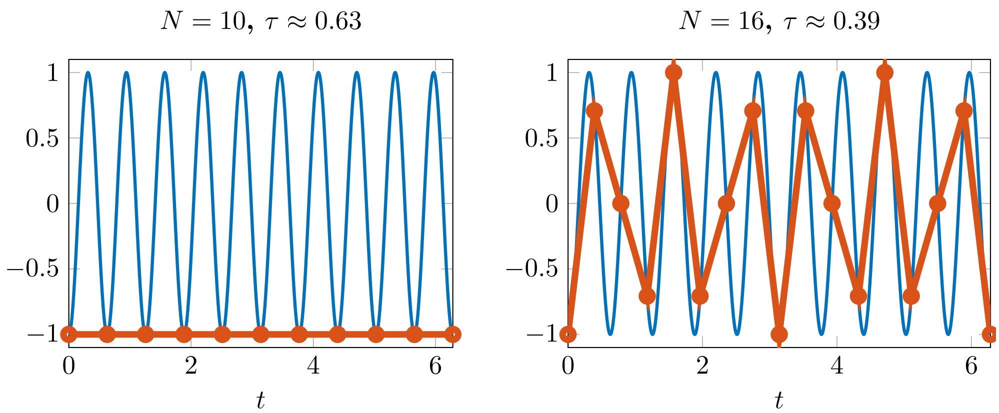

Figure 1.5: Plot of the exact solution of the harmonic oscillator for $\omega = 10$ in blue. Approximation in red for different grids.

In order to solve the equation of the harmonic oscillator numerically we rewrite (1.1) as a first-order system

$$\begin{aligned} y'(t) &= v(t), \\ v'(t) &= -\omega^2 y(t). \end{aligned}$$

We apply the variation of constants formula and obtain

$$
\begin{aligned}
y(t_n+\tau) &= y(t_n) + \int_0^\tau v(t_n+s)\mathrm{d}s,\\
v(t_n+\tau) &= v(t_n) - \omega^2 \int_0^\tau y(t_n+s)\mathrm{d}s.
\end{aligned}
$$

For more details on the variation of constants formula we refer to [2, 3]. Now, it remains to approximate the integrals in an appropriate way. Firstly, we apply the explicit Euler method, which reads

$$
\begin{aligned}
y^{n+1} &= y^n + \tau v^n, & y^0 &= -1,\\
v^{n+1} &= v^n - \tau\omega^2 y^n, & v^0 &= 0.
\end{aligned}
$$

We compare the exact solution with the numerical approximation of the explicit Euler method (see Figure 1.6). The figure underlines that the explicit Euler method is not stable, i.e., the solution grows as time progresses. Hence, the numerical solution fails to approximate the exact solution after a certain time. We would need to choose a much finer time step size, in order to obtain a better numerical approximation.

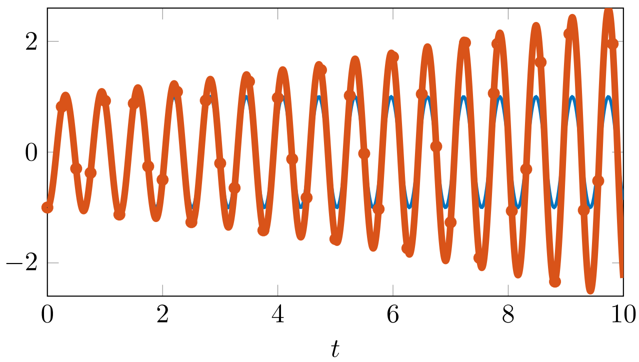

Figure 1.6: Plot of the exact solution of the harmonic oscillator for $\omega = 10$ in blue. Numerical approximation obtained via the explicit Euler method in red. Integration up to $T = 10$ with a step size $\tau \approx 10^{-3}$.

Next, we consider the implicit Euler method

$$
\begin{aligned}
y^{n+1} &= \frac{1}{1+\tau^2\omega^2}\left(y^n + \tau v^n\right),\\
v^{n+1} &= \frac{1}{1+\tau^2\omega^2}\left(v^n - \tau\omega^2 y^n\right).
\end{aligned}
$$

Again we compare the exact solution with the numerical approximation of the implicit Euler method (see Figure 1.7). The figure underlines that the implicit Euler method is stable, but damps the solution which means that the numerical solution again fails to approximate the exact solution after a certain time.

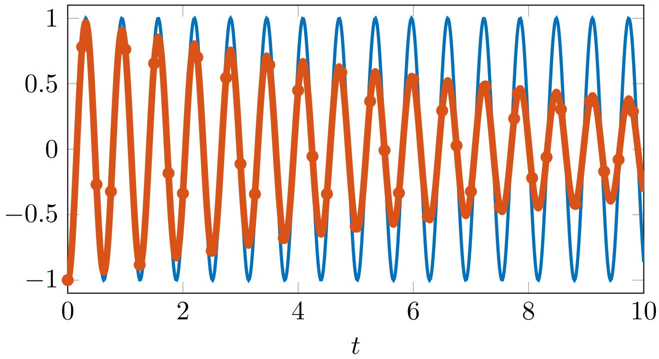

Figure 1.7: Plot of the exact solution of the harmonic oscillator for $\omega = 10$ in blue. Numerical approximation obtained via the implicit Euler method in red. Integration up to $T = 10$ with a step size $\tau \approx 10^{-3}$.

As we know that the exact solution conserves energy, we expect a better approximation with the energy conserving trapezoidal rule, also known as the Crank–Nicolson method (see [22]). It reads as follows

$$
\begin{aligned}
y^{n+1} &= \frac{1}{1+\omega^2\frac{\tau^2}{4}}\left(y^n + \tau v^n - \omega^2\frac{\tau^2}{4}y^n\right),\\
v^{n+1} &= \frac{1}{1+\omega^2\frac{\tau^2}{4}}\left(v^n - \omega^2\tau y^n - \omega^2\frac{\tau^2}{4}v^n\right).
\end{aligned}
$$

The Crank–Nicolson method approximates the solution of our linear ordinary differential equation very well (see Figure 1.8), but encounters difficulties if the underlying differential equation becomes nonlinear (see [47, 51]). In this thesis we are interested in nonlinear partial differential equations, the so-called Klein–Gordon type equations.

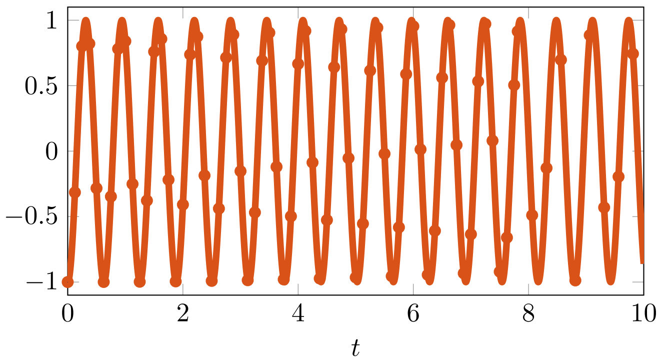

Figure 1.8: Plot of the exact solution of the harmonic oscillator for $\omega = 10$ in blue. Numerical approximation obtained via the Crank–Nicolson method in red. Integration up to $T = 10$ with a step size $\tau \approx 10^{-3}$.

As we have seen the simple explicit Euler and implicit Euler method fail even for linear equations and the Crank–Nicolson scheme fails for nonlinear equations (cf. [47, 51]). Therefore, numerical methods particularly suited for highly oscillatory differential equations, e.g., Gautschi-type methods and exponential integrators, were developed (see [32, 38, 39]).

In this thesis we consider Klein–Gordon type equations, the simplest one is the Klein–Gordon equation, which reads

$$c^{-2}\partial_{tt}z(t,x) - \Delta z(t,x) + c^2 z(t,x) = |z(t,x)|^2 z, \quad z(0,x) = z_0(x), \quad \partial_t z(0,x) = c^2 z_1(x).$$

Klein–Gordon type equations are very challenging to treat numerically, since the solutions become highly oscillatory in time for large values of c (see Figure 1.9 for the Klein–Gordon equation).

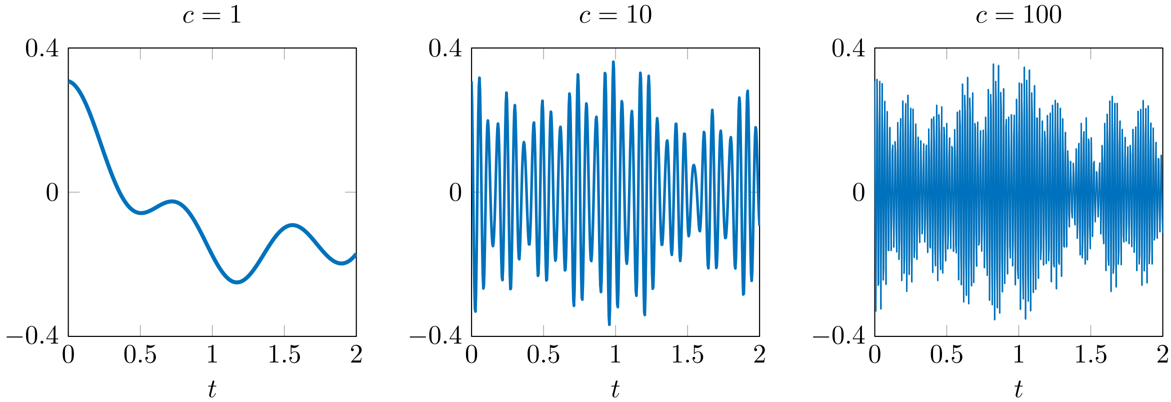

Figure 1.9: Plot of the solution of the Klein–Gordon equation for different values of c.

For these nonlinear equations we cannot state an exact solution explicitly. If we apply numerical methods like the Gautschi-type methods and exponential integrators to Klein–Gordon type equations, they suffer from severe time step restrictions (see Figure 1.10). The figure underlines that for finer time step sizes the numerical method approximates the solution of the Klein–Gordon equation better for a fixed value of c. If we plot the approximation for increasing c, we observe that for slowly varying solutions, i.e., small values of c these methods work well, but in the highly oscillatory case, i.e., large values of c the methods fail (see 1.11).

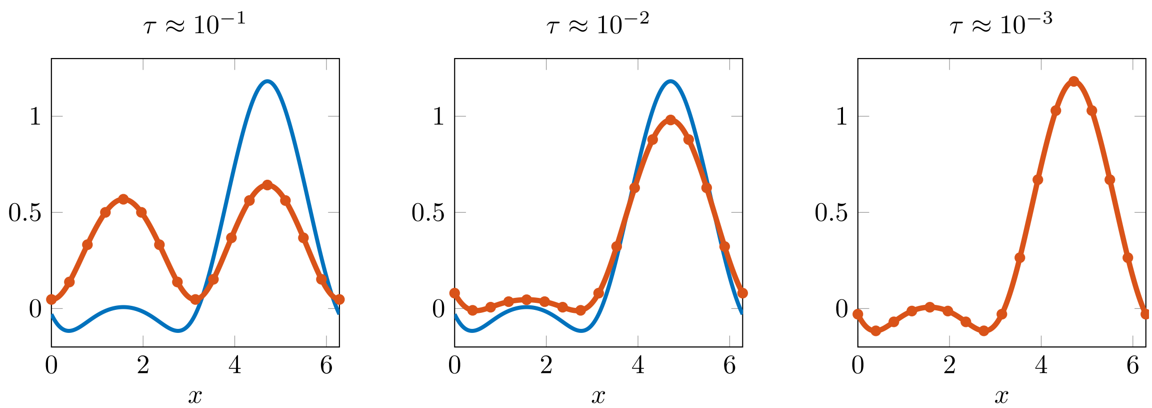

Figure 1.10: Plot of the numerical approximations of the Klein–Gordon equation for different time step sizes and fixed $c = 10$. Approximation computed via a classical exponential integrator in red, reference solution computed via the scheme itself with a finer time step size in blue.

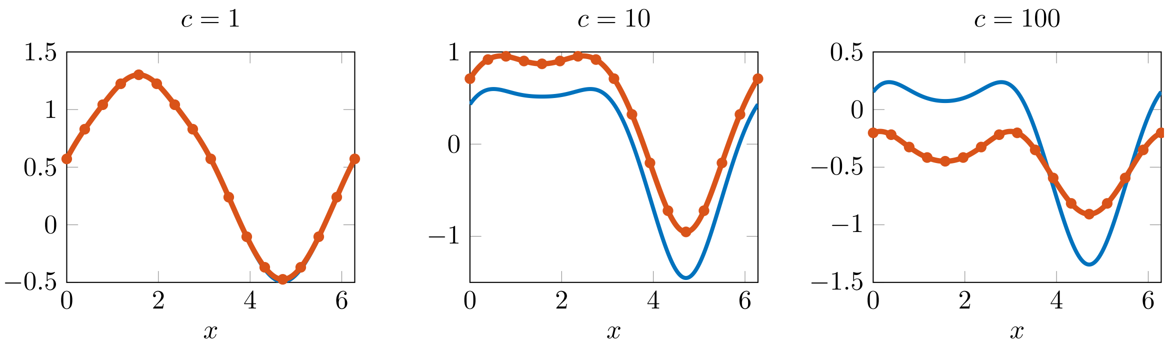

Figure 1.11: Plot of the numerical approximations of the Klein–Gordon equation for different values of c at time $T = 0.9$. Approximation computed via a classical exponential integrator in red, reference solution computed via the scheme itself with a finer time step size in blue.

For a large class of Klein–Gordon type equations we know how the oscillations look like. Hence, we can filter out the highly oscillatory phases and reduce the underlying differential equation to a non-oscillatory limit system. The solutions of the limit systems are slowly varying and we can solve them numerically in an efficient way (see [26, 53, 54]). For the Klein–Gordon equation the limit systems reads as follows

$$\begin{aligned} i\partial_t u_\infty &= \frac{1}{2}\Delta u_\infty + \frac{1}{8}\big(|u_\infty|^2 + 2\,|v_\infty|^2\big)u_\infty, & u_\infty(0) &= z_0 - iz_1, \\ i\partial_t v_\infty &= \frac{1}{2}\Delta v_\infty + \frac{1}{8}\big(|v_\infty|^2 + 2\,|u_\infty|^2\big)v_\infty, & v_\infty(0) &= \overline{z_0} - i\overline{z_1}. \end{aligned}$$

We can simply obtain an approximation to the original problem by multiplying the highly oscillatory phases with the solution of the limit system. For the solution of the Klein–Gordon equation we have

$$z(t,x) = \frac{1}{2}\left(\mathrm{e}^{ic^2t}\; u_\infty(t,x) + \mathrm{e}^{-ic^2t}\overline{v_\infty}(t,x)\right) + \mathcal{O}(c^{-2}),$$

where (u_∞, v_∞) satisfies the limit system. Those limit integrators only work well for highly oscillatory solutions, since the validity of such a limit integration method depends on the oscillations and so they fail in the slowly varying case (see Figure 1.12). On the other hand Gautschi-type methods and exponential integrators only work well in the slowly varying case (see [4, 7, 9]).

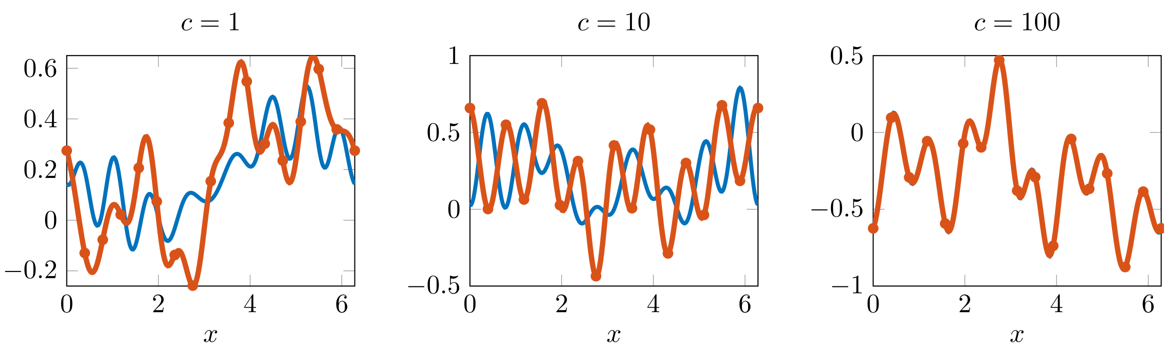

Figure 1.12: Plot of the numerical approximations of the Klein–Gordon equation for different values of c at time $T = 1$. Approximation computed via a limit integrator in red, reference solution computed via a classical exponential integrator with a finer time step size in blue.

Now, the main challenge is the development of numerical methods, that work well in both cases, i.e., in the slowly varying and in the highly oscillatory limit regime. We call such methods *uniformly accurate methods*.

1.2 Outline of the Thesis

In this thesis, we develop and analyze uniformly accurate methods for Klein–Gordon type equations. Uniformly accurate methods allow us to solve Klein–Gordon type equations numerically in the slowly varying as well as in the highly oscillatory regime without any step size restrictions. The thesis is organized as follows.

In Chapter 2, we start by developing uniformly accurate methods for the Klein–Gordon equation. After a short introduction to the Klein–Gordon equations we give a formal derivation of the limit system and the corresponding limit integrators. Then we focus on the derivation of a first- and second-order uniformly accurate method. We also state and prove convergence bounds for the first- and second-order schemes. At the end of this chapter we show numerical experiments, where we compare our methods with a standard Gautschi-type method and a classical exponential integrator. The comparison underlines the favorable error behavior of our new schemes.

In Chapter 3 we apply and expand the techniques, which were used for the Klein–Gordon equation, to the coupled Klein–Gordon–Schrödinger system, in order to construct uniformly accurate methods. Again we give a short introduction and derive formally the limit system and the corresponding limit scheme. Analogously to the previous chapter we derive a first- and second-order uniformly accurate scheme and prove their convergence. We close this chapter by presenting numerical experiments, where we compare our uniformly accurate methods with a standard Gautschi-type method and a classical exponential integrator. Again the comparison underlines the favorable error behavior of our new schemes.

In Chapter 4 we underline that the techniques, which we use for the Klein–Gordon equation and Klein–Gordon–Schrödinger system, do not yield a uniformly accurate method in the case of the Klein–Gordon–Zakahrov system. Here, we have to apply a refined approach. We develop a first-order uniformly accurate method with the refined approach and prove its first-order convergence. At the end of the chapter we compare our uniformly accurate method with a standard Gautschi-type method and a classical exponential integrator. This comparison underlines the favorable error behavior of our new uniformly accurate scheme.

Finally, in Chapter 5 we give a short summary and a brief outlook.

Prepublications

The results of Chapter 2 have been published in advance in [13]. Moreover, the results of Chapter 3 have been published in advance in [14]. The results of Chapter 4 have been published in the preprint [12]. We will point out these results at the appropriate place.

1.3 Notational Remarks

We start by listing some abbreviations which we will frequently use.

NLS	nonlinear Schrödinger	KG	Klein–Gordon
KGS	Klein–Gordon–Schrödinger	KGZ	Klein–Gordon–Zakharov
ODE	ordinary differential equation	PDE	partial differential equation
UA	uniformly accurate	MFE	modulated Fourier expansion
CFL	Courant–Friedrichs–Lewy		

The following notation will be used throughout this thesis. The sets $\mathbb{N}$, $\mathbb{Z}$, $\mathbb{R}$ and $\mathbb{C}$ denote the set of natural numbers, integers, real and complex numbers, respectively. The d-dimensional torus is denoted by $\mathbb{T}^d := (\mathbb{R}\backslash 2\pi\mathbb{Z})^d$. The one dimensional torus $\mathbb{T}$ is the interval of $[0, 2\pi]$. In this thesis $t \in [0, T]$ denotes the time variable and $x \in \mathbb{T}$ denotes the spatial variable. For notational simplicity we sometimes omit the spatial argument and just write $z(t)$ instead of $z(t, x)$ for a function $z : \mathbb{R} \times \mathbb{T} \to \mathbb{R}$.
The complex conjugate of a number $z \in \mathbb{C}$ is denoted by $\overline{z}$ and i denotes the imaginary unit, where we have $i := \sqrt{-1}$. The real and imaginary part of z is denoted by $\Re(z)$ and $\Im(z)$, respectively.
The partial derivatives with respect to x and t are denoted by ∂_x and ∂_t, respectively. The second derivative with respect to x and t is denoted by ∂_{xx} and ∂_{tt}, respectively. Sometimes we omit the time derivatives $\partial_t z$ and $\partial_{tt} z$ and write z', $\dot{z}$ and z'', $\ddot{z}$ instead, respectively. The Laplace operator Δ denotes the sum over the second spatial derivatives and is defined by

$$\Delta := \nabla^2 := \sum_{i=1}^{n} \frac{\partial^2}{\partial x_i^2}.$$

Applied on a sufficiently smooth scalar function $f(x) = f(x_1, ..., x_n)$ it reads

$$\Delta f(x) := \sum_{i=1}^{n} \frac{\partial^2 f(x)}{\partial x_i^2} = \partial_{x_1 x_1} f(x) + ... + \partial_{x_n x_n} f(x).$$

The big O notation is denoted by $\mathcal{O}(\cdot)$. If we write $z(t, x) = g(t, x) + \mathcal{O}(c^{-2})$ we mean that

$$\|z(t, x) - g(t, x)\| \leq K c^{-2},$$

for a constant $K \in \mathbb{R}$ independent of c and with respect to an appropriate norm $\|\cdot\|$.
We denote the standard Sobolev norm on $\mathbb{T}^d$ by the formula

$$\|u\|_r^2 = \sum_{k\in\mathbb{Z}^d} (1 + |k|^2)^r |\hat{u_k}|^2, \quad \text{where} \quad \hat{u_k} = \frac{1}{(2\pi)^d} \int_{\mathbb{T}^d} u(x) \mathrm{e}^{-ik\cdot x} \mathrm{d}x,$$

where for $k = (k_1, \ldots, k_d) \in \mathbb{Z}^d$, we set $k \cdot x = k_1 x_1 + \cdots + k_d x_d$ and $|k|^2 = k \cdot k$. Moreover, for a given linear bounded operator L we denote by $\|L\|_r$ its corresponding induced norm. For more details on Sobolev spaces we refer to [1, 26, 57, 73].
We mainly focus on the case $r > d/2$, which allows us to exploit the well-known bilinear estimate (for more details see [1, 42])

$$\|fg\|_r \leq K_{r,d} \|f\|_r \|g\|_r \tag{1.2}$$

which holds for some constant $K_{r,d} > 0$ and some sufficiently smooth functions f and g.

From [50] we know, that $f(t,x) = \mathrm{e}^{it\Omega_c} f_0$ solves the following differential equation

$$i\partial_t f(t,x) = -\Omega_c f(t,x), \qquad f(0,x) = f_0 \in H^r(\mathbb{T}^d)$$

with solution f on the torus $\mathbb{T}^d$ for $t \in \mathbb{R}$ and the operator $\Omega_c = \{c\langle\nabla\rangle_c, -\frac{1}{2}\Delta, c^2, \Delta, \mathcal{A}_c\}$. In Fourier space we denote the symbol of the operator $\mathrm{e}^{it\Omega_c}$ as

$$\left(\mathrm{e}^{it\Omega_c}\right)_k = \mathrm{e}^{it\omega_c(k)},$$

for $k \in \mathbb{Z}$, where $\omega_c : \mathbb{Z}^d \to \mathbb{R}$ denotes the corresponding symbol of Ω_c. For more details on the properties of groups and semi-groups we refer to [25, 26, 46, 50].

CHAPTER 2

The Klein–Gordon Equation

In this chapter we introduce the Klein–Gordon equation and derive uniformly accurate methods. In Section 2.1 we shortly give an overview of the limit regimes, limit integrators and different uniformly accurate methods for the Klein–Gordon equation. Then we focus in Section 2.2 on the formal derivation of the corresponding limit system. We finish this chapter with a detailed derivation of a first- and second-order uniformly accurate method for the Klein–Gordon equation (see Section 2.3). This chapter is based on [26], for the derivation of the limit system, and on our contribution [13], for the introduction of uniformly accurate methods. The results of this chapter, in particular Section 2.1 and Section 2.3, have been published together with Erwan Faou and Katharina Schratz in [13].

2.1 Introduction to Klein–Gordon Equations

The Klein–Gordon (KG) equation

$$c^{-2}\partial_{tt}z(t,x) - \Delta z(t,x) + c^2 z(t,x) = |z(t,x)|^2 z, \quad z(0,x) = z_0(x), \quad \partial_t z(0,x) = c^2 z_1(x) \tag{2.1}$$

is extensively studied numerically in the relativistic regime $c = 1$, see [31, 72] and the references therein. In the relativistic limit regime, the solution of the KG equation has a “nice” behavior, i.e. the solution is non-oscillatory and not hard to treat numerically. In contrast, the non-relativistic regime $c \gg 1$ is numerically much more involved due to the highly oscillatory behavior of the solution. We refer to Chapter 1 and [24, 36] for an introduction and overview on highly oscillatory problems.

Analytically, the non-relativistic limit regime $c \to \infty$ is extensively studied (see [52, 53]) and well understood nowadays. More precisely, assuming sufficiently smooth initial data the exact solution z of (2.1) allows the expansion

$$z(t,x) = \frac{1}{2}\left(\mathrm{e}^{ic^2 t}\, u_{*,\infty}(t,x) + \mathrm{e}^{-ic^2 t}\overline{v_{*,\infty}}(t,x)\right) + \mathcal{O}(c^{-2}),$$

where $(u_{*,\infty}, v_{*,\infty})$ satisfy the nonlinear Schrödinger (NLS) limit system

$$\begin{aligned} i\partial_t u_{*,\infty} &= \frac{1}{2}\Delta u_{*,\infty} + \frac{1}{8}\big(\,|u_{*,\infty}|^2 + 2\,|v_{*,\infty}|^2\,\big)u_{*,\infty}, \qquad u_{*,\infty}(0) = z_0 - iz_1,\\ i\partial_t v_{*,\infty} &= \frac{1}{2}\Delta v_{*,\infty} + \frac{1}{8}\big(\,|v_{*,\infty}|^2 + 2\,|u_{*,\infty}|^2\,\big)v_{*,\infty}, \qquad v_{*,\infty}(0) = \overline{z_0} - i\overline{z_1} \end{aligned} \tag{2.2}$$

with initial values

$$\begin{aligned} z(0,x) &\overset{c\to\infty}{\longrightarrow} z_0(x),\\ \frac{1}{c\sqrt{c^2-\Delta}}\partial_t z(0,x) = \frac{c}{\sqrt{c^2-\Delta}} z_1(x) &\overset{c\to\infty}{\longrightarrow} z_1(x). \end{aligned}$$

More details can be found in Section 2.2 and [26, Formula (37)] for the periodic setting (i.e. $x \in \mathbb{T}^d$) and [53, Formula (1.3)] for the case of $x \in \mathbb{R}$.

Also numerically, the non-relativistic limit regime $c \gg 1$ has recently gained a lot of attention. Due to the difficult structure of the problem Gautschi-type methods (see [38]) which have been analyzed in [4] suffer from severe time step restrictions as they introduce a global error of order $c^4\tau^2$. In order to obtain convergence we thus require the CFL-type condition $c^2\tau < 1$. We illustrate this behavior in Figure 2.1 and observe that the Gautschi-type method works well for small c and fails for large values of c.

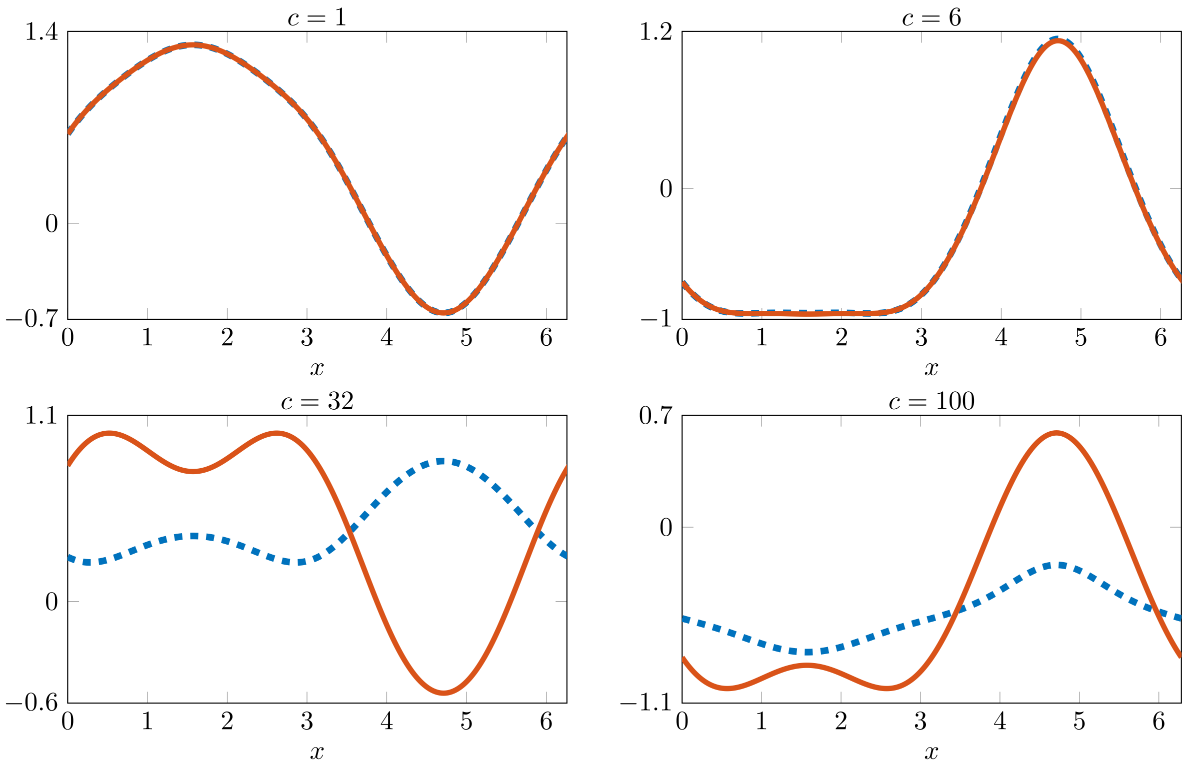

Figure 2.1: Numerical solution of the Klein–Gordon equation for different c. Exponential Gautschi-type scheme (red solid line) for different c with time step size $\tau \approx 10^{-2}$ at time $t = 1$. The blue dashed line represents the reference solution at time $t = 1$, computed via the same exponential Gautschi-type scheme with a small time step size $\tau \approx 10^{-6}$. The spatial discretization is done via a Fourier pseudospectral method with mesh-size $h = 0.0245$.

To overcome this difficulty, recently limit integrators were introduced (see [10, 18, 26]). This technique reduces the highly oscillatory problem to a corresponding non-oscillatory limit system (i.e., $c \to \infty$ in (2.1)). In the following, we give a comparison of these methods focusing on their convergence rates and regularity assumptions.

Limit integrators: Based on the modulated Fourier expansion (MFE) of the exact solution (see [19, 36]), numerical schemes for the Klein–Gordon equation in the strongly non-relativistic limit regime $c \gg 1$ were introduced in [26]. This MFE ansatz allows us to reduce the task of solving the highly oscillatory problem (2.1) to the integration of the corresponding *non-oscillatory limit Schrödinger system* (2.2). As the limit system is non-oscillatory, its numerical integration with standard numerical schemes is very efficient and does not require any $c-$dependent step size restriction. However, as this approach is based on the asymptotic expansion of the solution with respect to c^{-2}, it only allows error bounds of order

$$\mathcal{O}(c^{-2} + \tau^p)$$

when integrating the limit system with a numerical method of order p in time. For more details on the asymptotic expansion ansatz we refer to [26, 46]. However, the limit integration method only yields an accurate approximation of the exact solution for sufficiently large values of c (see Figure 2.2). For more details on the formal derivation of the limit system we refer to Section 2.2.

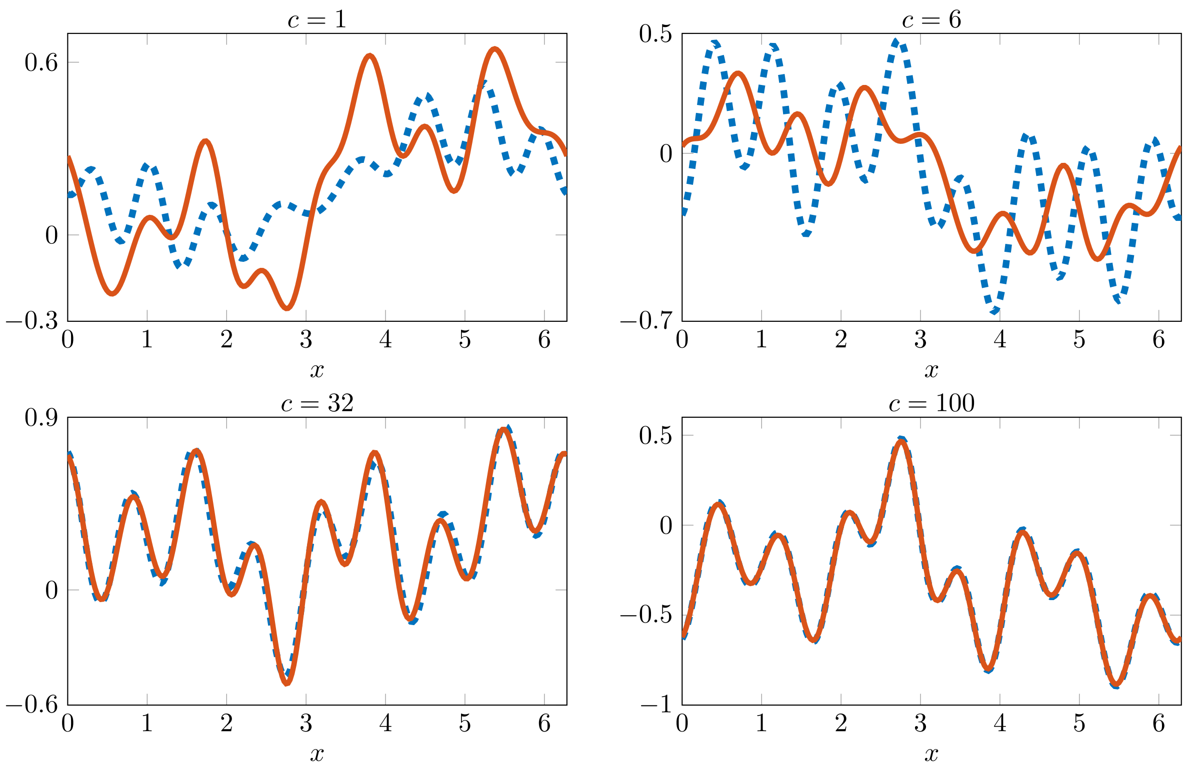

Figure 2.2: Numerical solution of the Klein–Gordon equation for different c. Limit integration scheme (red solid line) for different c with time step size $\tau \approx 10^{-2}$ at time $t = 1$. The blue dashed line represents the reference solution at time $t = 1$, computed via an exponential Gautschi-type scheme with a small time step size $\tau \approx 10^{-6}$. The spatial discretization is done via a Fourier pseudospectral method with mesh-size $h = 0.0245$.

Uniformly accurate schemes based on multiscale expansions: Uniformly accurate schemes, i.e., schemes that work well for small as well as for large values of c were recently introduced for Klein–Gordon equations in [10, 18]. The idea in the recent work is thereby based on a multiscale expansion of the exact solution. We also refer to [11] for the construction and analysis in the case of highly oscillatory second-order ordinary differential equations. The multiscale time integrator (MTI) pseudospectral method derived in [10] allows two independent error bounds at order

$$\mathcal{O}(\tau^2 + c^{-2}) \quad \text{and} \quad \mathcal{O}(\tau^2 c^2)$$

for sufficiently smooth solutions. These error bounds immediately imply that the MTI method converges uniformly in time with linear convergence rate at $\mathcal{O}(\tau)$ for all $c \geq 1$ thanks to the observation that $\min\{c^{-2}, \tau^2 c^2\} \leq \tau$. However, the optimal quadratic convergence rate of $\mathcal{O}(\tau^2)$ is only achieved in the regimes when either $0 < c = \mathcal{O}(1)$ (i.e., the relativistic regime) or $\frac{1}{\tau} \leq c$ (i.e., the strongly non-relativistic regime). In the context of ordinary differential equations similar error estimates were established for MTI methods in [11]. The first-order uniform convergence of the MTI-FP method [10] holds for sufficiently smooth solutions. First-order convergence in time holds in the Sobolev space H^2 uniformly in c for solutions in H^7 with $\sup_{0\leq t\leq T} \|z(t)\|_{H^7} + c^{-2}\|\partial_t z(t)\|_{H^6} \leq 1$ (see [10, Theorem 4.1]). First-order uniform convergence also holds in H^1 under weaker regularity assumptions, namely for solutions in H^6 satisfying $\sup_{0\leq t\leq T} \|z(t)\|_{H^6} + c^{-2}\|\partial_t z(t)\|_{H^5} \leq 1$ if an additional CFL-type condition is imposed in space dimensions $d = 2, 3$ (see [10, Theorem 4.9]).
A second-order uniformly accurate scheme based on the *Chapman-Enskog expansion* was derived in [18] for the Klein–Gordon equation. Thereby, to control the remainders in the expansion, second-order uniform convergence in H^r ($r > d/2$) requires sufficiently smooth solutions with in particular $z(0) \in H^{r+10}$. Also, due to the expansion, the *problem needs to be considered in $d + 1$ dimensions.*
For a comparison of asymptotic expansion techniques, i.e. a comparison of the modulated Fourier expansion, the multiscale frequency expansion and the Chapman-Enskog expansion, we refer to the preprint [68].

In Section 2.3 we establish exponential-type integrators of *second-order accuracy in time uniformly accurate in $c > 0$*. In comparison, the multiscale time integrators derived in [10, 11] only converge with first-order accuracy uniformly in all $c \geq 1$. This is due to the fact that the MTI methods are based on the multiscale decomposition

$$z(t, x) = \mathrm{e}^{ic^2 t} z_+^n(t, x) + \mathrm{e}^{-ic^2 t} \overline{z_-^n}(t, x) + r^n(t, x)$$

which leads to a coupled *second-order system in time* in the c^2-frequency waves $z_\pm^n$ and the remainder frequency waves r^n (cf. [10, System (2.4)]) and only allows numerical approximations at order $\mathcal{O}(\tau^2 + c^{-2})$ and $\mathcal{O}(\tau^2 c^2)$.
In contrast to [10, 18, 26], within this thesis we *do not* employ any asymptotic or multiscale expansion of the solution, but we construct exponential-type integrators based on the following strategy (see also [13, 14, 45]):

1. In a first step we reformulate the Klein–Gordon equation (2.1) as a coupled *first-order system in time* via the transformations

$$u = z - i\left(c\sqrt{-\Delta + c^2}\right)^{-1} \partial_t z, \quad v = \overline{z} - i\left(c\sqrt{-\Delta + c^2}\right)^{-1} \partial_t \overline{z}.$$

2. In a second step we rescale the coupled first-order system in time by considering at the so-called *twisted variables*
$$u_*(t) = \mathrm{e}^{ic^2 t} u(t), \qquad v_*(t) = \mathrm{e}^{ic^2 t} v(t).$$
Later on, this essential step will allow us to treat the highly oscillatory phases $\mathrm{e}^{\pm ic^2 t}$ and their interaction explicitly.

3. Finally, we iterate Duhamel's formula in $(u_*(t), v_*(t))$ and integrate the interactions of the highly oscillatory phases exactly by approximating only the slowly varying parts. For more details on the Duhamel's formula we refer to [43, 73].

In the last step, the exact integration of the highly oscillatory phases is significant for the uniformly accuracy of the scheme. If we only approximate the highly oscillatory phases, we obtain error bounds which depend on c (see also Section 2.3.1).
This strategy in particular allows us to construct uniformly accurate exponential-type integrators up to arbitrary order. Here in this thesis we derive methods up to order two (see Section 2.3.2 for the derivation of the first-order and Section 2.3.3 for the derivation of the second-order UA method) which in addition asymptotically converge to the classical splitting approximation of the corresponding nonlinear Schrödinger limit system (2.2) given in [26]. More precisely, the second-order exponential-type integrator converges for $c \to \infty$ to the classical Strang splitting scheme

$$u_{*,\infty}^{n+1} = \mathrm{e}^{-i\frac{\tau}{2}\frac{\Delta}{2}} \mathrm{e}^{-i\tau\frac{3}{8}|\mathrm{e}^{-i\frac{\tau}{2}\frac{\Delta}{2}} u_{*,\infty}^n|^2} \mathrm{e}^{-i\frac{\tau}{2}\frac{\Delta}{2}} u_{*,\infty}^n, \qquad u_{*,\infty}^0 = z_0 - iz_1 \tag{2.3}$$

associated to the nonlinear Schrödinger limit system (2.2) (see Remark 2.34) where for simplicity we assumed that z is real-valued such that $u_* = v_*$. A similar result holds for the asymptotic convergence of the first-order exponential-type integration scheme towards the classical Lie splitting approximation (see also Remark 2.16, below).
The Strang splitting (2.3) has been proposed in [26] for the numerical approximation of non-relativistic Klein–Gordon solutions. However, in contrast to the uniformly accurate exponential-type integrators derived here, the scheme in [26] only yields second-order convergence in the strongly non-relativistic regime $c > \frac{1}{\tau}$ due to its error bound at order $\mathcal{O}(\tau^2 + c^{-2})$.
The main novelty of our technique thus lies in the development and analysis of efficient and robust exponential-type integrators for the cubic Klein–Gordon equation (2.1) which

- allow second-order convergence uniformly in all $c > 0$ without adding an extra dimension to the problem,
- resolve the solution z in the relativistic regime $c = 1$ as well as in the non-relativistic regime $c \to \infty$ without any $c-$dependent step size restriction under the same regularity assumptions as needed for the integration of the corresponding limit system,
- converge uniformly in c and in addition converge asymptotically to the classical Lie and Strang splitting, respectively, for the corresponding nonlinear Schrödinger limit system (2.2) in the non-relativistic limit $c \to \infty$.

For notational simplicity, within this thesis we focus on the case of a cubic nonlinearity $f(z) = |z|^2 z$, but our strategy also applies to general polynomial nonlinearities $f(z) = |z|^{2p} z$ with $p \in \mathbb{N}$. Furthermore, for practical implementation issues we impose periodic boundary conditions, i.e., $x \in \mathbb{T}^d$.

Before presenting our new uniformly accurate technique, in the next section we start off with the formal derivation of the limit system. The benefit of the latter ansatz lies in the fact that it grants to reduce the highly oscillatory Klein–Gordon equation (2.1) to a non-oscillatory NLS limit system, which can be solved very efficiently with standard splitting methods (see also Section 2.4.2), but it only allows error bounds of order $\mathcal{O}(\tau^2 + c^{-2})$.

We commence with rescaling the Klein–Gordon equation (2.1) in Section 2.3. This enables us to construct first- and second-order schemes that converge uniformly in c, see Section 2.3.2 and 2.3.3, respectively.

2.2 Formal Derivation of the Limit System

In this section we give a detailed formal derivation the limit system of the Klein–Gordon equation (2.1) following the approach in [26]. Later on, in Chapter 3 and 4 we exploit this strategy for the derivation of the limit systems of the Klein–Gordon–Schrödinger and Klein–Gordon–Zakharov system in a more compact way.

In a first step we reformulate the Klein–Gordon equation (2.1) as a first-order system in time and apply a multi scale analysis and a formal asymptotic expansion. For a fixed $c > 0$, we define the operator

$$\langle \nabla \rangle_c = \sqrt{-\Delta + c^2}. \tag{2.4}$$

In this notation, equation (2.1) can be written as

$$\partial_{tt} z + c^2 \langle \nabla \rangle_c^2 z = c^2 |z|^2 z. \tag{2.5}$$

Applying the variable transformation

$$\begin{aligned} u &= z - ic^{-1} \langle \nabla \rangle_c^{-1} \partial_t z, \\ v &= \overline{z} - ic^{-1} \langle \nabla \rangle_c^{-1} \partial_t \overline{z}, \end{aligned}$$

we rewrite equation (2.5) as a first-order system in time, such that in particular

$$z = \tfrac{1}{2}(u + \overline{v}). \tag{2.6}$$

Remark 2.1. If z is real, i.e. $z \in \mathbb{R}$, then we have $u \equiv v$.

A short calculation shows that in terms of the variables u and v equation (2.5) reads

$$\begin{aligned} i\partial_t u &= -c\langle \nabla \rangle_c u + \tfrac{1}{8} c \langle \nabla \rangle_c^{-1} \left| u + \overline{v} \right|^2 (u + \overline{v}), \\ i\partial_t v &= -c\langle \nabla \rangle_c v + \tfrac{1}{8} c \langle \nabla \rangle_c^{-1} \left| \overline{u} + v \right|^2 (\overline{u} + v) \end{aligned} \tag{2.7}$$

with the initial conditions (see (2.1))

$$u(0) = z(0) - ic^{-1} \langle \nabla \rangle_c^{-1}\, \partial_t z(0) \quad \text{and} \quad v(0) = \overline{z}(0) - ic^{-1} \langle \nabla \rangle_c^{-1}\, \partial_t \overline{z}(0). \tag{2.8}$$

Based on the following strategy, now we derive the formal limit system.

1. **Multi scale analysis:**
Firstly, we introduce a new variable $\theta := c^2 t$ that defines the so-called long time scale. This time scale is called long, since θ is not negligible when t is of order $\mathcal{O}(c^{-2})$ or larger. We note that in the actual solution t and θ are in correlation to each other. However, the idea of the method of multiple scales (see [62]) is to treat t, θ as independent variables, which are connected to each other via the chain rule of the partial derivative $\partial_t \to \partial_t + c^2\partial_\theta$. Thus we replace ∂_t by $\partial_t + c^2\partial_\theta$ in the Klein–Gordon equation.

2. **Formal asymptotic expansion:**
Making an ansatz under the modulated Fourier expansion form (see [36, chapter XIII]) for u and v, we formally expand the functions u and v in the following way
$$u(t,x) = U_\infty + \sum_{m\geq 1} c^{-2m} U_m(t,\theta,x), \qquad v(t,x) = V_\infty + \sum_{m\geq 1} c^{-2m} V_n(t,\theta,x). \tag{2.9}$$
For more details on MFE we also refer to [19, 20, 34].

3. **Collecting same powers of c:**
Firstly, we expand the leading operator $c\langle\nabla\rangle_c$ and its inverse into its formal Taylor series expansion and plug it into the new PDE, we obtained from the multi scale analysis. Accordingly we expand the initial condition. This new PDE is obtained due to the fact that we introduced new variables and therefore we have a new time derivative operator. Then, we collect the terms of same powers of c. This yields a sequence of PDEs which is yet to be solved in order to find a representation for the coefficients U_m and V_m in the MFE (2.9).

The result of the procedure explained above is the first-order approximation term
$$z_\infty = \frac{1}{2}\left(U_\infty + V_\infty\right)$$
which formally satisfies
$$\|z - z_\infty\|_r = \mathcal{O}\left(c^{-2}\right).$$
Now we consider the different strategy points 1. to 3. in detail.

1. Multi scale analysis

Following our strategy above, we thus start with a multi scale analysis. Hence, we introduce the new variable $\theta = c^2 t$ and obtain
$$u(t,x) = U(t, c^2 t, x), \qquad v(t,x) = V(t, c^2 t, x)$$
with initial values
$$U(0,0,x) = z(0) - ic^{-1}\langle\nabla\rangle_c^{-1}\,\partial_t z(0), \qquad V(0,0,x) = \overline{z}(0) - ic^{-1}\langle\nabla\rangle_c^{-1}\,\partial_t \overline{z}(0).$$
Plugging U and V into equation (2.7) and after taking the derivative with respect to t, i.e. $\partial_t u = \partial_t U + c^2\partial_\theta U$ and $\partial_t v = \partial_t V + c^2\partial_\theta V$, we have
$$\begin{aligned} i\partial_t U + ic^2\partial_\theta U &= -c\langle\nabla\rangle_c U + \frac{1}{8}c\langle\nabla\rangle_c^{-1}|U+\overline{V}|^2\left(U+\overline{V}\right), \\ i\partial_t V + ic^2\partial_\theta V &= -c\langle\nabla\rangle_c V + \frac{1}{8}c\langle\nabla\rangle_c^{-1}|\overline{U}+V|^2\left(\overline{U}+V\right). \end{aligned} \tag{2.10}$$
Next we proceed with the formal asymptotic expansion of U, V.

2. Formal asymptotic expansion

In order to separate the highly oscillatory frequency terms from the slowly varying terms, we expand the whole system and introduce a formal asymptotic expansion of U and V in the following form

$$\begin{aligned} U(t,\theta,x) &= U_\infty + \sum_{m\geq 1} c^{-2m} U_m(t,\theta,x) = U_\infty(t,\theta,x) + \mathcal{O}(c^{-2}), \\ V(t,\theta,x) &= V_\infty + \sum_{m\geq 1} c^{-2m} V_m(t,\theta,x) = V_\infty(t,\theta,x) + \mathcal{O}(c^{-2}). \end{aligned} \tag{2.11}$$

We cut off the terms of order $\mathcal{O}(c^{-2})$, due to the fact, that we are only interested in the first-order correction term z_∞.

3. Collecting same powers of c

We devide this part into three subparts. Firstly, we expand the leading operator $c\langle\nabla\rangle_c$ and its inverse into its formal Taylor series expansion. Then, we plug the expansions into (2.10) and finally we collect the terms of the same powers of c.

a) Expanding the operators

In order to derive an asymptotic expansion step by step, we follow [26] and the procedure explained above. Firstly, we expand the operator $c\langle\nabla\rangle_c$. For given $k \in \mathbb{Z}$, the formal Taylor series expansion of this operator in Fourier space reads as follows

$$(c\langle\nabla\rangle_c)_k = c\sqrt{|k|^2 + c^2} = c^2\sqrt{1 + \frac{|k|^2}{c^2}} = c^2 + \frac{1}{2}|k|^2 + \sum_{m\geq 1} \mu_{m+1} c^{-2m} |k|^{2m+2}, \tag{2.12}$$

for some $\mu_n \in \mathbb{R}$. Since k is an arbitrary integer, the expansion for operators has to be understood as an asymptotic expansion, e.g., for a given sufficiently smooth function U we write

$$c\langle\nabla\rangle_c U = c^2 U - \frac{1}{2}\Delta U + \sum_{m\geq 1} \mu_{m+1} c^{-2m} (-\Delta)^{m+1} U. \tag{2.13}$$

This can be easily proven by using the Taylor series expansion. We estimate (2.13) as follows (see [26])

$$\left\| c\langle\nabla\rangle_c U - c^2 U + \frac{1}{2}\Delta U \right\|_r \leq \sum_{m\geq 1} \left\| \mu_{m+1} c^{-2m} (-\Delta)^{m+1} U \right\|_r \leq K c^{-2} \|U\|_{r+4},$$

for some constant $K > 0$. Analogously we expand $c\langle\nabla\rangle_c^{-1}$ and obtain

$$c\langle\nabla\rangle_c^{-1} = \left(1 - \frac{\Delta}{c^2}\right)^{-\frac{1}{2}} = 1 + \frac{1}{2c^2}\Delta + \sum_{m\geq 2} \beta_m c^{-2m} (-\Delta)^m, \tag{2.14}$$

for some coefficients $\beta_n \in \mathbb{R}$. Now, we expand the initial conditions with the help of (2.14) as follows

$$U(0,0,x) = \sum_{m\geq 0} c^{-2m} \Theta_m(x), \qquad V(0,0,x) = \sum_{m\geq 0} c^{-2m} \Phi_m(x), \tag{2.15}$$

where

$$\begin{aligned} \Theta_0 &= z_0 - i z_1, & \Theta_1 &= -\frac{i}{2}\Delta z_1, & \Theta_m &= \beta_m (-\Delta)^m z_1, \\ \Phi_0 &= \overline{z_0} - i\overline{z_1}, & \Phi_1 &= -\frac{i}{2}\Delta\overline{z_1}, & \Phi_m &= \beta_n (-\Delta)^m \overline{z_1}. \end{aligned}$$

b) Plugging the expansions into the PDE

Next we plug the expansion of functions u, v and the operators $c\langle\nabla\rangle_c$, $c\langle\nabla\rangle_c^{-1}$ into our differential equation (2.10) in order to collect the same powers of c. Plugging (2.13) and (2.14) into (2.11) we thus obtain

$$\begin{aligned} i\partial_t U + ic^2\partial_\theta U &= -c^2 U + \frac{1}{2}\Delta U + \frac{1}{8}|U+\overline{V}|^2\left(U+\overline{V}\right) + \mathcal{R}_0, \\ i\partial_t V + ic^2\partial_\theta V &= -c^2 V + \frac{1}{2}\Delta V + \frac{1}{8}|\overline{U}+V|^2\left(\overline{U}+V\right) + \mathcal{R}_0, \end{aligned} \tag{2.16}$$

where the remainder $\mathcal{R}_0$ is of order $\mathcal{O}\left(c^{-2}\Delta^2\right)$. Replacing U, V in (2.16) by their formal asymptotic expansions (2.11), we have

$$\begin{aligned} i\partial_t U_\infty + c^2(i\partial_\theta+1)\left(U_\infty + c^{-2}U_1\right) &= \frac{1}{2}\Delta U_\infty + \frac{1}{8}|U_\infty+\overline{V_\infty}|^2\left(U_\infty+\overline{V_\infty}\right) + \mathcal{R}_1, \\ i\partial_t V_\infty + c^2(i\partial_\theta+1)\left(V_\infty + c^{-2}V_1\right) &= \frac{1}{2}\Delta V_\infty + \frac{1}{8}|\overline{U_\infty}+V_\infty|^2\left(\overline{U_\infty}+V_\infty\right) + \mathcal{R}_1, \end{aligned}$$

where the $\mathcal{R}_1$ is of order $\mathcal{O}\left(c^{-2}\Delta^2\right)$. The above system can be rewritten as

$$\begin{aligned} i\partial_t U_\infty + c^2(i\partial_\theta+1)U_\infty + (i\partial_\theta+1)U_1 &= \frac{1}{2}\Delta U_\infty + \frac{1}{8}|U_\infty+\overline{V_\infty}|^2\left(U_\infty+\overline{V_\infty}\right) + \mathcal{R}_1, \\ i\partial_t V_\infty + c^2(i\partial_\theta+1)V_\infty + (i\partial_\theta+1)V_1 &= \frac{1}{2}\Delta V_\infty + \frac{1}{8}|\overline{U_\infty}+V_\infty|^2\left(\overline{U_\infty}+V_\infty\right) + \mathcal{R}_1. \end{aligned} \tag{2.17}$$

c) Collecting the same powers of U and V

Now, we collect the terms of same order in c. Firstly, we consider all terms of order $\mathcal{O}(c^2)$ in (2.17), and obtain

$$\begin{aligned} (i\partial_\theta+1)U_\infty &= 0, \\ (i\partial_\theta+1)V_\infty &= 0. \end{aligned} \tag{2.18}$$

The system above holds if

$$\begin{aligned} \partial_\theta U_\infty &= iU_\infty, \\ \partial_\theta V_\infty &= iV_\infty. \end{aligned}$$

The differential equations (2.18) have the following solutions

$$U_\infty(t,\theta,x) = \mathrm{e}^{i\theta}u_\infty(t,x), \qquad V_\infty(t,\theta,x) = \mathrm{e}^{i\theta}v_\infty(t,x), \tag{2.19}$$

where u_∞, v_∞ are yet to determine. Next, we collect all terms of order $\mathcal{O}(1)$ in (2.17) which yields

$$\begin{aligned} i\partial_t U_\infty + (i\partial_\theta+1)U_1 &= \frac{1}{2}\Delta U_\infty + \frac{1}{8}|U_\infty+\overline{V_\infty}|^2\left(U_\infty+\overline{V_\infty}\right), \\ i\partial_t V_\infty + (i\partial_\theta+1)V_1 &= \frac{1}{2}\Delta V_\infty + \frac{1}{8}|\overline{U_\infty}+V_\infty|^2\left(\overline{U_\infty}+V_\infty\right). \end{aligned} \tag{2.20}$$

In order to determine u_∞ and v_∞ we insert (2.19) into (2.20), and obtain

$$\begin{aligned} i\partial_t\left(\mathrm{e}^{i\theta}u_\infty\right) + (i\partial_\theta+1)U_1 &= \frac{1}{2}\Delta\mathrm{e}^{i\theta}u_\infty + \frac{1}{8}\left|\mathrm{e}^{i\theta}u_\infty + \mathrm{e}^{-i\theta}\overline{v_\infty}\right|^2\left(\mathrm{e}^{i\theta}u_\infty + \mathrm{e}^{-i\theta}\overline{v_\infty}\right), \\ i\partial_t\left(\mathrm{e}^{i\theta}v_\infty\right) + (i\partial_\theta+1)V_1 &= \frac{1}{2}\Delta\mathrm{e}^{i\theta}v_\infty + \frac{1}{8}\left|\mathrm{e}^{-i\theta}\overline{u_\infty} + \mathrm{e}^{i\theta}v_\infty\right|^2\left(\mathrm{e}^{-i\theta}\overline{u_\infty} + \mathrm{e}^{i\theta}v_\infty\right). \end{aligned}$$

Exploiting that

$$
\begin{aligned}
|e^{i\theta}a + e^{-i\theta}\overline{b}|^2 &= |a|^2 + |b|^2 + e^{-2i\theta}\overline{ab} + e^{2i\theta}ab, \\
|e^{i\theta}a + e^{-i\theta}\overline{b}|^2(e^{i\theta}a + e^{-i\theta}\overline{b}) &= \left(|a|^2 + |b|^2 + e^{-2i\theta}\overline{ab} + e^{2i\theta}ab\right) e^{i\theta}a + \left(|a|^2 + |b|^2 + e^{-2i\theta}\overline{ab} + e^{2i\theta}ab\right) e^{-i\theta}b \\
&= \left(|a|^2 + 2|b|^2\right) e^{i\theta}a + \left(2|a|^2 + |b|^2\right) e^{-i\theta}\overline{b} + e^{3i\theta}a^2b + e^{-3i\theta}\overline{ab^2},
\end{aligned}
$$

for $a, b \in \mathbb{C}$ and by orthogonalization with respect to the kernel of $(i\partial_\theta + 1)$, i.e. with respect to $e^{i\theta}$, which yields the system

$$
\begin{aligned}
i\partial_t u_\infty(t,x) &= \frac{1}{2}\Delta u_\infty(t,x) + \frac{1}{8}\left(\left|u_\infty(t,x)\right|^2 + 2\left|v_\infty(t,x)\right|^2\right) u_\infty(t,x), \\
i\partial_t v_\infty(t,x) &= \frac{1}{2}\Delta v_\infty(t,x) + \frac{1}{8}\left(\left|v_\infty(t,x)\right|^2 + 2\left|u_\infty(t,x)\right|^2\right) v_\infty(t,x).
\end{aligned}
$$

For more details on the orthogonality condition for MFE we refer to [26, Section 3]. The initial values are obtained by setting $t = 0$ in (2.19) and by comparison with (2.15), such that

$$
U_\infty(0,0,x) = z_0 - iz_1 \overset{!}{=} e^{i0}u_\infty(0,x) = u_\infty(0,x), \qquad V_\infty(0,0,x) = \overline{z_0} - i\overline{z_1} \overset{!}{=} e^{i0}v_\infty(0,x) = v_\infty(0,x).
$$

Lemma 2.2 (cf. Corollary 4.2 in [26]). *Fix $r > \frac{d}{2}$ and assume $z_0, z_1 \in H^{r+4}$. For the cubic Klein–Gordon equation (2.1) the first-order corrections term z_∞ reads*

$$
z_\infty(t,x) = \frac{1}{2}\left(e^{ic^2t}u_\infty(t,x) + e^{-ic^2t}\overline{v_\infty}(t,x)\right),
$$

where u_∞ and v_∞ are the solutions of the following cubic nonlinear Schrödinger limit system

$$
\begin{aligned}
i\partial_t u_\infty(t,x) &= \frac{1}{2}\Delta u_\infty(t,x) + \frac{1}{8}\left(\left|u_\infty(t,x)\right|^2 + 2\left|v_\infty(t,x)\right|^2\right) u_\infty(t,x), \\
i\partial_t v_\infty(t,x) &= \frac{1}{2}\Delta v_\infty(t,x) + \frac{1}{8}\left(\left|v_\infty(t,x)\right|^2 + 2\left|u_\infty(t,x)\right|^2\right) v_\infty(t,x),
\end{aligned}
\tag{2.21}
$$

with initial values given by

$$
u_\infty(0,x) = z_0 - iz_1, \qquad v_\infty(0,x) = \overline{z_0} - i\overline{z_1}.
$$

Then z_∞ approximates the exact solution z of (2.1) up to terms of order $\mathcal{O}(c^{-2})$.

Proof. For the detailed proof we refer to the proof of Theorem 3.2 in [26]. □

The benefit of this procedure is that it allows us to reduce the highly oscillatory problem (2.1) to a non-oscillatory system of PDEs which can be easily solved numerically, for example via a standard splitting method (see Section 2.4.2). For the theory of splitting methods and error bounds we also refer to [50]. In particular the Lie splitting method for the cubic NLS limit system (2.21) reads as follows

$$
\begin{aligned}
u_\infty^{n+1} &= e^{-i\tau\frac{\Delta}{2}} e^{-i\tau\frac{1}{8}\left(|u_\infty^n|^2 + 2|v_\infty^n|^2\right)} u_\infty^n, \qquad & u_\infty^0 &= z_0 - iz_1, \\
v_\infty^{n+1} &= e^{-i\tau\frac{\Delta}{2}} e^{-i\tau\frac{1}{8}\left(|v_\infty^n|^2 + 2|u_\infty^n|^2\right)} v_\infty^n, \qquad & v_\infty^0 &= \overline{z_0} - i\overline{z_1},
\end{aligned}
$$

and the Strang splitting scheme reads

$$
\begin{aligned}
u_\infty^{n+1} &= e^{-i\frac{\tau}{2}\frac{\Delta}{2}} e^{-i\tau\frac{1}{8}\left(\left|e^{-i\frac{\tau}{2}\frac{\Delta}{2}}u_\infty^n\right|^2 + 2\left|e^{-i\frac{\tau}{2}\frac{\Delta}{2}}v_\infty^n\right|^2\right)} e^{-i\frac{\tau}{2}\frac{\Delta}{2}} u_\infty^n, \qquad & u_\infty^0 &= z_0 - iz_1, \\
v_\infty^{n+1} &= e^{-i\frac{\tau}{2}\frac{\Delta}{2}} e^{-i\tau\frac{1}{8}\left(\left|e^{-i\frac{\tau}{2}\frac{\Delta}{2}}v_\infty^n\right|^2 + 2\left|e^{-i\frac{\tau}{2}\frac{\Delta}{2}}u_\infty^n\right|^2\right)} e^{-i\frac{\tau}{2}\frac{\Delta}{2}} v_\infty^n, \qquad & v_\infty^0 &= \overline{z_0} - i\overline{z_1}.
\end{aligned}
\tag{2.22}
$$

Remark 2.3. The error of the fully discrete scheme applied to the limit system of the Klein–Gordon equation is given by

$$\left\|z(t_n) - z_\infty^n\right\|_r \leq C\left(\tau^2 + h^{r'} + c^{-2}\right),$$

where $z_\infty^n = \frac{1}{2}\left(\mathrm{e}^{ic^2 t_n} u_\infty^n + \mathrm{e}^{-ic^2 t_n} \overline{v_\infty^n}\right)$ denotes the numerical approximation of the first-order correction term, obtained by the Strang splitting (2.22). For the space dsicretization we use a Fourier pseudospectral method with mesh-size h. For more details on the full discrete error result we refer to [26, Theorem 3].

In the next section we derive a uniformly accurate method for the cubic KG equation. Therefore we again use its representation as the coupled first-order system in time (2.7). Instead of employing asymptotic expansion techniques we rescale the system by looking at the so-called *twisted variables*. After this essential step we iterate Duhamel's formula in the new variables and integrate the interactions of the highly oscillatory phases exactly by approximating only the slowly varying parts. Also we show that our uniformly accurate scheme converges in the limit $c \to \infty$ to our numerical method for the limit system (see Section 2.3.2.3 and Section 2.3.3.3 for details).

2.3 Uniformly Accurate Methods for the Klein–Gordon Equation

In this section we give a detailed derivation of the first- and second-order uniformly accurate method for the KG equation. This section is a detailed version of [13, chapter 2-4].

In a first step, we reformulate the Klein–Gordon equation (2.1) as a first-order system in time which allows us to resolve the limit behavior of the solution, i.e., its behavior for $c \to \infty$ (see also [26, 53]). Due to the previous section (see equation (2.7)) we know that the first-order system reads

$$\begin{aligned} i\partial_t u &= -c\langle\nabla\rangle_c u + \tfrac{1}{8} c\langle\nabla\rangle_c^{-1} |u + \overline{v}|^2 (u + \overline{v}), \\ i\partial_t v &= -c\langle\nabla\rangle_c v + \tfrac{1}{8} c\langle\nabla\rangle_c^{-1} |\overline{u} + v|^2 (\overline{u} + v) \end{aligned}$$

with the initial conditions (see (2.8))

$$u(0) = z(0) - ic^{-1}\langle\nabla\rangle_c^{-1}\,\partial_t z(0) \quad \text{and} \quad v(0) = \overline{z}(0) - ic^{-1}\langle\nabla\rangle_c^{-1}\,\partial_t \overline{z}(0).$$

Formally, the definition of $\langle\nabla\rangle_c$ in (2.4) implies that for $c \to \infty$ we have

$$\begin{aligned} c\langle\nabla\rangle_c \omega &= c\sqrt{-\Delta + c^2}\omega \\ &= c^2\sqrt{1 - \tfrac{\Delta}{c^2}}\omega \\ &= c^2\left(\omega - \tfrac{1}{2}\tfrac{\Delta}{c^2}\omega + \mathcal{O}(\tfrac{\Delta^2}{c^4}\omega)\right) \\ &= c^2 + \text{“lower order terms in c”}, \end{aligned} \tag{2.23}$$

for a sufficiently smooth function ω.

This observation motivates us to look at the *twisted variables* by filtering out the highly oscillatory parts explicitly. More precisely, we define

$$u_*(t) = \mathrm{e}^{-ic^2 t} u(t), \qquad v_*(t) = \mathrm{e}^{-ic^2 t} v(t). \tag{2.24}$$

This idea of "twisting" the variable is well known in numerical analysis, for instance in the context of the modulated Fourier expansion [19, 36], adiabatic integrators [36, 49] as well as Lawson-type Runge–Kutta methods [48]. In the case of "multiple high frequencies" it is also widely used in the analysis of partial differential equations in low regularity spaces (see for instance [16]) and has been recently successfully employed numerically for the construction of low-regularity exponential-type integrators for the KdV and Schrödinger equation (see [40, 58]).

In terms of (u_*, v_*) the system (2.7) reads (cf. [53, Formula (2.1)])

$$\begin{aligned} i\partial_t u_* &= -\mathcal{A}_c u_* + c\langle\nabla\rangle_c^{-1}\, \mathrm{e}^{-ic^2t} f\left(\tfrac{1}{2}(\mathrm{e}^{ic^2t}u_* + \mathrm{e}^{-ic^2t}\overline{v_*})\right), \qquad u_*(0) = u(0),\\ i\partial_t v_* &= -\mathcal{A}_c v_* + c\langle\nabla\rangle_c^{-1}\, \mathrm{e}^{-ic^2t} f\left(\tfrac{1}{2}(\mathrm{e}^{ic^2t}v_* + \mathrm{e}^{-ic^2t}\overline{u_*})\right), \qquad v_*(0) = v(0) \end{aligned} \tag{2.25}$$

with $f(z) := |z|^2 z$ and the leading operator

$$\begin{aligned} \mathcal{A}_c :&= c\langle\nabla\rangle_c - c^2\\ &= c^2\sqrt{1 - \tfrac{\Delta}{c^2}} - c^2\\ &= c^2\left(1 - \tfrac{\Delta}{2}\tfrac{1}{c^2} + \mathcal{O}(\tfrac{\Delta^2}{c^4})\right) - c^2\\ &= -\tfrac{1}{2}\Delta + \mathcal{O}\left(\tfrac{\Delta^2}{c^2}\right). \end{aligned}$$

Remark 2.4. The numerical advantage of considering (u_*, v_*) instead of (u, v) lies in the fact that the leading operator $-c\langle\nabla\rangle_c$ in system (2.7) is of order c^2 (see (2.23)) whereas its counterpart $-\mathcal{A}_c$ in system (2.25) is "of order one in c" (see Lemma 2.5 below).

In the following we construct integration schemes for (2.25) based on Duhamel's formula

$$\begin{aligned} u_*(t_n + \tau) &= \mathrm{e}^{i\tau\mathcal{A}_c}u_*(t_n)\\ &\quad - ic\langle\nabla\rangle_c^{-1}\int_0^\tau \mathrm{e}^{i(\tau-s)\mathcal{A}_c}\mathrm{e}^{-ic^2(t_n+s)} f\left(\tfrac{1}{2}(\mathrm{e}^{ic^2(t_n+s)}u_*(t_n+s) + \mathrm{e}^{-ic^2(t_n+s)}\overline{v_*}(t_n+s))\right)\mathrm{d}s,\\ v_*(t_n + \tau) &= \mathrm{e}^{i\tau\mathcal{A}_c}v_*(t_n)\\ &\quad - ic\langle\nabla\rangle_c^{-1}\int_0^\tau \mathrm{e}^{i(\tau-s)\mathcal{A}_c}\mathrm{e}^{-ic^2(t_n+s)} f\left(\tfrac{1}{2}(\mathrm{e}^{ic^2(t_n+s)}v_*(t_n+s) + \mathrm{e}^{-ic^2(t_n+s)}\overline{u_*}(t_n+s))\right)\mathrm{d}s. \end{aligned} \tag{2.26}$$

Thereby, to guarantee *uniform convergence with respect to c* we make the following important observations.

Lemma 2.5 (Uniform bound on the operator $\mathcal{A}_c$, cf. Lemma 3 in [13])**.** *For all $c \in \mathbb{R}$ we have that*

$$\|\mathcal{A}_c u\|_r \le \tfrac{1}{2}\|u\|_{r+2}. \tag{2.27}$$

Proof. The operator $\mathcal{A}_c$ acts as the Fourier multiplier $(\mathcal{A}_c)_k = c\sqrt{c^2 + |k|^2} - c^2$, $k \in \mathbb{Z}^d$. Thus, the assertion follows thanks to the bound

$$\|\mathcal{A}_c u\|_r^2 = \sum_{k\in\mathbb{Z}^d}(1+|k|^2)^r\left(c\sqrt{c^2+|k|^2} - c^2\right)^2|\hat{u}_k|^2 \le \sum_{k\in\mathbb{Z}^d}(1+|k|^2)^r\left(\frac{|k|^2}{2}\right)^2|\hat{u}_k|^2,$$

where we have used that $\sqrt{1+x^2} \le 1 + \frac{1}{2}x^2$ for all $x \in \mathbb{R}$. □

Lemma 2.6 (cf. Lemma 4 in [13]). *For all $t \in \mathbb{R}$ we have that*

$$\|\mathrm{e}^{it\mathcal{A}_c}\|_r = 1 \quad \textit{and} \quad \left\|\left(\mathrm{e}^{-it\mathcal{A}_c} - 1\right) u\right\|_r \leq \frac{1}{2}|t|\|u\|_{r+2}. \tag{2.28}$$

Proof. The first assertion is obvious and the second follows thanks to the estimate $|(\mathrm{e}^{ix} - 1)| \leq |x|$ which holds for all $x \in \mathbb{R}$ together with the essential bound on the operator $\mathcal{A}_c$ given in (2.27). $\square$

In particular, the time derivatives $\big(\partial_t u_*(t), \partial_t v_*(t)\big) := \big(u_*'(t), v_*'(t)\big)$ can be bounded uniformly in c.

Lemma 2.7 (Uniform bounds on the derivatives $(u_*'(t), v_*'(t))$, cf. Lemma 5 in [13]). *Fix $r > d/2$. Solutions of (2.25) satisfy the following estimates*

$$\begin{aligned}
\|u_*(t_n + s) - u_*(t_n)\|_r &\leq \frac{1}{2}|s|\|u_*(t_n)\|_{r+2} + \frac{1}{8}|s| \sup_{0\leq\xi\leq s} \big(\, \|u_*(t_n+\xi)\|_r + \, \|v_*(t_n+\xi)\|_r\big)^3, \\
\|v_*(t_n + s) - v_*(t_n)\|_r &\leq \frac{1}{2}|s|\|v_*(t_n)\|_{r+2} + \frac{1}{8}|s| \sup_{0\leq\xi\leq s} \big(\, \|u_*(t_n+\xi)\|_r + \, \|v_*(t_n+\xi)\|_r\big)^3.
\end{aligned} \tag{2.29}$$

Proof. The assertion follows thanks to Lemma 2.6 together with the bound

$$\|c\langle\nabla\rangle_c^{-1}\|_r \leq 1. \tag{2.30}$$

Due to Duhamel's perturbation formula (2.26) this implies

$$\begin{aligned}
\|u_*(t_n + s) - u_*(t_n)\|_r &\leq |s|\|\mathcal{A}_c u_*(t_n)\|_r + \frac{1}{8}|s|\|c\langle\nabla\rangle_c^{-1}\,\|_r \sup_{0\leq\xi\leq s} \big(\, \|u_*(t_n+\xi)\|_r + \, \|v_*(t_n+\xi)\|_r\big)^3 \\
&\leq \frac{1}{2}|s|\|u_*(t_n)\|_{r+2} + \frac{1}{8}|s| \sup_{0\leq\xi\leq s} \big(\, \|u_*(t_n+\xi)\|_r + \, \|v_*(t_n+\xi)\|_r\big)^3.
\end{aligned}$$

Similarly, we can establish the bound on the derivative $v_*'(t)$. $\square$

In the following Definition, we employ the so-called "φ_j functions".

Definition 2.8 (φ_j functions [39]). *Let ξ be the generator of a (semi)group. Then we set*

$$\varphi_0(\xi) := \mathrm{e}^{\xi} \qquad \textit{and} \qquad \varphi_k(\xi) := \int_0^1 \mathrm{e}^{(1-\theta)\xi} \frac{\theta^{k-1}}{(k-1)!}\mathrm{d}\theta, \quad k \geq 1$$

such that in particular

$$\varphi_1(\xi) = \frac{\mathrm{e}^{\xi} - 1}{\xi}, \qquad \varphi_2(\xi) = \frac{\varphi_1(\xi) - 1}{\xi}.$$

In addition, we define

$$\Psi_k(\xi) := \int_0^1 \mathrm{e}^{\theta\xi} \frac{\theta^{k-1}}{(k-1)!}\mathrm{d}\theta, \quad k \geq 1$$

such that in particular we have that

$$\Psi_2(\xi) := \frac{\varphi_0(\xi) - \varphi_1(\xi)}{\xi}.$$

In the following, we assume local well-posedness (LWP) of (2.25) in H^r.

Assumption 2.9. *Fix $r > d/2$ and assume that there exists a $T > 0$ such that the solutions $(u_*(t), v_*(t))$ of (2.25) satisfy*

$$\sup_{0\le t\le T} \Big(\|u_*(t)\|_r + \|v_*(t)\|_r \Big) \le M$$

uniformly in c.

Remark 2.10. The previous assumption holds under the following condition on the initial data

$$\|z(0)\|_r + \|c^{-1}\langle\nabla\rangle_c^{-1}\partial_t z(0)\|_r \le M_0,$$

where M_0 does not depend on c. The c-independence of this bound can be easily proved from the formulation (2.26) by using a classical fixed point argument together with the essential uniform bound (2.30) and (2.28).

For further details on the local well-posedness of highly oscillatory Klein–Gordon equations we refer to [53, 73] and the references therein.
At this point, we have rewritten the Klein–Gordon equation into a twisted first-order system (2.25), which only involves bounded operators with respect to c (see Remark 2.4). Thus, why do not we use standard exponential integrators (see [39]) in order to solve the twisted first-order system numerically? The answer to this question will be given in the following section.

2.3.1 A Classical Exponential Integrator for the Twisted Klein–Gordon System

In this subsection we show that applying a classical exponential integrator (see [39]) on the twisted system is not an appropriate ansatz to obtain a uniformly accurate method. See Figure 2.3 for numerical illustration. In the following we construct an exponential integrator for the twisted system (2.25).
In order to obtain an exponential integrator for (2.25) in a classical way, we exploit Duhamel's formulas given in (2.26)

$$\begin{aligned}
u_*(t_n+\tau) &= \mathrm{e}^{i\tau\mathcal{A}_c}u_*(t_n)\\
&\quad - ic\langle\nabla\rangle_c^{-1}\int_0^\tau \mathrm{e}^{i(\tau-s)\mathcal{A}_c}\mathrm{e}^{-ic^2(t_n+s)} f\left(\tfrac12(\mathrm{e}^{ic^2(t_n+s)}u_*(t_n+s) + \mathrm{e}^{-ic^2(t_n+s)}\overline{v_*}(t_n+s))\right)\mathrm{d}s,\\
v_*(t_n+\tau) &= \mathrm{e}^{i\tau\mathcal{A}_c}v_*(t_n)\\
&\quad - ic\langle\nabla\rangle_c^{-1}\int_0^\tau \mathrm{e}^{i(\tau-s)\mathcal{A}_c}\mathrm{e}^{-ic^2(t_n+s)} f\left(\tfrac12(\mathrm{e}^{ic^2(t_n+s)}v_*(t_n+s) + \mathrm{e}^{-ic^2(t_n+s)}\overline{u_*}(t_n+s))\right)\mathrm{d}s.
\end{aligned}$$

We use the ansatz of exponential integrators and freeze the following terms of the Duhamel's formulas at $s = 0$

$$\begin{gathered}
\mathrm{e}^{-ic^2(t_n+s)} f\left(\tfrac12(\mathrm{e}^{ic^2(t_n+s)}u_*(t_n+s) + \mathrm{e}^{-ic^2(t_n+s)}\overline{v_*}(t_n+s))\right),\\
\mathrm{e}^{-ic^2(t_n+s)} f\left(\tfrac12(\mathrm{e}^{ic^2(t_n+s)}v_*(t_n+s) + \mathrm{e}^{-ic^2(t_n+s)}\overline{u_*}(t_n+s))\right)
\end{gathered}$$

which yields

$$\begin{aligned}
u_*(t_{n+1}) &\approx \mathrm{e}^{i\tau\mathcal{A}_c}u_*(t_n) - ic\langle\nabla\rangle_c^{-1}\int_0^\tau \mathrm{e}^{i(\tau-s)\mathcal{A}_c}\mathrm{d}s\, \mathrm{e}^{-ic^2t_n} f\left(\tfrac12(\mathrm{e}^{ic^2t_n}u_*(t_n) + \mathrm{e}^{-ic^2t_n}\overline{v_*}(t_n))\right),\\
v_*(t_{n+1}) &\approx \mathrm{e}^{i\tau\mathcal{A}_c}v_*(t_n) - ic\langle\nabla\rangle_c^{-1}\int_0^\tau \mathrm{e}^{i(\tau-s)\mathcal{A}_c}\mathrm{d}s\, \mathrm{e}^{-ic^2t_n} f\left(\tfrac12(\mathrm{e}^{ic^2t_n}v_*(t_n) + \mathrm{e}^{-ic^2t_n}\overline{u_*}(t_n))\right).
\end{aligned}$$

Integrating the remaining term $\int_0^\tau \mathrm{e}^{i(\tau-s)\mathcal{A}_c}\mathrm{d}s$ exactly and applying the Definition 2.8 of the φ_1 function we have

$$u_*(t_{n+1}) \approx \mathrm{e}^{i\tau\mathcal{A}_c}u_*(t_n) - i\tau c\langle\nabla\rangle_c^{-1}\varphi_1\left(i\tau\mathcal{A}_c\right)\mathrm{e}^{-ic^2t_n}f\left(\tfrac{1}{2}(\mathrm{e}^{ic^2t_n}u_*(t_n)+\mathrm{e}^{-ic^2t_n}\overline{v_*}(t_n))\right),$$
$$v_*(t_{n+1}) \approx \mathrm{e}^{i\tau\mathcal{A}_c}v_*(t_n) - i\tau c\langle\nabla\rangle_c^{-1}\varphi_1\left(i\tau\mathcal{A}_c\right)\mathrm{e}^{-ic^2t_n}f\left(\tfrac{1}{2}(\mathrm{e}^{ic^2t_n}v_*(t_n)+\mathrm{e}^{-ic^2t_n}\overline{u_*}(t_n))\right).$$

In particular, we obtain for $f(z)=|z|^2z$ the following exponential integration scheme

$$u_*^{n+1} = \mathrm{e}^{i\tau\mathcal{A}_c}u_*^n - \tfrac{i}{8}\tau c\langle\nabla\rangle_c^{-1}\varphi_1\left(i\tau\mathcal{A}_c\right)\left(\left|\mathrm{e}^{ic^2t_n}u_*^n+\mathrm{e}^{-ic^2t_n}\overline{v_*^n}\right|^2\left(u_*^n+\mathrm{e}^{-2ic^2t_n}\overline{v_*^n}\right)\right),$$
$$v_*^{n+1} = \mathrm{e}^{i\tau\mathcal{A}_c}v_*^n - \tfrac{i}{8}\tau c\langle\nabla\rangle_c^{-1}\varphi_1\left(i\tau\mathcal{A}_c\right)\left(\left|\mathrm{e}^{ic^2t_n}v_*^n+\mathrm{e}^{-ic^2t_n}\overline{u_*^n}\right|^2\left(v_*^n+\mathrm{e}^{-2ic^2t_n}\overline{u_*^n}\right)\right)$$

with initial values

$$u_*^0 = z_0 - ic\langle\nabla\rangle_c^{-1}\, z_1,$$
$$v_*^0 = \overline{z_0} - ic\langle\nabla\rangle_c^{-1}\, \overline{z_1}.$$

Figure 2.3 underlines that the exponential integrator scheme is not uniformly accurate with respect to c. More precisely for large values of c the exponential integrator scheme fails to approximate numerically the solution of the Klein–Gordon equation, which can be explained by the following approximation of the highly oscillatory terms

$$\mathrm{e}^{ic^2(t_n+s)} = \mathrm{e}^{ic^2t_n} + \mathcal{O}(sc^2).$$

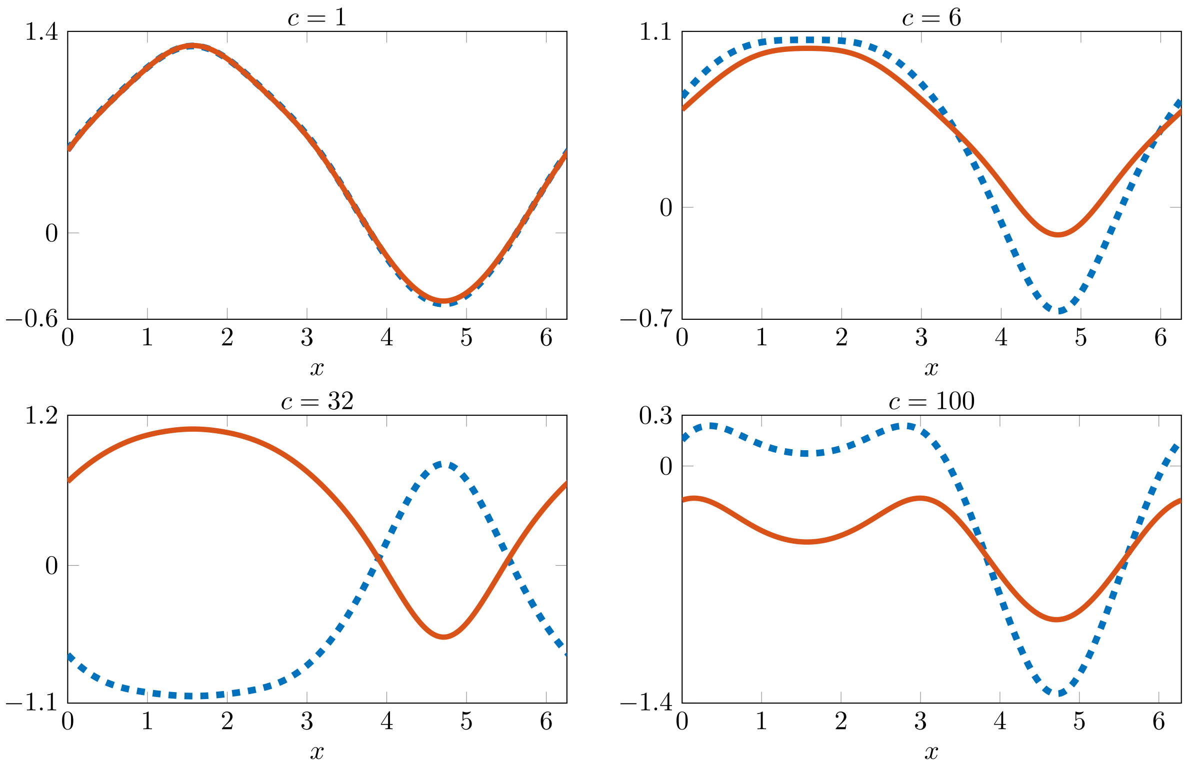

Figure 2.3: Numerical solution of the Klein–Gordon equation. Exponential integrator scheme (red solid line) for different c with time step size $\tau \approx 10^{-2}$ at time $t = 0.9$. The blue dashed line represents the reference solution at time $t = 0.9$, computed via the same exponential integrator scheme with a small time step size $\tau \approx 10^{-6}$. The spatial discretization is done via a Fourier pseudospectral method with with mesh-size $h = 0.0245$.

Thus, the exponential integrator also suffers from severe time step restrictions similarly to the Gautschi-type methods shown in Figure 2.1.
In the next section we construct our uniformly accurate exponential-type integrator. Therefore, we also integrate the highly oscillatory phase terms $\mathrm{e}^{\pm \ell i c^2 (t_n+s)}$, for $\ell \in \mathbb{N}$ in the Duhamel's formula exactly. This simple trick yields to our new uniformly accurate method.

2.3.2 Construction of a First-Order Uniformly Accurate Scheme

In this section we derive a first-order exponential-type integration scheme for the solutions (u_*, v_*) of (2.25) which allows *first-order time-convergence uniform with respect to c*. The construction is thereby based on Duhamel's formula (2.26) and the essential estimates in Lemma 2.5, 2.6 and 2.7. For the derivation we will for simplicity assume that z is real, which (by Remark 2.1) implies that $u = v$ such that system (2.25) reduces to

$$i\partial_t u_* = -\mathcal{A}_c u_* + \frac{1}{8} c \langle \nabla \rangle_c^{-1} \, \mathrm{e}^{-ic^2 t} \left(\mathrm{e}^{ic^2 t} u_* + \mathrm{e}^{-ic^2 t} \overline{u_*} \right)^3, \qquad u_*(0) = z_0 - ic\langle \nabla \rangle_c^{-1} z_1 \tag{2.31}$$

with the mild-solution

$$\begin{aligned} u_*(t_n + \tau) &= \mathrm{e}^{i\tau \mathcal{A}_c} u_*(t_n) \\ &\quad - \frac{i}{8} c \langle \nabla \rangle_c^{-1} \int_0^\tau \mathrm{e}^{i(\tau - s)\mathcal{A}_c} \mathrm{e}^{-ic^2(t_n+s)} \left(\mathrm{e}^{ic^2(t_n+s)} u_*(t_n+s) + \mathrm{e}^{-ic^2(t_n+s)} \overline{u_*}(t_n+s) \right)^3 \mathrm{d}s. \end{aligned} \tag{2.32}$$

2.3.2.1 Construction

In order to derive a first-order scheme, we need to impose additional regularity assumptions on the exact solution $u_*(t)$ of (2.31).

Assumption 2.11. *Fix $r > d/2$ and assume that $u_* \in \mathcal{C}([0,T]; H^{r+2}(\mathbb{T}^d))$ and in particular*

$$\sup_{0 \le t \le T} \|u_*(t)\|_{r+2} \le M_2,$$

where M_2 can be bounded uniformly in c.

Note that the above assumption can be easily played back to the initial value thanks to Remark 2.10.
Applying Lemma 2.6 and Lemma 2.7 in (2.32) allows us to employ the following expansion

$$\begin{aligned} u_*(t_n + \tau) &= \mathrm{e}^{i\tau \mathcal{A}_c} u_*(t_n) - \frac{i}{8} c \langle \nabla \rangle_c^{-1} \mathrm{e}^{i\tau \mathcal{A}_c} \int_0^\tau \mathrm{e}^{-ic^2(t_n+s)} \left(\mathrm{e}^{ic^2(t_n+s)} u_*(t_n) + \mathrm{e}^{-ic^2(t_n+s)} \overline{u_*}(t_n) \right)^3 \mathrm{d}s \\ &\quad + \mathcal{R}(\tau, t_n, u_*), \end{aligned} \tag{2.33}$$

where the remainder $\mathcal{R}(\tau, t_n, u_*)$ satisfies thanks to the bounds (2.28), (2.29) and (2.30) that

$$\|\mathcal{R}(\tau, t_n, u_*)\|_r \le \tau^2 k_{r,M_2}, \tag{2.34}$$

for some constant k_{r,M_2} which depends on M_2 (see Assumption 2.11) and r, but is independent of c. Furthermore, solving the integral in (2.33) (in particular, integrating the highly oscillatory phases $\mathrm{e}^{\pm i l c^2 s}$ exactly, for $\ell \in \mathbb{N}_0$) yields by adding and subtracting the term $\tau \frac{3i}{8} \mathrm{e}^{i\tau \mathcal{A}_c} |u_*(t_n)|^2 u_*(t_n)$ (see Remark 2.19

below for the purpose of this manipulation) that

$$
\begin{aligned}
u_*(t_n+\tau) = \mathrm{e}^{i\tau\mathcal{A}_c}\Big(1-\tau\frac{3i}{8}|u_*(t_n)|^2\Big)u_*(t_n) - \tau\frac{3i}{8}\left(c\langle\nabla\rangle_c^{-1}-1\right)\mathrm{e}^{i\tau\mathcal{A}_c}|u_*(t_n)|^2u_*(t_n)\\
-\tau\frac{i}{8}c\langle\nabla\rangle_c^{-1}\mathrm{e}^{i\tau\mathcal{A}_c}\Big\{\mathrm{e}^{2ic^2t_n}\varphi_1(2ic^2\tau)u_*^3(t_n)+\mathrm{e}^{-2ic^2t_n}\varphi_1(-2ic^2\tau)3|u_*(t_n)|^2\overline{u_*}(t_n)\\
+\mathrm{e}^{-4ic^2t_n}\ \varphi_1(-4ic^2\tau)\overline{u_*}^3(t_n)\Big\}+\mathcal{R}(\tau,t_n,u_*)
\end{aligned}
\tag{2.35}
$$

with φ_1 given in Definition 2.8. For more details on the practical implementation of the scheme we refer to Remark 2.12.

As the operator $\mathrm{e}^{it\mathcal{A}_c}$ is a linear isometry (see Lemma 2.6 or [25, 46, 50]) in H^r and by Taylor series expansion

$$
|1-x-\mathrm{e}^{-x}| = \mathcal{O}(x^2)
$$

we obtain for $r>d/2$ that

$$
\left\|\mathrm{e}^{i\tau\mathcal{A}_c}\Big(1-\tau\frac{3i}{8}|u_*(t_n)|^2\Big)u_*(t_n)-\mathrm{e}^{i\tau\mathcal{A}_c}\mathrm{e}^{-\tau\frac{3i}{8}|u_*(t_n)|^2}u_*(t_n)\right\|_r \le k_r3\tau^2\|u_*(t_n)\|_r^3,
\tag{2.36}
$$

for some constant k_r independent of c. Exploiting the bound (2.36) we can express (2.35) as follows

$$
\begin{aligned}
u_*(t_n+\tau) = \mathrm{e}^{i\tau\mathcal{A}_c}\mathrm{e}^{-\tau\frac{3i}{8}|u_*(t_n)|^2}u_*(t_n) - \tau\frac{3i}{8}\left(c\langle\nabla\rangle_c^{-1}-1\right)\mathrm{e}^{i\tau\mathcal{A}_c}|u_*(t_n)|^2u_*(t_n)\\
-\tau\frac{i}{8}c\langle\nabla\rangle_c^{-1}\mathrm{e}^{i\tau\mathcal{A}_c}\Big\{\mathrm{e}^{2ic^2t_n}\varphi_1(2ic^2\tau)u_*^3(t_n)+\mathrm{e}^{-2ic^2t_n}\varphi_1(-2ic^2\tau)3|u_*(t_n)|^2\overline{u_*}(t_n)\\
+\mathrm{e}^{-4ic^2t_n}\ \varphi_1(-4ic^2\tau)\overline{u_*}^3(t_n)\Big\}+\mathcal{R}(\tau,t_n,u_*),
\end{aligned}
\tag{2.37}
$$

where the remainder $\mathcal{R}(\tau,t_n,u_*)$ satisfies thanks to (2.34) and (2.36) that

$$
\|\mathcal{R}(\tau,t_n,u_*)\|_r \le \tau^2k_{r,M_2},
\tag{2.38}
$$

for some constant k_{r,M_2} which depends on M_2 (see Assumption 2.11) and r, but is independent of c.

Based on the expansion (2.37) we construct the following exponential-type integration scheme, in order to approximate the exact solution $u_*(t_{n+1})$ at time $t_{n+1} = t_n+\tau$. The scheme reads as follows

$$
\begin{aligned}
u_*^{n+1} &= \mathrm{e}^{i\tau\mathcal{A}_c}\mathrm{e}^{-\tau\frac{3i}{8}|u_*^n|^2}u_*^n - \tau\frac{3i}{8}\left(c\langle\nabla\rangle_c^{-1}-1\right)\mathrm{e}^{i\tau\mathcal{A}_c}|u_*^n|^2u_*^n\\
&\quad-\tau\frac{i}{8}c\langle\nabla\rangle_c^{-1}\mathrm{e}^{i\tau\mathcal{A}_c}\Big\{\mathrm{e}^{2ic^2t_n}\ \varphi_1(2ic^2\tau)(u_*^n)^3+\mathrm{e}^{-2ic^2t_n}\ \varphi_1(-2ic^2\tau)3|u_*^n|^2\overline{u_*^n}\\
&\quad+\mathrm{e}^{-4ic^2t_n}\varphi_1(-4ic^2\tau)(\overline{u_*^n})^3\Big\},\\
u_*^0 &= z(0)-ic^{-1}\langle\nabla\rangle_c^{-1}\ \partial_tz(0)
\end{aligned}
$$

with φ_1 given in Definition 2.8. Note that the definition of the initial value u_*^0 follows from (2.8).

For complex-valued functions z (i.e., for $u\not\equiv v$) we similarly derive the exponential-type integration scheme

$$
\begin{aligned}
u_*^{n+1} &= \mathrm{e}^{i\tau\mathcal{A}_c}\mathrm{e}^{-\tau\frac{i}{8}\left(|u_*^n|^2+2|v_*^n|^2\right)}u_*^n - \tau\frac{i}{8}\left(c\langle\nabla\rangle_c^{-1}-1\right)\mathrm{e}^{i\tau\mathcal{A}_c}\left(|u_*^n|^2+2|v_*^n|^2\right)u_*^n\\
&\quad-\tau\frac{i}{8}c\langle\nabla\rangle_c^{-1}\mathrm{e}^{i\tau\mathcal{A}_c}\Big\{\mathrm{e}^{2ic^2t_n}\ \varphi_1(2ic^2\tau)(u_*^n)^2v_*^n+\mathrm{e}^{-2ic^2t_n}\ \varphi_1(-2ic^2\tau)\left(2|u_*^n|^2+|v_*^n|^2\right)\overline{v_*^n}\\
&\quad+\mathrm{e}^{-4ic^2t_n}\varphi_1(-4ic^2\tau)(\overline{v_*^n})^2\overline{u_*^n}\Big\},\\
u_*^0 &= z(0)-ic^{-1}\langle\nabla\rangle_c^{-1}\partial_t\ z(0),
\end{aligned}
\tag{2.39}
$$

where the scheme in v_*^{n+1} is obtained by replacing $u_*^n \leftrightarrow v_*^n$ on the right-hand side of (2.39) with initial value $v_*^0 = \overline{z}(0) - ic^{-1}\langle\nabla\rangle_c^{-1}\partial_t\overline{z}(0)$ (see (2.8)).

Remark 2.12 (Practical implementation)**.** To reduce the computational effort we may express the first-order scheme (2.39) in its equivalent form

$$\begin{aligned}
u_*^{n+1} &= \mathrm{e}^{i\tau\mathcal{A}_c}\left(\mathrm{e}^{-\tau\frac{i}{8}\left(|u_*^n|^2+2|v_*^n|^2\right)}u_*^n + \tau\frac{i}{8}\left(|u_*^n|^2+2|v_*^n|^2\right)u_*^n\right)\\
&\quad - \frac{i\tau}{8}c\langle\nabla\rangle_c^{-1}\mathrm{e}^{i\tau\mathcal{A}_c}\Big\{\left(|u_*^n|^2+2|v_*^n|^2\right)u_*^n + \mathrm{e}^{2ic^2t_n}\ \varphi_1(2ic^2\tau)(u_*^n)^2v_*^n\\
&\qquad + \mathrm{e}^{-2ic^2t_n}\ \varphi_1(-2ic^2\tau)\left(2|u_*^n|^2+|v_*^n|^2\right)\overline{v_*^n} + \mathrm{e}^{-4ic^2t_n}\varphi_1(-4ic^2\tau)(\overline{v_*^n})^2\overline{u_*^n}\Big\},\\
u_*^0 &= z(0) - ic^{-1}\langle\nabla\rangle_c^{-1}\ \partial_t z(0)
\end{aligned}$$

which after a Fourier pseudo-spectral space discretization only requires the usage of two Fast Fourier transforms (and its corresponding inverse counter parts) instead of three.

In Section 2.3.2.2 below we prove that the exponential-type integration scheme (2.39) is first-order convergent uniformly in c for sufficiently smooth solutions. Furthermore, we give a fractional convergence result under weaker regularity assumptions and analyze its behavior in the non-relativistic limit regime $c \to \infty$. In Section 2.3.2.3 we give some simplifications in the latter regime.

2.3.2.2 Convergence Analysis

The exponential-type integration scheme (2.39) converges (by construction) with first-order in time uniformly with respect to c, see Theorem 2.13. Furthermore, a fractional convergence bound holds true for less regular solutions, see Theorem 2.15. In particular, in the limit $c \to \infty$ the scheme converges to the classical Lie splitting applied to the nonlinear Schrödinger limit system, see Lemma 2.17.

Theorem 2.13 (Convergence bound for the first-order scheme, cf. Theorem 11 in [13])**.** *Fix $r > d/2$ and assume that*

$$\|z(0)\|_{r+2} + \|c^{-1}\langle\nabla\rangle_c^{-1}\partial_t z(0)\|_{r+2} \leq M_2 \tag{2.40}$$

uniformly in c. For (u_*^n, v_*^n) defined in (2.39) we set

$$z^n \ := \frac{1}{2}\left(\mathrm{e}^{ic^2t_n}u_*^n + \mathrm{e}^{-ic^2t_n}\overline{v_*^n}\right).$$

Then, there exists a $T > 0$ and $\tau_0 > 0$ such that for all $\tau \leq \tau_0$ and $t_n \leq T$ we have for all $c > 0$ that

$$\|z(t_n) - z^n\|_r \ \leq \tau K^*_{r,T,M,M_2},$$

where the constant K^*_{r,T,M,M_2} can be chosen independently of c.

Now we state a detailed version of the proof of [13, Theorem 11].

Proof. Fix $r > d/2$. First note that the regularity assumption on the initial data in (2.40) implies the regularity Assumption 2.11 on (u_*, v_*), i.e., there exists a $T > 0$ such that

$$\sup_{0\leq t\leq T}\Big(\ \|u_*(t)\|_{r+2}\ + \|v_*(t)\|_{r+2}\Big)\ \leq k_{T,M_2},$$

for some constant k that depends on M_2 and T, but can be chosen independently of c. For the local well-posedness we refer to [73] and the references therein.

In the following let $(\phi^t_{u_*}, \phi^t_{v_*})$ denote the exact flow of (2.25) and let $(\Phi^\tau_{u_*}, \Phi^\tau_{v_*})$ denote the numerical flow defined in (2.39), i.e.,

$$u_*(t_{n+1}) = \phi^\tau_{u_*}(u_*(t_n), v_*(t_n)), \qquad u_*^{n+1} = \Phi^\tau_{u_*}(u_*^n, v_*^n),$$

and a similar formula for the functions $v_*(t_n)$ and v_*^n. For more details on numerical flows we refer to [25, 36]. In the literature the numerical flow is often denoted by φ, here we use ϕ, since φ denotes the φ functions (see Definition 2.8). This allows us to split the global error as follows

$$\begin{aligned} u_*(t_{n+1}) - u_*^{n+1} &= \phi^\tau_{u_*}(u_*(t_n), v_*(t_n)) - \Phi^\tau_{u_*}(u_*^n, v_*^n) \\ &= \Phi^\tau_{u_*}(u_*(t_n), v_*(t_n)) - \Phi^\tau_{u_*}(u_*^n, v_*^n) + \phi^\tau_{u_*}(u_*(t_n), v_*(t_n)) - \Phi^\tau_{u_*}(u_*(t_n), v_*(t_n)). \end{aligned} \tag{2.41}$$

Local error bound: With the aid of (2.38), the expansion of the exact solution in (2.37) and the definition of the numerical scheme (2.39) allows us to write

$$\|\phi^\tau_{u_*}(u_*(t_n), v_*(t_n)) - \Phi^\tau_{u_*}(u_*(t_n), v_*(t_n))\|_r = \|\mathcal{R}(\tau, t_n, u_*, v_*)\|_r \le \tau^2 k_{r,M_2}, \tag{2.42}$$

for some constant k which depends on M_2 and r, but can be chosen independently of c.
Stability bound: Note that for all $l \in \mathbb{Z}$ we have that

$$\left|\varphi_1(i\tau c^2 l)\right| \le 1 \tag{2.43}$$

which can be easily seen from the definition of the φ_1 function (see Definition 2.8). This yields that

$$\left|\varphi_1(i\tau c^2 l)\right| = \left|\int_0^1 \mathrm{e}^{(1-\theta)i\tau c^2 l} \mathrm{d}\theta\right| \le \int_0^1 \left|\mathrm{e}^{i\tau c^2 l}\right| \left|\mathrm{e}^{-\theta i\tau c^2 l}\right| \mathrm{d}\theta = \int_0^1 1 \mathrm{d}\theta = 1. \tag{2.44}$$

We have

$$\begin{aligned} \Phi^\tau_{u_*}(u_*(t_n), v_*(t_n)) = {} & \mathrm{e}^{i\tau\mathcal{A}_c} \mathrm{e}^{-\tau\frac{i}{8}\left(|u_*(t_n)|^2 + 2|v_*(t_n)|^2\right)} u_*(t_n) \\ & - \tau\frac{i}{8}\left(c\langle\nabla\rangle^{-1} - 1\right) \mathrm{e}^{i\tau\mathcal{A}_c}\left(|u_*(t_n)|^2 + 2|v_*(t_n)|^2\right) u_*(t_n) \\ & - \tau\frac{i}{8} c\langle\nabla\rangle^{-1} \mathrm{e}^{i\tau\mathcal{A}_c}\Big\{\mathrm{e}^{2ic^2t_n}\ \varphi_1(2ic^2\tau)(u_*(t_n))^2 v_*(t_n) \\ & \qquad + \mathrm{e}^{-4ic^2t_n}\varphi_1(-4ic^2\tau)(\overline{v_*}(t_n))^2\overline{u_*}(t_n) \\ & \qquad + \mathrm{e}^{-2ic^2t_n}\ \varphi_1(-2ic^2\tau)\left(2|u_*(t_n)|^2 + |v_*(t_n)|^2\right)\overline{v_*}(t_n)\Big\} \\ = {} & E_1 + E_2 + E_3, \end{aligned}$$

where we set

$$\begin{aligned} E_1 &:= \mathrm{e}^{i\tau\mathcal{A}_c} \mathrm{e}^{-\tau\frac{i}{8}\left(|u_*(t_n)|^2 + 2|v_*(t_n)|^2\right)} u_*(t_n), \\ E_2 &:= -\tau\frac{i}{8}\left(c\langle\nabla\rangle^{-1} - 1\right) \mathrm{e}^{i\tau\mathcal{A}_c}\left(|u_*(t_n)|^2 + 2|v_*(t_n)|^2\right) u_*(t_n), \\ E_3 &:= -\tau\frac{i}{8} c\langle\nabla\rangle^{-1} \mathrm{e}^{i\tau\mathcal{A}_c}\Big\{\mathrm{e}^{2ic^2t_n}\ \varphi_1(2ic^2\tau)(u_*(t_n))^2 v_*(t_n) + \mathrm{e}^{-4ic^2t_n}\varphi_1(-4ic^2\tau)(\overline{v_*}(t_n))^2\overline{u_*}(t_n) \\ &\qquad + \mathrm{e}^{-2ic^2t_n}\ \varphi_1(-2ic^2\tau)\left(2|u_*(t_n)|^2 + |v_*(t_n)|^2\right)\overline{v_*}(t_n)\Big\}. \end{aligned}$$

Furthermore, we have

$$\begin{aligned}
\Phi^{\tau}_{u_*}(u^n_*, v^n_*) &= \mathrm{e}^{i\tau\mathcal{A}_c}\mathrm{e}^{-\tau\frac{i}{8}\left(|u^n_*|^2+2|v^n_*|^2\right)}u^n_* \\
&\quad - \tau\frac{i}{8}\left(c\langle\nabla\rangle^{-1}-1\right)\mathrm{e}^{i\tau\mathcal{A}_c}\left(|u^n_*|^2+2|v^n_*|^2\right)u^n_* \\
&\quad - \tau\frac{i}{8}c\langle\nabla\rangle^{-1}\mathrm{e}^{i\tau\mathcal{A}_c}\Big\{\mathrm{e}^{2ic^2t_n}\ \varphi_1(2ic^2\tau)(u^n_*)^2v^n_* + \mathrm{e}^{-2ic^2t_n}\ \varphi_1(-2ic^2\tau)\big(2|u^n_*|^2+|v^n_*|^2\big)\overline{v^n_*} \\
&\qquad\qquad + \mathrm{e}^{-4ic^2t_n}\varphi_1(-4ic^2\tau)(\overline{v^n_*})^2\overline{u^n_*}\Big\} \\
&= N_1 + N_2 + N_3,
\end{aligned}$$

where we set

$$\begin{aligned}
N_1 &:= \mathrm{e}^{i\tau\mathcal{A}_c}\mathrm{e}^{-\tau\frac{i}{8}\left(|u^n_*|^2+2|v^n_*|^2\right)}u^n_*, \\
N_2 &:= -\tau\frac{i}{8}\left(c\langle\nabla\rangle^{-1}-1\right)\mathrm{e}^{i\tau\mathcal{A}_c}\left(|u^n_*|^2+2|v^n_*|^2\right)u^n_*, \\
N_3 &:= -\tau\frac{i}{8}c\langle\nabla\rangle^{-1}\mathrm{e}^{i\tau\mathcal{A}_c}\Big\{\mathrm{e}^{2ic^2t_n}\ \varphi_1(2ic^2\tau)(u^n_*)^2v^n_* + \mathrm{e}^{-4ic^2t_n}\varphi_1(-4ic^2\tau)(\overline{v^n_*})^2\overline{u^n_*} \\
&\qquad + \mathrm{e}^{-2ic^2t_n}\ \varphi_1(-2ic^2\tau)\big(2|u^n_*|^2+|v^n_*|^2\big)\overline{v^n_*}\Big\}.
\end{aligned}$$

Next we take the difference of E_1 and N_1. As $\mathrm{e}^{i\tau\mathcal{A}_c}$ and $\mathrm{e}^{-i\ell c^2t}$ are linear isometries for all $t \in \mathbb{R}$ and $\ell \in \mathbb{R}$ (see Lemma 2.6) we obtain that

$$\begin{aligned}
\|E_1 - N_1\|_r &= \left\|\mathrm{e}^{-\tau\frac{i}{8}\left(|u_*(t_n)|^2+2|v_*(t_n)|^2\right)}u_*(t_n) - \mathrm{e}^{-\tau\frac{i}{8}\left(|u^n_*|^2+2|v^n_*|^2\right)}u^n_*\right\|_r \\
&\le \left\|\mathrm{e}^{-\tau\frac{i}{8}\left(|u_*(t_n)|^2+2|v_*(t_n)|^2\right)}u_*(t_n) - \mathrm{e}^{-\tau\frac{i}{8}\left(|u_*(t_n)|^2+2|v_*(t_n)|^2\right)}u^n_*\right\|_r \\
&\quad + \left\|\mathrm{e}^{-\tau\frac{i}{8}\left(|u_*(t_n)|^2+2|v_*(t_n)|^2\right)}u^n_* - \mathrm{e}^{-\tau\frac{i}{8}\left(|u^n_*|^2+2|v^n_*|^2\right)}u^n_*\right\|_r \\
&\le \left\|\mathrm{e}^{-\tau\frac{i}{8}\left(|u_*(t_n)|^2+2|v_*(t_n)|^2\right)}\right\|_r\|u_*(t_n) - u^n_*\|_r \\
&\quad + \left\|\mathrm{e}^{-\tau\frac{i}{8}\left(|u_*(t_n)|^2+2|v_*(t_n)|^2\right)} - \mathrm{e}^{-\tau\frac{i}{8}\left(|u^n_*|^2+2|v^n_*|^2\right)}\right\|_r\|u^n_*\|_r.
\end{aligned} \tag{2.45}$$

In the following we assume that

$$\|u_*(t_n)\|_r \le M \qquad \text{and} \qquad \|u^n_*\|_r \le 2M. \tag{2.46}$$

Furthermore, we define constants K_r and $K_{r,M}$, which depend only on r and r, M respectively, but can be chosen independently of c. Exploiting the Taylor series expansion of the exponential function, we obtain

$$\left\|\mathrm{e}^{-\frac{i\tau}{8}\left(|u|^2+2|v|^2\right)} - 1\right\|_r \le \tau K_{r,M}$$

and

$$1 + \tau K_{r,M} \le \mathrm{e}^{\tau K_{r,M}}. \tag{2.47}$$

Therefore, (2.45) implies

$$\begin{aligned}
\|E_1 - N_1\|_r &\le (1+\tau K_{r,M})\|u_*(t_n) - u^n_*\|_r + \tau K_{r,M}\|u_*(t_n) - u^n_*\|_r \\
&\le (1+\tau K_{r,M})\|u_*(t_n) - u^n_*\|_r \\
&\le \mathrm{e}^{\tau K_{r,M}}\|u_*(t_n) - u^n_*\|_r.
\end{aligned} \tag{2.48}$$

Thanks to the bound $\|c\langle\nabla\rangle^{-1}\|_r \leq 1$, we obtain for the difference of E_2 and N_2 that

$$
\begin{aligned}
\|E_2 - N_2\|_r &\leq \tau K_r \left\|\left(|u_*(t_n)|^2 + 2\,|v_*(t_n)|^2\right) u_*(t_n) - \left(|u_*^n|^2 + 2\,|v_*^n|^2\right) u_*^n\right\|_r \\
&= \tau K_r \left\||u_*(t_n)|^2 u_*(t_n) + 2\,|v_*(t_n)|^2 u_*(t_n) - |u_*^n|^2 u_*^n - 2\,|v_*^n|^2 u_*^n\right\|_r \\
&= \tau K_r \left\||u_*(t_n)|^2 u_*(t_n) - |u_*^n|^2 u_*^n + 2\,|v_*(t_n)|^2 u_*(t_n) - 2\,|v_*^n|^2 u_*^n\right\|_r \\
&\leq \tau K_r \left(\left\||u_*(t_n)|^2 u_*(t_n) - |u_*^n|^2 u_*^n\right\|_r + 2\left\||v_*(t_n)|^2 u_*(t_n) - |v_*^n|^2 u_*^n\right\|_r \right) \\
&\leq \tau K_r \big(F_1 + 2F_2\big).
\end{aligned}
\tag{2.49}
$$

We estimate F_1 as follows

$$
\begin{aligned}
F_1 &= \big\||u_*(t_n)|^2 u_*(t_n) - |u_*^n|^2 u_*^n\big\|_r \\
&= \big\|u_*(t_n)\overline{u_*}(t_n)u_*(t_n) - u_*^n\overline{u_*^n}u_*^n\big\|_r \\
&= \big\|u_*(t_n)\big(\overline{u_*}(t_n)u_*(t_n)\big) - u_*^n\big(\overline{u_*}(t_n)u_*(t_n)\big) + u_*^n\big(\overline{u_*}(t_n)u_*(t_n)\big) - \big(u_*^n\overline{u_*^n}\big)u_*(t_n) \\
&\qquad + \big(u_*^n\overline{u_*^n}\big)u_*(t_n) - \big(u_*^n\overline{u_*^n}\big)u_*^n\big\|_r \\
&= \big\|\big(u_*(t_n) - u_*^n\big)\big(\overline{u_*}(t_n)u_*(t_n)\big) + \big(u_*^n u_*(t_n)\big)\big(\overline{u_*}(t_n) - \overline{u_*^n}\big) + \big(u_*^n\overline{u_*^n}\big)\big(u_*(t_n) - u_*^n\big)\big\|_r \\
&\leq \big\|u_*(t_n) - u_*^n\big\|_r \left(\big\|u_*(t_n)\big\|_r^2 + \big\|u_*(t_n)u_*^n\big\|_r + \big\|u_*^n\big\|_r^2\right).
\end{aligned}
$$

With the aid of (2.46) we find

$$
F_1 \leq K_{r,M}\big\|u_*(t_n) - u_*^n\big\|_r.
$$

Now, we estimate F_2 and using (2.46) we obtain the following bound for F_2

$$
\begin{aligned}
F_2 &= \big\||v_*(t_n)|^2 u_*(t_n) - |v_*^n|^2 u_*^n\big\|_r \\
&= \big\|v_*(t_n)\overline{v_*}(t_n)u_*(t_n) - v_*^n\overline{v_*^n}u_*^n\big\|_r \\
&= \big\|v_*(t_n)\overline{v_*}(t_n)u_*(t_n) - v_*^n\overline{v_*}(t_n)u_*(t_n) + v_*^n\overline{v_*}(t_n)u_*(t_n) - v_*^n\overline{v_*^n}u_*(t_n) + v_*^n\overline{v_*^n}u_*(t_n) - v_*^n\overline{v_*^n}u_*^n\big\|_r \\
&\leq \big\|\big(v_*(t_n) - v_*^n\big)\overline{v_*}(t_n)u_*(t_n) + \big(\overline{v_*(t_n)} - \overline{v_*^n}\big)v_*^n u_*(t_n) + \big(u_*(t_n) - u_*^n\big)v_*^n\overline{v_*^n}\big\|_r \\
&\leq K_{r,M}\left(\big\|u_*(t_n) - u_*^n\big\|_r + \big\|v_*(t_n) - v_*^n\big\|_r\right).
\end{aligned}
$$

Inserting the estimates of F_1 and F_2 into (2.49) and exploiting (2.47), yields

$$
\begin{aligned}
\big\|E_2 - N_2\big\|_r &\leq \tau K_{r,M}\left(\big\|u_*(t_n) - u_*^n\big\|_r + \big\|v_*(t_n) - v_*^n\big\|_r\right) \\
&\leq (1 + \tau K_{r,M})\left(\big\|u_*(t_n) - u_*^n\big\|_r + \big\|v_*(t_n) - v_*^n\big\|_r\right) \\
&\leq \mathrm{e}^{\tau K_{r,M}}\left(\big\|u_*(t_n) - u_*^n\big\|_r + \big\|v_*(t_n) - v_*^n\big\|_r\right).
\end{aligned}
\tag{2.50}
$$

Next, we take the difference of E_3 and N_3. We use that $\mathrm{e}^{i\tau\mathcal{A}_c}$, $\mathrm{e}^{-i\ell c^2 t}$ are linear isometries for all $t \in \mathbb{R}$ and $\ell \in \mathbb{R}$. We use (2.43) and $\|c\langle\nabla\rangle^{-1}\|_r \leq 1$ such that we obtain

$$
\begin{aligned}
\|E_3 - N_3\|_r \leq \tau K_r\Big(&\big\|(u_*(t_n))^2 v_*(t_n) - (u_*^n)^2 v_*^n\big\|_r + \big\|(\overline{v_*}(t_n))^2\overline{u_*}(t_n) - (\overline{v_*^n})^2\overline{u_*^n}\big\|_r \\
&+ \big\|\big(2|u_*(t_n)|^2 + |v_*(t_n)|^2\big)\overline{v_*}(t_n) - \big(2|u_*^n|^2 + |v_*^n|^2\big)\overline{v_*^n}\big\|_r\Big).
\end{aligned}
$$

With similar estimates as for F_1 , F_2 and with (2.47), we have that

$$\|E_3 - N_3\|_r \le \mathrm{e}^{\tau K_{r,M}} \Big(\big\|u_*(t_n) - u_*^n\big\|_r + \big\|v_*(t_n) - v_*^n\big\|_r \Big). \tag{2.51}$$

Combining the bounds (2.48), (2.50), and (2.51), we obtain that as long as (2.46) holds, that we have

$$\|\Phi^\tau_{u_*}(u_*(t_n), v_*(t_n)) - \Phi^\tau_{u_*}(u_*^n, v_*^n)\|_r \le \mathrm{e}^{\tau K_{r,M}} \Big(\|u_*(t_n) - u_*^n\|_r + \|v_*(t_n) - v_*^n\|_r \Big). \tag{2.52}$$

Analogously we can show that a similar bound holds for v_*, i.e.

$$\|\Phi^\tau_{v_*}(u_*(t_n), v_*(t_n)) - \Phi^\tau_{v_*}(u_*^n, v_*^n)\|_r \le \mathrm{e}^{\tau K_{r,M}} \Big(\|u_*(t_n) - u_*^n\|_r + \|v_*(t_n) - v_*^n\|_r \Big). \tag{2.53}$$

Global error bound: Plugging the stability bounds (2.52) and (2.53) as well as the local error bound (2.42) into (2.41) yields that the global error at time $t_{n+1} = t_n + \tau$ satisfies

$$\left\| \begin{pmatrix} u_*(t_{n+1}) - u_*^{n+1} \\ v_*(t_{n+1}) - v_*^{n+1} \end{pmatrix} \right\|_r \le \mathrm{e}^{\tau K_{r,M}} \left\| \begin{pmatrix} u_*(t_n) - u_*^n \\ v_*(t_n) - v_*^n \end{pmatrix} \right\|_r + \tau^2 k_{r,M_2}.$$

Iteratively applying the above local error and stability bounds implies that

$$\begin{aligned} \left\| \begin{pmatrix} u_*(t_{n+1}) - u_*^{n+1} \\ v_*(t_{n+1}) - v_*^{n+1} \end{pmatrix} \right\|_r &\le \mathrm{e}^{\tau K_{r,M}} \left\| \begin{pmatrix} u_*(t_n) - u_*^n \\ v_*(t_n) - v_*^n \end{pmatrix} \right\|_r + \tau^2 k_{r,M_2} \\ &\le \mathrm{e}^{\tau K_{r,M}} \left(\mathrm{e}^{\tau K^1_{r,M}} \left\| \begin{pmatrix} u_*(t_{n-1}) - u_*^{n-1} \\ v_*(t_{n-1}) - v_*^{n-1} \end{pmatrix} \right\|_r + \tau^2 k_{r,M_2} \right) + \tau^2 k_{r,M_2}. \end{aligned}$$

Using iteratively (2.42), (2.52) and (2.53) we have

$$\begin{aligned} \left\| \begin{pmatrix} u_*(t_{n+1}) - u_*^{n+1} \\ v_*(t_{n+1}) - v_*^{n+1} \end{pmatrix} \right\|_r &\le \mathrm{e}^{n\tau \sup_n K^n_{r,M}} \left(\left\| \begin{pmatrix} u_*(0) - u_*^0 \\ v_*(0) - v_*^0 \end{pmatrix} \right\| \right) + \mathrm{e}^{n\tau \sup_n K^n_{r,M}} n\tau^2 k_{r,M_2} \\ &= \mathrm{e}^{T \sup_n K^n_{r,M}} \left(\left\| \begin{pmatrix} u_*(0) - u_*^0 \\ v_*(0) - v_*^0 \end{pmatrix} \right\| \right) + \mathrm{e}^{T \sup_n K^n_{r,M}} T\tau k_{r,M_2}. \end{aligned}$$

Hence, we obtain the following bound by a *Lady Winderemere's fan* argument (see, e.g. [35, 50])

$$\|u_*(t_n) - u_*^n\|_r + \|v_*(t_n) - v_*^n\|_r \ \le \tau K_{r,M_2} \mathrm{e}^{T K_{r,M}} \le \tau K^*_{r,T,M,M_2}, \tag{2.54}$$

where the constant K^*_{r,T,M,M_2} is independent of c. This implies first-order convergence of (u_*^n, v_*^n) towards $(u_*(t_n), v_*(t_n))$ uniformly in c. Furthermore, by (2.6) and (2.24) we have

$$\begin{aligned} \|z(t_n) - z^n\|_r &= \left\| \tfrac{1}{2}\big(u(t_n) + \overline{v(t_n)}\big) - \tfrac{1}{2}\big(\mathrm{e}^{ic^2 t_n}\ u_*^n + \mathrm{e}^{-ic^2 t_n}\ \overline{v_*^n}\big) \right\|_r \\ &\le \left\| \mathrm{e}^{ic^2 t_n} \big(u_*(t_n) - u_*^n\big) \right\|_r + \left\| \mathrm{e}^{ic^2 t_n} \big(v_*(t_n) - v_*^n\big) \right\|_r \\ &= \|u_*(t_n) - u_*^n\|_r + \|v_*(t_n) - v_*^n\|_r. \end{aligned}$$

Together with the bounds in (2.54) this completes the proof. □

Remark 2.14. Note that the regularity assumption (2.40) is satisfied for initial values

$$z(0,x) = z_0(x), \qquad \partial_t z(0,x) = c^2 z_1(x) \qquad \text{with} \quad z_0, z_1 \in H^{r+2}.$$

Thanks to (2.30) we have as a consequence

$$\big\|c^{-1} \langle\nabla\rangle_c^{-1} \partial_t z(0)\big\|_r = \big\|c \langle\nabla\rangle_c^{-1} z_1\big\|_r \le \|z_1\|_r.$$

Under weaker regularity assumptions on the exact solution we obtain *uniform fractional convergence* of the formally first-order scheme (2.39).

Theorem 2.15 (Fractional convergence bound for the first-order scheme, cf. Theorem 13 in [13])**.** *Fix $r > d/2$ and assume that for some $0 < \gamma \leq 1$*

$$\|z(0)\|_{r+2\gamma} + \|c^{-1}\langle\nabla\rangle_c^{-1}\partial_t z(0)\|_{r+2\gamma} \ \leq M_{2\gamma} \tag{2.55}$$

uniformly in c. For (u_*^n, v_*^n) defined in (2.39) we set

$$z^n \ := \frac{1}{2}\left(\mathrm{e}^{ic^2 t_n} u_*^n + \mathrm{e}^{-ic^2 t_n}\overline{v_*^n}\right).$$

Then, there exists $T > 0$ and $\tau_0 > 0$ such that for all $\tau \leq \tau_0$ and $t_n \leq T$ we have for all $c > 0$ that

$$\|z(t_n) - z^n\|_r \ \leq \tau^\gamma K^*_{r,T,M,M_{2\gamma}},$$

where the constant $K^*_{r,T,M,M_{2\gamma}}$ can be chosen independently of c.

Proof. The proof follows the same steps as in the proof of Theorem 2.13 using "fractional estimates" of the operator $\mathcal{A}_c$.
Fix $r > d/2$ and $0 < \gamma \leq 1$. Firstly, note that similarly to Lemma 2.5 we obtain that

$$\|\mathcal{A}_c^\gamma f\|_r \leq 2^{-\gamma}\|f\|_{r+2\gamma}.$$

Furthermore, as $\left|\mathrm{e}^{ix} - 1\right| \leq 2|x|^\gamma$ for all $x \in \mathbb{R}$ we have that

$$\left\|\left(\mathrm{e}^{-it\mathcal{A}_c} - 1\right) f\right\|_r \leq 2\|\mathcal{A}_c^\gamma f\|_r \leq 2^{1-\gamma}|t|^\gamma\|f\|_{r+2\gamma}.$$

In particular, Duhamel's formula (2.26) together with the bound in (2.30) yields for $r > d/2$ that

$$\|u_*(t_n+s) - u_*(t_n)\|_r + \|v_*(t_n+s) - v_*(t_n)\|_r \leq |s|^\gamma\left(\|\mathcal{A}_c^\gamma u_*(t_n)\|_r + \|\mathcal{A}_c^\gamma v_*(t_n)\|\right) + |s|(1+M_0)^3.$$

The above bounds imply the corresponding fractional estimates of Lemma 2.5, 2.6, and 2.7. With these fractional error bounds, the proof then follows the same steps as in the proof of Theorem 2.13. □

Next, we point out the interesting observation, that for sufficiently smooth solutions the exponential-type integration scheme (2.39) converges in the limit $c \ \to \infty$ to the classical Lie splitting of the corresponding nonlinear Schrödinger limit (2.2).

Remark 2.16 (Approximation in the non-relativistic limit $c \to \infty$)**.** The exponential-type integration scheme (2.39) converges, for sufficiently smooth solutions, in the limit $(u_*^n, v_*^n) \overset{c\to\infty}{\longrightarrow} (u_{*,\infty}^n, v_{*,\infty}^n)$, essentially to the Lie Splitting (see [25, 50])

$$\begin{aligned} u_{*,\infty}^{n+1} &= \mathrm{e}^{-i\tau\frac{\Delta}{2}}\mathrm{e}^{-i\tau\frac{1}{8}\left(|u_{*,\infty}^n|^2+2|v_{*,\infty}^n|^2\right)}u_{*,\infty}^n, & u_{*,\infty}^0 &= z_0 - iz_1,\\ v_{*,\infty}^{n+1} &= \mathrm{e}^{-i\tau\frac{\Delta}{2}}\mathrm{e}^{-i\tau\frac{1}{8}\left(|v_{*,\infty}^n|^2+2|u_{*,\infty}^n|^2\right)}v_{*,\infty}^n, & v_{*,\infty}^0 &= \overline{z_0} - i\overline{z_1} \end{aligned} \tag{2.56}$$

applied to the cubic nonlinear Schrödinger system (2.2) which is the limit system of the Klein–Gordon equation (2.1) for $c \to \infty$ with initial values

$$z(0) \overset{c\to\infty}{\longrightarrow} z_0 \quad \text{and} \quad c^{-1}\langle\nabla\rangle_c^{-1}\partial_t z(0) \overset{c\to\infty}{\longrightarrow} z_1.$$

More precisely, the following Lemma holds.

Lemma 2.17 (cf. Lemma 15 in [13]). *Fix $r > d/2$ and let $0 < \delta \leq 2$. Assume that*

$$\|z(0)\|_{r+2\delta+\varepsilon} + \|c^{-1}\langle\nabla\rangle_c^{-1}\partial_t z(0)\|_{r+2\delta+\varepsilon} \leq M_{2\delta+\varepsilon} \tag{2.57}$$

for some $\varepsilon > 0$ uniformly in c and suppose that the initial value approximation (there exist functions z_0, z_1 such that)

$$\|z(0) - z_0\|_r + \|c^{-1}\langle\nabla\rangle_c^{-1}\partial_t z(0) - z_1\|_r \leq k_r c^{-\delta} \tag{2.58}$$

holds for some constant k_r independent of c.
Then, there exists $T > 0$ and $\tau_0 > 0$ such that for all $\tau \leq \tau_0$ the difference of the first-order scheme (2.39) for system (2.25) and the Lie splitting (2.56) for the limit Schrödinger equation (2.2) satisfies for $t_n \leq T$ and all $c > 0$ with

$$\tau c^{2-\delta} \geq 1 \tag{2.59}$$

that

$$\|u_*^n - u_{*,\infty}^n\|_r + \|v_*^n - v_{*,\infty}^n\|_r \leq c^{-\delta} k_{r,T,M_{2\delta+\varepsilon}},$$

for some constant $k_{r,T,M_{2\delta+\varepsilon}}$ that depends on $M_{2\delta+\varepsilon}$ and T, but is independent of c.

Proof. In the following fix $r > d/2$, $0 < \delta \leq 2$ and $\varepsilon > 0$:
1. Initial value approximation: Thanks to (2.58) and to the definition of the initial value u_*^0 in (2.39), respectively, $u_{*,\infty}^0$ in (2.56), we have that

$$\|u_*^0 - u_{*,\infty}^0\|_r = \|z(0) - ic^{-1}\langle\nabla\rangle_c^{-1}\ \partial_t z(0) - (z_0 - iz_1)\|_r \leq k_r c^{-\delta},$$

for some constant k_r independent of c. A similar bound holds for $v_*^0 - v_{*,\infty}^0$.
2. Regularity of the numerical solutions (u_*^n, v_*^n): Thanks to the regularity assumption (2.57) we have by Theorem 2.15 that there exists a $T > 0$ and $\tau_0 > 0$ such that for all $\tau \leq \tau_0$ we have

$$\|u_*^n\|_{r+2\delta} + \|v_*^n\|_{r+2\delta} \leq m_{2\delta} \tag{2.60}$$

as long as $t_n \leq T$ for some constant $m_{2\delta}$ depending on $M_{2\delta+\varepsilon}$ and T, but not on c.
3. Regularity of the numerical solutions $(u_{*,\infty}^n, v_{*,\infty}^n)$: Thanks to the regularity assumption (2.57) and due to the assumption on the initial data (2.58), the global first-order convergence result of the Lie splitting for semilinear Schrödinger equations (see for instance [25, 50]) implies that there exists a $T > 0$ and $\tau_0 > 0$ such that for all $\tau \leq \tau_0$ we have

$$\|u_{*,\infty}^n\|_r + \|v_{*,\infty}^n\|_r \leq m_0 \tag{2.61}$$

as long as $t_n \leq T$ for some constant m_0, which depends on M_r and T, but not on c.
4. Approximations: Using the following bounds

$$\left|\sqrt{1+x^2} - 1 - \frac{1}{2}x^2\right| \leq x^{2\gamma} \quad \text{and} \quad \left|\frac{1}{\sqrt{1+x^2}} - 1\right| \leq x^{2\gamma-2}, \quad \text{for } \gamma > 1.$$

Together with the Definition of φ_1 (see Definition 2.8) we have for every $f \in H^{r+2+2\delta}$,

$$\left\| \left(\mathcal{A}_c + \tfrac{\Delta}{2}\right) f\right\|_r + \left\| \left(c\langle\nabla\rangle_c^{-1} - 1\right) f\right\|_{r+2} + \left\|\varphi_1(i\ell c^2\tau) f\right\|_{r+2+\delta} \leq k_r c^{-\delta}\ \|f\|_{r+2+2\delta}, \tag{2.62}$$

for $\ell = \pm 2, -4$ and for some constant k_r independent of c. For the last estimate we used (2.59).

5. Difference of the numerical solutions: Thanks to the a priori regularity of the numerical solutions (2.60) and (2.61) we obtain with the aid of (2.62) under assumption (2.59) for the difference $u_*^n - u_{*,\infty}^n$ that

$$\begin{aligned}\left\|u_*^{n+1} - u_{*,\infty}^{n+1}\right\|_r &\leq \big(1 + \tau k(m_0)\big)\left\|u_*^n - u_{*,\infty}^n\right\|_r + (c^{-2+\delta} + \tau)c^{-\delta} k(m_{2\delta}) \\ &\leq \big(1 + \tau k(m_0)\big)\left\|u_*^n - u_{*,\infty}^n\right\|_r + 2\tau c^{-\delta} k(m_{2\delta})\end{aligned}$$

and a similar bound on $v_*^n - v_{*,\infty}^n$. Resolving the recursion yields the assertion. □

2.3.2.3 Simplifications in the "Weakly to Strongly non-relativistic Limit Regime"

In the strongly non-relativistic limit regime, i.e., for large values of c, we may simplify the first-order scheme (2.39) and nevertheless obtain a well suited, first-order approximation to (u_*, v_*) in (2.25).

Remark 2.18. Note that for $\ell = \pm 2, -4$ and $c > 0$ we have (see Definition 2.8)

$$\left\|\tau \varphi_1(i\ell c^2 \tau)\right\|_r = \left\|\frac{\mathrm{e}^{i\ell c^2 \tau} - 1}{i\ell c^2}\right\|_r \leq \frac{\|\mathrm{e}^{i\ell c^2\tau}\|_r + \|1\|_r}{\|\ell c^2\|_r} \leq \frac{1+1}{c^2} = 2c^{-2}.$$

Furthermore, (2.62) yields that

$$\|\left(c\langle\nabla\rangle_c^{-1} - 1\right) u_*(t)\|_r \leq c^{-2}\, k_r \|u_*(t)\|_{r+2},$$

for some constant k_r independent of c. Thus, for sufficiently large values of c, more precisely if

$$\tau c > 1,$$

and under the same regularity assumption (2.55) we may take instead of (2.39) the scheme

$$\begin{aligned}u_{*,c>\tau}^{n+1} &= \mathrm{e}^{i\tau \mathcal{A}_c} \mathrm{e}^{-i\tau \frac{1}{8}\left(|u_{*,c>\tau}^n|^2 + 2|v_{*,c>\tau}^n|^2\right)} u_{*,c>\tau}^n, \\ v_{*,c>\tau}^{n+1} &= \mathrm{e}^{i\tau \mathcal{A}_c} \mathrm{e}^{-i\tau \frac{1}{8}\left(|v_{*,c>\tau}^n|^2 + 2|u_{*,c>\tau}^n|^2\right)} v_{*,c>\tau}^n\end{aligned}$$

as a first-order numerical approximation to $\big(u_*(t_{n+1}), v_*(t_{n+1})\big)$ in (2.25).

However, note that in the strongly non-relativistic limit regime (such that in particular $c\tau \gg 1$) we may immediately take the Lie splitting scheme proposed in [26] as a suitable first-order approximation to (2.25) thanks to the following observation:

Remark 2.19 (Limit scheme [26])**.** For sufficiently large values of c and sufficiently smooth solutions, i.e., if

$$\|z(0)\|_{r+2} + \|c^{-1}\langle\nabla\rangle_c^{-1}\partial_t z(0)\|_{r+2} \leq M_2 \quad \text{and} \quad \tau c > 1,$$

the classical Lie splitting scheme (see [25, 50]) for the nonlinear Schrödinger limit equation (2.2)

$$\begin{aligned}u_{*,\infty}^{n+1} &= \mathrm{e}^{-i\tau\frac{1}{2}\Delta} \mathrm{e}^{-i\tau\frac{1}{8}\left(|u_{*,\infty}^n|^2 + 2|v_{*,\infty}^n|^2\right)} u_{*,\infty}^n, \\ v_{*,\infty}^{n+1} &= \mathrm{e}^{-i\tau\frac{1}{2}\Delta} \mathrm{e}^{-i\tau\frac{1}{8}\left(|v_{*,\infty}^n|^2 + 2|u_{*,\infty}^n|^2\right)} v_{*,\infty}^n\end{aligned}$$

yields a first-order numerical approximation to $(u_*(t_{n+1}), v_*(t_{n+1}))$ in (2.25).

This assertion follows from [26] thanks to the approximation

$$\|u_*(t_n) - u_{*,\infty}^n\|_r \leq \|u_*(t_n) - u_{*,\infty}(t_n)\|_r + \|u_{*,\infty}(t_n) - u_{*,\infty}^n\|_r = \mathcal{O}\big(c^{-2} + \tau\big),$$

and a similar bound on $v_*(t_n) - v_{*,\infty}^n$.

2.3.3 Construction of a Second-Order Uniformly Accurate Scheme

In this section we derive a second-order exponential-type integration scheme for the solutions (u_*, v_*) of (2.25) which allows *second-order time-convergence uniform with respect to c*. For notational simplicity we assume that z is real, i.e. $z(t,x) \in \mathbb{R}$, which reduces the coupled system (2.25) to equation (2.31) with mild-solutions (2.32) (see also Remark 2.1).
The construction of the second-order scheme is again based on Duhamel's formula (2.32) and the essential estimates in Lemma 2.5, 2.6 and 2.7. However, the construction of a second-order approximation is much more involved due to the fact that

$$u_*'(t) = \mathcal{O}(1), \quad \text{but} \quad u_*''(t) = \mathcal{O}(c^2).$$

The latter observation prevents us from simply applying the higher-order Taylor series expansion

$$u_*(t_n + s) = u_*(t_n) + s u_*'(t_n) + \mathcal{O}\big(s^2 u_*''(t_n + \xi)\big)$$

in Duhamel's formula (2.32) as this would lead to the "classical" $c-$dependent error at order $\mathcal{O}(\tau^2 c^2)$. Therefore, we need to carry out a much more careful frequency analysis by iterating Duhamel's formula (2.32) twice and controlling the appearing highly oscillatory terms $\mathrm{e}^{\pm ic^2 t}$ and their interactions $\mathrm{e}^{i\ell c^2 t}$ $(\ell \in \mathbb{Z})$ precisely.

2.3.3.1 Construction of a Second-Order Uniformly Accurate Scheme

In this subsection we state the necessary regularity assumptions on the solution u_* and derive two useful expansions. Moreover, we collect some useful lemmata on highly oscillatory integrals and their approximations. These approximations then allow us to construct a uniformly accurate second-order scheme. The rigorous convergence analysis is given in Section 2.3.3.2.

Regularity and expansion of the exact solution

In order to derive a second-order scheme, we need to impose additional regularity on the exact solution $u_*(t)$ of (2.31).

Assumption 2.20. *Fix $r > d/2$ and assume that $u_* \in \mathcal{C}([0,T]; H^{r+4}(\mathbb{T}^d))$ and in particular*

$$\sup_{0 \le t \le T} \|u_*(t)\|_{r+4} \le M_4,$$

where M_4 can be bounded uniformly in c.

In Lemma 2.23 below we derive two useful expansions of the exact solution u_* of (2.31). For this purpose we introduce the following definition.

Definition 2.21. *For some function v and $t_n, t \in \mathbb{R}$ we set*

$$\begin{aligned} \Psi_{c^2}(t_n, t, v) :=& \frac{1}{2ic^2}\left(\mathrm{e}^{2ic^2(t_n+t)} - \mathrm{e}^{2ic^2 t_n}\right) v^3 + \frac{3}{-2ic^2}\left(\mathrm{e}^{-2ic^2(t_n+t)} - \mathrm{e}^{-2ic^2 t_n}\right) |v|^2 \overline{v} \\ &+ \frac{1}{-4ic^2}\left(\mathrm{e}^{-4ic^2(t_n+t)} - \mathrm{e}^{-4ic^2 t_n}\right) \overline{v}^3 \\ =& t\mathrm{e}^{2ic^2 t_n}\varphi_1\left(2ic^2 t\right) v^3 + 3t\mathrm{e}^{-2ic^2 t_n}\varphi_1\left(-2ic^2 t\right)|v|^2\overline{v} + t\mathrm{e}^{-4ic^2 t_n}\varphi_1\left(-4ic^2 t\right)\overline{v}^3. \end{aligned} \tag{2.63}$$

Remark 2.22. With the above definition, the first-order scheme (2.39) for real valued z, i.e. for $u_* = v_*$, may be written in compact form as

$$u_*^{n+1} = \mathrm{e}^{i\tau\mathcal{A}_c}\Big(\mathrm{e}^{-i\tau\frac{3}{8}|u_*^n|^2}u_*^n + \tau\frac{3i}{8}|u_*^n|^2u_*^n\Big) - \frac{i}{8}c\langle\nabla\rangle_c^{-1}\,\mathrm{e}^{i\tau\mathcal{A}_c}\Big(\Psi_{c^2}(t_n,\tau,u_*^n) + 3\tau|u_*^n|^2u_*^n\Big).$$

Furthermore, Defintion 2.21 allows us the following expansions of the exact solution u_*.

Lemma 2.23 (cf. Lemma 20 in [13])**.** *Fix $r > d/2$. Then the exact solution of (2.31) satisfies the expansions*

$$\begin{aligned}u_*(t_n+s) = \mathrm{e}^{is\mathcal{A}_c}u_*(t_n) &- \frac{3i}{8}c\langle\nabla\rangle_c^{-1}\int_0^s \mathrm{e}^{i(s-\xi)\mathcal{A}_c}\left|\mathrm{e}^{i\xi\mathcal{A}_c}u_*(t_n)\right|^2\left(\mathrm{e}^{i\xi\mathcal{A}_c}u_*(t_n)\right)\mathrm{d}\xi\\ &- \frac{i}{8}c\langle\nabla\rangle_c^{-1}\Psi_{c^2}(t_n,s,u_*(t_n)) + \mathcal{R}_1(t_n,s,u_*)\end{aligned}$$

and

$$u_*(t_n+s) = \mathrm{e}^{is\mathcal{A}_c}u_*(t_n) - \frac{i}{8}c\langle\nabla\rangle_c^{-1}\Big(3s\left|u_*(t_n)\right|^2u_*(t_n) + \Psi_{c^2}(t_n,s,u_*(t_n))\Big) + \mathcal{R}_2(t_n,s,u_*)$$

with Ψ_{c^2} defined in (2.63). The remainders satisfy

$$\|\mathcal{R}_1(t_n,s,u_*)\|_r + \|\mathcal{R}_2(t_n,s,u_*)\|_r \le s^2k_{r,M_2},$$

for some constant k_{r,M_2} which depends on M_2, but is independent of c.

Proof. Note that by Duhamel's perturbation formula (2.32) we have that

$$\begin{aligned}u_*(t_n+s) = \mathrm{e}^{is\mathcal{A}_c}u_*(t_n) - \frac{i}{8}c\langle\nabla\rangle_c^{-1}\int_0^s \mathrm{e}^{i(s-\xi)\mathcal{A}_c}\Big(3\left|u_*(t_n+\xi)\right|^2u_*(t_n+\xi) + \mathrm{e}^{2ic^2(t_n+\xi)}u_*(t_n+\xi)^3\\ +3\mathrm{e}^{-2ic^2(t_n+\xi)}\left|u_*(t_n+\xi)\right|^2\overline{u_*}(t_n+\xi) + \mathrm{e}^{-4ic^2(t_n+\xi)}\overline{u_*}(t_n+\xi)^3\Big)\mathrm{d}\xi.\end{aligned}$$

Therefore, the bound on $c\langle\nabla\rangle_c^{-1}$ given in (2.30) in particular implies that for $\xi \in \mathbb{R}$

$$\|u_*(t_n+\xi) - \mathrm{e}^{i\xi\mathcal{A}_c}u_*(t_n)\|_r \le \xi k_r(1+M_0)^3,$$

for some constant k_r which is independent of c. Together with Lemma 2.6 and 2.7 the assertion then follows by integrating the highly oscillatory phases $\mathrm{e}^{\pm i\ell c^2\xi}$ exactly. □

In the next section we collect important definitions and useful lemmata on highly oscillatory integrals.

Preliminary lemmata on highly oscillatory integrals

The construction of a second-order approximation to u_* based on the iteration of Duhamel's formula (2.32) that holds uniformly in all $c > 0$ leads to interactions of the highly oscillatory phases e^{ic^2t}. More precisely, we need to handle highly oscillatory integrals of type

$$\int_0^\tau \mathrm{e}^{is(\delta c^2-\mathcal{A}_c)}\left(\mathrm{e}^{is\mathcal{A}_c}v\right)^\ell\left(\mathrm{e}^{-is\mathcal{A}_c}\overline{v}\right)^m\mathrm{d}s, \qquad \delta \in \{-4,-2,2\}. \tag{2.64}$$

In order to control these integrals, we first need to distinguish the non-resonant case $\delta \in \{-4,-2\}$ where

$$\forall c > 0,\, k \in \mathbb{N}: \quad (\delta c^2 - \mathcal{A}_c)_k = \delta c^2 - c\sqrt{c^2+k^2} + c^2 \neq 0$$

from the resonant case $\delta = 2$ in which the operator $\delta c^2 - \mathcal{A}_c$ may become singular.
In Lemma 2.24 we outline how to control the non-resonant case $\delta \in \{-4, -2\}$. Lemma 2.26 treats the resonant case $\delta = 2$.

Lemma 2.24 (cf. Lemma 21 in [13]). *Fix $r > d/2$ and assume that $v \in \mathcal{C}\left([0, T]; H^{r+4}(\mathbb{T}^d)\right)$. Then we have $\delta_1 = -2$ and $\delta_2 = -4$ that for $j = 1, 2$ and $\ell, m \in \mathbb{N}^*$,*

$$\begin{aligned}\int_0^\tau \mathrm{e}^{is(\delta_j c^2 - \mathcal{A}_c)} \left(\mathrm{e}^{is\mathcal{A}_c} v\right)^\ell \left(\mathrm{e}^{-is\mathcal{A}_c} \overline{v}\right)^m \mathrm{d}s = \tau\varphi_1\left(i\tau(\delta_j c^2 - \mathcal{A}_c)\right) v^\ell \overline{v}^m \\ + i\tau^2 \Psi_2\left(i\tau(\delta_j c^2 - \mathcal{A}_c)\right) \left(\ell v^{\ell-1} \overline{v}^m \mathcal{A}_c v - m v^\ell \overline{v}^{m-1} \mathcal{A}_c \overline{v}\right) \\ + \mathcal{R}(t_n, s, v),\end{aligned} \tag{2.65}$$

where the remainder satisfies

$$\|\mathcal{R}(t_n, s, v)\|_r \le k_r \tau^3 \|v\|_{r+4} \|v\|_r^{\ell+m-1}, \tag{2.66}$$

for some constant k_r which is independent of c.

Proof. By Taylor series expansion of $\mathrm{e}^{is\mathcal{A}_c}$ and from (2.27) we obtain that

$$\begin{aligned}\int_0^\tau \mathrm{e}^{-is\mathcal{A}_c} \mathrm{e}^{i\delta_j c^2 s} \left(\mathrm{e}^{is\mathcal{A}_c} v\right)^\ell \left(\mathrm{e}^{-is\mathcal{A}_c} \overline{v}\right)^m \mathrm{d}s = \int_0^\tau \mathrm{e}^{is(\delta_j c^2 - \mathcal{A}_c)} \left(v^\ell \overline{v}^m + is\left(\ell v^{\ell-1} \overline{v}^m \mathcal{A}_c v - m v^\ell \overline{v}^{m-1} \mathcal{A}_c \overline{v}\right)\right) \mathrm{d}s \\ + \mathcal{R}(t_n, s, v),\end{aligned}$$

where thanks to (2.27) we have for $r > d/2$ that (2.66) holds for the remainder $\mathcal{R}(t_n, s, v)$. The assertion then follows by the definition of the φ_j and Ψ_j functions given in Definition 2.8. □

As the construction of our numerical scheme is based on the approximation in (2.65) we need to guarantee that the constructed term

$$\tau^2 \Psi_2\left(i\tau(\delta_j c^2 - \mathcal{A}_c)\right) \left(\ell v^{\ell-1} \overline{v}^m \mathcal{A}_c v - m v^\ell \overline{v}^{m-1} \mathcal{A}_c \overline{v}\right)$$

is uniformly bounded with respect to c in H^r for all functions $v \in H^r$. This stability analysis is carried out in Remark 2.25 below, where we especially exploit the bilinear estimate (see (1.2))

$$\|vw\|_r \le k \|v\|_{r_1} \|w\|_{r_2} \quad \text{for all } r \le r_1 + r_2 - \tfrac{d}{2} \quad \text{with} \quad r_1, r_2, -r \ne \tfrac{d}{2} \quad \text{and} \quad r_1 + r_2 \ge 0. \tag{2.67}$$

Remark 2.25 (Stability in Lemma 2.24). Note that for $\delta_1 = -2$, respectively, $\delta_2 = -4$ we have that

$$0 \ne \delta_j c^2 - \mathcal{A}_c = \delta_j c^2 - c\langle\nabla\rangle_c + c^2 = \begin{cases} -(c^2 + c\langle\nabla\rangle_c) & \text{if } j = 1 \\ -(3c^2 + c\langle\nabla\rangle_c) & \text{if } j = 2 \end{cases}. \tag{2.68}$$

With

$$(\langle\nabla\rangle_c)_k = \sqrt{c^2 + |k|^2} \le \sqrt{c^2} + \sqrt{|k|^2} = c + |k|,$$

and

$$\frac{1}{c^2 + c\left(\langle\nabla\rangle_c\right)_k} \le \min\left\{|c|^{-2}, |c\sqrt{c^2 + k^2}|^{-1}\right\} \le \min\left\{|c|^{-2}, (c|k|)^{-1}\right\},$$

we obtain together with the bilinear estimate (2.67) and (2.68) that for $\delta_j = -2, -4$ we have

$$\begin{aligned}
\left\|\tau^2\Psi_2\left(i\tau(\delta_j c^2 - \mathcal{A}_c)\right)(v\mathcal{A}_c w)\right\|_r &= \tau\left\|\frac{\varphi_0(i\tau(\delta_j c^2 - \mathcal{A}_c)) - \varphi_1(i\tau(\delta_j c^2 - \mathcal{A}_c))}{(\delta_j c^2 - \mathcal{A}_c)}(v\mathcal{A}_c w)\right\|_r \\
&\leq 2\tau\left\|\frac{1}{(c^2 + c\langle\nabla\rangle_c)}(v\mathcal{A}_c w)\right\|_r \\
&\leq 2\tau\left\|\frac{1}{(c^2 + c\langle\nabla\rangle_c)}\left(v2c^2 w\right)\right\|_r + 2\tau\left\|\frac{1}{(c^2 + c\langle\nabla\rangle_c)}(vc\langle\nabla\rangle_c w)\right\|_r \\
&\leq 4k_r\tau\|v\|_r\|w\|_r,
\end{aligned} \tag{2.69}$$

for all $r > d/2$ and all functions $v, w \in H^r$, and some constant $k_r > 0$. The estimate (2.69) guarantees stability of our numerical scheme built on the approximation in (2.65).

A simple manipulation allows us to treat the resonant case, i.e., $\delta = 2$ in (2.64), similarly to Lemma 2.24.

Lemma 2.26 (cf. Lemma 23 in [13])**.** *Fix $r > d/2$, assume that $v \in \mathcal{C}([0,T]; H^{r+4}(\mathbb{T}^d))$ and let $c \neq 0$. Then we have that*

$$\begin{aligned}
\int_0^\tau \mathrm{e}^{is(2c^2 - \mathcal{A}_c)}\left(\mathrm{e}^{is\mathcal{A}_c}v\right)^\ell\left(\mathrm{e}^{-is\mathcal{A}_c}\overline{v}\right)^m \mathrm{d}s &= \tau\varphi_1\left(i\tau(2c^2 - \tfrac{1}{2}\Delta)\right)\left(v^\ell\overline{v}^m\right) \\
&\quad + i\tau^2\Psi_2\left(i\tau(2c^2 - \tfrac{1}{2}\Delta)\right)\left[\left(\tfrac{1}{2}\Delta - \mathcal{A}_c\right)\left(v^\ell\overline{v}^m\right) + \left(\ell v^{\ell-1}\overline{v}^m\mathcal{A}_c v - m v^\ell\overline{v}^{m-1}\mathcal{A}_c\overline{v}\right)\right] \\
&\quad + \mathcal{R}(t_n, s, v),
\end{aligned} \tag{2.70}$$

where the remainder satisfies

$$\|\mathcal{R}(t_n, s, v)\|_r \leq k_r\tau^3\|v\|_{r+4}\|v\|_r^{\ell+m-1}, \tag{2.71}$$

for some constant k_r which is independent of c.

Proof. Due to the identity

$$2c^2 - \mathcal{A}_c = 2c^2 - \tfrac{1}{2}\Delta + \tfrac{1}{2}\Delta - \mathcal{A}_c$$

we obtain

$$\begin{aligned}
\int_0^\tau \mathrm{e}^{is(2c^2 - \mathcal{A}_c)}\left(\mathrm{e}^{is\mathcal{A}_c}v\right)^\ell\left(\mathrm{e}^{-is\mathcal{A}_c}\overline{v}\right)^m \mathrm{d}s &= \int_0^\tau \mathrm{e}^{is(2c^2 - \frac{1}{2}\Delta)}\mathrm{e}^{is(\frac{1}{2}\Delta - \mathcal{A}_c)}\left(\mathrm{e}^{is\mathcal{A}_c}v\right)^\ell\left(\mathrm{e}^{-is\mathcal{A}_c}\overline{v}\right)^m \mathrm{d}s \\
= \int_0^\tau \mathrm{e}^{is(2c^2 - \frac{1}{2}\Delta)}\Big[\left(1 + is(\tfrac{1}{2}\Delta - \mathcal{A}_c)\right)\left(v^\ell\overline{v}^m\right) &+ is\left(\ell v^{\ell-1}\overline{v}^m\mathcal{A}_c v - m v^\ell\overline{v}^{m-1}\mathcal{A}_c\overline{v}\right)\Big]\mathrm{d}s + \mathcal{R}(t_n, s, v).
\end{aligned}$$

Thanks to (2.27) we have for $r > d/2$ that (2.71) holds for the remainder $\mathcal{R}$. The assertion then follows by the definition of the φ_j and Ψ_j functions given in Definition 2.8. □

Again, we need to verify that the term

$$\tau^2\Psi_2\left(i\tau(2c^2 - \tfrac{1}{2}\Delta)\right)\left[\left(\tfrac{1}{2}\Delta - \mathcal{A}_c\right)\left(v^\ell\overline{v}^m\right) + \left(\ell v^{\ell-1}\overline{v}^m\mathcal{A}_c v - m v^\ell\overline{v}^{m-1}\mathcal{A}_c\overline{v}\right)\right]$$

in (2.70) can be bounded uniformly with respect to c in H^r for all functions $v \in H^r$. This is done in the following remark.

Remark 2.27 (Stability in Lemma 2.26)**.** Note that the operator $2c^2 - \frac{1}{2}\Delta$ satisfies the bounds

$$\begin{aligned}
\frac{c|k|}{\left(2c^2 - \frac{1}{2}\Delta\right)_k} &= \frac{c|k|}{2c^2 + \frac{1}{2}|k|^2} \leq 2, \\
\frac{c^2}{\left(2c^2 - \frac{1}{2}\Delta\right)_k} &= \frac{c^2}{2c^2 + \frac{1}{2}|k|^2} \leq \frac{1}{2},
\end{aligned}$$

and furthermore

$$(\mathcal{A}_c)_k = c\sqrt{c^2+|k|^2} - c^2 \leq 2c^2 + c|k|.$$

The above estimates together with the bilinear estimate (2.67) imply that for $r > d/2$

$$\begin{aligned}
&\left\|\tau^2\Psi_2\left(i\tau(2c^2-\tfrac{1}{2}\Delta)\right)(v\mathcal{A}_c w)\right\|_r^2 \leq \tau\sum_k \frac{(1+|k|^2)^r}{(2c^2+\frac{1}{2}|k|^2)^2}\Big|\sum_{k=k_1+k_2} v_{k_1}(\mathcal{A}_c)_{k_2}w_{k_2}\Big|^2\\
&\leq \tau m_r\sum_k \frac{(1+|k|^2)^r c^4}{(2c^2+\frac{1}{2}|k|^2)^2}\Big(\sum_{k=k_1+k_2}|v_{k_1}||w_{k_2}|\Big)^2 + \tau m_r\sum_k \frac{(1+|k|^2)^r c^2}{(2c^2+\frac{1}{2}|k|^2)^2}\Big(\sum_{k=k_1+k_2}|v_{k_1}||k_2||w_{k_2}|\Big)^2\\
&\leq \tau m_r\sum_k(1+|k|^2)^r\Big(\sum_{k=k_1+k_2}|v_{k_1}||w_{k_2}|\Big)^2 + \tau m_r\sum_k(1+|k|^2)^{r-1}\Big(\sum_{k=k_1+k_2}|v_{k_1}||k_2||w_{k_2}|\Big)^2\\
&\leq \tau m_r\|v\|_r^2\|w\|_r^2 + \tau k_r\|v\|_r^2\|\partial_x w\|_{r-1}^2\\
&\leq \tau k m_r\|v\|_r^2\|w\|_r^2,
\end{aligned} \tag{2.72}$$

for some constant $m_r > 0$ which guarantees stability of the numerical method built on the approximation in Lemma 2.26.

Next, we need to analyze integrals involving the highly oscillatory function Ψ_{c^2} defined in (2.21). The following lemma yields a uniform approximation.

Lemma 2.28 (cf. Lemma 25 in [13]). *Fix $r > d/2$. Then for any polynomial $p(v)$ in v and $\overline{v}$ we have that*

$$\int_0^\tau \mathrm{e}^{i(\tau-s)\mathcal{A}_c}p\left(\mathrm{e}^{is\mathcal{A}_c}v\right)c\langle\nabla\rangle_c^{-1}\Psi_{c^2}(t_n,s,v)\mathrm{d}s = \tau^2 p(v)c\langle\nabla\rangle_c^{-1}\vartheta_{c^2}(t_n,\tau,v) + \mathcal{R}(t_n,\tau,v)$$

with

$$\begin{aligned}
\vartheta_{c^2}(t_n,\tau,v) &:= \mathrm{e}^{2ic^2t_n}\frac{\varphi_1\left(2ic^2\tau\right)-1}{2i\tau c^2}v^3 + 3\mathrm{e}^{-2ic^2t_n}\frac{\varphi_1\left(-2ic^2\tau\right)-1}{-2i\tau c^2}|v|^2\overline{v} + \mathrm{e}^{-4ic^2t_n}\frac{\varphi_1\left(-4ic^2\tau\right)-1}{-4i\tau c^2}\overline{v}^3\\
&= \mathrm{e}^{2ic^2t_n}\varphi_2\left(2i\tau c^2\right)v^3 + 3\mathrm{e}^{-2ic^2t_n}\varphi_2\left(-2i\tau c^2\right)|v|^2\overline{v} + \mathrm{e}^{-4ic^2t_n}\varphi_2\left(-4i\tau c^2\right)\overline{v}^3.
\end{aligned} \tag{2.73}$$

The remainder satisfies

$$\|\mathcal{R}(t_n,\tau,v)\|_r \leq k_r\tau^3\left(1+\|v\|_{r+2}\right)^5, \tag{2.74}$$

for some constant k_r independent of c.

Proof. Thanks to the approximation (2.28) and the fact that $\Psi_{c^2}(t_n,s,u_*(t_n))$ is of order one in s uniformly in c we have that

$$\int_0^\tau \mathrm{e}^{i(\tau-s)\mathcal{A}_c}p\left(\mathrm{e}^{is\mathcal{A}_c}v\right)c\langle\nabla\rangle_c^{-1}\Psi_{c^2}(t_n,s,v)\mathrm{d}s = p(v)\,c\langle\nabla\rangle_c^{-1}\int_0^\tau\Psi_{c^2}(t_n,s,v)\mathrm{d}s + \mathcal{R}(t_n,\tau,v),$$

where the remainder satisfies the bound (2.74) for $r > d/2$. □

Finally, we need to handle the interaction of highly oscillatory phases $\mathrm{e}^{i\ell c^2 t}$ with the highly oscillatory function Ψ_{c^2} defined in (2.21).

Lemma 2.29 (cf. Lemma 26 in [13]). *Let $c \neq 0$. Then, we have for $\ell \in \mathbb{N}$ that*

$$\begin{aligned}
\Omega_{c^2,\ell}(t_n,\tau,v) &:= \frac{1}{\tau^2}\int_0^\tau \mathrm{e}^{i\ell c^2 s}\Psi_{c^2}(t_n,s,v)\mathrm{d}s\\
&= \mathrm{e}^{2ic^2t_n}\frac{\varphi_1\left((\ell+2)ic^2\tau\right)-\varphi_1\left(\ell ic^2\tau\right)}{2i\tau c^2}v^3 + \mathrm{e}^{-4ic^2t_n}\frac{\varphi_1\left((\ell-4)ic^2\tau\right)-\varphi_1\left(\ell ic^2\tau\right)}{-4i\tau c^2}\overline{v}^3\\
&\quad + 3\mathrm{e}^{-2ic^2t_n}\frac{\varphi_1\left((\ell-2)ic^2\tau\right)-\varphi_1\left(\ell ic^2\tau\right)}{-2i\tau c^2}|v|^2\overline{v}
\end{aligned} \tag{2.75}$$

and that

$$\int_0^\tau \mathrm{e}^{i\ell c^2 s} s\mathrm{d}s = \tau^2 \ \Psi_2(i\ell c^2\tau).$$

Proof. Due to Definition 2.21 we have that

$$\mathrm{e}^{i\ell c^2 s}\Psi_{c^2}(t_n, s, v) = \mathrm{e}^{i\ell c^2 s}\Big(s\mathrm{e}^{2ic^2 t_n}\varphi_1(2ic^2 s)v^3 + 3s\mathrm{e}^{-2ic^2 t_n}\varphi_1(-2ic^2 s)|v|^2\overline{v} + s\mathrm{e}^{-4ic^2 t_n} s\varphi_1(-4ic^2 s)\overline{v}^3\Big)$$

which implies the assertion by the Definition 2.8 of φ_1 and Ψ_2. □

With the above lemmata we can commence the construction of the second-order uniformly accurate scheme.

Uniform second-order discretization of Duhamel's formula

Our starting point is again Duhamel's perturbation formula (see (2.32))

$$\begin{aligned} u_*(t_n+\tau) &= \mathrm{e}^{i\tau\mathcal{A}_c}u_*(t_n) \\ &\quad - \frac{i}{8}c\langle\nabla\rangle_c^{-1}\int_0^\tau \mathrm{e}^{i(\tau-s)\mathcal{A}_c}\mathrm{e}^{-ic^2(t_n+s)}\left(\mathrm{e}^{ic^2(t_n+s)}u_*(t_n+s) + \mathrm{e}^{-ic^2(t_n+s)}\overline{u_*}(t_n+s)\right)^3 \mathrm{d}s \end{aligned}$$

which we split into two parts by separating the linear and classical cubic part $|u_*|^2 u_*$ from the terms involving u_*^3, $\overline{u_*}^3$ and $|u_*|^2\overline{u_*}$. More precisely, we set

$$u_*(t_n+\tau) = I_*(\tau, t_n, u_*) - \frac{i}{8}c\langle\nabla\rangle_c^{-1} I_{c^2}(\tau, t_n, u_*) \tag{2.76}$$

with the linear as well as classical cubic part $|u_*|^2 u_*$ defined in I_*

$$I_*(\tau, t_n, u_*) := \mathrm{e}^{i\tau\mathcal{A}_c}u_*(t_n) - \frac{3i}{8}c\langle\nabla\rangle_c^{-1}\int_0^\tau \mathrm{e}^{i(\tau-s)\mathcal{A}_c}|u_*(t_n+s)|^2 u_*(t_n+s)\mathrm{d}s \tag{2.77}$$

and the terms involving $u_*^3, \overline{u_*}^3$ and $|u_*|^2\overline{u_*}$ defined in I_{c^2}

$$\begin{aligned} I_{c^2}(\tau, t_n, u_*) := \int_0^\tau \mathrm{e}^{i(\tau-s)\mathcal{A}_c}\Big(&\mathrm{e}^{2ic^2(t_n+s)}u_*^3(t_n+s) \\ &+ 3\mathrm{e}^{-2ic^2(t_n+s)}|u_*(t_n+s)|^2\overline{u_*}(t_n+s) + \mathrm{e}^{-4ic^2(t_n+s)}\overline{u_*}^3(t_n+s)\Big)\mathrm{d}s. \end{aligned} \tag{2.78}$$

In order to obtain a second-order uniformly accurate scheme based on the decomposition (2.76) we need to carefully analyze the highly oscillatory phases in $I_*(\tau, t_n, u_*)$ and $I_{c^2}(\tau, t_n, u_*)$. We commence with the analysis of $I_*(\tau, t_n, u_*)$.

1.) First term $I_*(\tau, t_n, u_*)$: By Lemma 2.23 we have that

$$\begin{aligned} u_*(t_n+s) = \mathrm{e}^{is\mathcal{A}_c}u_*(t_n) &- \frac{3i}{8}c\langle\nabla\rangle_c^{-1}\int_0^s \mathrm{e}^{i(s-\xi)\mathcal{A}_c}\left|\mathrm{e}^{i\xi\mathcal{A}_c}u_*(t_n)\right|^2\left(\mathrm{e}^{i\xi\mathcal{A}_c}u_*(t_n)\right)\mathrm{d}\xi \\ &- \frac{i}{8}c\langle\nabla\rangle_c^{-1}\Psi_{c^2}(t_n, s, u_*(t_n)) + \mathcal{R}_1(t_n, s, u_*) \end{aligned} \tag{2.79}$$

with Ψ_{c^2} defined in (2.63) and where the remainder $\mathcal{R}_1$ is of order $\mathcal{O}(s^2)$ uniformly in c. Plugging the approximation (2.79) into $I_*(\tau,t_n,u_*)$ defined in (2.77) yields that

$$\begin{aligned} I_*(\tau,t_n,u_*) &= \mathrm{e}^{i\tau\mathcal{A}_c}u_*(t_n) - \frac{3i}{8}c\langle\nabla\rangle_c^{-1}\int_0^\tau \mathrm{e}^{i(\tau-s)\mathcal{A}_c}|u_*(t_n+s)|^2u_*(t_n+s)\mathrm{d}s \\ &= \mathrm{e}^{i\tau\mathcal{A}_c}u_*(t_n) - \frac{3i}{8}c\langle\nabla\rangle_c^{-1}I_*^1(\tau,t_n,u_*) \\ &\quad + \frac{3i}{8}c\langle\nabla\rangle_c^{-1}\frac{i}{8}\int_0^\tau \mathrm{e}^{i(\tau-s)\mathcal{A}_c}\Big\{2\left|\mathrm{e}^{is\mathcal{A}_c}u_*(t_n)\right|^2 c\langle\nabla\rangle_c^{-1}\Psi_{c^2}(t_n,s,u_*(t_n)) \\ &\qquad\qquad - \left(\mathrm{e}^{is\mathcal{A}_c}u_*(t_n)\right)^2 c\langle\nabla\rangle_c^{-1}\overline{\Psi_{c^2}}(t_n,s,u_*(t_n))\Big\}\mathrm{d}s \\ &\quad + \mathcal{R}(\tau,t_n,u_*), \end{aligned} \tag{2.80}$$

where we have set

$$\begin{aligned} I_*^1(\tau,t_n,u_*) := \int_0^\tau \mathrm{e}^{i(\tau-s)\mathcal{A}_c}\Bigg\{&\left|\mathrm{e}^{is\mathcal{A}_c}u_*(t_n)\right|^2\mathrm{e}^{is\mathcal{A}_c}u_*(t_n) \\ &- \frac{3i}{4}\left|\mathrm{e}^{is\mathcal{A}_c}u_*(t_n)\right|^2 c\langle\nabla\rangle_c^{-1}\int_0^s \mathrm{e}^{i(s-\xi)\mathcal{A}_c}|\mathrm{e}^{i\xi\mathcal{A}_c}u_*(t_n)|^2\mathrm{e}^{i\xi\mathcal{A}_c}u_*(t_n)\mathrm{d}\xi \\ &+ \frac{3i}{8}\left(\mathrm{e}^{is\mathcal{A}_c}u_*(t_n)\right)^2 c\langle\nabla\rangle_c^{-1}\int_0^s \mathrm{e}^{-i(s-\xi)\mathcal{A}_c}|\mathrm{e}^{i\xi\mathcal{A}_c}u_*(t_n)|^2\mathrm{e}^{-i\xi\mathcal{A}_c}\overline{u_*(t_n)}\mathrm{d}\xi\Bigg\}\,\mathrm{d}s. \end{aligned}$$

The remainder satisfies

$$\|\mathcal{R}(\tau,t_n,u_*)\|_r \le \tau^3 k_{r,M_4}, \tag{2.81}$$

for some constant k_{r,M_4} which depends on M_4, but is independent of c.
Lemma 2.28 allows us to handle the highly oscillatory integrals involving the function Ψ_{c^2} in (2.80). Thus, in order to obtain a uniform second-order approximation of $I_*(\tau,t_n,u_*)$, it remains to derive a suitable second-order approximation to $I_*^1(\tau,t_n,u_*)$.
1.1.) Approximation of $I_*^1(\tau,t_n,u_*)$: The midpoint rule yields the following approximation

$$\begin{aligned} I_*^1(\tau,t_n,u_*) = \tau\mathrm{e}^{i\frac{\tau}{2}\mathcal{A}_c}\Bigg\{&\left|\mathrm{e}^{i\frac{\tau}{2}\mathcal{A}_c}u_*(t_n)\right|^2\mathrm{e}^{i\frac{\tau}{2}\mathcal{A}_c}u_*(t_n) \\ &- \frac{3i}{4}\left|\mathrm{e}^{i\frac{\tau}{2}\mathcal{A}_c}u_*(t_n)\right|^2 c\langle\nabla\rangle_c^{-1}\int_0^{\tau/2}\mathrm{e}^{i(\frac{\tau}{2}-\xi)\mathcal{A}_c}|\mathrm{e}^{i\xi\mathcal{A}_c}u_*(t_n)|^2\mathrm{e}^{i\xi\mathcal{A}_c}u_*(t_n)\mathrm{d}\xi \\ &+ \frac{3i}{8}\left(\mathrm{e}^{i\frac{\tau}{2}\mathcal{A}_c}u_*(t_n)\right)^2 c\langle\nabla\rangle_c^{-1}\int_0^{\tau/2}\mathrm{e}^{-i(\frac{\tau}{2}-\xi)\mathcal{A}_c}|\mathrm{e}^{i\xi\mathcal{A}_c}u_*(t_n)|^2\mathrm{e}^{-i\xi\mathcal{A}_c}\overline{u_*(t_n)}\mathrm{d}\xi\Bigg\} \\ &+ \mathcal{R}(\tau,t_n,u_*(t_n)), \end{aligned} \tag{2.82}$$

where the remainder satisfies thanks to (2.27) and (2.30) that

$$\|\mathcal{R}(\tau,t_n,u_*(t_n))\|_r \le \tau^3 k_{r,M_4} \tag{2.83}$$

with k_{r,M_4} independent of c.
Next, we approximate the two remaining integrals in (2.82) with the right rectangular rule, i.e.,

$$\int_0^{\tau/2}\mathrm{e}^{i(\frac{\tau}{2}-\xi)\mathcal{A}_c}|\mathrm{e}^{i\xi\mathcal{A}_c}u_*(t_n)|^2\mathrm{e}^{i\xi\mathcal{A}_c}u_*(t_n)\mathrm{d}\xi = \frac{\tau}{2}|\mathrm{e}^{i\frac{\tau}{2}\mathcal{A}_c}u_*(t_n)|^2\mathrm{e}^{i\frac{\tau}{2}\mathcal{A}_c}u_*(t_n) + \mathcal{R}(\tau,t_n,u_*(t_n)), \tag{2.84}$$

where, again thanks to (2.27), the remainder satisfies

$$\|\mathcal{R}(\tau,t_n,u_*(t_n))\|_r \le \tau^2 k_{r,M_4} \tag{2.85}$$

with k_{r,M_4} independent of c.
Plugging (2.84) into (2.82) and using the notation

$$\mathcal{U}_*(t_n) = \mathrm{e}^{i\frac{\tau}{2}\mathcal{A}_c} u_*(t_n)$$

yields that

$$\begin{aligned} I_*^1(\tau, t_n, u_*) = \mathrm{e}^{i\frac{\tau}{2}\mathcal{A}_c} \Big\{ & \tau \left|\mathcal{U}_*(t_n)\right|^2 \mathcal{U}_*(t_n) \\ & - \frac{\tau^2}{2}\frac{3i}{4} \left|\mathcal{U}_*(t_n)\right|^2 c\langle\nabla\rangle_c^{-1} |\mathcal{U}_*(t_n)|^2 \mathcal{U}_*(t_n) + \frac{\tau^2}{2}\frac{3i}{8} \mathcal{U}_*(t_n)^2 c\langle\nabla\rangle_c^{-1} |\mathcal{U}_*(t_n)|^2 \overline{\mathcal{U}_*(t_n)} \Big\} \\ + \mathcal{R}(\tau, t_n, u_*(t_n)), & \end{aligned}$$

where thanks to (2.81), (2.83) and (2.85) the remainder satisfies the bound $\|\mathcal{R}(\tau, t_n, u_*(t_n))\|_r \leq \tau^2 k_{r,M_4}$ with k_{r,M_4} independent of c.
In order to obtain asymptotic convergence to the classical Strang splitting scheme (2.3) associated to the nonlinear Schrödinger limit (2.2), we add and subtract the term

$$\mathrm{e}^{i\frac{\tau}{2}\mathcal{A}_c} \frac{\tau^2}{2}\frac{3i}{8} |\mathcal{U}_*(t_n)|^4 \mathcal{U}_*(t_n)$$

in the above approximation to $I_*^1(\tau, t_n, u_*)$. This yields that

$$\begin{aligned} I_*^1(\tau, t_n, u_*) = \mathrm{e}^{i\frac{\tau}{2}\mathcal{A}_c} \Big\{ & \tau \left|\mathcal{U}_*(t_n)\right|^2 \mathcal{U}_*(t_n) - \frac{\tau^2}{2}\frac{3i}{8} |\mathcal{U}_*(t_n)|^4 \mathcal{U}_*(t_n) \\ & - \frac{\tau^2}{2}\frac{3i}{4} \left|\mathcal{U}_*(t_n)\right|^2 \left(c\langle\nabla\rangle_c^{-1} - 1\right) |\mathcal{U}_*(t_n)|^2 \mathcal{U}_*(t_n) \\ & + \frac{\tau^2}{2}\frac{3i}{8} \mathcal{U}_*(t_n)^2 \left(c\langle\nabla\rangle_c^{-1} - 1\right) |\mathcal{U}_*(t_n)|^2 \overline{\mathcal{U}_*(t_n)} \Big\} + \mathcal{R}(\tau, t_n, u_*(t_n)). \end{aligned} \tag{2.86}$$

The above decomposition allows us a second-order approximation of $I_*(\tau, t_n, u_*)$ which holds uniformly in all c.
1.2.) Final approximation of $I_*(\tau, t_n, u_*)$: Plugging (2.86) into (2.80) and exploiting Lemma 2.28 yields that

$$\begin{aligned} I_*(\tau, t_n, u_*) = \mathrm{e}^{i\frac{\tau}{2}\mathcal{A}_c} & \left\{ \mathcal{U}_*(t_n) - \frac{3i}{8}\tau \left|\mathcal{U}_*(t_n)\right|^2 \mathcal{U}_*(t_n) + \left(-\frac{3i}{8}\right)^2 \frac{\tau^2}{2} |\mathcal{U}_*(t_n)|^4 \mathcal{U}_*(t_n) \right\} \\ & - \tau \frac{3i}{8} \left(c\langle\nabla\rangle_c^{-1} - 1\right) \mathrm{e}^{i\frac{\tau}{2}\mathcal{A}_c} \left|\mathcal{U}_*(t_n)\right|^2 \mathcal{U}_*(t_n) + \tau^2 \theta_{c\langle\nabla\rangle_c - 1}(t_n, \tau, \mathcal{U}_*(t_n)) \\ & - \tau^2 \frac{3}{32} c\langle\nabla\rangle_c^{-1} \left|u_*(t_n)\right|^2 c\langle\nabla\rangle_c^{-1} \vartheta_{c^2}(t_n, \tau, u_*(t_n)) \\ & + \tau^2 \frac{3}{64} c\langle\nabla\rangle_c^{-1} \left(u_*(t_n)\right)^2 c\langle\nabla\rangle_c^{-1} \overline{\vartheta_{c^2}}(t_n, \tau, u_*(t_n)) + \mathcal{R}(\tau, t_n, u_*) \end{aligned}$$

with a remainder $\mathcal{R}$ of order $\mathcal{O}(\tau^3)$ uniformly in c. Furthermore, The formal Taylor series expansion

$$\left| 1 + x + \frac{x^2}{2} - \mathrm{e}^x \right| = \mathcal{O}(x^3)$$

allows us the following final representation of I_*:

$$\begin{aligned} I_*(\tau, t_n, u_*) = \mathrm{e}^{i\frac{\tau}{2}\mathcal{A}_c} & \exp\left(-\frac{3i}{8}\tau |\mathcal{U}_*(t_n)|^2\right) \mathcal{U}_*(t_n) \\ & - \tau \frac{3i}{8} \left(c\langle\nabla\rangle_c^{-1} - 1\right) \mathrm{e}^{i\frac{\tau}{2}\mathcal{A}_c} \left|\mathcal{U}_*(t_n)\right|^2 \mathcal{U}_*(t_n) + \tau^2 \theta_{c\langle\nabla\rangle_c - 1}(t_n, \tau, \mathcal{U}_*(t_n)) \\ & - \tau^2 \frac{3}{32} c\langle\nabla\rangle_c^{-1} \left|u_*(t_n)\right|^2 c\langle\nabla\rangle_c^{-1} \vartheta_{c^2}(t_n, \tau, u_*(t_n)) \\ & + \tau^2 \frac{3}{64} c\langle\nabla\rangle_c^{-1} \left(u_*(t_n)\right)^2 c\langle\nabla\rangle_c^{-1} \overline{\vartheta_{c^2}}(t_n, \tau, u_*(t_n)) + \mathcal{R}(\tau, t_n, u_*) \end{aligned} \tag{2.87}$$

with

$$\begin{aligned}\theta_{c\langle\nabla\rangle_c-1}(t_n,\tau,v) := &-\frac{1}{2}\frac{9}{64}\mathrm{e}^{i\frac{\tau}{2}\mathcal{A}_c}\Big(c\langle\nabla\rangle_c^{-1}-1\Big)\,|v|^4\,v-\frac{1}{2}\frac{9}{32}c\langle\nabla\rangle_c^{-1}\mathrm{e}^{i\frac{\tau}{2}\mathcal{A}_c}\,|v|^2\,\Big(c\langle\nabla\rangle_c^{-1}-1\,\Big)|v|^2v\\ &+\frac{1}{2}\frac{9}{64}c\langle\nabla\rangle_c^{-1}\mathrm{e}^{i\frac{\tau}{2}\mathcal{A}_c}v^2\Big(c\langle\nabla\rangle_c^{-1}-1\,\Big)|v|^2\overline{v}\end{aligned} \tag{2.88}$$

and where ϑ_{c^2} is defined in (2.73) and the remainder $\mathcal{R}(\tau,t_n,u_*)$ satisfies

$$\|\mathcal{R}(\tau,t_n,u_*(t_n))\|_r\le\tau^3k_{r,M_4} \tag{2.89}$$

with k_{r,M_4} independent of c. The approximation of $I_*(\tau,t_n,u_*)$ given in (2.87) provides the first terms in our numerical scheme. In order to obtain a full approximation to $u_*(t_n+\tau)$ in (2.76) we next derive a second-order approximation to the integral term $I_{c^2}(\tau,t_n,u_*)$.

2.) Second term $I_{c^2}(\tau,t_n,u_*)$: Combining the second approximation in Lemma 2.23 yields together with Lemma 2.6 and by the definition of $I_{c^2}(\tau,t_n,u_*)$ in (2.78) that

$$\begin{aligned}I_{c^2}(\tau,t_n,u_*) = &\int_0^\tau \mathrm{e}^{i(\tau-s)\mathcal{A}_c}\Big\{\mathrm{e}^{2ic^2(t_n+s)}\left(\mathrm{e}^{is\mathcal{A}_c}u_*(t_n)\right)^3+3\mathrm{e}^{-2ic^2(t_n+s)}\left|\mathrm{e}^{is\mathcal{A}_c}u_*(t_n)\right|^2\mathrm{e}^{-is\mathcal{A}_c}\overline{u_*}(t_n)\\ &\qquad+\mathrm{e}^{-4ic^2(t_n+s)}\left(\mathrm{e}^{-is\mathcal{A}_c}\overline{u_*}(t_n)\right)^3\Big\}\mathrm{d}s\\ &+\int_0^\tau\Big\{-\frac{3i}{8}\mathrm{e}^{2ic^2(t_n+s)}\left(u_*(t_n)\right)^2c\langle\nabla\rangle_c^{-1}\left[3s|u_*(t_n)|^2u_*(t_n)+\Psi_{c^2}(t_n,s,u_*(t_n))\right]\\ &\qquad+3\mathrm{e}^{-2ic^2(t_n+s)}\Big(-\frac{i}{8}\left(\overline{u_*}(t_n)\right)^2c\langle\nabla\rangle_c^{-1}\left[3s|u_*(t_n)|^2u_*(t_n)+\Psi_{c^2}(t_n,s,u_*(t_n))\right]\\ &\qquad+\frac{2i}{8}\left|u_*(t_n)\right|^2c\langle\nabla\rangle_c^{-1}\left[3s|u_*(t_n)|^2\overline{u_*}(t_n)+\overline{\Psi}_{c^2}(t_n,s,u_*(t_n))\right]\Big)\\ &\qquad+\frac{3i}{8}\mathrm{e}^{-4ic^2(t_n+s)}\left(\overline{u_*}(t_n)\right)^2c\langle\nabla\rangle_c^{-1}\left[3s|u_*(t_n)|^2\overline{u_*}(t_n)+\overline{\Psi}_{c^2}(t_n,s,u_*(t_n))\right]\Big\}\,\mathrm{d}s\\ &+\mathcal{R}(t_n,\tau,u_*)\end{aligned}$$

with Ψ_{c^2} defined in (2.63) and where thanks to Lemma 2.6, Lemma 2.23, and due to the fact that Ψ_{c^2} is of order one in s uniformly in c the remainder satisfies $\|\mathcal{R}(\tau,t_n,u_*(t_n))\|_r\le\tau^3k_{r,M_4}$ with k_r independent of c.

Lemma 2.24, 2.26 together with Lemma 2.29 thus allow us the following expansion of I_{c^2}, i.e., we have

$$I_{c^2}(\tau,t_n,u_*) = I^1_{c^2}(\tau,t_n,u_*)+\mathcal{R}(t_n,\tau,u_*) \tag{2.90}$$

with the highly oscillatory term

$$
\begin{aligned}
I^1_{c^2}(\tau, t_n, u_*) := {} & \tau \mathrm{e}^{2ic^2 t_n} \mathrm{e}^{i\tau\mathcal{A}_c} \varphi_1\left(i\tau(2c^2 - \tfrac{1}{2}\Delta)\right) u_*^3(t_n) \\
& + i\tau^2 \mathrm{e}^{2ic^2 t_n} \mathrm{e}^{i\tau\mathcal{A}_c} \Psi_2\left(i\tau(2c^2 - \tfrac{1}{2}\Delta)\right) \left[(\tfrac{1}{2}\Delta - \mathcal{A}_c) u_*^3(t_n) + 3u_*^2(t_n)\mathcal{A}_c u_*(t_n)\right] \\
& + 3\tau \mathrm{e}^{-2ic^2 t_n} \mathrm{e}^{i\tau\mathcal{A}_c} \varphi_1(i\tau(-2c^2 - \mathcal{A}_c)) \left|u_*(t_n)\right|^2 \overline{u_*}(t_n) \\
& + 3i\tau^2 \mathrm{e}^{-2ic^2 t_n} \mathrm{e}^{i\tau\mathcal{A}_c} \Psi_2(i\tau(-2c^2 - \mathcal{A}_c)) \left[\overline{u_*}^2(t_n)\mathcal{A}_c u_*(t_n) - 2|u_*(t_n)|^2 \mathcal{A}_c \overline{u_*}(t_n)\right] \\
& + \tau \mathrm{e}^{-4ic^2 t_n} \mathrm{e}^{i\tau\mathcal{A}_c} \varphi_1(i\tau(-4c^2 - \mathcal{A}_c)) \overline{u_*}^3(t_n) \\
& - i\tau^2 \mathrm{e}^{-4ic^2 t_n} \mathrm{e}^{i\tau\mathcal{A}_c} \Psi_2(i\tau(-4c^2 - \mathcal{A}_c)) 3\overline{u_*}^2(t_n)\mathcal{A}_c \overline{u_*}(t_n) \\
& - \tau^2 \frac{3i}{8} \mathrm{e}^{2ic^2 t_n} \left(u_*(t_n)\right)^2 c\langle\nabla\rangle_c^{-1} \left[3\Psi_2(2ic^2\tau)|u_*(t_n)|^2 u_*(t_n) + \Omega_{c^2,2,}(t_n, \tau, u_*(t_n))\right] \\
& - \tau^2 \frac{3i}{8} \mathrm{e}^{-2ic^2 t_n} \left(\overline{u_*}(t_n)\right)^2 c\langle\nabla\rangle_c^{-1} \left[3\Psi_2(-2ic^2\tau)|u_*(t_n)|^2 u_*(t_n) + \Omega_{c^2,-2}(t_n, \tau, u_*(t_n))\right] \\
& + \tau^2 \frac{6i}{8} \mathrm{e}^{-2ic^2 t_n} \left|u_*(t_n)\right|^2 c\langle\nabla\rangle_c^{-1} \left[3\Psi_2(-2ic^2\tau)|u_*(t_n)|^2 \overline{u_*}(t_n) + \overline{\Omega}_{c^2,-2}(t_n, \tau, u_*(t_n))\right] \\
& + \tau^2 \frac{3i}{8} \mathrm{e}^{-4ic^2 t_n} \left(\overline{u_*}(t_n)\right)^2 c\langle\nabla\rangle_c^{-1} \left[3\Psi_2(-4ic^2\tau)|u_*(t_n)|^2 \overline{u_*}(t_n) + \overline{\Omega}_{c^2,-4}(t_n, \tau, u_*(t_n))\right] \\
& + \mathcal{R}(t_n, \tau, u_*),
\end{aligned}
\tag{2.91}
$$

where $\Omega_{c^2,\ell}$ is defined in Lemma 2.29, and the remainder satisfies

$$
\|\mathcal{R}(t_n, \tau, u_*)\|_r \leq \tau^3 k_{r,M_4} \tag{2.92}
$$

with k_{r,M_4} independent of c.

3.) Final approximation of $u_*(t_n + \tau)$*:* Plugging (2.87) as well as (2.90) into (2.76) builds the basis of our second-order scheme. As a numerical approximation to the exact solution u_* at time t_{n+1} we take the second-order uniform accurate exponential-type integrator

$$
\mathcal{U}_*^n = \mathrm{e}^{i\frac{\tau}{2}\mathcal{A}_c} u_*^n
$$

and obtain

$$
\begin{aligned}
u_*^{n+1} = {} & \mathrm{e}^{i\frac{\tau}{2}\mathcal{A}_c} \mathrm{e}^{-i\tau\frac{3}{8}|\mathcal{U}_*^n|^2} \mathcal{U}_*^n \\
& - \tau\frac{3i}{8}\left(c\langle\nabla\rangle_c^{-1} - 1\right) \mathrm{e}^{i\frac{\tau}{2}\mathcal{A}_c} \left|\mathcal{U}_*^n\right|^2 \mathcal{U}_*^n + \tau^2 \theta_{c\langle\nabla\rangle_c - 1}(t_n, \tau, \mathcal{U}_*^n) \\
& - \tau^2 \frac{3}{64} c\langle\nabla\rangle_c^{-1} \left[2\left|u_*^n\right|^2 c\langle\nabla\rangle_c^{-1} \vartheta_{c^2}(t_n, \tau, u_*^n) - \left(u_*^n\right)^2 c\langle\nabla\rangle_c^{-1} \overline{\vartheta_{c^2}}(t_n, \tau, u_*^n)\right] \\
& - \frac{i}{8} c\langle\nabla\rangle_c^{-1} I^1_{c^2}(\tau, t_n, u_*^n), \\
u_*^0 = {} & z(0) - ic^{-1}\langle\nabla\rangle_c^{-1}\partial_t z(0),
\end{aligned}
\tag{2.93}
$$

where $I^1_{c^2}(\tau, t_n, u_*^n)$ is defined in (2.91) and with φ_1, Ψ_2 given in Definition 2.8, $\theta_{c\langle\nabla\rangle_c - 1}$ given in (2.88), ϑ_{c^2} in (2.73) and $\Omega_{c^2,\ell}$ in (2.75).

We continue with the convergence analysis of the uniformly accurate second-order scheme.

2.3.3.2 Convergence Analysis

By construction the exponential-type integration scheme (2.93) converges with second-order accuracy in time uniformly with respect to c.

Theorem 2.30 (Convergence bound for the second-order scheme, cf. Theorem 27 in [13])**.** *Fix $r > d/2$ and assume that*

$$\|z(0)\|_{r+4} + \|c^{-1}\langle\nabla\rangle_c^{-1}\partial_t z(0)\|_{r+4} \leq M_4 \tag{2.94}$$

uniformly in c. For u_*^n defined in (2.93) we set

$$z^n := \frac{1}{2}\left(\mathrm{e}^{ic^2 t_n} u_*^n + \mathrm{e}^{-ic^2 t_n}\overline{u_*^n}\right).$$

Then, there exists a $T > 0$ and $\tau_0 > 0$ such that for all $\tau \leq \tau_0$ and $t_n \leq T$ we have for all $c > 0$ that

$$\|z(t_n) - z^n\|_r \leq \tau^2 K^*_{r,T,M,M_4},$$

where the constant K^*_{r,T,M,M_4} can be chosen independently of c.

Proof. Firstly, note that the regularity assumption on the initial data in (2.94) implies the regularity Assumption 2.20 on $u_*(t)$, i.e., there exists a $T > 0$ such that

$$\sup_{0\leq t\leq T} \|u_*(t)\|_{r+4} \leq k(M_4),$$

for some constant k that depends on M_4 and T, but can be chosen independently of c.
Furthermore in the following, we denote by k_r, K_r and $K_{r,M}$ constants depending only on r or r, M respectively, but which can be chosen independently of c.
In the following let ϕ^t denote the exact flow of (2.31), i.e., $u_*(t_{n+1}) = \phi^\tau(u_*(t_n))$ and let Φ^τ denote the numerical flow defined in (2.93), i.e.,

$$u_*^{n+1} = \Phi^\tau(u_*^n).$$

For the further analysis, we consider the difference of (2.32) and (2.93), i.e.,

$$\begin{aligned} u_*(t_{n+1}) - u_*^{n+1} &= \phi^\tau(u_*(t_n)) - \Phi^\tau(u_*^n) \\ &= \Phi^\tau(u_*(t_n)) - \Phi^\tau(u_*^n) + \phi^\tau(u_*(t_n)) - \Phi^\tau(u_*(t_n))\end{aligned} \tag{2.95}$$

which represents an expression of the global error of our scheme.
Local error bound: With the aid of the expansions (2.87) and (2.90) we obtain by the representation of the exact solution in (2.76) together with the error bounds (2.89) and (2.92) that

$$\|\phi^\tau(u_*(t_n)) - \Phi^\tau(u_*(t_n))\|_r = \|\mathcal{R}(\tau, t_n, u_*)\|_r \leq \tau^3 k_{r,M_4}, \tag{2.96}$$

for some constant k_{r,M_4} which depends on M_4 and r, but can be chosen independently of c.
Stability bound: Note that by definition of Ψ_2 in Definition 2.8, $\theta_{c\langle\nabla\rangle_c-1}$ in (2.88), ϑ_{c^2} in (2.73) and $\Omega_{c^2,\ell}$ in (2.75) we have for $\ell = -4, -2, 2$ that

$$\begin{aligned}\tau^2\Big(\|\Psi_2(\ell i c^2 t)(f-g)\|_r + \|\Omega_{c^2,\ell}(t_n,\tau,f) - \Omega_{c^2,\ell}(t_n,\tau,g)\|_r + \|\vartheta_{c^2}(t_n,\tau,f) - \vartheta_{c^2}(t_n,\tau,g)\|_r\Big) \\ \leq \tau k_r\left(\|f\|_r, \|g\|_r\right)\|f-g\|_r\end{aligned} \tag{2.97}$$

for some constant k_r independent of c .

We have

$$\begin{aligned}
u_*(t_{n+1}) &= \mathrm{e}^{i\frac{\tau}{2}\mathcal{A}_c}\mathrm{e}^{-i\tau\frac{3}{8}|\mathcal{U}_*(t_n)|^2}\mathcal{U}_*(t_n) - \tau\frac{3i}{8}\left(c\langle\nabla\rangle_c^{-1} - 1\right)\mathrm{e}^{i\frac{\tau}{2}\mathcal{A}_c}\left|\mathcal{U}_*(t_n)\right|^2\mathcal{U}_*(t_n) \\
&\quad + \tau^2\theta_{c\langle\nabla\rangle_c-1}\left(t_n,\tau,\mathcal{U}_*(t_n)\right) \\
&\quad - \tau^2\frac{3}{64}c\langle\nabla\rangle_c^{-1}\left[2\left|u_*(t_n)\right|^2 c\langle\nabla\rangle_c^{-1}\vartheta_{c^2}(t_n,\tau,u_*(t_n)) - (u_*(t_n))^2 c\langle\nabla\rangle_c^{-1}\overline{\vartheta_{c^2}}(t_n,\tau,u_*(t_n))\right] \\
&\quad - \frac{i}{8}c\langle\nabla\rangle_c^{-1}I^1_{c^2}(\tau,t_n,u_*(t_n)) \\
&= E_1 + E_2 + E_3 + E_4 + E_5
\end{aligned}$$

with $\mathcal{U}_*(t_n) = \mathrm{e}^{i\frac{\tau}{2}\mathcal{A}_c}u_*(t_n)$ and where we set

$$\begin{aligned}
E_1 &:= \mathrm{e}^{i\frac{\tau}{2}\mathcal{A}_c}\mathrm{e}^{-i\tau\frac{3}{8}|\mathcal{U}_*(t_n)|^2}\mathcal{U}_*(t_n), \\
E_2 &:= -\tau\frac{3i}{8}\left(c\langle\nabla\rangle_c^{-1} - 1\right)\mathrm{e}^{i\frac{\tau}{2}\mathcal{A}_c}\left|\mathcal{U}_*(t_n)\right|^2\mathcal{U}_*(t_n), \\
E_3 &:= \tau^2\theta_{c\langle\nabla\rangle_c-1}\left(t_n,\tau,\mathcal{U}_*(t_n)\right), \\
E_4 &:= -\tau^2\frac{3}{64}c\langle\nabla\rangle_c^{-1}\left[2\left|u_*(t_n)\right|^2 c\langle\nabla\rangle_c^{-1}\vartheta_{c^2}(t_n,\tau,u_*(t_n)) - (u_*(t_n))^2 c\langle\nabla\rangle_c^{-1}\overline{\vartheta_{c^2}}(t_n,\tau,u_*(t_n))\right], \\
E_5 &:= -\frac{i}{8}c\langle\nabla\rangle_c^{-1}I^1_{c^2}(\tau,t_n,u_*(t_n)).
\end{aligned}$$

We also have

$$\begin{aligned}
u_*^{n+1} &= \mathrm{e}^{i\frac{\tau}{2}\mathcal{A}_c}\mathrm{e}^{-i\tau\frac{3}{8}|\mathcal{U}_*^n|^2}\mathcal{U}_*^n - \tau\frac{3i}{8}\left(c\langle\nabla\rangle_c^{-1} - 1\right)\mathrm{e}^{i\frac{\tau}{2}\mathcal{A}_c}\left|\mathcal{U}_*^n\right|^2\mathcal{U}_*^n + \tau^2\theta_{c\langle\nabla\rangle_c-1}\left(t_n,\tau,\mathcal{U}_*^n\right) \\
&\quad - \tau^2\frac{3}{64}c\langle\nabla\rangle_c^{-1}\left[2\left|u_*^n\right|^2 c\langle\nabla\rangle_c^{-1}\vartheta_{c^2}(t_n,\tau,u_*^n) - (u_*^n)^2 c\langle\nabla\rangle_c^{-1}\overline{\vartheta_{c^2}}(t_n,\tau,u_*^n)\right] \\
&\quad - \frac{i}{8}c\langle\nabla\rangle_c^{-1}I^1_{c^2}(\tau,t_n,u_*^n) \\
&= N_1 + N_2 + N_3 + N_4 + N_5
\end{aligned}$$

with $\mathcal{U}_*^n = \mathrm{e}^{i\frac{\tau}{2}\mathcal{A}_c}u_*^n$ and where we set

$$\begin{aligned}
N_1 &:= \mathrm{e}^{i\frac{\tau}{2}\mathcal{A}_c}\mathrm{e}^{-i\tau\frac{3}{8}|\mathcal{U}_*^n|^2}\mathcal{U}_*^n, \\
N_2 &:= -\tau\frac{3i}{8}\left(c\langle\nabla\rangle_c^{-1} - 1\right)\mathrm{e}^{i\frac{\tau}{2}\mathcal{A}_c}\left|\mathcal{U}_*^n\right|^2\mathcal{U}_*^n, \\
N_3 &:= \tau^2\theta_{c\langle\nabla\rangle_c-1}\left(t_n,\tau,\mathcal{U}_*^n\right), \\
N_4 &:= -\tau^2\frac{3}{64}c\langle\nabla\rangle_c^{-1}\left[2\left|u_*^n\right|^2 c\langle\nabla\rangle_c^{-1}\vartheta_{c^2}(t_n,\tau,u_*^n) - (u_*^n)^2 c\langle\nabla\rangle_c^{-1}\overline{\vartheta_{c^2}}(t_n,\tau,u_*^n)\right], \\
N_5 &:= -\frac{i}{8}c\langle\nabla\rangle_c^{-1}I^1_{c^2}(\tau,t_n,u_*^n).
\end{aligned}$$

Now, we take the difference of E_1 and N_1. As $\mathrm{e}^{it\mathcal{A}_c}$ is a linear isometry (see Lemma 2.6) for all $t \in \mathbb{R}$ we obtain

$$\begin{aligned}
\|E_1 - N_1\|_r &= \left\|\mathrm{e}^{i\frac{\tau}{2}\mathcal{A}_c}\mathrm{e}^{-i\tau\frac{3}{8}|\mathcal{U}_*(t_n)|^2}\mathcal{U}_*(t_n) - \mathrm{e}^{i\frac{\tau}{2}\mathcal{A}_c}\mathrm{e}^{-i\tau\frac{3}{8}|\mathcal{U}_*^n|^2}\mathcal{U}_*^n\right\|_r \\
&= \left\|\mathrm{e}^{-i\tau\frac{3}{8}|\mathcal{U}_*(t_n)|^2}\mathcal{U}_*(t_n) - \mathrm{e}^{-i\tau\frac{3}{8}|\mathcal{U}_*^n|^2}\mathcal{U}_*^n\right\|_r \\
&\le \left\|\mathrm{e}^{-i\tau\frac{3}{8}|\mathcal{U}_*(t_n)|^2}\mathcal{U}_*(t_n) - \mathrm{e}^{-i\tau\frac{3}{8}|\mathcal{U}_*(t_n)|^2}\mathcal{U}_*^n\right\|_r + \left\|\mathrm{e}^{-i\tau\frac{3}{8}|\mathcal{U}_*(t_n)|^2}\mathcal{U}_*^n - \mathrm{e}^{-i\tau\frac{3}{8}|\mathcal{U}_*^n|^2}\mathcal{U}_*^n\right\|_r \\
&\le \left\|\mathrm{e}^{-i\tau\frac{3}{8}|\mathcal{U}_*(t_n)|^2}\right\|_r\|\mathcal{U}_*(t_n) - \mathcal{U}_*^n\|_r + \left\|\mathrm{e}^{-i\tau\frac{3}{8}|\mathcal{U}_*(t_n)|^2} - \mathrm{e}^{-i\tau\frac{3}{8}|\mathcal{U}_*^n|^2}\right\|_r\|\mathcal{U}_*^n\|_r.
\end{aligned}$$

We use the definitions of $\mathcal{U}_*^n$, $\mathcal{U}_*(t_n)$ and obtain

$$\begin{aligned}\|E_1 - N_1\|_r &\le \left\|\mathrm{e}^{-i\tau\frac{3}{8}\left|\mathrm{e}^{i\frac{\tau}{2}\mathcal{A}_c}u_*(t_n)\right|^2}\right\|_r \|\mathrm{e}^{i\frac{\tau}{2}\mathcal{A}_c}u_*(t_n) - \mathrm{e}^{i\frac{\tau}{2}\mathcal{A}_c}u_*^n\|_r \\ &\quad + \left\|\mathrm{e}^{-i\tau\frac{3}{8}\left|\mathrm{e}^{i\frac{\tau}{2}\mathcal{A}_c}u_*(t_n)\right|^2} - \mathrm{e}^{-i\tau\frac{3}{8}\left|\mathrm{e}^{i\frac{\tau}{2}\mathcal{A}_c}u_*^n\right|^2}\right\|_r \|\mathrm{e}^{i\frac{\tau}{2}\mathcal{A}_c}u_*^n\|_r \\ &= \left\|\mathrm{e}^{-i\tau\frac{3}{8}\left|\mathrm{e}^{i\frac{\tau}{2}\mathcal{A}_c}u_*(t_n)\right|^2}\right\|_r \|u_*(t_n) - u_*^n\|_r + \left\|\mathrm{e}^{-i\tau\frac{3}{8}\left|\mathrm{e}^{i\frac{\tau}{2}\mathcal{A}_c}u_*(t_n)\right|^2} - \mathrm{e}^{-i\tau\frac{3}{8}\left|\mathrm{e}^{i\frac{\tau}{2}\mathcal{A}_c}u_*^n\right|^2}\right\|_r \|u_*^n\|_r.\end{aligned}$$

In the following we assume that

$$\|u_*(t_n)\|_r \le M \qquad \text{and} \qquad \|u_*^n\|_r \le 2M.$$

Exploiting these assumptions, the linear isometry property of $\mathrm{e}^{it\mathcal{A}_c}$ and the Taylor series expansion of the exponential function we obtain that

$$\begin{aligned}\left\|\mathrm{e}^{-i\tau\frac{3}{8}\left|\mathrm{e}^{i\frac{\tau}{2}\mathcal{A}_c}u_*(t_n)\right|^2} - 1\right\|_r &\le \tau K_{r,M}, \\ 1 + \tau K_{r,M} &\le \mathrm{e}^{\tau K_{r,M}}.\end{aligned}$$

Therefore, we have

$$\|E_1 - N_1\|_r \le \mathrm{e}^{\tau K_{r,M}}\, \|u_*(t_n) - u_*^n\|_r + K_M \left\|\mathrm{e}^{-i\tau\frac{3}{8}\left|\mathrm{e}^{i\frac{\tau}{2}\mathcal{A}_c}u_*(t_n)\right|^2} - \mathrm{e}^{-i\tau\frac{3}{8}\left|\mathrm{e}^{i\frac{\tau}{2}\mathcal{A}_c}u_*^n\right|^2}\right\|_r.$$

Applying once more the Taylor series expansion of the exponential function again and using that $\mathrm{e}^{it\mathcal{A}_c}$ is a linear isometry for all $t \in \mathbb{R}$ we obtain analogously to the proof of Theorem 2.13 that

$$\|E_1 - N_1\|_r \le e^{\tau K_{r,M}}\|u_*(t_n) - u_*^n\|_r.$$

Similar bounds can be established for $\|E_2 - N_2\|_r$, $\|E_3 - N_3\|_r$, $\|E_4 - N_4\|_r$, and $\|E_5 - N_5\|_r$ by using the same trick as for $\|E_1 - N_1\|_r$ and applying the estimate (2.97) together with the bound (2.30), the definition of φ_1 in Definition 2.8, and the stability estimates (2.69) and (2.72). For $\|E_5 - N_5\|_r$ we have also take into account Remark 2.25 and in particular the estimate (2.72).
As long as $\|u_*(t_n)\|_r \le M$ and $\|u_*^n\|_r \le 2M$, we thus find the stability bound

$$\|\Phi^\tau(u_*(t_n)) - \Phi^\tau(u_*^n)\|_r \le \mathrm{e}^{\tau K_{r,M}}\|u_*(t_n) - u_*^n\|_r, \tag{2.98}$$

where the constant $K_{r,M}$ depends on r and M, but can be chosen independently of c.
Global error bound: Plugging the stability bound (2.98) as well as the local error bound (2.96) into (2.95) yields by a bootstrap argument that

$$\|u_*(t_n) - u_*^n\|_r \le \tau^2 K_{r,M_4}\mathrm{e}^{TK_{r,M}} \le \tau^2 K^*_{r,T,M,M_4}, \tag{2.99}$$

where the constants K_{r,M_4}, $K_{r,M}$, and K^*_{r,T,M,M_4} are uniformly bounded in c. Since z is real and thus $u = v$, the identities $z = \frac{1}{2}(u + \overline{v})$ from (2.6) and $u_* = \mathrm{e}^{-ic^2t}u$, $v_* = \mathrm{e}^{-ic^2t}v$ from (2.24) imply that

$$\begin{aligned}\|z(t_n) - z^n\|_r &= \left\|\tfrac{1}{2}\big(u(t_n) + \overline{u}(t_n)\big) - \tfrac{1}{2}\big(\mathrm{e}^{ic^2t_n}\, u_*^n + \mathrm{e}^{-ic^2t_n}\, \overline{u_*^n}\big)\right\|_r \\ &\le \|u(t_n) - \mathrm{e}^{ic^2t_n}u_*^n\|_r \\ &= \|\mathrm{e}^{ic^2t_n}(u_*(t_n) - u_*^n)\|_r = \|u_*(t_n) - u_*^n\|_r.\end{aligned}$$

Together with the bound in (2.99) this completes the proof. □

Remark 2.31 (Fractional convergence and convergence in L^2)**.** A fractional convergence result as Theorem 2.15 for the first-order scheme also holds for the second-order exponential-type integrator (2.93): Fix $r > d/2$ and let $0 \leq \gamma \leq 1$. Assume that

$$\|z(0)\|_{r+2+2\gamma} + \|c^{-1}\langle\nabla\rangle_c^{-1}\partial_t z(0)\|_{r+2+2\gamma} \leq M_{2+2\gamma}.$$

Then, the scheme (2.93) is convergent of order $\tau^{1+\gamma}$ in H^r uniformly with respect to c.
Furthermore, for initial values satisfying

$$\|z(0)\|_{r+4} + \|c^{-1}\langle\nabla\rangle_c^{-1}\partial_t z(0)\|_{r+4} \leq M_4$$

the exponential-type integration scheme (2.93) is second-order convergent in L^2 uniformly with respect to c by the strategy presented in [50].

In analogy to Remark 2.16 we make the following observation: for sufficiently smooth solutions the exponential-type integration scheme (2.93) converges in the limit $c \to \infty$ to the classical Strang splitting of the corresponding nonlinear Schrödinger limit equation (2.2).

Remark 2.32 (Approximation in the non-relativistic limit $c \to \infty$)**.** The exponential-type integration scheme (2.93) converges for sufficiently smooth solutions in the limit $u_*^n \overset{c\to\infty}{\longrightarrow} u_{*,\infty}^n$, essentially to the Strang Splitting (see [25, 50])

$$u_{*,\infty}^{n+1} = \mathrm{e}^{-i\frac{\tau}{2}\frac{\Delta}{2}}\mathrm{e}^{-i\tau\frac{3}{8}|\mathrm{e}^{-i\frac{\tau}{2}\frac{\Delta}{2}}u_{*,\infty}^n|^2}\mathrm{e}^{-i\frac{\tau}{2}\frac{\Delta}{2}}u_{*,\infty}^n, \qquad u_{*,\infty}^0 = z_0 - iz_1, \tag{2.100}$$

for the cubic nonlinear Schrödinger limit system (2.2).

More precisely, the following Lemma holds.

Lemma 2.33 (cf. Lemma 30 in [13])**.** *Fix $r > d/2$. Assume that*

$$\|z(0)\|_{r+3} + \|c^{-1}\langle\nabla\rangle_c^{-1}\partial_t z(0)\|_{r+3} \leq M_3,$$

for some $\varepsilon > 0$ uniformly in c and let the initial value approximation (there exist functions z_0, z_1 such that)

$$\|z(0) - z_0\|_r + \|c^{-1}\langle\nabla\rangle_c^{-1}\partial_t z(0) - z_1\|_r \leq k_r c^{-1}$$

hold for some constant k_r independent of c.
Then, there exists a $T > 0$ and $\tau_0 > 0$ such that for all $\tau \leq \tau_0$ the difference of the second-order scheme (2.93) *for system* (2.31) *and the Strang splitting* (2.100) *for the limit Schrödinger equation* (2.2) *satisfies for $t_n \leq T$ and all $c > 0$ with*

$$\tau c \geq 1$$

that

$$\|u_*^n - u_{*,\infty}^n\|_r \leq c^{-1}k_{r,T,M_3},$$

for some constant k_{r,T,M_3} that depends on M_3 and T, but is independent of c.

Proof. The proof follows the same step as in the proof of Lemma 2.17 by noting that for $\ell = -4, -2$ and $n = -4, -2, 2$

$$\tau\Big(\|\varphi_j(2i\tau\langle\nabla\rangle_c^2)\|_r + \|\varphi_j\big(i\tau(\ell c^2 - \mathcal{A}_c)\big)\|_r + \|\varphi_j(nic^2\tau)\|_r\Big) \leq k_r c^{-2},$$

for some constant k_r independent of c. $\square$

2.3.3.3 Simplifications in the "Weakly to Strongly non-relativistic Limit Regime"

In the "weakly to strongly non-relativistic limit regime", i.e., for large values of c, we may again (substantially) simplify the second-order scheme (2.93) and nevertheless obtain a well suited, second-order approximation to $u_*(t_n)$ in (2.31).

Remark 2.34 (Limit scheme [26])**.** For sufficiently large values of c and sufficiently smooth solutions, more precisely, if

$$\|z(0)\|_{r+4} + \|c^{-1}\langle\nabla\rangle_c^{-1}\partial_t z(0)\|_{r+4} \leq M_4 \quad \text{and} \quad \tau c > 1$$

we may take instead of (2.93) the classical Strang splitting (see [25, 50]) for the nonlinear Schrödinger limit equation (2.2), this yields

$$u_{*,\infty}^{n+1} = \mathrm{e}^{-i\frac{\tau}{2}\frac{\Delta}{2}} \mathrm{e}^{-i\tau\frac{3}{8}|\mathrm{e}^{-i\frac{\tau}{2}\frac{\Delta}{2}} u_{*,\infty}^n|^2} \mathrm{e}^{-i\frac{\tau}{2}\frac{\Delta}{2}} u_{*,\infty}^n$$

as a second-order numerical approximation to $u_*(t_n)$ in (2.31). The assertion follows from [26] thanks to the approximation

$$\|u_*(t_n) - u_{*,\infty}^n\|_r \leq \|u_*(t_n) - u_{*,\infty}(t_n)\|_r + \|u_{*,\infty}(t_n) - u_{*,\infty}^n\|_r = \mathcal{O}\big(c^{-2} + \tau^2\big).$$

In the next section we numerically underline the first- and second-order convergence results of the uniformly accurate exponential-type integration schemes. Furthermore, we numerically compare our uniformly accurate methods with standard time integration schemes in Section 2.4.4.

2.4 Numerical Experiments for the Klein–Gordon Equation

In this section we numerically underline first-, respectively, second-order convergence uniformly in c of the newly developed exponential-type integration schemes (2.39) and (2.93). We also confirm the convergence of the first- and second-order uniformly accurate schemes to the corresponding limit integrator for $c \to \infty$. We consider the Klein–Gordon equation on the one dimensional torus, i.e. $x \in \mathbb{T} = [0, 2\pi]$ and on a finite time interval, i.e. $t \in [0, T]$. In all numerical experiments we use a standard Fourier pseudospectral method for the spatial discretization. For more details on pseudospectral methods we refer to [27, 69, 70]. The mesh-size is denoted by $h = \frac{2\pi}{M}$, for $M \in \mathbb{N}$ with grid points $x_j = jh$ and time step size $\tau = \frac{T}{N}$ with grid points $t_n = n\tau$, for $j = 0, ..., M$ and $n = 0, ..., N$, respectively. In order to use the Fourier transform efficiently we choose $M = 2^k$, with $k \in \mathbb{N}$. For practical implementation of the Fourier transform in Matlab, we introduce the Fourier grid $K = \big[-\frac{M}{2} : -1, 0, 1 : \frac{M}{2} - 1\big]$.
In the following we choose $M = 2^{10}$, i.e. we have the spatial mesh-size $h = 0.0061$, and integrate up to $T = 1$ in all numerical simulations.
In all numerical methods for the Klein–Gordon equation we use the following initial values

$$\begin{aligned} z(0, x) &= \frac{1}{2}\frac{\cos(3x)^2 \sin(2x)}{2 - \cos(x)}, \\ \partial_t z(0, x) &= c^2 \frac{1}{2}\frac{\sin(x)\cos(2x)}{2 - \cos(x)}. \end{aligned} \tag{2.101}$$

Since we cannot state an exact solution of the Klein–Gordon we have to compute a reference solution. Therefore, in Section 2.4.1 we derive a Gautschi-type method following the ansatz of [9] in order to compute the reference solution. We also derive a classical exponential integrator. Then, we recall the numerical method for the limit system in Section 2.4.2 and the uniformly accurate methods in Section 2.4.3. Finally, we compare the different numerical methods in Section 2.4.4.

2.4.1 Numerical Methods for the Reference Solution

In this subsection based on [4, 39] we state two types of numerical reference methods, namely a second-order Gautschi-type method in Section 2.4.1.1 and a first-order exponential integrator in Section 2.4.1.2 for the Klein–Gordon equation.

2.4.1.1 A Gautschi-type Method for the Klein–Gordon Equation

We use the techniques of [4] for the construction of a two step Gautschi-type method. Therefore, we recall the Klein–Gordon equation

$$\partial_{tt} z + c^2 \langle\nabla\rangle_c^2 z = c^2 |z|^2 z, \qquad z(0) = z_0, \quad \partial_t z(0) = c^2 z_1.$$

Using the variation of constants formula for second-order equations, we obtain

$$\begin{aligned} z(t_n+\tau) &= \cos(\tau c\langle\nabla\rangle_c) z(t_n) + \tau \frac{\sin(\tau c\langle\nabla\rangle_c)}{\tau c\langle\nabla\rangle_c} \dot z(t_n) + c^2 \int_0^\tau \frac{\sin\left((\tau-s)c\langle\nabla\rangle_c\right)}{c\langle\nabla\rangle_c} |z(t_n+s)|^2 z(t_n+s) \mathrm{d}s, \\ \dot z(t_n+\tau) &= -c\langle\nabla\rangle_c \sin(\tau c\langle\nabla\rangle_c) z(t_n) + \cos(\tau c\langle\nabla\rangle_c)\dot z(t_n) \\ &\qquad + c^2 \int_0^\tau \cos\left((\tau-s)c\langle\nabla\rangle_c\right) |z(t_n+s)|^2 z(t_n+s) \mathrm{d}s, \end{aligned} \tag{2.102}$$

where $\dot z$ denotes the partial derivative of z with respect to t.

For $n=0$ we have

$$\begin{aligned} z(t_1) &= \cos(\tau c\langle\nabla\rangle_c) z(0) + \tau \frac{\sin(\tau c\langle\nabla\rangle_c)}{\tau c\langle\nabla\rangle_c} \dot z(0) + c^2 \int_0^\tau \frac{\sin\left((\tau-s)c\langle\nabla\rangle_c\right)}{c\langle\nabla\rangle_c} |z(s)|^2 z(s) \mathrm{d}s, \\ \dot z(t_1) &= -c\langle\nabla\rangle_c \sin(\tau c\langle\nabla\rangle_c) z(0) + \cos(\tau c\langle\nabla\rangle_c)\dot z(0) + c^2 \int_0^\tau \cos\left((\tau-s)c\langle\nabla\rangle_c\right) |z(s)|^2 z(s) \mathrm{d}s. \end{aligned} \tag{2.103}$$

For $n \geq 1$, we consider the solution z in t_{n+1} and t_{n-1} in (2.102) and add $z(t_{n+1})$ and $z(t_{n-1})$, such that with $\cos(-x) = \cos(x)$ and $\sin(-x) = -\sin(x)$ we have that

$$\begin{aligned} z(t_{n+1}) + z(t_{n-1}) &= 2\cos(\tau c\langle\nabla\rangle_c) z(t_n) \\ &\qquad + c^2 \int_0^\tau \frac{\sin\left((\tau-s)c\langle\nabla\rangle_c\right)}{c\langle\nabla\rangle_c} \Big(|z(t_n+s)|^2 z(t_n+s) + |z(t_n-s)|^2 z(t_n-s) \Big) \mathrm{d}s, \\ \dot z(t_{n+1}) + \dot z(t_{n-1}) &= 2\cos(\tau c\langle\nabla\rangle_c) \dot z(0) \\ &\qquad + c^2 \int_0^\tau \cos\left((\tau-s)c\langle\nabla\rangle_c\right) \Big(|z(t_n+s)|^2 z(t_n+s) + |z(t_n-s)|^2 z(t_n-s) \Big) \mathrm{d}s. \end{aligned}$$

We solve the equations for $z(t_{n+1})$, $\dot{z}(t_{n+1})$ and obtain

$$\begin{aligned} z(t_{n+1}) &= 2\cos(\tau c\langle\nabla\rangle_c)z(t_n) - z(t_{n-1}) \\ &\quad + c^2 \int_0^\tau \frac{\sin\left((\tau-s)c\langle\nabla\rangle_c\right)}{c\langle\nabla\rangle_c}\Big(|z(t_n+s)|^2 z(t_n+s) + |z(t_n-s)|^2 z(t_n-s)\Big)\mathrm{d}s, \\ \dot{z}(t_{n+1}) &= 2\cos(\tau c\langle\nabla\rangle_c)\dot{z}(t_n) - \dot{z}(t_{n-1}) \\ &\quad + c^2 \int_0^\tau \cos\left((\tau-s)c\langle\nabla\rangle_c\right)\Big(|z(t_n+s)|^2 z(t_n+s) + |z(t_n-s)|^2 z(t_n-s)\Big)\mathrm{d}s. \end{aligned} \tag{2.104}$$

We approximate the integrals in (2.104) as follows

$$\begin{aligned} &\int_0^\tau \frac{\sin\left((\tau-s)c\langle\nabla\rangle_c\right)}{c\langle\nabla\rangle_c}\Big(|z(t_n+s)|^2 z(t_n+s) + |z(t_n-s)|^2 z(t_n-s)\Big)\mathrm{d}s \\ &\qquad\approx 2\int_0^\tau \frac{\sin\left((\tau-s)c\langle\nabla\rangle_c\right)}{c\langle\nabla\rangle_c}\mathrm{d}s\,|z(t_n)|^2 z(t_n) \\ &\qquad= 2\frac{1-\cos(\tau c\langle\nabla\rangle_c)}{c^2\langle\nabla\rangle_c^2}|z(t_n)|^2 z(t_n), \\ &\int_0^\tau \cos\left((\tau-s)c\langle\nabla\rangle_c\right)\Big(|z(t_n+s)|^2 z(t_n+s) + |z(t_n-s)|^2 z(t_n-s)\Big)\mathrm{d}s \\ &\qquad\approx 2\int_0^\tau \cos\left((\tau-s)c\langle\nabla\rangle_c\right)\mathrm{d}s\,|z(t_n)|^2 z(t_n) \\ &\qquad= 2\frac{\sin(\tau c\langle\nabla\rangle_c)}{c\langle\nabla\rangle_c}|z(t_n)|^2 z(t_n). \end{aligned} \tag{2.105}$$

Next, we compute the integrals in (2.103) with the same approximation as in (2.105) and insert the approximations (2.105) into (2.104). Therefore, we obtain the following two step iteration scheme for $n = 0$

$$\begin{aligned} z^1 &= \cos(\tau c\langle\nabla\rangle_c)z^0 + \tau\frac{\sin(\tau c\langle\nabla\rangle_c)}{\tau c\langle\nabla\rangle_c}\dot{z}^0 + c^2\frac{1-\cos(\tau c\langle\nabla\rangle_c)}{c^2\langle\nabla\rangle_c^2}|z^0|^2 z^0, \\ \dot{z}^1 &= -c\langle\nabla\rangle_c\sin(\tau c\langle\nabla\rangle_c)z^0 + \cos(\tau c\langle\nabla\rangle_c)\dot{z}^0 + c^2\frac{\sin(\tau c\langle\nabla\rangle_c)}{c\langle\nabla\rangle_c}|z^0|^2 z^0, \end{aligned}$$

and for $n \geq 1$

$$\begin{aligned} z^{n+1} &= 2\cos(\tau c\langle\nabla\rangle_c)z^n - z^{n-1} + 2c^2\frac{1-\cos(\tau c\langle\nabla\rangle_c)}{c^2\langle\nabla\rangle_c^2}|z^n|^2 z^n, \\ \dot{z}^{n+1} &= 2\cos(\tau c\langle\nabla\rangle_c)\dot{z}^n - \dot{z}^{n-1} + 2c^2\frac{\sin(\tau c\langle\nabla\rangle_c)}{c\langle\nabla\rangle_c}|z^n|^2 z^n \end{aligned}$$

with initial data

$$z^0 = z(0), \qquad \dot{z}^0 = \partial_t z(0).$$

For a detailed error analysis of this method we refer to [4]. We implement the Gautschi-type method in order to obtain a reference solution for our Klein–Gordon equation. For the spatial discretization we use a Fourier pseudospectral method with the largest Fourier mode $M = 2^{10}$ (i.e., the spatial mesh-size $h = 0.0061$) and integrate up to time $T = 1$. In Figure 2.4 we plot (double logarithmic) the time step size versus the error in z measured in a discrete H^1 norm for different values $c = 1, 5, 10, 50, 100$. As a reference solution we use the scheme itself with a finer time step size $\tau \approx 10^{-6}$. Figure 2.4 confirms the behavior of the numerical solution, shown in Figure 2.1, i.e., that it suffers from severe time step restrictions.

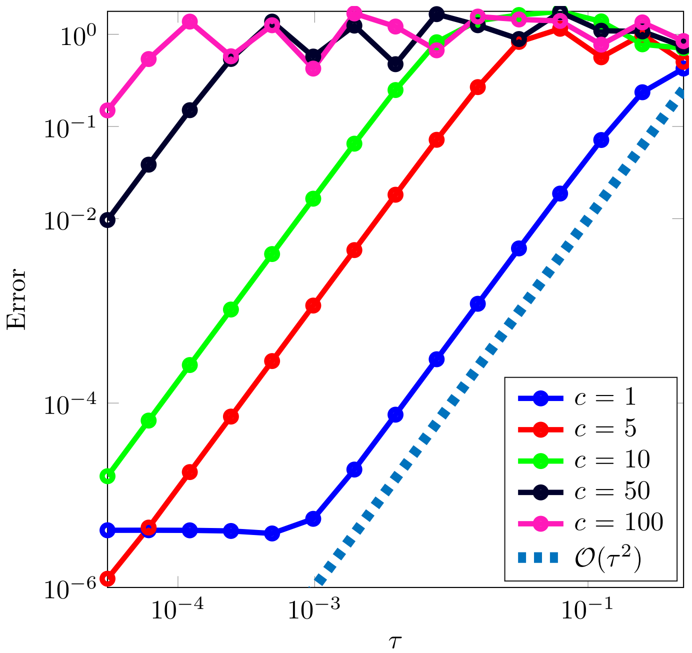

Figure 2.4: Order plot of the Gautschi-type method (double logarithmic scale). Time step size versus error. The slope of the dashed line is two. Reference solution computed via the scheme itself with a finer time step size $\tau \approx 10^{-6}$.

2.4.1.2 A Classical Exponential Integrator for the Klein–Gordon Equation

Based on [39], we now derive a classical exponential integration scheme for the Klein–Gordon equation. For more details and a rigorous error analysis of exponential integrators we refer to [39]. The KG equation in its first-order formulation in time (see (2.7)) reads

$$\begin{aligned} i\partial_t u &= -c\langle\nabla\rangle_c u + \frac{1}{8}c\langle\nabla\rangle_c^{-1}|u+\overline{v}|^2(u+\overline{v}), \qquad u(0) = z_0 - ic\langle\nabla\rangle_c^{-1} z_1, \\ i\partial_t v &= -c\langle\nabla\rangle_c v + \frac{1}{8}c\langle\nabla\rangle_c^{-1}|\overline{u}+v|^2(\overline{u}+v), \qquad v(0) = \overline{z}_0 - ic\langle\nabla\rangle_c^{-1} \overline{z}_1. \end{aligned}$$

In a first step, we apply Duhamel's formula to the above system, i.e.,

$$\begin{aligned} u(t_n+\tau) &= \mathrm{e}^{i\tau c\langle\nabla\rangle_c} u(t_n) - \frac{i}{8}c\langle\nabla\rangle_c^{-1}\int_0^\tau \mathrm{e}^{i(\tau-s)c\langle\nabla\rangle_c}|u(t_n+s)+\overline{v}(t_n+s)|^2(u(t_n+s)+\overline{v}(t_n+s))\mathrm{d}s, \\ v(t_n+\tau) &= \mathrm{e}^{i\tau c\langle\nabla\rangle_c} v(t_n) - \frac{i}{8}c\langle\nabla\rangle_c^{-1}\int_0^\tau \mathrm{e}^{i(\tau-s)c\langle\nabla\rangle_c}|\overline{u}(t_n+s)+v(t_n+s)|^2(\overline{u}(t_n+s)+v(t_n+s))\mathrm{d}s \end{aligned}$$

and then approximate the integrals in the simplest way, i.e. by freezing the nonlinearity at $s = 0$ and integrating the remaining exponential term exactly. This yields the following first-order exponential integration scheme

$$\begin{aligned} u^{n+1} &= \mathrm{e}^{i\tau c\langle\nabla\rangle_c} u^n - \tau\frac{i}{8}c\langle\nabla\rangle_c^{-1}\mathrm{e}^{i\tau c\langle\nabla\rangle_c}\varphi_1\left(-i\tau c\langle\nabla\rangle_c\right)|u^n+\overline{v}^n|^2(u^n+\overline{v}^n), \\ v^{n+1} &= \mathrm{e}^{i\tau c\langle\nabla\rangle_c} v^n - \tau\frac{i}{8}c\langle\nabla\rangle_c^{-1}\mathrm{e}^{i\tau c\langle\nabla\rangle_c}\varphi_1\left(-i\tau c\langle\nabla\rangle_c\right)|\overline{u}^n+v^n|^2(\overline{u}^n+v^n), \end{aligned}$$

which we implement for our numerical experiments, in order to obtain a reference solution for our Klein–Gordon equation. In Figure 2.5 we plot (double logarithmic) the time step size versus the error in z

measured in a discrete H^1 norm for different values $c = 1, 5, 10, 50, 100, 500$. As a reference solution we use the scheme itself with a finer time step size $\tau \approx 10^{-7}$. Furthermore, Figure 2.5 also underlines the time step restrictions for large values of c, similar to the Gautschi scheme (see Figure 2.4).

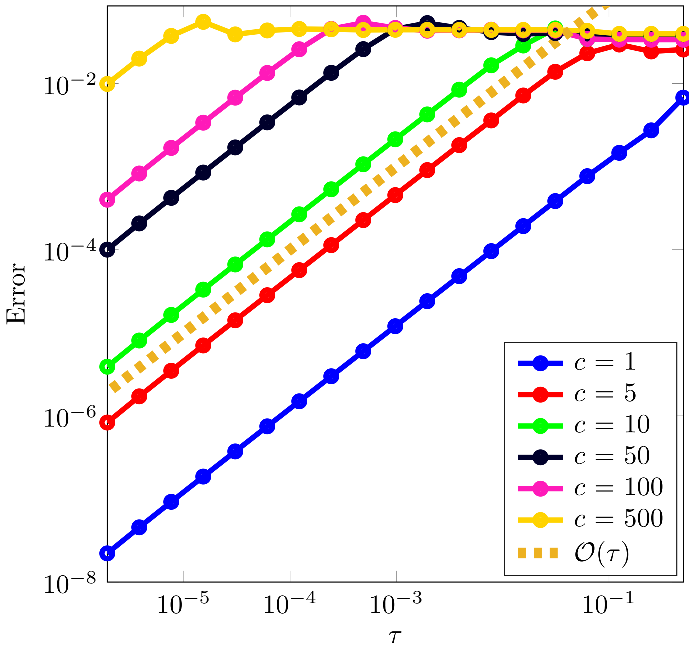

Figure 2.5: Order plot of the first-order exponential integrator (double logarithmic scale). The slope of the dashed line is one. Reference solution computed via the scheme itself with a finer time step size $\tau \approx 10^{-7}$.

2.4.2 Numerical Methods for the Limit System

In Section 2.2 we derived the following limit system of the Klein–Gordon equation for $c \to \infty$, were the solution z satisfies

$$z(t,x) = \frac{1}{2}\left(\mathrm{e}^{ic^2t}u_\infty(t,x) + \mathrm{e}^{-ic^2t}\overline{v_\infty}(t,x)\right) + \mathcal{O}(c^{-2}),$$

where u_∞, v_∞ solve the following NLS system

$$\begin{aligned} i\partial_t u_\infty &= \frac{1}{2}\Delta u_\infty + \frac{1}{8}\left(\left|u_\infty\right|^2 + 2\left|v_\infty\right|^2\right)u_\infty, \\ i\partial_t v_\infty &= \frac{1}{2}\Delta v_\infty + \frac{1}{8}\left(\left|v_\infty\right|^2 + 2\left|u_\infty\right|^2\right)v_\infty \end{aligned} \tag{2.106}$$

with initial values

$$u_\infty(0) = z_0 - iz_1, \qquad v_\infty(0) = \overline{z_0} - i\overline{z_1}.$$

Because this system is independent of c, its solution is non-oscillatory, which is a huge benefit from the numerical point of view. This allows us to solve it via a classical splitting method. For more details on splitting methods and a detailed analysis we refer to [25, 50]. Thus, we naturally split the right hand side of (2.106) for u_∞ into the subproblems

$$\begin{aligned} &\text{(S1)} \qquad i\partial_t u_\infty = \frac{1}{2}\Delta u_\infty, \\ &\text{(S2)} \qquad i\partial_t u_\infty = \frac{1}{8}\left(|u_\infty|^2 + 2|v_\infty|^2\right)u_\infty. \end{aligned}$$

Analogously we split the equation for v_∞. The solution of (S1) is given through

$$u_\infty(t_n+\tau) = \mathrm{e}^{-\frac{i}{2}\tau\Delta} u_\infty(t_n).$$

Before considering (S2) we take a closer look on $|u_\infty|^2$ and derivate it with respect to t. This yields

$$\begin{aligned}
\partial_t |u_\infty|^2 &= \partial_t (u_\infty \overline{u_\infty}) = \overline{u_\infty}\partial_t u_\infty + u_\infty \partial_t \overline{u_\infty} \\
&= \overline{u_\infty}\left(-\frac{i}{8}\left(|u_\infty|^2 + 2|v_\infty|^2\right) u_\infty\right) + u_\infty \overline{\left(-\frac{i}{8}\left(|u_\infty|^2 + 2|v_\infty|^2\right) u_\infty\right)} \\
&= -\frac{i}{8}\left(|u_\infty|^2 + 2|v_\infty|^2\right)|u_\infty|^2 + \frac{i}{8}\left(|u_\infty|^2 + 2|v_\infty|^2\right)|u_\infty|^2 = 0.
\end{aligned}$$

Thus, the term $|u_\infty(t)|^2 = |u_\infty(0)|^2$ is constant with respect to t, which allows us to also solve subproblem (S2) exactly in time. Therefore, we obtain

$$u_\infty(t_n+\tau) = \mathrm{e}^{-\frac{i}{8}\tau\left(|u_\infty(t_n)|^2 + 2|v_\infty(t_n)|^2\right)} u_\infty(t_n).$$

Connecting the two subproblems, we obtain the following iterative Lie splitting scheme

$$u_\infty^{n+1} = \mathrm{e}^{-\frac{i}{2}\tau\Delta}\mathrm{e}^{-\frac{i}{8}\tau\left(|u_\infty^n|^2 + 2|v_\infty^n|^2\right)} u_\infty^n.$$

The Lie splitting scheme is a first-order numerical method. In order to compare the limit integration scheme with the methods for the reference solution and our uniformly accurate methods, we state a second-order splitting method called Strang splitting scheme. The Strang splitting reads

$$u_\infty^{n+1} = \mathrm{e}^{-\frac{i}{2}\frac{\tau}{2}\Delta}\mathrm{e}^{-\frac{i}{8}\tau\left(\left|\mathrm{e}^{-\frac{i}{2}\frac{\tau}{2}\Delta}u_\infty^n\right|^2 + 2\left|\mathrm{e}^{-\frac{i}{2}\frac{\tau}{2}\Delta}v_\infty^n\right|^2\right)}\mathrm{e}^{-\frac{i}{2}\frac{\tau}{2}\Delta} u_\infty^n.$$

In Figure 2.6 we numerically confirm the convergence order in time of our first- and second-order splitting method for our limit system, respectively. In the figure we plot time step size versus the error of the Lie and Strang splitting method. The error in u_∞ is measured in a discrete H^1 norm. As a reference solution we use the scheme itself with a finer time step size $\tau \approx 10^{-7}$. For the spatial discretization we use a Fourier pseudospectral method with the largest Fourier mode $M = 2^{10}$ and integrate up to $T = 1$.

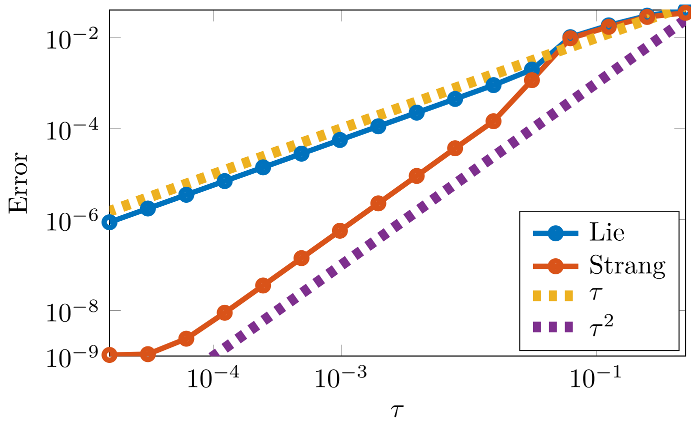

Figure 2.6: Order plot of the first- and second-order limit method (double logarithmic scale). The slope of the yellow dashed line is one and the slope of the purple dashed line is two. Reference solution computed via the scheme itself with a finer time step size $\tau \approx 10^{-7}$.

2.4.3 Uniformly Accurate Methods for the Klein–Gordon Equation

In this subsection we underline the first- and second-order convergence rate of our newly derived uniformly accurate methods with numerical experiments. Recall that in Section 2.3.2 we derived the first-order uniformly accurate scheme for the Klein–Gordon equation, which reads

$$\begin{aligned}
u_*^{n+1} &= \mathrm{e}^{i\tau\mathcal{A}_c}\mathrm{e}^{-\tau\frac{3i}{8}|u_*^n|^2}u_*^n - \tau\frac{3i}{8}\left(c\langle\nabla\rangle_c^{-1}-1\right)\mathrm{e}^{i\tau\mathcal{A}_c}|u_*^n|^2u_*^n\\
&\quad - \tau\frac{i}{8}c\langle\nabla\rangle_c^{-1}\mathrm{e}^{i\tau\mathcal{A}_c}\Big\{\mathrm{e}^{2ic^2t_n}\ \varphi_1(2ic^2\tau)(u_*^n)^3 + 3\mathrm{e}^{-2ic^2t_n}\ \varphi_1(-2ic^2\tau)|u_*^n|^2\overline{u_*^n}\\
&\qquad\qquad + \mathrm{e}^{-4ic^2t_n}\varphi_1(-4ic^2\tau)(\overline{u_*^n})^3\Big\},\\
u_*^0 &= z_0 - ic\langle\nabla\rangle_c^{-1}z_1,
\end{aligned}$$

and in Section 2.3.3 the second-order uniformly accurate method

$$\begin{aligned}
u_*^{n+1} &= \mathrm{e}^{i\frac{\tau}{2}\mathcal{A}_c}\mathrm{e}^{-i\tau\frac{3}{8}\left|\mathrm{e}^{i\frac{\tau}{2}\mathcal{A}_c}u_*^n\right|^2}\mathrm{e}^{i\frac{\tau}{2}\mathcal{A}_c}u_*^n\\
&\quad - \tau\frac{3i}{8}\Big(c\langle\nabla\rangle_c^{-1}-1\Big)\mathrm{e}^{i\frac{\tau}{2}\mathcal{A}_c}\left|\mathrm{e}^{i\frac{\tau}{2}\mathcal{A}_c}u_*^n\right|^2\mathrm{e}^{i\frac{\tau}{2}\mathcal{A}_c}u_*^n + \tau^2\theta_{c\langle\nabla\rangle_c-1}\left(t_n,\tau,\mathrm{e}^{i\frac{\tau}{2}\mathcal{A}_c}u_*^n\right)\\
&\quad - \tau^2\frac{3}{64}c\langle\nabla\rangle_c^{-1}\Big[2\,|u_*^n|^2\,c\langle\nabla\rangle_c^{-1}\vartheta_{c^2}(t_n,\tau,u_*^n) - (u_*^n)^2\,c\langle\nabla\rangle_c^{-1}\overline{\vartheta_{c^2}}(t_n,\tau,u_*^n)\Big]\\
&\quad - \frac{i}{8}c\langle\nabla\rangle_c^{-1}I_{c^2}^1(\tau,t_n,u_*^n),\\
u_*^0 &= z_0 - ic\langle\nabla\rangle_c^{-1}z_1
\end{aligned}$$

with the abbreviations

$$\begin{aligned}
\theta_{c\langle\nabla\rangle_c-1}\left(t_n,\tau,\mathrm{e}^{i\frac{\tau}{2}\mathcal{A}_c}u_*^n\right) &= -\frac{1}{2}\frac{9}{64}\mathrm{e}^{i\frac{\tau}{2}\mathcal{A}_c}\Big(c\langle\nabla\rangle_c^{-1}-1\Big)\left|\mathrm{e}^{i\frac{\tau}{2}\mathcal{A}_c}u_*^n\right|^4\mathrm{e}^{i\frac{\tau}{2}\mathcal{A}_c}u_*^n\\
&\quad - \frac{1}{2}\frac{9}{32}c\langle\nabla\rangle_c^{-1}\mathrm{e}^{i\frac{\tau}{2}\mathcal{A}_c}\left|\mathrm{e}^{i\frac{\tau}{2}\mathcal{A}_c}u_*^n\right|^2\Big(c\langle\nabla\rangle_c^{-1}-1\Big)\left|\mathrm{e}^{i\frac{\tau}{2}\mathcal{A}_c}u_*^n\right|^2\mathrm{e}^{i\frac{\tau}{2}\mathcal{A}_c}u_*^n\\
&\quad + \frac{1}{2}\frac{9}{64}c\langle\nabla\rangle_c^{-1}\mathrm{e}^{i\frac{\tau}{2}\mathcal{A}_c}v^2\Big(c\langle\nabla\rangle_c^{-1}-1\Big)\left|\mathrm{e}^{i\frac{\tau}{2}\mathcal{A}_c}u_*^n\right|^2\mathrm{e}^{-i\frac{\tau}{2}\mathcal{A}_c}\overline{u_*^n},\\
\vartheta_{c^2}(t_n,\tau,u_*^n) &= \mathrm{e}^{2ic^2t_n}\varphi_2\left(2i\tau c^2\right)(u_*^n)^3 + 3\mathrm{e}^{-2ic^2t_n}\varphi_2\left(-2i\tau c^2\right)|u_*^n|^2\overline{u_*^n}\\
&\quad + \mathrm{e}^{-4ic^2t_n}\varphi_2\left(-4i\tau c^2\right)(\overline{u_*^n})^3,
\end{aligned}$$

and

$$\begin{aligned}
I_{c^2}^1(\tau,t_n,u_*^n) &= \tau\mathrm{e}^{2ic^2t_n}\mathrm{e}^{i\tau\mathcal{A}_c}\varphi_1\left(i\tau(2c^2-\tfrac{1}{2}\Delta)\right)(u_*^n)^3\\
&\quad + i\tau^2\mathrm{e}^{2ic^2t_n}\mathrm{e}^{i\tau\mathcal{A}_c}\Psi_2\left(i\tau(2c^2-\tfrac{1}{2}\Delta)\right)\Big[(\tfrac{1}{2}\Delta-\mathcal{A}_c)(u_*^n)^3 + 3(u_*^n)^2\mathcal{A}_cu_*^n\Big]\\
&\quad + 3\tau\mathrm{e}^{-2ic^2t_n}\mathrm{e}^{i\tau\mathcal{A}_c}\varphi_1(i\tau(-2c^2-\mathcal{A}_c))\,|u_*^n|^2\,\overline{u_*^n}\\
&\quad + 3i\tau^2\mathrm{e}^{-2ic^2t_n}\mathrm{e}^{i\tau\mathcal{A}_c}\Psi_2(i\tau(-2c^2-\mathcal{A}_c))\Big[\overline{u_*^n}^2\mathcal{A}_cu_*^n - 2|u_*^n|^2\mathcal{A}_c\overline{u_*^n}\Big]\\
&\quad + \tau\mathrm{e}^{-4ic^2t_n}\mathrm{e}^{i\tau\mathcal{A}_c}\varphi_1(i\tau(-4c^2-\mathcal{A}_c))\overline{u_*^n}^3\\
&\quad - i\tau^2\mathrm{e}^{-4ic^2t_n}\mathrm{e}^{i\tau\mathcal{A}_c}\Psi_2(i\tau(-4c^2-\mathcal{A}_c))3\overline{u_*^n}^2\mathcal{A}_c\overline{u_*^n}\\
&\quad - \tau^2\frac{3i}{8}\mathrm{e}^{2ic^2t_n}\,(u_*^n)^2\,c\langle\nabla\rangle_c^{-1}\,\Big[3\Psi_2(2ic^2\tau)|u_*^n|^2u_*^n + \Omega_{c^2,2,}(t_n,\tau,u_*^n)\Big]\\
&\quad - \tau^2\frac{3i}{8}\mathrm{e}^{-2ic^2t_n}\,(\overline{u_*^n})^2\,c\langle\nabla\rangle_c^{-1}\Big[3\Psi_2(-2ic^2\tau)|u_*^n|^2u_*^n + \Omega_{c^2,-2}(t_n,\tau,u_*^n)\Big]\\
&\quad + \tau^2\frac{6i}{8}\mathrm{e}^{-2ic^2t_n}\,|u_*^n|^2\,c\langle\nabla\rangle_c^{-1}\,\Big[3\Psi_2(-2ic^2\tau)|u_*^n|^2\overline{u_*^n} + \overline{\Omega}_{c^2,-2}(t_n,\tau,u_*^n)\Big]\\
&\quad + \tau^2\frac{3i}{8}\mathrm{e}^{-4ic^2t_n}\,(\overline{u_*^n})^2\,c\langle\nabla\rangle_c^{-1}\,\Big[3\Psi_2(-4ic^2\tau)|u_*^n|^2\overline{u_*^n} + \overline{\Omega}_{c^2,-4}(t_n,\tau,u_*^n)\Big]
\end{aligned}$$

and

$$\begin{aligned}\Omega_{c^2,l}(t_n,\tau,u_*^n) = \mathrm{e}^{2ic^2t_n}&\frac{\varphi_1\left((l+2)ic^2\tau\right)-\varphi_1\left(lic^2\tau\right)}{2i\tau c^2}(u_*^n)^3\\ &+3\mathrm{e}^{-2ic^2t_n}\frac{\varphi_1\left((l-2)ic^2\tau\right)-\varphi_1\left(lic^2\tau\right)}{-2i\tau c^2}|u_*^n|^2\overline{u_*^n}\\ &+\mathrm{e}^{-4ic^2t_n}\frac{\varphi_1\left((l-4)ic^2\tau\right)-\varphi_1\left(lic^2\tau\right)}{-4i\tau c^2}(\overline{u_*^n})^3.\end{aligned}$$

In Figure 2.7 we numerically confirm the convergence order in time of the first- and second-order uniformly accurate method, respectively. We plot time step size versus the error of our uniformly accurate schemes for different values of $c = 1, 5, 10, 50, 100, 500, 1000, 5000, 10000$. The error in z is measured in a discrete H^1 norm. As a reference solution we use the scheme itself with a finer time step size $\tau \approx 10^{-7}$.

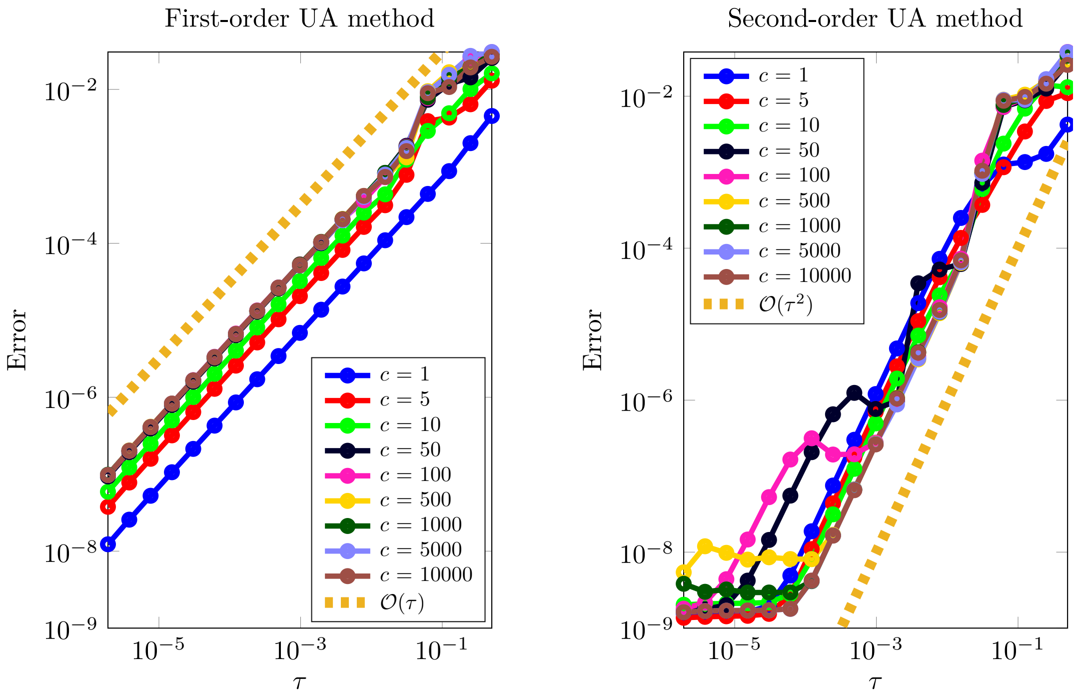

Figure 2.7: Order plot of the first- and second-order uniformly accurate method (double logarithmic scale). First-order method on the left, second-order method on the right. The slope of the dashed line is one and two, respectively. Reference solution computed via the scheme itself with a finer time step size $\tau \approx 10^{-7}$.

2.4.4 Comparison of the Numerical Methods

In this subsection we compare our uniformly accurate methods with the established Gautschi-type method, exponential integrator and limit scheme. We confirm that our newly derived uniformly accurate methods are uniformly accurate with respect to c and that they converge asymptotically to the corresponding limit scheme. Finally, we consider work-precision plots and compare the error constants.

We compare our newly derived uniformly accurate first- and second-order method with the first-order exponential integrator. This comparison (see Figure 2.8) confirms that our UA methods are uniformly accurate with respect to c. We use the first-order exponential integrator in order to compute the reference solution with time step size $\tau \approx 10^{-7}$ for different values of $c = 1, 5, 10, 50, 100$. The error between the exponential integrator and our uniformly accurate methods is measured in a discrete H^1 norm.

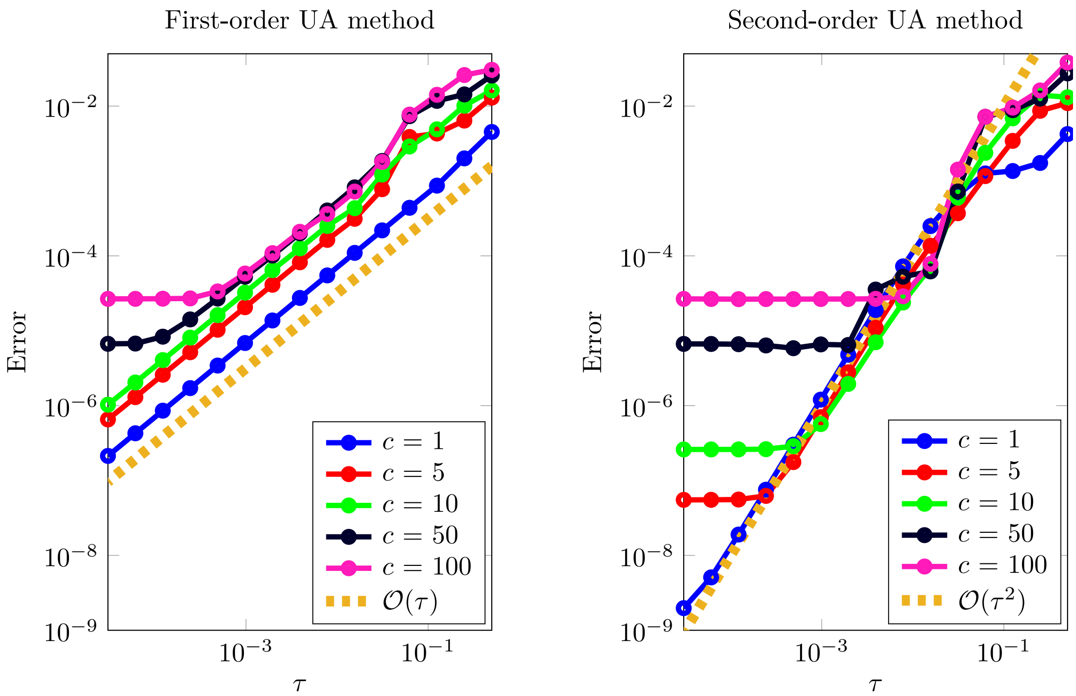

Figure 2.8: Order plot of the first- and second-order uniformly accurate method (double logarithmic scale). First-order method on the left, second-order method on the right. The slope of the dashed line is one and two, respectively. Reference solution computed via the classical exponential integrator with a finer time step size $\tau \approx 10^{-7}$.

Figure 2.9 confirms the asymptotic convergence to the corresponding numerical method for the limit system. Therefore, we plot the error of the UA method and the limit method versus different values of c. This yields the $\mathcal{O}(c^{-2})$ convergence, which is shown in Section 2.3 (Remark 2.19 and 2.34). The error in z is measured in a discrete H^1 norm.

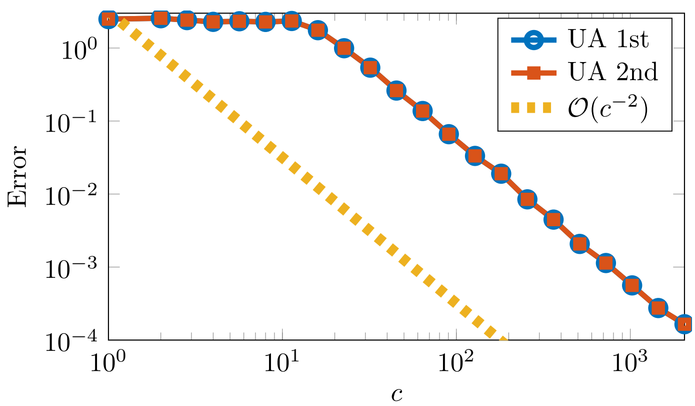

Figure 2.9: Asymptotic consistency plot (double logarithmic scale). The slope of the dashed line is -2.

Next, we compare the error of the different methods versus the computation time. Such an efficency plot is also called a work-precision plot and is given in Figure 2.10 and 2.11. The work-precision plots show the efficiency of the numerical methods for different values of c. We plot the corresponding error against the computation time (in seconds) of the corresponding numerical method. We desire values in the lower left corner, i.e. a small error at a short computation time. For the reference solution we use the exponential integrator with time step size $\tau \approx 10^{-6}$. We compare the error of the exponential integrator with the error of the Gautschi-type method, our uniformly accurate methods and the limit scheme. The errors are measured in a discrete H^1 norm.

We observe that the Gautschi-type method performs good for small c and fails for large c. For the limit scheme we observe this behavior vice versa, i.e. the limit scheme fails for small c and performs good for large c. Our uniformly accurate schemes show a good behavior for all values of c. We note that our uniformly accurate schemes reach smaller errors than both, the Gautschi-type method and the limit scheme.

We simulate the solution of the Klein–Gordon equation for two different initial values. Firstly, in Figure 2.10 we show a work-precision plot with the standard initial values (see (2.101)) and then in Figure 2.11 with the following initial values

$$z(0) = \frac{\cos(x)\sin(x)}{2-\cos(x)}, \qquad \partial_t z(0) = c^2 \frac{\sin(x)^2}{2-\cos(x)}.$$

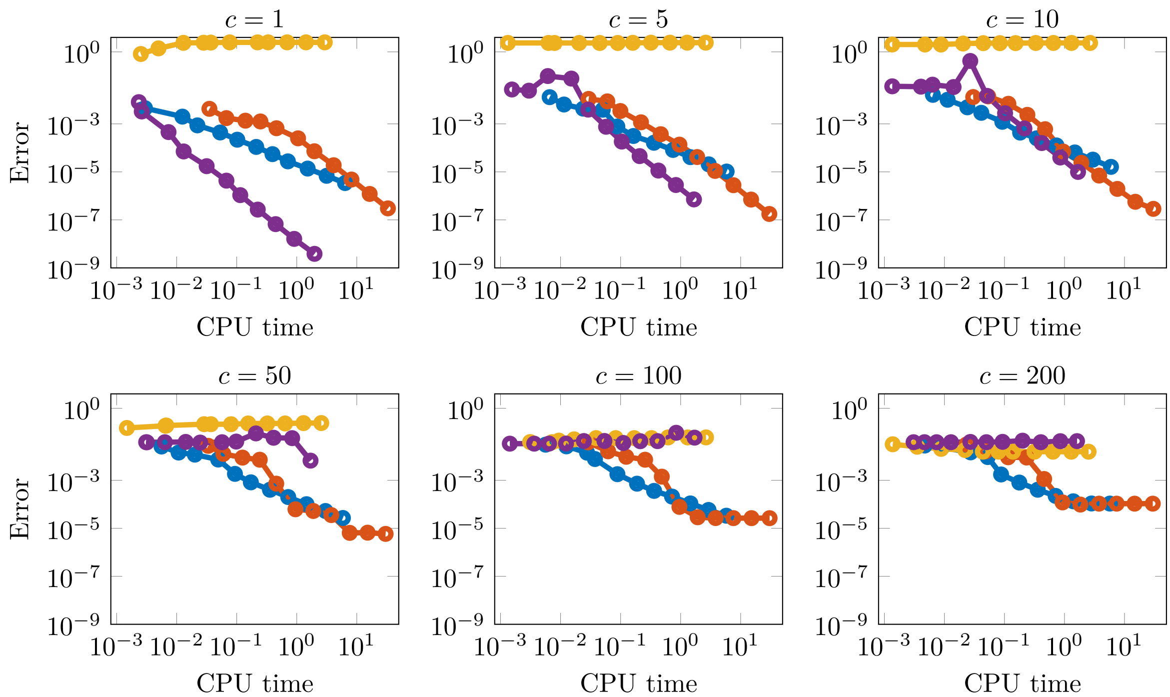

Figure 2.10: Work-precision plot (double logarithmic scale). The yellow lines mark the error of the limit scheme. The purple lines mark the error of the Gautschi-type method. The blue lines mark the error of our first-order uniformly accurate method and the red line mark the error of our second-order uniformly accurate method. The CPU time is measured in seconds. Reference solution computed via the classical exponential integrator with a finer time step size $\tau \approx 10^{-7}$.

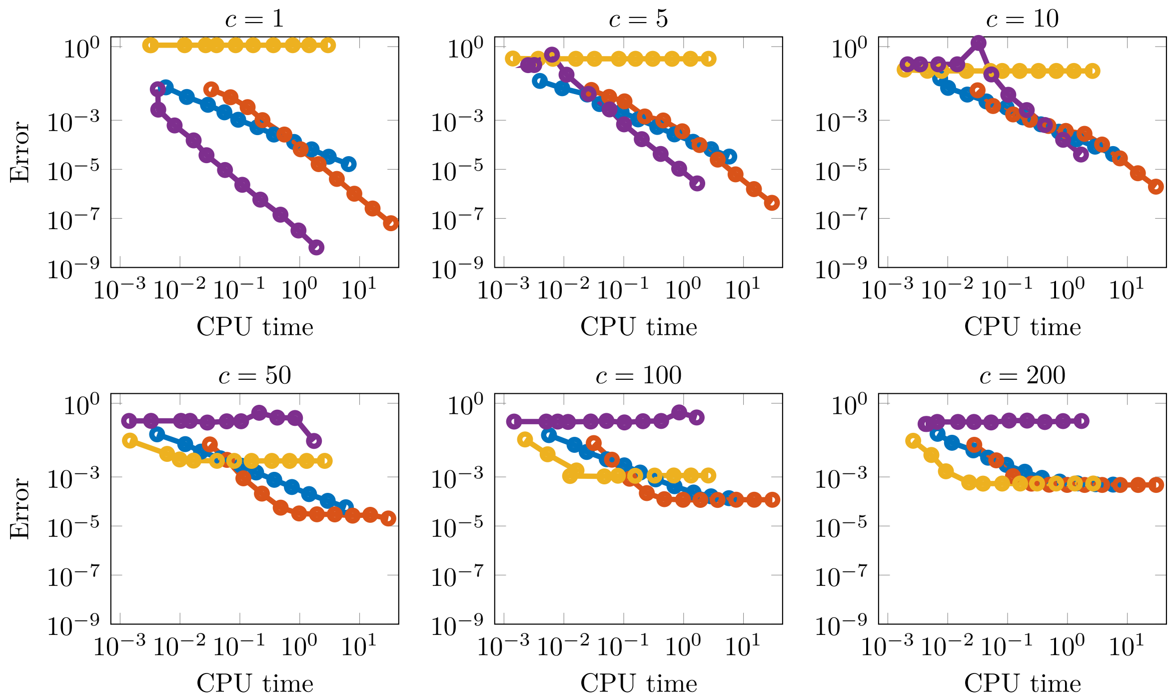

Figure 2.11: Work-precision plot (double logarithmic scale). The yellow lines mark the error of the limit scheme. The purple lines mark the error of the Gautschi-type method. The blue lines mark the error of our first-order uniformly accurate method and the red line mark the error of our second-order uniformly accurate method. The CPU time is measured in seconds. Reference solution computed via the classical exponential integrator with a finer time step size $\tau \approx 10^{-7}$.

Figure 2.11 shows a similar behavior as the plot in Figure 2.10. But we observe a better behavior of the limit scheme for large c in Figure 2.11. More precisely, we see in Figure 2.11 that for $c \geq 50$ the limit scheme is faster and more accurate than all the other schemes.

Now, we underline the different error constant behaviors of our UA methods. As a reference solution we use the classical exponential integrator with time step size $\tau \approx 10^{-6}$. We plot the numerical error of the corresponding numerical method against different values of c for different time step sizes τ. For our uniformly accurate methods we observe uniform bounds, whereas for the Gautschi-type method we obtain the expected $\mathcal{O}(c^4)$ error behavior (see Figure 2.12). In the plots of the uniformly accurate methods the error of the exponential integrator of order $\mathcal{O}(c^2)$ is obtained.

In the next chapter we consider the Klein–Gordon–Schrödinger system, which is a Klein–Gordon equation coupled with a Schrödinger equation. For this system we also derive a limit system and a uniformly accurate method analogously to the derivation for the KG equation.

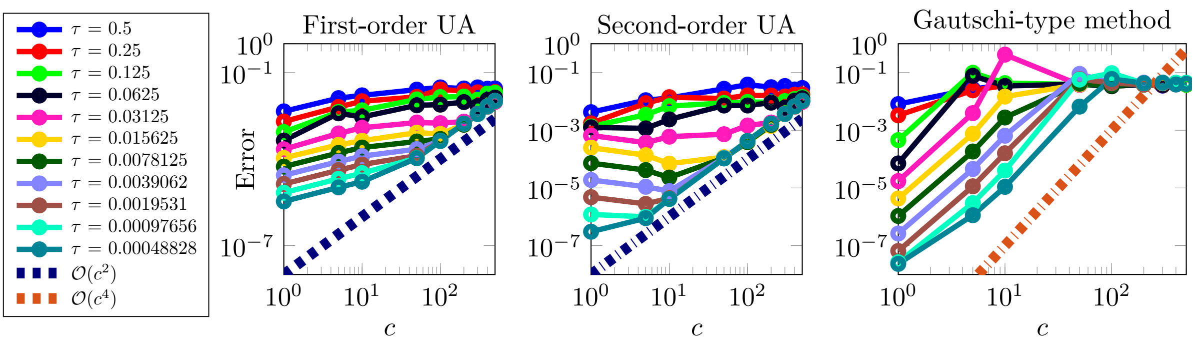

Figure 2.12: Error constant comparison plot (double logarithmic scale). On the left for the first-order uniformly accurate method, in the middle for the second-order uniformly accurate method and on the right for the Gautschi-type method. The slope of the dashed and dash-dotted line is two and four, respectively. Reference solution computed via the classical exponential integrator with a finer time step size $\tau \approx 10^{-6}$.

CHAPTER 3

The Klein–Gordon–Schrödinger System

In this chapter we focus on the construction of uniformly accurate methods for the Klein–Gordon–Schrödinger system. Thereby, we proceed analogously to Chapter 2 for the Klein–Gordon equation. In Section 3.1 we give a short overview of the limit regime and different standard methods for the Klein–Gordon–Schrödinger system. Then we focus in Section 3.2 on the formal derivation of the corresponding limit system. We close this chapter with a detailed derivation of a first- and second-order uniformly accurate method for the Klein–Gordon–Schrödinger system (see Section 3.3). The main references for this chapter are [26] for the derivation of the limit system and [14] for the overview and the uniformly accurate methods. The results of this chapter, in particular Section 3.3, have been published together with Georgia Kokkala and Katharina Schratz in [14]. The first-order uniformly accurate method, which will be derived within this chapter, was also introduced in the master thesis of Georgia Kokkala. In addition, we construct and analyze a second-order method in this thesis.

3.1 Introduction to Klein–Gordon–Schrödinger Systems

The Klein–Gordon–Schrödinger (KGS) system

$$\begin{aligned} c^{-2}\partial_{tt} z(t,x) - \Delta z(t,x) + c^2 z(t,x) &= |\mathfrak{n}(t,x)|^2, \\ i\partial_t \mathfrak{n}(t,x) + \Delta \mathfrak{n}(t,x) + \mathfrak{n}(t,x) z(t,x) &= 0 \end{aligned} \tag{3.1}$$

with initial conditions

$$\begin{aligned} z(0,x) &= z_0(x), \qquad \partial_t z(0,x) = c^2 z_1(x), \\ \mathfrak{n}(0,x) &= \mathfrak{n}_0(x), \end{aligned}$$

describes physically the dynamics of a complex-valued nucleon field $\mathfrak{n}$ interacting with a neutral real-valued scalar meson field z. In addition to the numerical challenge of the highly oscillatory Klein–Gordon equation from the previous chapter, we have to cope with the nonlinear coupling of the Klein–Gordon equation to a classical Schrödinger equation. For existence and uniqueness of global smooth solutions we refer to [28–30] and the references therein. Numerically, the Klein–Gordon–Schrödinger system is extensively studied in the *relativistic regime* $c = 1$, see for instance [7, 41, 44]. In contrast, the *non-relativistic regime*, where the speed of light c formally tends to infinity, is due to the highly oscillatory behavior of the solution much more demanding numerically. Similar to the Klein–Gordon equation in Chapter 2 classical numerical methods break down, also for the Klein–Gordon–Schrödinger system, as they fail to resolve the oscillations of the solution. In particular, severe step size restrictions need to be imposed which lead to huge computational efforts and which do not permit reasonably accurate simulations. Even more suitable Gautschi-type methods which are especially designed for numerically solving oscillatory second-order differential equations (see, e.g., [4, 36, 38]) do not allow a reasonable approximation as they fail to capture the highly oscillatory parts. This phenomenon is illustrated in Figure 3.1. In the slowly varying relativistic regime ($c = 1$) the Gautschi-type method allows a precise approximation of the solution, whereas it fails in the highly oscillatory non-relativistic regime ($c \gg 1$). For classical splitting-type methods we observe a similar error behavior as for the Gautschi-type methods. We refer to [25, 50] for their analysis in the context of Schrödinger equations.

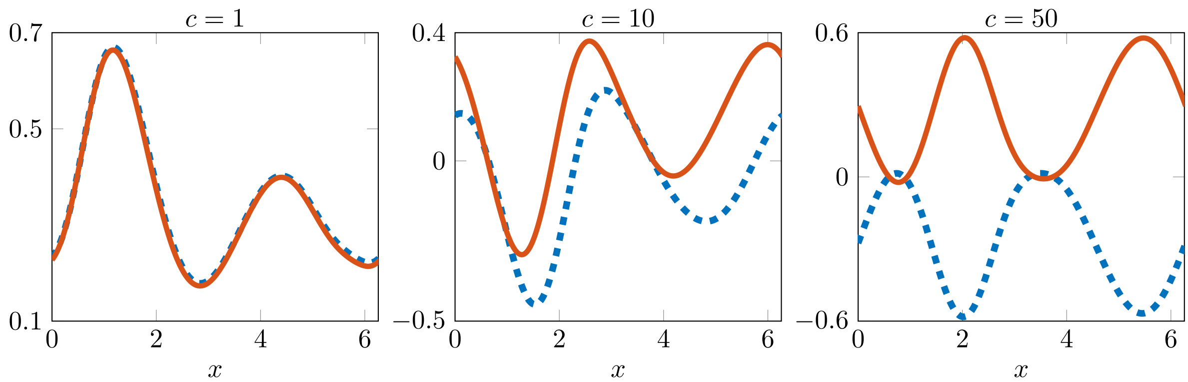

Figure 3.1: Numerical solution of the Klein–Gordon–Schrödinger system for z. Exponential Gautschi-type scheme (red solid line) for different c with time step size $\tau \approx 10^{-2}$ at time $t = 0.6$. The blue dashed line represents the reference solution at time $t = 0.6$, computed via the same exponential Gautschi-type scheme with a small time step size $\tau \approx 10^{-6}$. The spatial discretization is done via a Fourier pseudospectral method with mesh-size $h = 0.0245$.

Based on the modulated Fourier expansion of the exact solution (see [19, 36]) numerical schemes for the Klein–Gordon–Schrödinger system in the strongly non-relativistic limit regime $c \gg 1$ are introduced in Section 3.2. This ansatz allows us to reduce the highly oscillatory problem (3.1) to the integration of the corresponding *non-oscillatory free decoupled Schrödinger limit equation.* The limit system can be solved numerically very efficiently without imposing any $c-$dependent step size restriction, since we can solve it exactly in Fourier space (see Section 3.2). However, as this approach is based on the asymptotic expansion of the solution with respect to c^{-2} (see also Chapter 2), it only allows error bounds of order

$$\mathcal{O}(c^{-2}).$$

Henceforth, the limit integration method only yields an accurate approximation of the exact solution for sufficiently large values of c (see Figure 3.2). For more details on the formal derivation of the limit system we refer to Section 3.2.

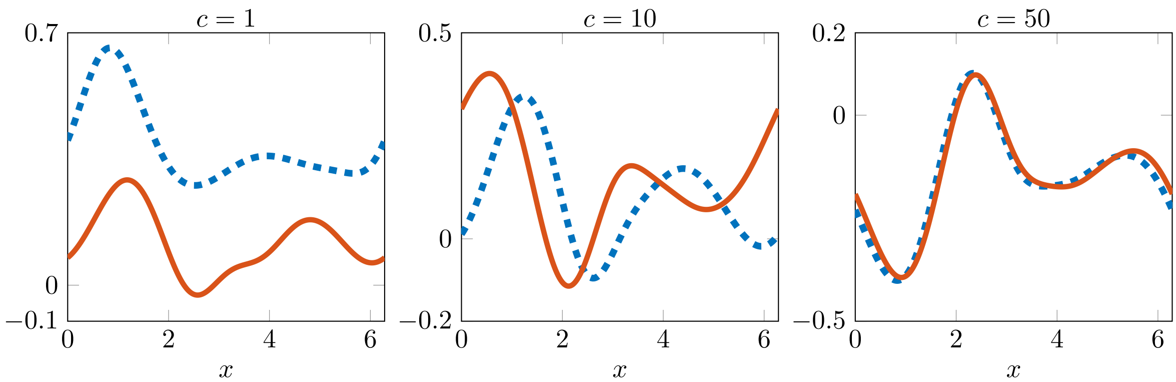

Figure 3.2: Numerical solution of the Klein–Gordon–Schrödinger system for z for different c. Limit integration scheme (red solid line) for different c with time step size $\tau \approx 10^{-2}$ at time $t = 1$. The blue dashed line represents the reference solution at time $t = 1$, computed via an exponential Gautschi-type scheme with a small time step size $\tau \approx 10^{-6}$. The spatial discretization is done via a Fourier pseudospectral method with mesh-size $h = 0.0245$.

Based on a multiscale expansion technique, an unconditionally stable accurate method for the Klein–Gordon–Schrödinger system with (and without) damping was recently presented in [8] (see also [10, 18] for results on classical Klein–Gordon equations). The corresponding method converges, for sufficiently smooth solutions, uniformly in time with linear convergence rate $\mathcal{O}(\tau)$ for $c \in [1, \infty)$. However, optimal quadratic convergence rate $\mathcal{O}(\tau^2)$ is only reached in the regime when either $c = \mathcal{O}(1)$ or $c\tau \geq 1$.

In comparison, we establish a novel class of exponential-type integrators which allow convergence with second-order accuracy in time uniformly for all $c > 0$. As we have seen in the previous Chapter 2 the key idea thereby lies again in exploiting the so-called *twisted variables* (see, e.g., [16, 17, 33, 73]). For more details on *twisted variables* in numerical analysis, for instance in the context of the modulated Fourier expansion we refer to [20, 36], for adiabatic integrators (see [36, 49]) and for Lawson-type Runge-Kutta methods (see [48]). Recently, this technique was also established in the numerical analysis of low-regularity problems (see [40, 58]). Compared to the previous chapter, the analysis of the numerical scheme in the Klein–Gordon–Schrödinger setting is much more involved due to the coupled structure of the underlying system. In particular, because their nonlinear resonance interaction strongly differs, we thus need to develop new, adapted techniques.

Let us explain the underlying strategy again in a nutshell. It follows the ideas of Section 2.3, but differs a litte bit due to the fact that in this chaper we consider a coupled system of PDEs.

In a first step we reformulate the Klein–Gordon part (in z) as a *first-order system in time* via the transformation

$$u = z - ic^{-1}\langle\nabla\rangle_c^{-1}\partial_t z$$

which allows us to reformulate the KGS system (3.1) as a coupled first-order system in the new variables $(u, \mathfrak{n})$ (see Section 3.3 for details). Then, by applying the key idea of *twisted variables*, we filter out the highly oscillatory phases

$$\mathrm{e}^{\pm i\ell c^2 t} \quad \text{with} \quad \ell \in \mathbb{Z}$$

explicitly (see also Section 3.3). Again the major numerical advantage of looking at the system in $(u_*, \mathfrak{n}_*)$ instead of $(u, \mathfrak{n})$ lies in the fact that $(\partial_t u_*, \partial_t \mathfrak{n}_*)$ is *bounded uniformly in* c, whereas $(\partial_t u, \partial_t \mathfrak{n})$ is of order c^2. This allows us to develop a novel class of *uniformly accurate* exponential-type integrators by iterating

Duhamel's formula in $(u_*, \mathfrak{n}_*)$. The essential point thereby lies in integrating the interactions of the highly oscillatory phases exactly and only approximating the slowly varying parts (see Section 3.3.2 and Section 3.3.3 for more details).

Analogously to the previous chapter, this strategy allows us to develop high-order uniformly accurate numerical methods which approximate Klein–Gordon–Schrödinger solutions from relativistic ($c = 1$) up to non-relativistic ($c \gg 1$) regimes. In addition to this uniform approximation property, another advantage of the novel class of integrators compared to classical methods is the following: the method converges asymptotically (i.e., for $c \to \infty$) to the numerical scheme of the corresponding decoupled free Schrödinger limit system ($c \to \infty$ in (3.1)). For details see Section 3.3.4.

Our theoretical convergence results are underlined with numerical experiments in Section 2.4.

For practical implementation issues, we impose in the following periodic boundary conditions, i.e., $x \in \mathbb{T}^d := [0, 2\pi]^d$.

3.2 Formal Derivation of the Limit System

In this section we start off with a formal derivation of the decoupled free Schrödinger limit system of the KGS system (3.1) by applying a multiscale analysis and a formal asymptotic expansion to the KGS system. In order to do this, we follow the ideas and techniques shown in [26]. Furthermore, we derive a numerical limit scheme that solves the decoupled free Schrödinger limit system. Essentially, the limit system is of great interest, because compared to the original system, which is highly oscillatory, the limit system is non-oscillatory. Furthermore, the limit system is linear so it can be solved numerically very easily compared to the original KGS system.

Analogously to the KG equation (see Section 2.2), we rewrite the KGS system with the transformation $u = z - ic^{-1}\langle\nabla\rangle_c^{-1}\partial_t z$ as a first-order system in time which reads

$$\begin{aligned} i\partial_t u &= -c\langle\nabla\rangle_c u + c\langle\nabla\rangle_c^{-1}|\mathfrak{n}|^2, \qquad & u(0) &= z_0 - ic\langle\nabla\rangle_c^{-1} z_1,\\ i\partial_t \mathfrak{n} &= -\Delta\mathfrak{n} - \frac{1}{2}(u+v)\mathfrak{n}, & \mathfrak{n}(0) &= \mathfrak{n}_0. \end{aligned} \tag{3.2}$$

Now, we use this first-order system to apply the formal asymptotic expansion. In order to derive the limit system and the first-order correction term z_∞ formally, we follow the steps from Section 2.2.

1. Multiscale analysis

Our aim is to separate the high oscillations from the slow time dependency of the solution. Hence, we introduce a new variable $\theta := c^2 t$ which defines the so-called long time scale. The multiscale ansatz treats t and θ as independent variables where in fact, in the actual solution, t and θ are correlated. The relation appears through the new time derivative operator, i.e., $\partial_t \to \partial_t + c^2\partial_\theta$.

We introduce the new time variable θ and obtain

$$\begin{aligned} u(t,x) &= U(t,\theta,x), \quad & U(0,0,x) &= u_0(x),\\ \mathfrak{n}(t,x) &= H(t,\theta,x), & H(0,0,x) &= \mathfrak{n}_0(x). \end{aligned}$$

The functions $U(t,\theta,x)$, $H(t,\theta,x)$ are defined on $\mathbb{T}\times\mathbb{T}\times\mathbb{T}^d$. We plug the function U, H into (3.2) and take the derivative with respect to t. This yields

$$\begin{aligned} i\partial_t U + ic^2\partial_\theta U &= -c\langle\nabla\rangle_c U + c\langle\nabla\rangle_c^{-1}|H|^2,\\ i\partial_t H + ic^2\partial_\theta H &= -\Delta H - \frac{1}{2}(U+\overline{U})H. \end{aligned} \tag{3.3}$$

2. Formal asymptotic expansion

We make an ansatz which corresponds to the *modulated Fourier expansion* form (see [36]) of u and $\mathfrak{n}$. For more insight in MFE see also [19, 20, 34] and the references therein. In particular, we expand u and $\mathfrak{n}$ in the following way

$$\begin{aligned} U(t,\theta,x) &= U_\infty + \sum_{m\geq 1} c^{-2m}U_m(t,\theta,x),\\ H(t,\theta,x) &= H_\infty + \sum_{m\geq 1} c^{-2m}H_m(t,\theta,x), \end{aligned}$$

where here we cut off the terms of order $\mathcal{O}(c^{-2})$.

3. Collecting terms with same powers of c

Analogously to the previous chapter, we devide this part into three subparts. First, we expand the leading operator $c\langle\nabla\rangle_c$ and its inverse. Then, we plug the expansions into (2.10) and finally, we collect the terms of the same powers of c.

a) Expanding the operators

We expand the operators $c\langle\nabla\rangle_c$ and $c\langle\nabla\rangle_c^{-1}$ with the formal Taylor series expansion analogously to Section 2.2 and obtain

$$\begin{aligned} c\langle\nabla\rangle_c &= c^2 - \frac{1}{2}\Delta + \sum_{m\geq 1}\mu_{m+1}c^{-2m}(-\Delta)^{m+1},\\ c\langle\nabla\rangle_c^{-1} &= 1 + \frac{1}{2c^2}\Delta + \sum_{m\geq 2}\beta_m c^{-2m}(-\Delta)^m \end{aligned}$$

with coefficients μ_m, $\beta_m \in \mathbb{R}$.

The expansion of the operators $c\langle\nabla\rangle_c$ and $c\langle\nabla\rangle_c^{-1}$ has to be considered again as an asymptotic expansion (for more details see Section 2.2 equation (2.13), (2.14)). We also expand the initial condition $U(0,0,x)$ and obtain

$$U(0,0,x) = \sum_{m\geq 0} c^{-2m}\Theta_m(x),$$

where

$$\Theta_0 = z_0 - iz_1, \qquad \Theta_1 = -\frac{i}{2}\Delta z_1, \qquad \Theta_m = \beta_m(-\Delta)^m z_1.$$

b) Plug the expansions into the PDE

Now, we plug the expansions of the operators into (3.3). This yields

$$i\partial_t U + ic^2\partial_\theta U = -c^2 U + \frac{1}{2}\Delta U + |H|^2 + \mathcal{R}_0,$$

where the remainder $\mathcal{R}_0$ is formally of order $\mathcal{O}(c^{-2}\Delta^2)$. We rewrite the equation as follows

$$i\partial_t U + c^2(i\partial_\theta + 1)U = \frac{1}{2}\Delta U + |H|^2 + \mathcal{R}_0.$$

Together with (3.3), we obtain formally the following system

$$\begin{aligned} i\partial_t U + c^2(i\partial_\theta + 1)U &= \frac{1}{2}\Delta U + |H|^2 + \mathcal{R}_0, \\ i\partial_t H + ic^2\partial_\theta H &= -\Delta H - \frac{1}{2}(U + \overline{U})H. \end{aligned} \tag{3.4}$$

Now, we treat the equation for U and H separately. Next, we plug the expansion of U and H into (3.4). For U we have

$$i\partial_t U_\infty + c^2(i\partial_\theta + 1)(U_\infty + c^{-2}U_1) = \frac{1}{2}\Delta U_\infty + |H_\infty + c^{-2}H_1|^2 + \mathcal{R}_0,$$

which we rewrite, via a short calculation, formally as

$$i\partial_t U_\infty + c^2(i\partial_\theta + 1)U_\infty + (i\partial_\theta + 1)U_1 = \frac{1}{2}\Delta U_\infty + |H_\infty|^2 + \mathcal{R}_0.$$

We plug the expansion of H into (3.4) and obtain

$$i\partial_t H_\infty + ic^2\partial_\theta(H_\infty + c^{-2}H_1) = -\Delta H_\infty - \frac{1}{2}(U_\infty + \overline{U_\infty})H_\infty + \mathcal{R}_1,$$

where $\mathcal{R}_1$ is of order $\mathcal{O}(c^{-2}\Delta)$. By a short calculation we have

$$i\partial_t H_\infty + ic^2\partial_\theta H_\infty + i\partial_\theta H_1 = -\Delta H_\infty - \frac{1}{2}(U_\infty + \overline{U_\infty})H_\infty + \mathcal{R}_1.$$

After plugging the ansatz for U and H into (3.4), we formally obtain the following system

$$\begin{aligned} i\partial_t U_\infty + c^2(i\partial_\theta + 1)U_\infty + (i\partial_\theta + 1)U_1 &= \frac{1}{2}\Delta U_\infty + |H_\infty|^2 + \mathcal{R}_0, \\ i\partial_t H_\infty + ic^2\partial_\theta H_\infty + i\partial_\theta H_1 &= -\Delta H_\infty - \frac{1}{2}(U_\infty + \overline{U_\infty})H_\infty + \mathcal{R}_1. \end{aligned} \tag{3.5}$$

c) Collecting the same powers of U and H

We collect the same powers in c and start with the terms of order $\mathcal{O}(c^2)$. This yields

$$\begin{aligned} (i\partial_\theta + 1)U_\infty &= 0, \\ i\partial_\theta H_\infty &= 0, \end{aligned}$$

which implies that $\partial_\theta U_\infty = iU_\infty$ and $\partial_\theta H_\infty = 0$, i.e., H_∞ is independent of θ, such that we have

$$H_\infty(t, \theta, x) = \mathfrak{n}_\infty(t, x). \tag{3.6}$$

Analogously to the previous chapter, U_∞ has the following solution

$$U_\infty(t, \theta, x) = \mathrm{e}^{i\theta}u_\infty(t, x). \tag{3.7}$$

We proceed by collecting the terms of order $\mathcal{O}(1)$ in the equation for U_∞ and find

$$\left(i\partial_t - \tfrac{1}{2}\Delta\right)U_\infty + (i\partial_\theta + 1)U_1 = |H_\infty|^2. \tag{3.8}$$

Plugging (3.6) and (3.7) into (3.8), we have

$$\big(i\partial_t - \tfrac{1}{2}\Delta\big)\mathrm{e}^{i\theta}u_\infty + (i\partial_\theta + 1)U_1 = |\mathfrak{n}_\infty|^2.$$

By orthogonalization with respect to the kernel of $(i\partial_\theta + 1)$ (see [26]), i.e., with respect to $\mathrm{e}^{i\theta}$, we obtain

$$\big(i\partial_t - \tfrac{1}{2}\Delta\big)u_\infty = 0,$$

which implies that

$$i\partial_t u_\infty = \tfrac{1}{2}\Delta u_\infty.$$

We collect the terms of order $\mathcal{O}(1)$ in (3.5) for H_∞ and plug in (3.6) and (3.7) this yields that

$$i\partial_\theta H_1 = -(i\partial_t + \Delta)\mathfrak{n}_\infty - \tfrac{1}{2}\big(\mathrm{e}^{i\theta}u_\infty + \mathrm{e}^{-i\theta}\overline{u_\infty}\big)\mathfrak{n}_\infty.$$

By orthogonalization with respect to the kernel of $i\partial_\theta$, the following holds

$$(i\partial_t + \Delta)\mathfrak{n}_\infty = 0,$$

and we obtain

$$i\partial_t \mathfrak{n}_\infty = -\Delta\mathfrak{n}_\infty.$$

Remark 3.1. Similar to Lemma (2.2) we can state the first-order correction term and the convergence to the limit system. We fix $r > \frac{d}{2}$ and assume that $z_0,\, z_1 \in H^{r+4}$. Then, for the Klein–Gordon–Schrödinger system (3.1) the first-order correction term z_∞ reads

$$z_\infty(t,x) = \frac{1}{2}\Big(\mathrm{e}^{ic^2t}u_\infty(t,x) + \mathrm{e}^{-ic^2t}\overline{u_\infty}(t,x)\Big),$$

where u_∞ and $\mathfrak{n}_\infty$ are the solutions of the following decoupled free Schrödinger limit system

$$\begin{aligned} i\partial_t u_\infty(t,x) &= \tfrac{1}{2}\Delta u_\infty(t,x), \qquad & u_\infty(0) &= z_0 - iz_1,\\ i\partial_t \mathfrak{n}_\infty(t,x) &= -\Delta\mathfrak{n}_\infty(t,x), \qquad & \mathfrak{n}_\infty(0) &= \mathfrak{n}_0. \end{aligned} \tag{3.9}$$

Then z_∞ approximates the exact solution $(z, \mathfrak{n})$ of (3.1) up to terms of order $\mathcal{O}(c^{-2})$.

The limit Schrödinger system (3.9) is linear and additionally the highly oscillatory part in the first-order correction term

$$z_\infty(t,x) = \frac{1}{2}\Big(\mathrm{e}^{ic^2t}u_\infty(t,x) + \mathrm{e}^{-ic^2t}\overline{u_\infty}(t,x)\Big)$$

is only contained in the phases e^{ic^2t} and e^{-ic^2t}, but does not appear in the Schrödinger limit system. A big advantage is that the limit system (3.9) can be solved exactly in time in Fourier space. By multiplying the limit solution with the highly oscillatory phases we obtain an approximation to the solution of the original system up to an error of order $\mathcal{O}(c^{-2})$. Therefore, the numerical integration of the system (3.9) can be carried out without any c-dependent time step restriction. Hence, we only solve the limit system (3.9) and multiply the numerical approximation of u_∞ with the highly oscillatory phases e^{ic^2t} and e^{-ic^2t}, respectively, to obtain a suitable numerical approximation to the exact solution z in the non-relativistic

limit regime $c \gg 1$.
We can solve the Schrödinger limit system exactly in Fourier space

$$
\begin{aligned}
u_\infty(t,x) &= \mathrm{e}^{-\frac{i}{2}t\Delta}u_\infty(t,x),\\
\mathfrak{n}_\infty(t,x) &= \mathrm{e}^{it\Delta}\mathfrak{n}_\infty(t,x).
\end{aligned}
$$

In the next section we also show that our uniformly accurate method converges in the limit to the numerical method for the limit system, therefore we define the numerical solution of u_∞, $\mathfrak{n}_\infty$

$$
\begin{aligned}
u_\infty^{n+1} &= \mathrm{e}^{-\frac{i}{2}\tau\Delta}u_\infty^n, \quad & u_\infty^0 &= z_0 - iz_1,\\
\mathfrak{n}_\infty^{n+1} &= \mathrm{e}^{i\tau\Delta}\mathfrak{n}_\infty^n, & \mathfrak{n}_\infty^0 &= \mathfrak{n}_0.
\end{aligned} \tag{3.10}
$$

However, this method only allows error bounds of order $\mathcal{O}(c^{-2})$. Therefore, the aim of the next section is to derive a uniformly accurate method for the KGS system.
We proceed as in Chapter 2 and reformulate the KGS system as a coupled first-order system in time. Then we rescale the system by considering the so-called *twisted variables*. After this essential step we iterate Duhamel's formual in the new variables and integrate the interactions of the highly oscillatory phases exactly by approximating only the slowly varying parts. Analogously to the previous chapter we show that our uniformly accurate scheme converges in the limit to our derived numerical scheme for the limit system.

3.3 Uniformly Accurate Methods for the Klein–Gordon–Schrödinger System

This section is a detailed version of [14, chapter 2-5]. In a first step, we rewrite the Klein–Gordon part (in z) of the Klein–Gordon–Schrödinger system (3.1) as a first-order system in time. This allows us to resolve the limit-behavior $c \to \infty$ of the solution. Therefore, we use the operator $\langle\nabla\rangle_c$ defined in (2.4). Rewriting (3.1) with real solution $z(t,x) \in \mathbb{R}$ as a first-order system in time via the transformation (see, e.g., [53])

$$
u = z - ic^{-1}\langle\nabla\rangle_c^{-1}\partial_t z. \tag{3.11}
$$

As z is real-valued we have

$$
z = \frac{1}{2}(u + \overline{u}). \tag{3.12}
$$

Taking the derivative of the ansatz of u in (3.11) with respect to t we obtain

$$
\partial_t u = \partial_t z - ic^{-1}\langle\nabla\rangle_c^{-1}\partial_{tt} z.
$$

Inserting $\partial_t z = ic\langle\nabla\rangle_c(u-z)$ and $\partial_{tt} z = c^2|\mathfrak{n}|^2 - c^2\langle\nabla\rangle_c^2 z$ we find

$$
\begin{aligned}
\partial_t u &= ic\langle\nabla\rangle_c(u-z) - ic^{-1}\langle\nabla\rangle_c^{-1}\left(c^2|\mathfrak{n}|^2 - c^2\langle\nabla\rangle_c^2 z\right)\\
&= ic\langle\nabla\rangle_c u - ic\langle\nabla\rangle_c z - ic^{-1}\langle\nabla\rangle_c^{-1}c^2|\mathfrak{n}|^2 + ic^{-1}\langle\nabla\rangle_c^{-1}c^2\langle\nabla\rangle_c^2 z\\
&= ic\langle\nabla\rangle_c u - ic\langle\nabla\rangle_c z - ic\langle\nabla\rangle_c^{-1}|\mathfrak{n}|^2 + ic\langle\nabla\rangle_c z\\
&= ic\langle\nabla\rangle_c u - ic\langle\nabla\rangle_c^{-1}|\mathfrak{n}|^2.
\end{aligned}
$$

The corresponding KGS system in $(u, \mathfrak{n})$ reads

$$\begin{aligned} i\partial_t u &= -c\langle\nabla\rangle_c u + c\langle\nabla\rangle_c^{-1}|\mathfrak{n}|^2, \quad && u(0) = z(0) - ic^{-1}\langle\nabla\rangle_c^{-1}\partial_t z(0), \\ i\partial_t \mathfrak{n} &= -\Delta\mathfrak{n} - \mathfrak{n}\frac{1}{2}\big(u + \overline{u}\big), && \mathfrak{n}(0) = \mathfrak{n}_0. \end{aligned} \tag{3.13}$$

We note again (see (2.23)) the definition of the operator $\langle\nabla\rangle_c$ formally implies that we have

$$c\langle\nabla\rangle_c = c^2 + \text{“lower order terms in c”}, \qquad \text{for } c \to \infty. \tag{3.14}$$

Next, following the approach in [13], we consider the corresponding *twisted variables* by multiplying u with the phases $\mathrm{e}^{-ic^2 t}$. More precisely, we set

$$u_*(t) = \mathrm{e}^{-ic^2 t}u(t).$$

Note that for the Schrödinger part $\mathfrak{n}$ of the KGS system (3.13) we do not need to apply this twisting since no highly oscillatory action is linked to this variable. However, for notational reasons, we write $\mathfrak{n}_*$ instead of $\mathfrak{n}$.

A simple calculation shows that

$$\begin{aligned} i\partial_t u_* &= i\partial_t\big(\mathrm{e}^{-ic^2 t}u\big) = -i^2c^2\mathrm{e}^{-ic^2 t}u + \mathrm{e}^{-ic^2 t}i\partial_t u = c^2\mathrm{e}^{-ic^2 t}u + \mathrm{e}^{-ic^2 t}\Big(-c\langle\nabla\rangle_c u + c\langle\nabla\rangle_c^{-1}|\mathfrak{n}|^2\Big) \\ &= c^2u_* - c\langle\nabla\rangle_c u_* + c\langle\nabla\rangle_c^{-1}\mathrm{e}^{-ic^2 t}|\mathfrak{n}|^2 \\ &= -\mathcal{A}_c u_* + c\langle\nabla\rangle_c^{-1}\mathrm{e}^{-ic^2 t}|\mathfrak{n}|^2 \end{aligned} \tag{3.15}$$

with leading operator $\mathcal{A}_c = c\langle\nabla\rangle_c - c^2$. As we saw in Remark 2.4 for the Klein–Gordon equation, the advantage of considering the twisted system in u_* (instead of u) lies in the fact that the leading operator formally satisfies $\mathcal{A}_c = \mathcal{O}(1)$ in c (cf. (2.27)), whereas $c\langle\nabla\rangle_c = \mathcal{O}(c^2)$ see (3.14).

Replacing the first line in (3.13) by (3.15) yields the twisted KGS system

$$\begin{aligned} i\partial_t u_* &= -\mathcal{A}_c u_* + c\langle\nabla\rangle_c^{-1}\mathrm{e}^{-ic^2 t}|\mathfrak{n}_*|^2, && u_*(0) = z(0) - ic^{-1}\langle\nabla\rangle_c^{-1}\partial_t z(0), \\ i\partial_t \mathfrak{n}_* &= -\Delta\mathfrak{n}_* - \tfrac{1}{2}\left(\mathrm{e}^{ic^2 t}u_* + \mathrm{e}^{-ic^2 t}\overline{u_*}\right)\mathfrak{n}_*, && \mathfrak{n}_*(0) = \mathfrak{n}(0) \end{aligned} \tag{3.16}$$

with mild solutions

$$\begin{aligned} u_*(t_n+\tau) &= \mathrm{e}^{i\tau\mathcal{A}_c}u_*(t_n) - ic\langle\nabla\rangle_c^{-1}\int_0^\tau \mathrm{e}^{i(\tau-s)\mathcal{A}_c}\mathrm{e}^{-ic^2(t_n+s)}|\mathfrak{n}_*(t_n+s)|^2\mathrm{d}s, \\ \mathfrak{n}_*(t_n+\tau) &= \mathrm{e}^{i\tau\Delta}\mathfrak{n}_*(t_n) + \frac{i}{2}\int_0^\tau \mathrm{e}^{i(\tau-s)\Delta}\big[\mathrm{e}^{ic^2(t_n+s)}u_*(t_n+s) + \mathrm{e}^{-ic^2(t_n+s)}\overline{u_*}(t_n+s)\big]\mathfrak{n}_*(t_n+s)\mathrm{d}s. \end{aligned} \tag{3.17}$$

In the following remark we recall some essential operator bounds.

Remark 3.2. As we have seen in Lemma 2.5 and Lemma 2.6 the benefit in the above formulation is the uniform bound with respect to c of the leading operator $\mathcal{A}_c$

$$\|\mathcal{A}_c u\|_r \le \frac{1}{2}\|u\|_{r+2}\,, \tag{3.18}$$

as well as of the operator in front of the nonlinear coupling which satisfies

$$\left\|c\langle\nabla\rangle_c^{-1}u\right\|_r \le \|u\|_r\,, \tag{3.19}$$

see also [13, Lemma 3]. This in particular implies that for all $t \in \mathbb{R}$ (see [13, Lemma 4])

$$\left\|\mathrm{e}^{it\mathcal{A}_c}\right\|_r = 1 \quad \text{and} \quad \left\|(\mathrm{e}^{-it\mathcal{A}_c} - 1)u\right\|_r \le \frac{1}{2}|t|\, \|u\|_{r+2}. \tag{3.20}$$

Thanks to the essential bound (3.18) the derivatives $\big(u_*'(t), \mathfrak{n}_*'(t)\big)$ can also be bounded uniformly. More precisely, the solutions of (3.16) satisfy

$$\begin{aligned} \|u_*(t_n+s) - u_*(t_n)\|_r &\le \frac{1}{2}|s|\, \|u_*(t_n)\|_{r+2} + |s| \sup_{0\le\xi\le s} \|\mathfrak{n}_*(t_n+\xi)\|_r^2, \\ \|\mathfrak{n}_*(t_n+s) - \mathfrak{n}_*(t_n)\|_r &\le |s|\, \|\mathfrak{n}_*(t_n)\|_{r+2} + |s| \sup_{0\le\xi\le s} \big(\|u_*(t_n+\xi)\|_r \|\mathfrak{n}_*(t_n+\xi)\|_r \big). \end{aligned} \tag{3.21}$$

The above estimates on the derivatives can be proven by using Duhamel's formula for u_* and $\mathfrak{n}_*$, respectively, and then employing the estimates (3.19) and (3.20) (see [13, Lemma 5]).
Next, we state the necessary local well-posedness assumptions.

Assumption 3.3. *Fix $r > d/2$ and assume that there exists a $T > 0$ such that the solution $u_*(t)$, $\mathfrak{n}_*(t)$ of (3.16) satisfies*

$$\sup_{0\le t\le T} \Big(\|u_*(t)\|_r + \|\mathfrak{n}_*(t)\|_r \Big) \le M,$$

uniformly in c.

Remark 3.4. Note that Assumption 3.3 holds under the following conditions on the initial data

$$\begin{aligned} \|\mathfrak{n}(0)\|_r &\le M_1, \\ \|z(0)\|_r + \left\|c^{-1}\langle\nabla\rangle_c^{-1}\partial_t z(0)\right\|_r &\le M_2, \end{aligned}$$

where M_1, M_2 do not depend on c. This can be easily seen by using a classical fixed point argument in Duhamel's formula (3.17) together with the essential uniform bound (3.19) and (3.20).

For further details on the local well-posedness of highly oscillatory Klein–Gordon type equations we refer to [53, 73] and the references therein. Analogously to the previous chapter, in our analysis we will employ the concept of the so-called φ-functions (see [39]) which are defined in Section 2.3. Recall that by Definition 2.8 the φ-functions read

$$\varphi_0(\xi) = \mathrm{e}^{\xi}, \qquad \varphi_1(\xi) = \frac{\mathrm{e}^{\xi} - 1}{\xi}, \qquad \varphi_2(\xi) = \frac{\varphi_1(\xi) - 1}{\xi}$$

and

$$\Psi_2(\xi) = \frac{\varphi_0(\xi) - \varphi_1(\xi)}{\xi},$$

for $\xi \in \mathbb{C}$.

3.3.1 A Classical Exponential Integrator for the Twisted Klein–Gordon–Schrödinger System

In this subsection we formally show that applying a classical exponential integrator on the twisted system is not an appropriate ansatz in order to obtain a uniformly accurate method. This behavior is underlined in numerical experiments (see Figure 3.3). In the following, we formally construct an exponential integrator for the twisted system.

In order to obtain an exponential integrator for (3.16), we use Duhamel's formulas given in (3.17)

$$
\begin{aligned}
u_*(t_n+\tau) &= \mathrm{e}^{i\tau\mathcal{A}_c}u_*(t_n) - ic\langle\nabla\rangle_c^{-1}\int_0^\tau \mathrm{e}^{i(\tau-s)\mathcal{A}_c}\mathrm{e}^{-ic^2(t_n+s)}|\mathfrak{n}_*(t_n+s)|^2\mathrm{d}s,\\
\mathfrak{n}_*(t_n+\tau) &= \mathrm{e}^{i\tau\Delta}\mathfrak{n}_*(t_n) + \frac{i}{2}\int_0^\tau \mathrm{e}^{i(\tau-s)\Delta}\Big[\mathrm{e}^{ic^2(t_n+s)}u_*(t_n+s) + \mathrm{e}^{-ic^2(t_n+s)}\overline{u_*}(t_n+s)\Big]\mathfrak{n}_*(t_n+s)\mathrm{d}s.
\end{aligned}
$$

We use the ansatz of exponential integrators (see [39]) and freeze the following terms in Duhamel's formulas at $s=0$

$$
\begin{aligned}
&\mathrm{e}^{-ic^2(t_n+s)}|\mathfrak{n}_*(t_n+s)|^2,\\
&\Big[\mathrm{e}^{ic^2(t_n+s)}u_*(t_n+s) + \mathrm{e}^{-ic^2(t_n+s)}\overline{u_*}(t_n+s)\Big]\mathfrak{n}_*(t_n+s),
\end{aligned}
$$

such that we obtain

$$
\begin{aligned}
u_*(t_{n+1}) &\approx \mathrm{e}^{i\tau\mathcal{A}_c}u_*(t_n) - ic\langle\nabla\rangle_c^{-1}\int_0^\tau \mathrm{e}^{i(\tau-s)\mathcal{A}_c}\mathrm{e}^{-ic^2t_n}|\mathfrak{n}_*(t_n)|^2\mathrm{d}s,\\
\mathfrak{n}_*(t_{n+1}) &\approx \mathrm{e}^{i\tau\Delta}\mathfrak{n}_*(t_n) + \frac{i}{2}\int_0^\tau \mathrm{e}^{i(\tau-s)\Delta}\Big[\mathrm{e}^{ic^2t_n}u_*(t_n) + \mathrm{e}^{-ic^2t_n}\overline{u_*}(t_n)\Big]\mathfrak{n}_*(t_n)\mathrm{d}s.
\end{aligned}
$$

Then, we integrate the remaining terms $\mathrm{e}^{i(\tau-s)\mathcal{A}_c}$ and $\mathrm{e}^{i(\tau-s)\Delta}$ exactly. Thus, with the Definition 2.8 of the φ_1-function we have

$$
\begin{aligned}
u_*(t_{n+1}) &\approx \mathrm{e}^{i\tau\mathcal{A}_c}u_*(t_n) - ic\langle\nabla\rangle_c^{-1}\tau\varphi_1(i\tau\mathcal{A}_c)\mathrm{e}^{-ic^2t_n}|\mathfrak{n}_*(t_n)|^2,\\
\mathfrak{n}_*(t_{n+1}) &\approx \mathrm{e}^{i\tau\Delta}\mathfrak{n}_*(t_n) + \tfrac{i}{2}\tau\varphi_1(i\tau\Delta)\Big[\mathrm{e}^{ic^2t_n}u_*(t_n) + \mathrm{e}^{-ic^2t_n}\overline{u_*}(t_n)\Big]\mathfrak{n}_*(t_n).
\end{aligned}
$$

Therefore, we obtain the following exponential integration scheme

$$
\begin{aligned}
u_*^{n+1} &= \mathrm{e}^{i\tau\mathcal{A}_c}u_*^n - i\tau c\langle\nabla\rangle_c^{-1}\varphi_1\left(i\tau\mathcal{A}_c\right)\mathrm{e}^{-ic^2t_n}|\mathfrak{n}_*^n|^2,\\
\mathfrak{n}_*^{n+1} &= \mathrm{e}^{i\tau\Delta}\mathfrak{n}_*^n + \tfrac{i}{2}\tau\varphi_1\left(i\tau\Delta\right)\left[\mathrm{e}^{ic^2t_n}u_*^n + \mathrm{e}^{-ic^2t_n}\overline{u_*^n}\right]\mathfrak{n}_*^n
\end{aligned}
$$

with initial values

$$
\begin{aligned}
u_*^0 &= z_0 - ic\langle\nabla\rangle_c^{-1}\, z_1,\\
\mathfrak{n}_*^0 &= \mathfrak{n}_0.
\end{aligned}
$$

Figure 3.3 underlines that the exponential integrator scheme is not uniformly accurate with respect to c. For large values of c the exponential integrator scheme fails to numerically approximate the solution of the Klein–Gordon–Schrödinger system. Thus, classical exponential integrators also suffer from severe time step restrictions similarly to the Gautschi-type methods shown in Figure 3.1.

In the next section we construct our uniformly accurate exponential-type integrator, similar to Section 2.3. Therefore, we also integrate the highly oscillatory phase terms $\mathrm{e}^{\pm\ell ic^2(t_n+s)}$, for $\ell\in\mathbb{N}$ of the Duhamel's formulas exactly. This simple trick yields our new uniformly accurate methods.

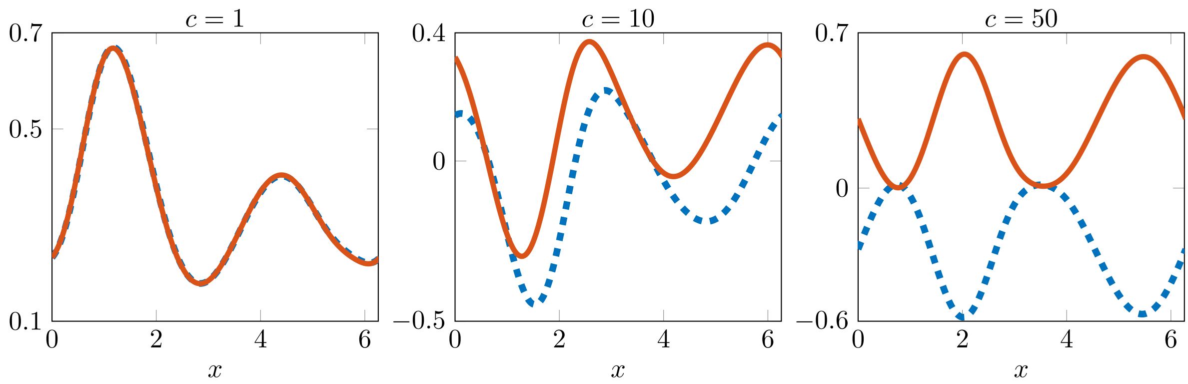

Figure 3.3: Numerical solution of the Klein–Gordon–Schrödinger system for z. Exponential integrator scheme (red solid line) for different c with time step size $\tau \approx 10^{-2}$ at time $t = 0.6$. The blue dashed line represents the reference solution at time $t = 0.6$, computed via the same exponential integrator scheme with a small time step size $\tau \approx 10^{-6}$. The spatial discretization is done via a Fourier pseudospectral method with with mesh-size $h = 0.0245$.

3.3.2 Construction of a First-Order Uniformly Accurate Integrator

In this section we derive a first-order exponential-type integrator for the solution $(u_*, \mathfrak{n}_*)$ based on Duhamel's formula (3.17). For the analysis in the classical Klein–Gordon setting we refer to Section 2.3. In order to construct a scheme of first-order, we need to impose some additional regularity assumptions on the exact solutions.

Assumption 3.5. *Fix $r > d/2$ and assume that $u_*, \mathfrak{n}_* \in \mathcal{C}\big([0,T]; H^{r+2}(\mathbb{T}^d)\big)$ with in particular*

$$\sup_{0\leq t\leq T} \Big(\|u_*(t)\|_{r+2} + \|\mathfrak{n}_*(t)\|_{r+2} \Big) \leq M_3,$$

where M_3 can be bounded uniformly in c.

Note that the above assumption can be easily played back to the initial values thanks to Remark 3.4.

Now, we give a detailed derivation of the numerical scheme for u_*^{n+1} approximating $u_*(t_{n+1})$, with $t_{n+1} = t_n + \tau$, followed by a more compact derivation of the schemes for $\mathfrak{n}_*^{n+1}$. Recall Duhamel's formula for u_* (see (3.17))

$$u_*(t_n + \tau) = \mathrm{e}^{i\tau\mathcal{A}_c} u_*(t_n) - ic\langle\nabla\rangle_c^{-1} \int_0^\tau \mathrm{e}^{i(\tau-s)\mathcal{A}_c} \mathrm{e}^{-ic^2(t_n+s)} |\mathfrak{n}_*(t_n+s)|^2 \mathrm{d}s.$$

The exponential term $\mathrm{e}^{i\tau\mathcal{A}_c}$ is uniformly bounded in c thanks to (3.20). Therefore, the remaining task lies in resolving the highly oscillatory phases in the integral. Using the formal Taylor series expansions

$$\mathfrak{n}_*(t_n + s) = \mathfrak{n}_*(t_n) + \mathcal{O}(s\partial_t \mathfrak{n}_*) \quad \text{and} \quad \mathrm{e}^{-is\mathcal{A}_c} = 1 + \mathcal{O}(s\mathcal{A}_c) \tag{3.22}$$

in the above integral allows us to integrate the highly oscillatory phases

$$\int_0^\tau \mathrm{e}^{-ic^2 s} \mathrm{d}s = \tau\varphi_1\left(-ic^2\tau\right)$$

exactly. The formal expansion of $\mathrm{e}^{is\mathcal{A}_c}$ given in (3.22) is thereby understood as the application of the operator $\mathrm{e}^{is\mathcal{A}_c}$ to some sufficiently smooth function f in the sense that

$$\mathrm{e}^{-is\mathcal{A}_c} f = f + s\mathcal{R}(\mathcal{A}_c f), \tag{3.23}$$

where the remainder $\mathcal{R}(\mathcal{A}_c f)$ satisfies the bound

$$\|\mathcal{R}(\mathcal{A}_c f)\|_r \leq \tfrac{1}{2}\|f\|_{r+2}.$$

The above bound on the remainder is a direct consequence of (3.20). It is important to note that additional smoothness on f is needed in the expansion (3.23).

Combined with the definition of φ_1 (Definition 2.8), we thus obtain that

$$u_*(t_n+\tau) = \mathrm{e}^{i\tau\mathcal{A}_c} u_*(t_n) - ic\langle\nabla\rangle_c^{-1}\mathrm{e}^{i\tau\mathcal{A}_c}\mathrm{e}^{-ic^2 t_n}\tau\varphi_1(-ic^2\tau)|\mathfrak{n}_*(t_n)|^2 + R_1(\tau, t_n, u_*, \mathfrak{n}_*), \tag{3.24}$$

where the remainder $R_1(\tau, t_n, u_*, \mathfrak{n}_*)$ satisfies thanks to the bounds (3.18), (3.19) and (3.21) (which hold uniformly in c)

$$\|R_1(\tau, t_n, u_*, \mathfrak{n}_*)\|_r \leq \tau^2 k_{r,M_3}, \tag{3.25}$$

for a constant k_{r,M_3} which can be chosen independently of c.
This motivates us to define the following numerical scheme in u_*

$$u_*^{n+1} = \mathrm{e}^{i\tau\mathcal{A}_c} u_*^n - i\tau c\langle\nabla\rangle_c^{-1}\mathrm{e}^{i\tau\mathcal{A}_c}\mathrm{e}^{-ic^2 t_n}\varphi_1(-ic^2\tau)|\mathfrak{n}_*^n|^2.$$

Given the numerical scheme in u_*^{n+1} we compute z^{n+1} as (see (3.12))

$$z^{n+1} = \frac{1}{2}\left(\mathrm{e}^{ic^2 t_{n+1}} u_*^{n+1} + \mathrm{e}^{-ic^2 t_{n+1}}\overline{u_*^{n+1}}\right).$$

For $\mathfrak{n}_*$ we proceed as follows. Recall Duhamel's formula (see (3.17))

$$\mathfrak{n}_*(t_n+\tau) = \mathrm{e}^{i\tau\Delta}\mathfrak{n}_*(t_n) + \frac{i}{2}\int_0^\tau \mathrm{e}^{i(\tau-s)\Delta}\left[\mathrm{e}^{ic^2(t_n+s)}u_*(t_n+s) + \mathrm{e}^{-ic^2(t_n+s)}\overline{u_*}(t_n+s)\right]\mathfrak{n}_*(t_n+s)\mathrm{d}s.$$

Carrying out the formal Taylor series expansions

$$u_*(t_n+s) = u_*(t_n) + \mathcal{O}(su_*'), \quad \mathfrak{n}_*(t_n+s) = \mathfrak{n}_*(t_n) + \mathcal{O}(s\mathfrak{n}_*') \quad \text{and} \quad \mathrm{e}^{-is\Delta} = 1 + \mathcal{O}(s\Delta) \tag{3.26}$$

in the above integral allows us to freeze the functions u_*, $\mathfrak{n}_*$ and integrate the highly oscillatory phases $\mathrm{e}^{\pm ic^2 s}$ exactly. Together with the definition of φ_1 (Definition 2.8) we therefore obtain that

$$\begin{aligned}\mathfrak{n}_*(t_n+\tau) = {} & \mathrm{e}^{i\tau\Delta}\mathfrak{n}_*(t_n) + \frac{i}{2}\mathrm{e}^{i\tau\Delta}\tau\left[\mathrm{e}^{ic^2 t_n}\varphi_1(ic^2\tau)u_*(t_n)\mathfrak{n}_*(t_n) + \mathrm{e}^{-ic^2 t_n}\varphi_1(-ic^2\tau)\overline{u_*}(t_n)\mathfrak{n}_*(t_n)\right] \\ & + R_1(\tau, t, u_*, \mathfrak{n}_*),\end{aligned} \tag{3.27}$$

where the remainder $R_1(\tau, t, u_*, \mathfrak{n}_*)$ satisfies a similar (in particular uniform) bound to (3.25) thanks to (3.21).
This motivates us to define the following numerical scheme in $\mathfrak{n}_*$

$$\mathfrak{n}_*^{n+1} = \mathrm{e}^{i\tau\Delta}\mathfrak{n}_*^n + \frac{i}{2}\tau\mathrm{e}^{i\tau\Delta}\left[\mathrm{e}^{ic^2 t_n}\varphi_1(ic^2\tau)u_*^n\mathfrak{n}_*^n + \mathrm{e}^{-ic^2 t_n}\varphi_1(-ic^2\tau)\overline{u_*^n}\mathfrak{n}_*^n\right].$$

Collecting the results yields the following full numerical scheme in u_* and $\mathfrak{n}_*$

$$\begin{aligned} u_*^{n+1} &= \mathrm{e}^{i\tau\mathcal{A}_c}u_*^n - i\tau\mathrm{e}^{-ic^2t_n}\varphi_1(-ic^2\tau)c\langle\nabla\rangle_c^{-1}\mathrm{e}^{i\tau\mathcal{A}_c}|\mathfrak{n}_*^n|^2, & u_*^0 &= z_0 - ic\langle\nabla\rangle_c^{-1}z_1, \\ \mathfrak{n}_*^{n+1} &= \mathrm{e}^{i\tau\Delta}\mathfrak{n}_*^n + \frac{i}{2}\tau\mathrm{e}^{i\tau\Delta}\left[\mathrm{e}^{ic^2t_n}\varphi_1(ic^2\tau)u_*^n\mathfrak{n}_*^n + \mathrm{e}^{-ic^2t_n}\varphi_1(-ic^2\tau)\overline{u_*^n}\mathfrak{n}_*^n\right], & \mathfrak{n}_*^0 &= \mathfrak{n}_0, \end{aligned} \tag{3.28}$$

where we used the transformation (3.11) for the initial value.

3.3.2.1 Convergence Analysis of the First-Order Uniformly Accurate Scheme

The exponential-type integration scheme (3.28) converges (by construction) with first-order in time uniformly with respect to c, see Theorem 3.6 below.

Theorem 3.6 (Convergence bound for the first-order scheme, cf. Theorem 5 in [14])**.** *Fix $r > d/2$, and assume that Assumption 3.5 holds. For u_*^n defined in (3.28), we set*

$$z^n := \frac{1}{2}\left(\mathrm{e}^{ic^2t_n}u_*^n + \mathrm{e}^{-ic^2t_n}\overline{u_*^n}\right).$$

Then, there exists a $T > 0$ and $\tau_0 > 0$ such that for $\tau \le \tau_0$ and $t_n \le T$ we have for all $c > 0$ that

$$\|z(t_n) - z^n\|_r + \|\mathfrak{n}(t_n) - \mathfrak{n}^n\|_r \le \tau K_{r,T,M,M_3},$$

where the constant K_{r,T,M,M_3} can be chosen independently of c.

Proof. Fix $r > d/2$. For notational reasons we write again $\mathfrak{n}_*$ instead of $\mathfrak{n}$. In the following, let $(\phi^\tau_{u_*}, \phi^\tau_{\mathfrak{n}_*})$ denote the exact flow of (3.16) and let $(\Phi^\tau_{u_*}, \Phi^\tau_{\mathfrak{n}_*})$ denote the numerical flow defined in (3.28), i.e.,

$$\begin{aligned} u_*(t_{n+1}) &= \phi^\tau_{u_*}(u_*(t_n), \mathfrak{n}_*(t_n)), & u_*^{n+1} &= \Phi^\tau_{u_*}(u_*^n, \mathfrak{n}_*^n), \\ \mathfrak{n}_*(t_{n+1}) &= \phi^\tau_{\mathfrak{n}_*}(u_*(t_n), \mathfrak{n}_*(t_n)), & \mathfrak{n}_*^{n+1} &= \Phi^\tau_{\mathfrak{n}_*}(u_*^n, \mathfrak{n}_*^n). \end{aligned}$$

Again we denote the numerical flow by ϕ instead of the standard notation φ. For more details on flows we refer to [25, 36]. This allows us to decompose the global error as follows

$$\begin{aligned} u_*(t_{n+1}) - u_*^{n+1} &= \phi^\tau_{u_*}(u_*(t_n), \mathfrak{n}_*(t_n)) - \Phi^\tau_{u_*}(u_*^n, \mathfrak{n}_*^n) \\ &= \phi^\tau_{u_*}(u_*(t_n), \mathfrak{n}_*(t_n)) - \Phi^\tau_{u_*}(u_*(t_n), \mathfrak{n}_*(t_n)) + \Phi^\tau_{u_*}(u_*(t_n), \mathfrak{n}_*(t_n)) - \Phi^\tau_{u_*}(u_*^n, \mathfrak{n}_*^n), \end{aligned} \tag{3.29}$$

where a similar equation holds for $\mathfrak{n}_*$. By splitting the global error as shown above, we can treat the terms that appear separately. In particular, the first term describes the local error and the second term the stability. Therefore, we look at them one by one and derive a local error bound and a stability bound. In the following we define by k_r, K_r, $K_{r,M}$ constants depending only on r and r, M respectively, but which can be chosen independently of c.

Local error: With the aid of $\|R_1(\tau, t_n, u_*, \mathfrak{n}_*)\|_r \le \tau^2 k_{r,M_3}$ we have by the expansion of the exact solution for $u_*(t_n + \tau)$ together with $z = \frac{1}{2}(u + \overline{u})$ and by the numerical schemes (3.28) that

$$\left\|\phi^\tau_{u_*}(u_*(t_n), \mathfrak{n}_*(t_n)) - \Phi^\tau_{u_*}(u_*(t_n), \mathfrak{n}_*(t_n))\right\|_r \le \|R_1(\tau, t_n, u_*, \mathfrak{n}_*)\|_r \le \tau^2 k_{r,M_3}, \tag{3.30}$$

where the constant k_{r,M_3} can be chosen independently of c. The same estimate holds for $\mathfrak{n}_*$.

Stability: Now, we have to establish bounds on

$$\left\|\Phi^\tau_{u_*}(u_*(t_n),\mathfrak{n}_*(t_n)) - \Phi^\tau_{u_*}(u^n_*,\mathfrak{n}^n_*)\right\|_r \qquad \text{and} \qquad \left\|\Phi^\tau_{\mathfrak{n}_*}(u_*(t_n),\mathfrak{n}_*(t_n)) - \Phi^\tau_{\mathfrak{n}_*}(u^n_*,\mathfrak{n}^n_*)\right\|_r .$$

For this purpose, we set in the following for $f,g\in H^r$

$$\begin{aligned}
\Gamma_\tau(f,g) &:= \mathrm{e}^{i\tau\mathcal{A}_c} f - i\tau \mathrm{e}^{-ic^2t_n}\varphi_1(-i\tau c^2)c\langle\nabla\rangle_c^{-1}\mathrm{e}^{i\tau\mathcal{A}_c}|g|^2,\\
\Theta_\tau(f,g) &:= \mathrm{e}^{i\tau\Delta} g + \frac{i}{2}\tau\mathrm{e}^{i\tau\Delta}\left[\mathrm{e}^{ic^2t_n}\varphi_1(ic^2\tau)fg + \mathrm{e}^{-ic^2t_n}\varphi_1(-ic^2\tau)\overline{f}g\right],
\end{aligned}$$

such that in particular we have

$$\begin{aligned}
\|\Phi^\tau_{u_*}\big(u_*(t_n),\mathfrak{n}_*(t_n)\big) - \Phi^\tau_{u_*}(u^n_*,\mathfrak{n}^n_*)\|_r &= \|\Gamma_\tau\big(u_*(t_n),\mathfrak{n}_*(t_n)\big) - \Gamma_\tau(u^n_*,\mathfrak{n}^n_*)\|_r,\\
\|\Phi^\tau_{\mathfrak{n}_*}\big(u_*(t_n),\mathfrak{n}_*(t_n)\big) - \Phi^\tau_{\mathfrak{n}_*}(u^n_*,\mathfrak{n}^n_*)\|_r &= \|\Theta_\tau\big(u_*(t_n),\mathfrak{n}_*(t_n)\big) - \Theta_\tau(u^n_*,\mathfrak{n}^n_*)\|_r.
\end{aligned}$$

Note for all $t\in\mathbb{R}$ we have that $\|\mathrm{e}^{it\mathcal{A}_c}\|_r = 1$ and $\|c\langle\nabla\rangle_c^{-1}\|_r \le 1$ (see (3.19) and (3.20), respectively). Furthermore, the following stability bound holds for the φ_1-function (see also (2.44) or [39])

$$\left\|\varphi_1(i\tau c^2\xi)\right\|_r \le 1 \quad \text{for all} \quad \xi\in\mathbb{R}. \tag{3.31}$$

This implies (together with the bilinear estimate (1.2)) that

$$\begin{aligned}
\|\Gamma_\tau(f_1,g_1) - \Gamma_\tau(f_2,g_2)\|_r &\le \|\mathrm{e}^{i\tau\mathcal{A}_c}\|_r\,\|f_1-f_2\|_r\\
&\quad + \tau\|\frac{i}{2}c\langle\nabla\rangle_c^{-1}\|_r\left\|\mathrm{e}^{i\tau\mathcal{A}_c}\right\|_r\|\mathrm{e}^{-ic^2t_n}\varphi_1(-ic^2\tau)\|_r\||g_1|^2-|g_2|^2\|_r\\
&\le \|f_1-f_2\|_r + \tau K\||g_1|^2-|g_2|^2\|_r\\
&\le \|f_1-f_2\|_r + \tau K\|g_1\overline{g_1} - \overline{g_1}g_2 + \overline{g_1}g_2 - g_2\overline{g_2}\|_r\\
&\le \|f_1-f_2\|_r + \tau K\Big[\|\overline{g_1}\|_r\|g_1-g_2\|_r + \|g_2\|_r\|\overline{g_1}-\overline{g_2}\|_r\Big]\\
&\le \|f_1-f_2\|_r + \tau K\left(\|g_1\|_r,\|g_2\|_r\right)\|g_1-g_2\|_r,
\end{aligned} \tag{3.32}$$

where the constant K depends on $\|g_1\|_r$ and $\|g_2\|_r$, but can be chosen independently of c. In the following we assume that $\|u_*(t_n)\|_r\le M$, $\|\mathfrak{n}_*(t_n)\|_r\le 2M$, $\|u^n_*\|_r\le 3M$, and $\|\mathfrak{n}^n_*\|_r\le 4M$. We furthermore abbreviate $K\left(\|v_1\|_r,\|v_2\|_r\right) = K_{r,M}$, where $\|v_i\|_r\le kM$ for $i=1,2$ and some constant k independent of c. A similar bound holds for Θ_τ

$$\begin{aligned}
\|\Theta_\tau(f_1,g_1) - \Theta_\tau(f_2,g_2)\|_r &\le \|g_1-g_2\|_r + \tau K_{r,M}\left(\|f_1-f_2\|_r + \|g_1-g_2\|_r\right)\\
&\quad + \tau K_{r,M}\left(\|\overline{f_1}-\overline{f_2}\|_r + \|g_1-g_2\|_r\right)\\
&\le \|g_1-g_2\|_r + \tau K_{r,M}(\|g_1-g_2\|_r + \|f_1-f_2\|_r).
\end{aligned} \tag{3.33}$$

Global error: Plugging the local error bounds (3.30) as well as the stability bounds (3.32) and (3.33) into (3.29), we have that

$$\begin{aligned}
\left\|u_*(t_{n+1}) - u^{n+1}_*\right\|_r &= \|u_*(t_n)-u^n_*\|_r + \tau K_{r,M}\|\mathfrak{n}_*(t_n)-\mathfrak{n}^n_*\|_r + \tau^2 k_{r,M_3},\\
\left\|\mathfrak{n}_*(t_{n+1}) - \mathfrak{n}^{n+1}_*\right\|_r &= \|\mathfrak{n}_*(t_n)-\mathfrak{n}^n_*\|_r + \tau K_{r,M}(\|\mathfrak{n}_*(t_n)-\mathfrak{n}^n_*\|_r + \|u_*(t_n)-u^n_*\|_r) + \tau^2 k_{r,M_3}.
\end{aligned}$$

We consider each equation individually. For the equation of u_* we obtain

$$\begin{aligned}
\left\|u_*(t_{n+1}) - u^{n+1}_*\right\|_r &= \|u_*(t_n)-u^n_*\|_r + \tau K_{r,M}\|\mathfrak{n}_*(t_n)-\mathfrak{n}^n_*\|_r + \tau^2 k_{r,M_3}\\
&\le \|u_*(t_n)-u^n_*\|_r + \|\mathfrak{n}_*(t_n)-\mathfrak{n}^n_*\|_r\\
&\quad + \tau K_{r,M}(\|\mathfrak{n}_*(t_n)-\mathfrak{n}^n_*\|_r + \|u_*(t_n)-u^n_*\|_r) + \tau^2 k_{r,M_3}\\
&\le (1+\tau K_{r,M})(\|u_*(t_n)-u^n_*\|_r + \|\mathfrak{n}_*(t_n)-\mathfrak{n}^n_*\|_r) + \tau^2 k_{r,M_3}.
\end{aligned} \tag{3.34}$$

For the equation of $\mathfrak{n}_*$ we have

$$\begin{aligned}\left\|\mathfrak{n}_*(t_{n+1})-\mathfrak{n}_*^{n+1}\right\|_r &= \|\mathfrak{n}_*(t_n)-\mathfrak{n}_*^n\|_r + \tau K_{r,M}(\|\mathfrak{n}_*(t_n)-\mathfrak{n}_*^n\|_r + \|u_*(t_n)-u_*^n\|_r) + \tau^2 k_{r,M_3}\\ &\leq \|\mathfrak{n}_*(t_n)-\mathfrak{n}_*^n\|_r + \|u_*(t_n)-u_*^n\|_r\\ &\quad + \tau K_{r,M}(\|\mathfrak{n}_*(t_n)-\mathfrak{n}_*^n\|_r + \|u_*(t_n)-u_*^n\|_r) + \tau^2 k_{r,M_3}\\ &\leq (1+\tau K_{r,M})(\|\mathfrak{n}_*(t_n)-\mathfrak{n}_*^n\|_r + \|u_*(t_n)-u_*^n\|_r) + \tau^2 k_{r,M_3}.\end{aligned} \tag{3.35}$$

Combining the above bounds (3.34) and (3.35), we thus find

$$\left\|\begin{pmatrix} u_*(t_{n+1})-u_*^{n+1}\\ \mathfrak{n}_*(t_{n+1})-\mathfrak{n}_*^{n+1}\end{pmatrix}\right\|_r \leq (1+\tau K_{r,M})\left\|\begin{pmatrix} u_*(t_n)-u_*^n\\ \mathfrak{n}_*(t_n)-\mathfrak{n}_*^n\end{pmatrix}\right\|_r + \tau^2 k_{r,M_3}. \tag{3.36}$$

Exploiting

$$1+\tau K_{r,M} \leq \mathrm{e}^{\tau K_{r,M}},$$

and iterating (3.36) we obtain

$$\begin{aligned}\left\|\begin{pmatrix} u_*(t_{n+1})-u_*^{n+1}\\ \mathfrak{n}_*(t_{n+1})-\mathfrak{n}_*^{n+1}\end{pmatrix}\right\|_r &\leq \mathrm{e}^{\tau K_{r,M}}\left\|\begin{pmatrix} u_*(t_n)-u_*^n\\ \mathfrak{n}_*(t_n)-\mathfrak{n}_*^n\end{pmatrix}\right\|_r + \tau^2 k_{r,M_3}\\ &\leq \mathrm{e}^{\tau K_{r,M}}\left(\mathrm{e}^{\tau K^1_{r,M}}\left\|\begin{pmatrix} u_*(t_{n-1})-u_*^{n-1}\\ \mathfrak{n}_*(t_{n-1})-\mathfrak{n}_*^{n-1}\end{pmatrix}\right\|_r + \tau^2 k_{r,M_3}\right) + \tau^2 k_{r,M_3}\\ &\leq \mathrm{e}^{n\tau \sup_n K^n_{r,M}}\left(\left\|\begin{pmatrix} u_*(0)-u_*^0\\ \mathfrak{n}_*(0)-\mathfrak{n}_*^0\end{pmatrix}\right\|_r\right) + \mathrm{e}^{n\tau\sup_n K^n_{r,M}} n\tau^2 k_{r,M_3}\\ &= \mathrm{e}^{T \sup_n K^n_{r,M}}\left(\left\|\begin{pmatrix} u_*(0)-u_*^0\\ \mathfrak{n}_*(0)-\mathfrak{n}_*^0\end{pmatrix}\right\|_r\right) + \mathrm{e}^{T\sup_n K^n_{r,M}} T\tau k_{r,M_3}.\end{aligned}$$

Hence, a *Lady Windermere's fan* argument (see, e.g., [35, 50]) yields

$$\|u_*(t_n)-u_*^n\|_r + \|\mathfrak{n}_*(t_n)-\mathfrak{n}_*^n\|_r \leq \tau K_{r,T,M_3}\mathrm{e}^{TK_{r,M}} \leq \tau K_{r,T,M,M_3}, \tag{3.37}$$

where the constants K_{r,T,M_3} and K_{r,T,M,M_3} are uniformly bounded in c.
The identity with $z=\frac{1}{2}(u+\overline{u})$ and the definition of the twisted variable $u_*(t)=\mathrm{e}^{-ic^2t}u(t)$ imply

$$\begin{aligned}\|z(t_n)-z^n\|_r &= \left\|\tfrac{1}{2}(u(t_n)-\overline{u}(t_n)) - \tfrac{1}{2}(\mathrm{e}^{ic^2t_n}u_*^n + \mathrm{e}^{-ic^2t_n}\overline{u_*^n})\right\|_r\\ &\leq \frac{1}{2}\left\|\mathrm{e}^{ic^2t_n}(u_*(t_n)-u_*^n)\right\|_r + \frac{1}{2}\left\|\mathrm{e}^{ic^2t_n}(u_*(t_n)-u_*^n)\right\|_r\\ &= \frac{1}{2}\|u_*(t_n)-u_*^n\|_r + \frac{1}{2}\|u_*(t_n)-u_*^n\|_r\\ &= \|u_*(t_n)-u_*^n\|_r.\end{aligned}$$

Employing the essential bound (3.37) we finally conclude

$$\|z(t_n)-z^n\|_r + \|\mathfrak{n}(t_n)-\mathfrak{n}^n\|_r \leq \tau K_{r,T,M,M_3},$$

where the constant K_{r,T,M,M_3} is uniform in c. This finishes the proof. □

In the next subsection we derive the second-order uniformly accurate method for the KGS system and state the corresponding convergence result.

3.3.3 Construction of a Second-Order Uniformly Accurate Integrator

In this section we derive a second-order integrator for the KGS system (3.1) based on Duhamel's formula (3.17) in the twisted variables $(u_*, \mathfrak{n}_*)$.

Naively, we would think that the second-order integrator can be derived by simply including the next terms (of order s) in the Taylor series expansions (3.22) and (3.26). However, as we have seen for the KG equation in Section 2.3.3, this would *not allow a uniform approximation* in c due to the observation that formally

$$\partial_t u_* = \mathcal{O}(1) \quad \text{in} \quad c \qquad \text{however} \qquad \partial_{tt} u_*(t) = \mathcal{O}(c^2).$$

A similar observation holds for $\mathfrak{n}_*$. The construction of a numerical scheme based on a second-order Taylor series expansion of $u_*(t)$ would thus introduce an error of order $\mathcal{O}(\tau^2 c^2)$, but would not yield the desired uniform second-order error bound $\mathcal{O}(\tau^2)$.
Therefore, we need to carry out a much more careful analysis by iterating Duhamel's formula twice which allows us to integrate the highly oscillatory terms $\mathrm{e}^{\pm ic^2 \ell t}$ (with $\ell \in \mathbb{Z}$) exactly. In addition, in order to obtain second-order approximations we need to impose additional regularity on the exact solutions $u_*(t)$ and $\mathfrak{n}_*(t)$.

Assumption 3.7. *Fix $r > d/2$ and assume that $u_*, \mathfrak{n}_* \in \mathcal{C}\big([0,T]; H^{r+4}(\mathbb{T}^d)\big)$ with in particular*

$$\sup_{0 \le t \le T} \Big(\|u_*(t)\|_{r+4} + \|\mathfrak{n}_*(t)\|_{r+4} \Big) \le M_4,$$

where M_4 can be bounded uniformly in c.

3.3.3.1 Second-Order Approximation of u_*

In a first step we iterate Duhamel's formula (3.17) in $u_*(t_n + \tau)$ by plugging Duhamel's formula for $\mathfrak{n}_*(t_n + s)$ into the corresponding integral in $u_*(t_n + \tau)$. This yields that

$$\begin{aligned} u_*(t_n+\tau) &= \mathrm{e}^{i\mathcal{A}_c\tau} u_*(t_n) - ic\langle\nabla\rangle_c^{-1} \int_0^\tau \mathrm{e}^{i(\tau-s)\mathcal{A}_c} \mathrm{e}^{-ic^2(t_n+s)} \Big| \mathrm{e}^{i\Delta s} \mathfrak{n}_*(t_n) \\ &\quad + \frac{i}{2} \int_0^s \mathrm{e}^{i(s-\theta)\Delta} \mathfrak{n}_*(t_n+\theta) \big(\mathrm{e}^{ic^2(t_n+\theta)} u_*(t_n+\theta) + \mathrm{e}^{-ic^2(t_n+\theta)} \overline{u_*}(t_n+\theta) \big) \mathrm{d}\theta \Big|^2 \mathrm{d}s \\ &= \mathrm{e}^{i\mathcal{A}_c\tau} u_*(t_n) - ic\langle\nabla\rangle_c^{-1} \int_0^\tau \mathrm{e}^{i(\tau-s)\mathcal{A}_c} \mathrm{e}^{-ic^2(t_n+s)} \mathcal{U}\left(\mathfrak{n}_*, u_*, s\right) \mathrm{d}s, \end{aligned} \tag{3.38}$$

where $\mathcal{U}\left(\mathfrak{n}_*, u_*, s\right)$ is defined as follows

$$\mathcal{U}\left(\mathfrak{n}_*, u_*, s\right) := \Big| \mathrm{e}^{i\Delta s} \mathfrak{n}_*(t_n) + \frac{i}{2} \int_0^s \mathrm{e}^{i(s-\theta)\Delta} \mathfrak{n}_*(t_n+\theta) \big(\mathrm{e}^{ic^2(t_n+\theta)} u_*(t_n+\theta) + \mathrm{e}^{-ic^2(t_n+\theta)} \overline{u_*}(t_n+\theta) \big) \mathrm{d}\theta \Big|^2.$$

We rewrite $\mathcal{U}$ and obtain

$$\begin{aligned}\mathcal{U}\left(\mathfrak{n}_*, u_*, s\right) &= \Bigg| \mathrm{e}^{i\Delta s}\mathfrak{n}_*(t_n) + \frac{i}{2}\int_0^s \mathrm{e}^{i(s-\theta)\Delta}\mathrm{e}^{ic^2(t_n+\theta)}\Big(\mathfrak{n}_*(t_n+\theta)u_*(t_n+\theta)\Big)d\theta \\ &\qquad + \frac{i}{2}\int_0^s \mathrm{e}^{i(s-\theta)\Delta}\mathrm{e}^{-ic^2(t_n+\theta)}\Big(\mathfrak{n}_*(t_n+\theta)\overline{u_*}(t_n+\theta)d\theta\Big)\Bigg|^2 \\ &= \Bigg| \mathrm{e}^{i\Delta s}\mathfrak{n}_*(t_n) + \frac{i}{2}\mathrm{e}^{is\Delta}\mathrm{e}^{ic^2 t_n}\int_0^s \mathrm{e}^{-i\theta\Delta}\mathrm{e}^{ic^2\theta}\Big(\mathfrak{n}_*(t_n+\theta)u_*(t_n+\theta)\Big)d\theta \\ &\qquad + \frac{i}{2}\mathrm{e}^{is\Delta}\mathrm{e}^{-ic^2 t_n}\int_0^s \mathrm{e}^{-i\theta\Delta}\mathrm{e}^{-ic^2\theta}\Big(\mathfrak{n}_*(t_n+\theta)\overline{u_*}(t_n+\theta)d\theta\Big)\Bigg|^2\end{aligned}$$

Now, we apply Taylor series expansion (see (3.26)), this implies that

$$\begin{aligned}\mathcal{U}\left(\mathfrak{n}_*, u_*, s\right) &= \Bigg| \mathrm{e}^{i\Delta s}\mathfrak{n}_*(t_n) + \frac{i}{2}\mathrm{e}^{is\Delta}\mathrm{e}^{ic^2 t_n}\int_0^s \mathrm{e}^{ic^2\theta}d\theta\,\Big(\mathfrak{n}_*(t_n)u_*(t_n)\Big) \\ &\qquad + \frac{i}{2}\mathrm{e}^{is\Delta}\mathrm{e}^{-ic^2 t_n}\int_0^s \mathrm{e}^{-ic^2\theta}d\theta\,\Big(\mathfrak{n}_*(t_n)\overline{u_*}(t_n)\Big)\Bigg|^2 + R_3(\tau, t_n, u_*, \mathfrak{n}_*) \\ &= \Bigg| \mathrm{e}^{i\Delta s}\mathfrak{n}_*(t_n) + \frac{i}{2}s\mathrm{e}^{is\Delta}\mathrm{e}^{ic^2 t_n}\varphi_1\left(ic^2 s\right)\Big(\mathfrak{n}_*(t_n)u_*(t_n)\Big) \\ &\qquad + \frac{i}{2}s\mathrm{e}^{is\Delta}\mathrm{e}^{-ic^2 t_n}\varphi_1\left(-ic^2 s\right)\Big(\mathfrak{n}_*(t_n)\overline{u_*}(t_n)\Big)\Bigg|^2 + R_3(\tau, t_n, u_*, \mathfrak{n}_*),\end{aligned}$$

where the remainder satisfies the estimate

$$\|R_3(s, t_n, u_*, \mathfrak{n}_*)\|_r \le s^2 k_{r,M_3}$$

uniformly in c.

And with $\mathrm{e}^{is\Delta} = 1 + is\Delta + \mathcal{O}(s^2\Delta^2)$ we have that

$$\begin{aligned}\mathcal{U}\left(\mathfrak{n}_*, u_*, s\right) &= \left| \mathrm{e}^{is\Delta}\mathfrak{n}_*(t_n) + \frac{i}{2}s\mathfrak{n}_*(t_n)\left(\mathrm{e}^{ic^2 t_n}\varphi_1(ic^2 s)u_*(t_n) + \mathrm{e}^{-ic^2 t_n}\varphi_1(-ic^2 s)\overline{u_*}(t_n)\right)\right|^2 \\ &\quad + R_3(s, t_n, u_*, \mathfrak{n}_*).\end{aligned}$$

Simplifying the absolute value square in U_1 yields

$$\begin{aligned}\mathcal{U} &= \left| \mathrm{e}^{i\Delta s}\mathfrak{n}_*(t_n) + \frac{i}{2}s\mathrm{e}^{ic^2 t_n}\varphi_1\left(ic^2 s\right)\mathfrak{n}_*(t_n)u_*(t_n) + \frac{i}{2}s\mathrm{e}^{-ic^2 t_n}\varphi_1\left(-ic^2 s\right)\mathfrak{n}_*(t_n)\overline{u_*}(t_n)\right|^2 \\ &= \left(\mathrm{e}^{i\Delta s}\mathfrak{n}_*(t_n) + \frac{i}{2}s\mathrm{e}^{ic^2 t_n}\varphi_1\left(ic^2 s\right)\mathfrak{n}_*(t_n)u_*(t_n) + \frac{i}{2}s\mathrm{e}^{-ic^2 t_n}\varphi_1\left(-ic^2 s\right)\mathfrak{n}_*(t_n)\overline{u_*}(t_n)\right) \\ &\quad \left(\mathrm{e}^{-i\Delta s}\overline{\mathfrak{n}_*}(t_n) - \frac{i}{2}s\mathrm{e}^{-ic^2 t_n}\varphi_1\left(-ic^2 s\right)\overline{\mathfrak{n}_*}(t_n)\overline{u_*}(t_n) - \frac{i}{2}s\mathrm{e}^{ic^2 t_n}\varphi_1\left(ic^2 s\right)\overline{\mathfrak{n}_*}(t_n)u_*(t_n)\right).\end{aligned}$$

Employing again the Taylor series expansion $\mathrm{e}^{is\Delta} = 1 + \mathcal{O}(s\Delta)$ in the terms of order s furthermore implies that

$$\begin{aligned}
\mathcal{U} = \mathfrak{n}_*(t_n)\Big(&\overline{\mathfrak{n}_*}(t_n) - is\left(\Delta\overline{\mathfrak{n}_*}(t_n)\right) - \frac{i}{2}s\mathrm{e}^{-ic^2t_n}\varphi_1\left(-ic^2s\right)\overline{\mathfrak{n}_*}(t_n)\overline{u_*}(t_n) - \frac{i}{2}s\mathrm{e}^{ic^2t_n}\varphi_1\left(ic^2s\right)\overline{\mathfrak{n}_*}(t_n)u_*(t_n)\Big)\\
&+ is\left(\Delta\mathfrak{n}_*(t_n)\right)\overline{\mathfrak{n}_*}(t_n) + \frac{i}{2}s\mathrm{e}^{ic^2t_n}\varphi_1\left(ic^2s\right)|\mathfrak{n}_*(t_n)|^2u_*(t_n) + \frac{i}{2}s\mathrm{e}^{-ic^2t_n}\varphi_1\left(-ic^2s\right)|\mathfrak{n}_*(t_n)|^2\overline{u_*}(t_n)\\
&+ R_3(\tau, t_n, u_*, \mathfrak{n}_*)\\
= &|\mathfrak{n}_*(t_n)|^2 - is\left(\Delta\overline{\mathfrak{n}_*}(t_n)\right)\mathfrak{n}_*(t_n) + is\left(\Delta\mathfrak{n}_*(t_n)\right)\overline{\mathfrak{n}_*}(t_n)\\
&- \frac{i}{2}s\mathrm{e}^{-ic^2t_n}\varphi_1\left(-ic^2s\right)|\mathfrak{n}_*(t_n)|^2\overline{u_*}(t_n) - \frac{i}{2}s\mathrm{e}^{ic^2t_n}\varphi_1\left(ic^2s\right)|\mathfrak{n}_*(t_n)|^2u_*(t_n)\\
&+ \frac{i}{2}s\mathrm{e}^{ic^2t_n}\varphi_1\left(ic^2s\right)|\mathfrak{n}_*(t_n)|^2u_*(t_n) + \frac{i}{2}s\mathrm{e}^{-ic^2t_n}\varphi_1\left(-ic^2s\right)|\mathfrak{n}_*(t_n)|^2\overline{u_*}(t_n) + R_3(\tau, t_n, u_*, \mathfrak{n}_*).
\end{aligned}$$

Finally, we have

$$\mathcal{U}\left(\mathfrak{n}_*, u_*, s\right) = |\mathfrak{n}_*(t_n)|^2 - is\left(\Delta\overline{\mathfrak{n}_*}(t_n)\right)\mathfrak{n}_*(t_n) + is\left(\Delta\mathfrak{n}_*(t_n)\right)\overline{\mathfrak{n}_*}(t_n) + R_3(s, t_n, u_*, \mathfrak{n}_*).$$

Plugging $\mathcal{U}$ into (3.38) we thus obtain together with the identity $\mathcal{A}_c + c^2 = c\langle\nabla\rangle_c$ the following second-order expansion in u_*

$$\begin{aligned}
u_*(t_n + \tau) = \mathrm{e}^{i\mathcal{A}_c\tau}u_*(t_n) &- ic\langle\nabla\rangle_c^{-1}\mathrm{e}^{i\tau\mathcal{A}_c}\mathrm{e}^{-ic^2t_n}\\
&\int_0^\tau \mathrm{e}^{-isc\langle\nabla\rangle_c}\Big(|\mathfrak{n}_*(t_n)|^2 - is\left(\Delta\overline{\mathfrak{n}_*}(t_n)\right)\mathfrak{n}_*(t_n) + is\left(\Delta\mathfrak{n}_*(t_n)\right)\overline{\mathfrak{n}_*}(t_n)\Big)\mathrm{d}s + R_4(\tau, t_n, u_*, \mathfrak{n}_*),
\end{aligned}$$

where the remainder satisfies

$$\|R_4(\tau, t_n, u_*, \mathfrak{n}_*)\|_r \leq \tau^3 k_{r,M_4} \tag{3.39}$$

uniformly in c.

In order to derive a *stable numerical scheme* we carry out the following manipulation in the exponential based on the observation (2.27), i.e.,

$$s\mathrm{e}^{-isc\langle\nabla\rangle_c} = s\mathrm{e}^{-is\left(c\langle\nabla\rangle_c - \frac{1}{2}\Delta\right)} + \mathcal{O}(s^2\Delta).$$

The above relation allows the following expansion of $u_*(t_n + \tau)$

$$\begin{aligned}
u_*(t_n + \tau) &= \mathrm{e}^{i\mathcal{A}_c\tau}u_*(t_n) - ic\langle\nabla\rangle_c^{-1}\mathrm{e}^{i\tau\mathcal{A}_c}\mathrm{e}^{-ic^2t_n}\\
&\qquad\int_0^\tau \mathrm{e}^{-isc\langle\nabla\rangle_c}|\mathfrak{n}_*(t_n)|^2 + is\mathrm{e}^{-is\left(c\langle\nabla\rangle_c - \frac{1}{2}\Delta\right)}\Big(-\left(\Delta\overline{\mathfrak{n}_*}(t_n)\right)\mathfrak{n}_*(t_n) + \left(\Delta\mathfrak{n}_*(t_n)\right)\overline{\mathfrak{n}_*}(t_n)\Big)\mathrm{d}s\\
&\qquad+ R_4(\tau, t_n, u_*, \mathfrak{n}_*)\\
&= \mathrm{e}^{i\mathcal{A}_c\tau}u_*(t_n) - ic\langle\nabla\rangle_c^{-1}\mathrm{e}^{i\tau\mathcal{A}_c}\mathrm{e}^{-ic^2t_n}\int_0^\tau \mathrm{e}^{-isc\langle\nabla\rangle_c}|\mathfrak{n}_*(t_n)|^2\mathrm{d}s\\
&\qquad- ic\langle\nabla\rangle_c^{-1}\mathrm{e}^{i\tau\mathcal{A}_c}\mathrm{e}^{-ic^2t_n}\int_0^\tau is\mathrm{e}^{-is\left(c\langle\nabla\rangle_c - \frac{1}{2}\Delta\right)}\Big(\left(\Delta\mathfrak{n}_*(t_n)\right)\overline{\mathfrak{n}_*}(t_n) - \left(\Delta\overline{\mathfrak{n}_*}(t_n)\right)\mathfrak{n}_*(t_n)\Big)\mathrm{d}s\\
&\qquad+ R_4(\tau, t_n, u_*, \mathfrak{n}_*),
\end{aligned}$$

where the remainder R_4 satisfies the bound (3.39). By Definition 2.8 and application of integration by part yields

$$\int_0^\tau \mathrm{e}^{-isc\langle\nabla\rangle_c}\mathrm{d}s = \tau\varphi_1\big(-i\tau c\langle\nabla\rangle_c\big),$$

$$\int_0^\tau s\mathrm{e}^{-is\left(c\langle\nabla\rangle_c - \frac{1}{2}\Delta\right)}\mathrm{d}s = \tau^2\Psi_2\left(-i\tau\big(c\langle\nabla\rangle_c - \tfrac{1}{2}\Delta\big)\right).$$

Therefore, we have

$$u_*(t_n+\tau) = \mathrm{e}^{i\mathcal{A}_c\tau}u_*(t_n) - ic\langle\nabla\rangle_c^{-1}\mathrm{e}^{i\tau\mathcal{A}_c}\mathrm{e}^{-ic^2t_n}\Bigg(\tau\varphi_1\big(-i\tau c\langle\nabla\rangle_c\big)|\mathfrak{n}_*(t_n)|^2$$
$$+ i\tau^2\Psi_2\left(-i\tau\big(c\langle\nabla\rangle_c - \tfrac{1}{2}\Delta\big)\right)\left(\overline{\mathfrak{n}_*}(t_n)\left(\Delta\mathfrak{n}_*(t_n)\right) - \mathfrak{n}_*(t_n)\left(\Delta\overline{\mathfrak{n}_*}(t_n)\right)\right)\Bigg) + R_4(\tau,t_n,u_*,\mathfrak{n}_*).$$

This motivates us to define the following scheme in u_*

$$u_*^{n+1} = \mathrm{e}^{i\mathcal{A}_c\tau}u_*^n - ic\langle\nabla\rangle_c^{-1}\mathrm{e}^{i\tau\mathcal{A}_c}\mathrm{e}^{-ic^2t_n}I_{u_*}^n\left(\mathfrak{n}_*^n\right) \tag{3.40}$$

with

$$I_{u_*}^n\left(\mathfrak{n}_*^n\right) := \tau\varphi_1\big(-i\tau c\langle\nabla\rangle_c\big)|\mathfrak{n}_*^n|^2 + i\tau^2\Psi_2\left(-i\tau\big(c\langle\nabla\rangle_c - \tfrac{1}{2}\Delta\big)\right)\left(\overline{\mathfrak{n}_*^n}\left(\Delta\mathfrak{n}_*^n\right) - \mathfrak{n}_*^n\left(\Delta\overline{\mathfrak{n}_*^n}\right)\right),$$

and initial value

$$u_*^0 = z_0 - ic\langle\nabla\rangle_c^{-1}z_1.$$

3.3.3.2 Second-Order Approximation of $\mathfrak{n}_*$

In order to approximate $\mathfrak{n}_*$ up to second-order uniformly in c we proceed similarly to the last subsection for u_*. Recall Duhamel's formula (3.17) in the twisted variable $\mathfrak{n}_*$

$$\mathfrak{n}_*(t_n+\tau) = \mathrm{e}^{i\tau\Delta}\mathfrak{n}_*(t_n) + \frac{i}{2}\int_0^\tau \mathrm{e}^{i(\tau-s)\Delta}\left[\mathrm{e}^{ic^2(t_n+s)}u_*(t_n+s) + \mathrm{e}^{-ic^2(t_n+s)}\overline{u_*}(t_n+s)\right]\mathfrak{n}_*(t_n+s)\mathrm{d}s. \tag{3.41}$$

In a first step we derive uniform approximations in $\mathfrak{n}_*(t_n+s)$ and $u_*(t_n+s)$ up to order $\mathcal{O}(s^2)$.

1) Approximation of $\mathfrak{n}_*(t_n+s)$:
Thanks to the first-order approximation in $\mathfrak{n}_*$ given in (3.27) we know that

$$\mathfrak{n}_*(t_n+s) = \mathrm{e}^{i\Delta s}\mathfrak{n}_*(t_n) + \frac{i}{2}\mathrm{e}^{ic^2t_n}s\varphi_1\big(ic^2s\big)\mathfrak{n}_*(t_n)u_*(t_n) + \frac{i}{2}\mathrm{e}^{-ic^2t_n}s\varphi_1\big(-ic^2s\big)\mathfrak{n}_*(t_n)\overline{u_*}(t_n) + R_3(s,t_n,u_*,\mathfrak{n}_*), \tag{3.42}$$

where the remainder satisfies

$$\|R_3(s,t_n,u_*,\mathfrak{n}_*)\|_r \le s^2k_{r,M_3} \tag{3.43}$$

uniformly in c.

2) Approximation of $u_*(t_n+s)$:
Thanks to the first-order approximation (3.24) we obtain together with (3.22) that

$$u_*(t_n+s) = \mathrm{e}^{is\mathcal{A}_c}u_*(t_n) - i\mathrm{e}^{-ic^2t_n}c\langle\nabla\rangle_c^{-1}s\varphi_1\left(-ic^2s\right)|\mathfrak{n}_*(t_n)|^2 + R_3(s,t_n,u_*,\mathfrak{n}_*), \tag{3.44}$$

where the remainder satisfies (3.43) for some constant k_{r,M_3} independent of c.

Plugging the first-order approximations (3.42) and (3.44) into (3.41) yields that

$$\begin{aligned}\mathfrak{n}_*(t_n+\tau) = \mathrm{e}^{i\Delta\tau}\mathfrak{n}_*(t_n) + \frac{i}{2}\mathrm{e}^{i\tau\Delta}\int_0^\tau \mathrm{e}^{-is\Delta}\\ \Big[\mathrm{e}^{i\Delta s}\mathfrak{n}_*(t_n) + \frac{i}{2}\mathrm{e}^{ic^2t_n}s\varphi_1\big(ic^2s\big)\mathfrak{n}_*(t_n)u_*(t_n) + \frac{i}{2}\mathrm{e}^{-ic^2t_n}s\varphi_1\big(-ic^2s\big)\mathfrak{n}_*(t_n)\overline{u_*}(t_n)\Big]\\ \Big[\mathrm{e}^{ic^2(t_n+s)}\mathrm{e}^{i\mathcal{A}_cs}u_*(t_n) - i\mathrm{e}^{ic^2s}c\langle\nabla\rangle_c^{-1}s\varphi_1\left(-ic^2s\right)|\mathfrak{n}_*(t_n)|^2\\ + \mathrm{e}^{-ic^2(t_n+s)}\mathrm{e}^{-i\mathcal{A}_cs}\overline{u_*}(t_n) + i\mathrm{e}^{-ic^2s}c\langle\nabla\rangle_c^{-1}s\varphi_1\left(ic^2s\right)|\mathfrak{n}_*(t_n)|^2\Big]\mathrm{d}s + R_4(\tau,t_n,u_*,\mathfrak{n}_*),\end{aligned} \tag{3.45}$$

where the remainder satisfies

$$\|R_4(\tau,t_n,u_*,\mathfrak{n}_*)\|_r \le \tau^3 k_{r,M_4}.$$

uniformly in c.

3) Approximation of the integral:

It remains to approximate the integral in (3.45), called $I_{\mathfrak{n}_*}$, which reads

$$\begin{aligned}I_{\mathfrak{n}_*}(u_*(t_n),\mathfrak{n}_*(t_n)) :=\\ \int_0^\tau \mathrm{e}^{-is\Delta}\Big[\mathrm{e}^{i\Delta s}\mathfrak{n}_*(t_n) + \frac{i}{2}\mathrm{e}^{ic^2t_n}s\varphi_1\big(ic^2s\big)\mathfrak{n}_*(t_n)u_*(t_n) + \frac{i}{2}\mathrm{e}^{-ic^2t_n}s\varphi_1\big(-ic^2s\big)\mathfrak{n}_*(t_n)\overline{u_*}(t_n)\Big]\\ \Big[\mathrm{e}^{ic^2(t_n+s)}\mathrm{e}^{i\mathcal{A}_cs}u_*(t_n) - i\mathrm{e}^{ic^2s}c\langle\nabla\rangle_c^{-1}s\varphi_1\left(-ic^2s\right)|\mathfrak{n}_*(t_n)|^2\\ + \mathrm{e}^{-ic^2(t_n+s)}\mathrm{e}^{-i\mathcal{A}_cs}\overline{u_*}(t_n) + i\mathrm{e}^{-ic^2s}c\langle\nabla\rangle_c^{-1}s\varphi_1\left(ic^2s\right)|\mathfrak{n}_*(t_n)|^2\Big]\mathrm{d}s.\end{aligned}$$

Multiplying the brackets yields

$$I_{\mathfrak{n}_*} = I_{\mathfrak{n}_*,a} + I_{\mathfrak{n}_*,b}$$

where we set

$$\begin{aligned}I_{\mathfrak{n}_*,a} :=& \int_0^\tau \mathrm{e}^{-is\Delta}\Big(\mathrm{e}^{i\Delta s}\mathfrak{n}_*(t_n)\mathrm{e}^{ic^2(t_n+s)}\mathrm{e}^{i\mathcal{A}_cs}u_*(t_n)\Big)\mathrm{d}s\\ &+ \int_0^\tau \mathrm{e}^{-is\Delta}\Big(\mathrm{e}^{i\Delta s}\mathfrak{n}_*(t_n)\mathrm{e}^{-ic^2(t_n+s)}\mathrm{e}^{-i\mathcal{A}_cs}\overline{u_*}(t_n)\Big)\mathrm{d}s\\ &- \int_0^\tau \mathrm{e}^{-is\Delta}\Big(\mathrm{e}^{i\Delta s}\mathfrak{n}_*(t_n)i\mathrm{e}^{ic^2s}c\langle\nabla\rangle_c^{-1}s\varphi_1\left(-ic^2s\right)|\mathfrak{n}_*(t_n)|^2\Big)\mathrm{d}s\\ &+ \int_0^\tau \mathrm{e}^{-is\Delta}\Big(\mathrm{e}^{i\Delta s}\mathfrak{n}_*(t_n)i\mathrm{e}^{-ic^2s}c\langle\nabla\rangle_c^{-1}s\varphi_1\left(ic^2s\right)|\mathfrak{n}_*(t_n)|^2\Big)\mathrm{d}s\\ &+ \int_0^\tau \mathrm{e}^{-is\Delta}\Big(\frac{i}{2}\mathrm{e}^{ic^2t_n}s\varphi_1\big(ic^2s\big)\mathfrak{n}_*(t_n)u_*(t_n)\mathrm{e}^{ic^2(t_n+s)}\mathrm{e}^{i\mathcal{A}_cs}u_*(t_n)\Big)\mathrm{d}s\\ &+ \int_0^\tau \mathrm{e}^{-is\Delta}\Big(\frac{i}{2}\mathrm{e}^{ic^2t_n}s\varphi_1\big(ic^2s\big)\mathfrak{n}_*(t_n)u_*(t_n)\mathrm{e}^{-ic^2(t_n+s)}\mathrm{e}^{-i\mathcal{A}_cs}\overline{u_*}(t_n)\Big)\mathrm{d}s\\ &+ \int_0^\tau \mathrm{e}^{-is\Delta}\Big(\frac{i}{2}\mathrm{e}^{-ic^2t_n}s\varphi_1\big(-ic^2s\big)\mathfrak{n}_*(t_n)\overline{u_*}(t_n)\Big)\mathrm{e}^{ic^2(t_n+s)}\mathrm{e}^{i\mathcal{A}_cs}u_*(t_n)\mathrm{d}s\\ &+ \int_0^\tau \mathrm{e}^{-is\Delta}\Big(\frac{i}{2}\mathrm{e}^{-ic^2t_n}s\varphi_1\big(-ic^2s\big)\mathfrak{n}_*(t_n)\overline{u_*}(t_n)\mathrm{e}^{-ic^2(t_n+s)}\mathrm{e}^{-i\mathcal{A}_cs}\overline{u_*}(t_n)\Big)\mathrm{d}s\end{aligned}$$

and

$$\begin{aligned}
I_{\mathfrak{n}_*,b} := &-\int_0^\tau \mathrm{e}^{-is\Delta}\Big(\frac{i}{2}\mathrm{e}^{ic^2t_n}s\varphi_1\big(ic^2s\big)\mathfrak{n}_*(t_n)u_*(t_n)i\mathrm{e}^{ic^2s}c\langle\nabla\rangle_c^{-1}s\varphi_1\left(-ic^2s\right)|\mathfrak{n}_*(t_n)|^2\Big)\mathrm{d}s\\
&+\int_0^\tau \mathrm{e}^{-is\Delta}\Big(\frac{i}{2}\mathrm{e}^{ic^2t_n}s\varphi_1\big(ic^2s\big)\mathfrak{n}_*(t_n)u_*(t_n)i\mathrm{e}^{-ic^2s}c\langle\nabla\rangle_c^{-1}s\varphi_1\left(ic^2s\right)|\mathfrak{n}_*(t_n)|^2\Big)\mathrm{d}s\\
&-\int_0^\tau \mathrm{e}^{-is\Delta}\Big(\frac{i}{2}\mathrm{e}^{-ic^2t_n}s\varphi_1\big(-ic^2s\big)\mathfrak{n}_*(t_n)\overline{u_*}(t_n)i\mathrm{e}^{ic^2s}c\langle\nabla\rangle_c^{-1}s\varphi_1\left(-ic^2s\right)|\mathfrak{n}_*(t_n)|^2\Big)\mathrm{d}s\\
&+\int_0^\tau \mathrm{e}^{-is\Delta}\Big(\frac{i}{2}\mathrm{e}^{-ic^2t_n}s\varphi_1\big(-ic^2s\big)\mathfrak{n}_*(t_n)\overline{u_*}(t_n)i\mathrm{e}^{-ic^2s}c\langle\nabla\rangle_c^{-1}s\varphi_1\left(ic^2s\right)|\mathfrak{n}_*(t_n)|^2\Big)\mathrm{d}s.
\end{aligned}$$

Using the approximation $s\mathrm{e}^{-is\Delta} = s+\mathcal{O}(s^2\Delta)$, the estimate for $c\langle\nabla\rangle_c^{-1}$ (see (3.19)) and for φ_1 (see (3.31)) we obtain that all terms in $I_{\mathfrak{n}_*,b}$ are of order $\mathcal{O}(\tau^3)$, such that we have

$$\begin{aligned}
I_{\mathfrak{n}_*} &= I_{\mathfrak{n}_*,a} + R_4(\tau,t_n,u_*,\mathfrak{n}_*)\\
&= \int_0^\tau \mathrm{e}^{-is\Delta}\left[\left(\mathrm{e}^{i\Delta s}\mathfrak{n}_*(t_n)\right)\left(\mathrm{e}^{ic^2(t_n+s)}\mathrm{e}^{is\mathcal{A}_c}u_*(t_n)\right)\right]\mathrm{d}s\\
&\quad+\int_0^\tau \mathrm{e}^{-is\Delta}\left[\left(\mathrm{e}^{i\Delta s}\mathfrak{n}_*(t_n)\right)\left(\mathrm{e}^{-ic^2(t_n+s)}\mathrm{e}^{-is\mathcal{A}_c}\overline{u_*}(t_n)\right)\right]\mathrm{d}s\\
&\quad+i\int_0^\tau sn_*(t_n)\left[c\langle\nabla\rangle_c^{-1}|\mathfrak{n}_*(t_n)|^2\right]\Big(-\mathrm{e}^{ic^2s}\varphi_1\left(-ic^2s\right)+\mathrm{e}^{-ic^2s}\varphi_1\left(ic^2s\right)\Big)\mathrm{d}s\\
&\quad+\frac{i}{2}\int_0^\tau s\left[\mathrm{e}^{ic^2t_n}\varphi_1\big(ic^2s\big)\mathfrak{n}_*(t_n)u_*(t_n)+\mathrm{e}^{-ic^2t_n}\varphi_1\big(-ic^2s\big)\mathfrak{n}_*(t_n)\overline{u_*}(t_n)\right]\\
&\qquad\qquad\left[\mathrm{e}^{ic^2(t_n+s)}u_*(t_n)+\mathrm{e}^{-ic^2(t_n+s)}\overline{u_*}(t_n)\right]\mathrm{d}s + R_4(\tau,t_n,u_*,\mathfrak{n}_*),
\end{aligned} \tag{3.46}$$

where the remainder R_4 satisfies

$$\|R_4(\tau,t_n,u_*,\mathfrak{n}_*)\|_r \leq \tau^3 k_{r,M_4}$$

uniformly in c. Note that the latter two integrals in (3.46) can be easily solved by exploiting the relations for $\sigma \in \mathbb{R}$, such that

$$\begin{aligned}
\int_0^\tau s\,\mathrm{e}^{-\sigma ic^2s}\varphi_1(\sigma ic^2s)\mathrm{d}s &= \int_0^\tau s\,\varphi_1(-\sigma ic^2s)\mathrm{d}s = \tau^2\varphi_2\left(-\sigma ic^2\tau\right),\\
\int_0^\tau s\,\mathrm{e}^{\sigma ic^2s}\varphi_1(\sigma ic^2s)\mathrm{d}s &= \sigma\frac{1}{ic^2}\int_0^\tau\Big(\varphi_0(\sigma 2ic^2s)-\varphi_0(\sigma ic^2s)\Big)\mathrm{d}s\\
&= \sigma\frac{\tau}{ic^2}\Big(\varphi_1(\sigma 2ic^2\tau)-\varphi_1(\sigma ic^2\tau)\Big)
\end{aligned}$$

which follows from integration by parts together with the observation

$$\mathrm{e}^{\sigma ic^2\tau}\varphi_1\left(-\sigma ic^2\tau\right) = \varphi_1\left(\sigma ic^2\tau\right)$$

which is an immediate consequence of Definition 2.8.

The first two integrals of $I_{\mathfrak{n}_*}$ (see (3.46)) need to be analyzed with care. For the first integral, henceforth called $I_{\mathfrak{n}_*,1}$, we obtain by Taylor series expansion of $\mathrm{e}^{is\Delta}$ and $\mathrm{e}^{is\mathcal{A}_c}$ together with the relation (see also Definition 2.8)

$$\int_0^\tau s\mathrm{e}^{\sigma is(c^2-\Delta)}\mathrm{d}s = \tau^2\Psi_2\left(\sigma i\tau(c^2-\Delta)\right), \quad \sigma = \pm 1 \tag{3.47}$$

that

$$
\begin{aligned}
I_{\mathfrak{n}_*,1} &:= \int_0^\tau \mathrm{e}^{-is\Delta}\left[\left(\mathrm{e}^{i\Delta s}\mathfrak{n}_*(t_n)\right)\left(\mathrm{e}^{ic^2(t_n+s)}\mathrm{e}^{is\mathcal{A}_c}u_*(t_n)\right)\right]\mathrm{d}s\\
&= \mathrm{e}^{ic^2t_n}\int_0^\tau \mathrm{e}^{is(c^2-\Delta)}\left[\mathfrak{n}_*(t_n)u_*(t_n) + \left(is\Delta\mathfrak{n}_*(t_n)\right)u_*(t_n) + \mathfrak{n}_*(t_n)\left(is\mathcal{A}_c u_*(t_n)\right)\right]\mathrm{d}s\\
&\quad + R_4(\tau,t_n,u_*,\mathfrak{n}_*)\\
&= \mathrm{e}^{ic^2t_n}\tau\varphi_1\left(i\tau(c^2-\Delta)\right)\mathfrak{n}_*(t_n)u_*(t_n)\\
&\quad + \tau^2\mathrm{e}^{ic^2t_n}\Psi_2\left(i\tau(c^2-\Delta)\right)\left[\left(i\Delta\mathfrak{n}_*(t_n)\right)u_*(t_n) + \mathfrak{n}_*(t_n)\left(i\mathcal{A}_c u_*(t_n)\right)\right] + R_4(\tau,t_n,u_*,\mathfrak{n}_*).
\end{aligned}
\tag{3.48}
$$

For the second integral in (3.46), henceforth called $I_{\mathfrak{n}_*,2}$, we analogously have

$$
\begin{aligned}
I_{\mathfrak{n}_*,2} &:= \int_0^\tau \mathrm{e}^{-is\Delta}\left[\left(\mathrm{e}^{i\Delta s}\mathfrak{n}_*(t_n)\right)\left(\mathrm{e}^{-ic^2(t_n+s)}\mathrm{e}^{-is\mathcal{A}_c}\overline{u_*}(t_n)\right)\right]\mathrm{d}s\\
&= \mathrm{e}^{-ic^2t_n}\int_0^\tau \mathrm{e}^{-is(c^2-\Delta)}\mathrm{e}^{-2is\Delta}\left[\left(\mathrm{e}^{i\Delta s}\mathfrak{n}_*(t_n)\right)\left(\mathrm{e}^{-is\mathcal{A}_c}\overline{u_*}(t_n)\right)\right]\mathrm{d}s\\
&= \mathrm{e}^{-ic^2t_n}\int_0^\tau \mathrm{e}^{-is(c^2-\Delta)}\left[\mathfrak{n}_*(t_n)\overline{u_*}(t_n)\right]\mathrm{d}s\\
&\quad + \mathrm{e}^{-ic^2t_n}\int_0^\tau \mathrm{e}^{-is(c^2-\Delta)}\left(-2is\Delta\right)\left[\mathfrak{n}_*(t_n)\overline{u_*}(t_n)\right]\mathrm{d}s\\
&\quad + \mathrm{e}^{-ic^2t_n}\int_0^\tau \mathrm{e}^{-is(c^2-\Delta)}\left[\left(is\Delta\mathfrak{n}_*(t_n)\right)\overline{u_*}(t_n) + \mathfrak{n}_*(t_n)\Big(-is\mathcal{A}_c\overline{u_*}(t_n)\Big)\right]\mathrm{d}s + R_4(\tau,t_n,u_*,\mathfrak{n}_*).
\end{aligned}
$$

By the definition of the φ-functions (Definition 2.8) and relation (3.47), we thus obtain that

$$
\begin{aligned}
I_{\mathfrak{n}_*,2} &= \mathrm{e}^{-ic^2t_n}\tau\varphi_1\left(-i\tau(c^2-\Delta)\right)\left[\mathfrak{n}_*(t_n)\overline{u_*}(t_n)\right]\\
&\quad + \mathrm{e}^{-ic^2t_n}\tau^2\Psi_2\left(-i\tau(c^2-\Delta)\right)\left(-2i\Delta\right)\left[\mathfrak{n}_*(t_n)\overline{u_*}(t_n)\right]\\
&\quad + \mathrm{e}^{-ic^2t_n}\tau^2\Psi_2\left(-i\tau(c^2-\Delta)\right)\left[\left(i\Delta\mathfrak{n}_*(t_n)\right)\overline{u_*}(t_n) + \mathfrak{n}_*(t_n)\Big(-i\mathcal{A}_c\overline{u_*}(t_n)\Big)\right] + R_4(\tau,t_n,u_*,\mathfrak{n}_*).
\end{aligned}
\tag{3.49}
$$

Recall that by (3.45) combining with (3.46) we have

$$
\mathfrak{n}_*(t_n+\tau) = \mathrm{e}^{i\tau\Delta}\,\mathfrak{n}_*(t_n) + \frac{i}{2}\mathrm{e}^{i\tau\Delta}\,I_{\mathfrak{n}_*}\big(u_*(t_n),\mathfrak{n}_*(t_n)\big).
$$

Thus, plugging (3.48) and (3.49) into (3.46) motivates us (together with (3.40)) to define the following numerical scheme

$$
\begin{aligned}
u_*^{n+1} &= \mathrm{e}^{i\mathcal{A}_c\tau}u_*^n - ic\langle\nabla\rangle_c^{-1}\mathrm{e}^{i\tau\mathcal{A}_c}\mathrm{e}^{-ic^2t_n}I_{u_*}^n(\mathfrak{n}_*^n), &\qquad u_*^0 &= z_0 - ic\langle\nabla\rangle_c^{-1}z_1,\\
\mathfrak{n}_*^{n+1} &= \mathrm{e}^{i\Delta\tau}\mathfrak{n}_*^n + \frac{i}{2}\mathrm{e}^{i\tau\Delta}I_{\mathfrak{n}_*}^n(u_*^n,\mathfrak{n}_*^n), &\qquad \mathfrak{n}_*^0 &= \mathfrak{n}_0
\end{aligned}
\tag{3.50}
$$

with

$$
I_{u_*}^n(\mathfrak{n}_*^n) := \tau\varphi_1\big(-i\tau c\langle\nabla\rangle_c\big)|\mathfrak{n}_*^n|^2 + i\tau^2\Psi_2\left(-i\tau\big(c\langle\nabla\rangle_c - \tfrac{1}{2}\Delta\big)\right)\left(\overline{\mathfrak{n}_*^n}\left(\Delta\mathfrak{n}_*^n\right) - \mathfrak{n}_*^n\left(\Delta\overline{\mathfrak{n}_*^n}\right)\right)
$$

and

$$
\begin{aligned}
I^n_{\mathfrak{n}_*} &:= \mathrm{e}^{ic^2 t_n}\tau\varphi_1\left(i\tau(c^2-\Delta)\right)\mathfrak{n}^n_* u^n_* + \tau^2\mathrm{e}^{ic^2 t_n}\Psi_2\left(i\tau(c^2-\Delta)\right)\Big[\left(i\Delta\mathfrak{n}^n_*\right)u^n_* + \mathfrak{n}^n_*\left(i\mathcal{A}_c u^n_*\right)\Big]\\
&\quad + \mathrm{e}^{-ic^2 t_n}\tau\varphi_1\left(-i\tau(c^2-\Delta)\right)\Big[\mathfrak{n}^n_*\overline{u^n_*}\Big]\\
&\quad + \mathrm{e}^{-ic^2 t_n}\tau^2\Psi_2\left(-i\tau(c^2-\Delta)\right)\Big[\left(-2i\Delta\right)\left(\mathfrak{n}^n_*\overline{u^n_*}\right) + \left(i\Delta\mathfrak{n}^n_*\right)\overline{u^n_*} + \mathfrak{n}^n_*\Big(-i\mathcal{A}_c\overline{u^n_*}\Big)\Big]\\
&\quad + \frac{\tau}{2c^2}\mathrm{e}^{2ic^2 t_n}\Big(\varphi_1\left(2ic^2\tau\right) - \varphi_1\left(ic^2\tau\right)\Big)\mathfrak{n}^n_*(u^n_*)^2 - \frac{\tau}{2c^2}\mathrm{e}^{-2ic^2 t_n}\Big(\varphi_1\left(-2ic^2\tau\right) - \varphi_1\left(-ic^2\tau\right)\Big)\mathfrak{n}^n_*(\overline{u^n_*})^2\\
&\quad + i\tau^2\Big(-\varphi_2\left(ic^2\tau\right) + \varphi_2\left(-ic^2\tau\right)\Big)\mathfrak{n}^n_*\left(c\langle\nabla\rangle_c^{-1}|\mathfrak{n}^n_*|^2\right)\\
&\quad + \frac{i\tau^2}{2}\Big(\varphi_2\left(ic^2\tau\right) + \varphi_2\left(-ic^2\tau\right)\Big)\mathfrak{n}^n_*|u^n_*|^2,
\end{aligned}
$$

where φ_1, φ_2, and Ψ_2 are given in Definition 2.8.

3.3.3.3 Convergence Analysis of the Second-Order Scheme

The exponential-type integration scheme (3.50) converges (by construction) with second-order in time uniformly with respect to c, see Theorem 3.8 below.

Theorem 3.8 (Convergence bound for the second-order scheme, cf. Theorem 7 in [14])**.** *Fix $r > d/2$ and assume that Assumption 3.7 holds. For u_* defined in (3.50) we set*

$$
z^n := \frac{1}{2}\left(\mathrm{e}^{ic^2 t_n}u^n_* + \mathrm{e}^{-ic^2 t_n}\overline{u^n_*}\right).
$$

Then, there exists a $T > 0$ and $\tau_0 > 0$ such that for $\tau \le \tau_0$ and $t_n \le T$ we have for all $c > 0$ that

$$
\|z(t_n) - z^n\|_r + \|\mathfrak{n}(t_n) - \mathfrak{n}^n\|_r \le \tau^2 K_{r,T,M,M_4},
$$

where the constant K_{r,T,M_4} can be chosen independently of c.

Proof. Fix $r > d/2$. In the following we denote by k_r, K_r and $K_{r,M}$ constants depending only on r and r, M respectively, but which can be chosen independently of c.
The regularity assumptions on the initial values implies Assumption 3.7 on $u_*(t)$. In addition we assume that

$$
\|u_*(t_n)\|_r \le M, \quad \|u^n_*\|_r \le 2M, \quad \|\mathfrak{n}_*(t_n)\|_r \le 3M, \quad \|\mathfrak{n}^n_*\|_r \le 4M.
$$

Again let $(\phi^\tau_{u_*}, \phi^\tau_{\mathfrak{n}_*})$ denote the exact flow and let $(\Phi^\tau_{u_*}, \Phi^\tau_{\mathfrak{n}_*})$ denote the numerical flow, i.e.,

$$
\begin{aligned}
u_*(t_{n+1}) &= \phi^\tau_{u_*}\left(u_*(t_n), \mathfrak{n}_*(t_n)\right), \quad u^{n+1}_* = \Phi^\tau_{u_*}\left(u^n_*, \mathfrak{n}^n_*\right),\\
\mathfrak{n}_*(t_{n+1}) &= \phi^\tau_{\mathfrak{n}_*}\left(u_*(t_n), \mathfrak{n}_*(t_n)\right), \quad \mathfrak{n}^{n+1}_* = \Phi^\tau_{\mathfrak{n}_*}\left(u^n_*, \mathfrak{n}^n_*\right).
\end{aligned}
$$

Again we split the global error as follows

$$
u_*(t_{n+1}) - u^{n+1}_* = \phi^\tau_{u_*}(u_*(t_n), \mathfrak{n}_*(t_n)) - \Phi^\tau_{u_*}(u_*(t_n), \mathfrak{n}_*(t_n)) + \Phi^\tau_{u_*}(u_*(t_n), \mathfrak{n}_*(t_n)) - \Phi^\tau_{u_*}(u^n_*, \mathfrak{n}^n_*).
$$

Local error bound: With the aid of the estimate $\|R_1(\tau, t_n, u_*, \mathfrak{n}_*)\|_r \le \tau^2 k_{r,M_3}$ we have

$$
\left\|\phi^\tau_{u_*}(u_*(t_n), \mathfrak{n}_*(t_n)) - \Phi^\tau_{u_*}(u_*(t_n), \mathfrak{n}_*(t_n))\right\|_r \le \|R_4(\tau, t_n, u_*, \mathfrak{n}_*)\|_r \le \tau^3 k_{r,M_4}.
$$

The same estimate holds for $\mathfrak{n}_*$.

Stability bound: We have to estimate

$$\left\|\Phi^\tau_{u_*}(u_*(t_n),\mathfrak{n}_*(t_n)) - \Phi^\tau_{u_*}(u_*^n,\mathfrak{n}_*^n)\right\|_r, \qquad \left\|\Phi^\tau_{\mathfrak{n}_*}(u_*(t_n),\mathfrak{n}_*(t_n)) - \Phi^\tau_{\mathfrak{n}_*}(u_*^n,\mathfrak{n}_*^n)\right\|_r.$$

Note that for all $t \in \mathbb{R}$ we have that $\|\mathrm{e}^{it\mathcal{A}_c}\|_r = 1$, $\|\mathrm{e}^{it\Delta}\|_r = 1$, and $\|c\langle\nabla\rangle_c^{-1}\|_r \le 1$ (see (3.19) and (3.20), respectively), thus we have

$$\begin{aligned}\left\|\Phi^\tau_{u_*}(f_1,g_1) - \Phi^\tau_{u_*}(f_2,g_2)\right\|_r &= \Big\|\mathrm{e}^{i\mathcal{A}_c\tau} f_1 - ic\langle\nabla\rangle_c^{-1}\mathrm{e}^{i\tau\mathcal{A}_c}\mathrm{e}^{-ic^2t_n} I^n_{u_*}(g_1)\\ &\qquad - \mathrm{e}^{i\mathcal{A}_c\tau} f_2 + ic\langle\nabla\rangle_c^{-1}\mathrm{e}^{i\tau\mathcal{A}_c}\mathrm{e}^{-ic^2t_n} I^n_{u_*}(g_2)\Big\|_r\\ &\le \left\|\mathrm{e}^{i\mathcal{A}_c\tau} f_1 - \mathrm{e}^{i\mathcal{A}_c\tau} f_2\right\|_r\\ &\quad + \left\|ic\langle\nabla\rangle_c^{-1}\mathrm{e}^{i\tau\mathcal{A}_c}\mathrm{e}^{-ic^2t_n} I^n_{u_*}(g_2) - ic\langle\nabla\rangle_c^{-1}\mathrm{e}^{i\tau\mathcal{A}_c}\mathrm{e}^{-ic^2t_n} I^n_{u_*}(g_1)\right\|_r\\ &\le \left\|f_1 - f_2\right\|_r + \left\|I^n_{u_*}(g_1) - I^n_{u_*}(g_2)\right\|_r\end{aligned} \tag{3.51}$$

and analogously

$$\|\Phi^\tau_{\mathfrak{n}_*}(f_1,g_1) - \Phi^\tau_{\mathfrak{n}_*}(f_2,g_2)\|_r \le \|g_1 - g_2\|_r + \|I^n_{\mathfrak{n}_*}(f_1,g_1) - I^n_{\mathfrak{n}_*}(f_2,g_2)\|_r. \tag{3.52}$$

In order to estimate the remaining terms

$$\begin{aligned}\|I^n_{u_*}(g_1) - I^n_{u_*}(g_2)\|_r = \Big\|&\tau\varphi_1\big(-i\tau c\langle\nabla\rangle_c\big)|g_1|^2 + i\tau^2\Psi_2\left(-i\tau\big(c\langle\nabla\rangle_c - \tfrac12\Delta\big)\right)\left(\overline{g_1}\,(\Delta g_1) - g_1\,(\Delta\overline{g_1})\right)\\ &- \tau\varphi_1\big(-i\tau c\langle\nabla\rangle_c\big)|g_2|^2 + i\tau^2\Psi_2\left(-i\tau\big(c\langle\nabla\rangle_c - \tfrac12\Delta\big)\right)\left(\overline{g_2}\,(\Delta g_2) - g_2\,(\Delta\overline{g_2})\right)\Big\|_r\end{aligned} \tag{3.53}$$

and $\|I^n_{\mathfrak{n}_*}(f_1,g_1) - I^n_{\mathfrak{n}_*}(f_2,g_2)\|_r$ we need the following definitions and estimates: recall that by Definition 2.8 we have that

$$\Psi_2(\xi) = \frac{\varphi_0(\xi) - \varphi_1(\xi)}{\xi}.$$

This implies (by looking at the corresponding operators in Fourier space) that the k-th Fourier coefficient satisfies

$$\tau\Psi_2\Big(i\tau\big(c\langle\nabla\rangle_c - \frac12\Delta\big)\Big)_k = \frac{\varphi_0\left(i\tau\big(c\sqrt{c^2+|k|^2} + \frac12|k|^2\big)\right) - \varphi_1\left(i\tau\big(c\sqrt{c^2+|k|^2} + \frac12|k|^2\big)\right)}{i\big(c\sqrt{c^2+|k|^2} + \frac12|k|^2\big)}.$$

Note that for all $k \in \mathbb{Z}^d$ we have

$$\frac{|k|^2}{c\sqrt{c^2+|k|^2} + \frac12|k|^2} \le 2.$$

As $|\varphi_0(i\xi)| \le 1$ for all $\xi \in \mathbb{R}$ and φ_1 satisfies (3.31) this allows us to derive the essential stability bound

$$\left\|\tau^2\Psi_2\Big(i\tau\big(c\langle\nabla\rangle_c - \frac12\Delta\big)\Big)\Delta f\right\|_r \le 4\tau\|f\|_r. \tag{3.54}$$

Similarly, we obtain due to the observations for the k-th Fourier coefficients

$$\left(\frac{-\Delta}{c^2-\Delta}\right)_k \sim \frac{|k|^2}{c^2+|k\ |^2} \leq 1 \quad \text{and} \quad \left(\frac{\mathcal{A}_c}{c^2-\Delta}\right)_k \sim \frac{c\sqrt{c^2+|k|^2}-c^2}{c^2+|k\ |^2} \leq 1$$

that

$$\tau^2 \left\|\Psi_2\big(\pm i\tau(c^2-\Delta)\big)Op\, f\right\|_r \leq \tau K \|f\|_r \quad \text{for} \quad Op=\Delta \quad \text{or} \quad Op=\mathcal{A}_c,$$

for some constant $K>0$ independent of c.

Furthermore, by the definition of φ_2 together with the relation $\varphi_2(\xi)=\frac{\varphi_1(\xi)-1}{\xi}$ (see Definition 2.8) we readily obtain that

$$\tau^2 \left|\varphi_2(i\ell c^2\tau)\right| \leq \tau \min\left\{\frac{2}{|\ell|c^2},\tau\right\} \quad \text{for all } \ell\in\mathbb{Z}, \ell\neq 0$$

such that

$$\tau^2 \left\|\varphi_2(i\ell c^2\tau) f\right\|_r \leq \tau \min\left\{\frac{2}{|\ell|c^2},\tau\right\} \|f\|_r \quad \text{for all } \ell\in\mathbb{Z}, \ell\neq 0.$$

Now, we split (3.53) into two terms

$$\begin{aligned}
\|I^n_{u_*}(g_1)-I^n_{u_*}(g_2)\|_r \leq\ & \Big\|\tau\varphi_1\big(-i\tau c\langle\nabla\rangle_c\big)|g_1|^2-\tau\varphi_1\big(-i\tau c\langle\nabla\rangle_c\big)|g_2|^2\|_r \\
& + \Big\| i\tau^2\Psi_2\left(-i\tau\big(c\langle\nabla\rangle_c-\tfrac{1}{2}\Delta\big)\right)\Big(\overline{g_1}\,(\Delta g_1)-g_1\,(\Delta\overline{g_1})\Big) \\
& - i\tau^2\Psi_2\left(-i\tau\big(c\langle\nabla\rangle_c-\tfrac{1}{2}\Delta\big)\right)\Big(\overline{g_2}\,(\Delta g_2)-g_2\,(\Delta\overline{g_2})\Big)\Big\|_r \\
=\ & T_1+T_2,
\end{aligned}$$

where we set

$$\begin{aligned}
T_1 &:= \Big\|\tau\varphi_1\big(-i\tau c\langle\nabla\rangle_c\big)|g_1|^2-\tau\varphi_1\big(-i\tau c\langle\nabla\rangle_c\big)|g_2|^2\Big\|_r, \\
T_2 &:= \Big\| i\tau^2\Psi_2\left(-i\tau\big(c\langle\nabla\rangle_c-\tfrac{1}{2}\Delta\big)\right)\Big(\overline{g_1}\,(\Delta g_1)-g_1\,(\Delta\overline{g_1})\Big) \\
&\quad - i\tau^2\Psi_2\left(-i\tau\big(c\langle\nabla\rangle_c-\tfrac{1}{2}\Delta\big)\right)\Big(\overline{g_2}\,(\Delta g_2)-g_2\,(\Delta\overline{g_2})\Big)\Big\|_r.
\end{aligned}$$

We consider only T_1, this yields with (3.31) and with the bilinear estimate (1.2) that

$$\begin{aligned}
T_1 &\leq \left\|\tau\varphi_1\big(-i\tau c\langle\nabla\rangle_c\big)\right\|_r \Big\||g_1|^2-|g_2|^2\Big\|_r \\
&\leq \tau K_r\|g_1\overline{g_1}-g_2\overline{g_2}\|_r \\
&\leq \tau K_r\|g_1\overline{g_1}-g_2\overline{g_1}\|_r+\tau K_r\|g_2\overline{g_1}-g_2\overline{g_2}\|_r \\
&\leq \tau K_r\|\overline{g_1}\|_r\|g_1-g_2\|_r+\tau K_r\|g_2\|_r\|\overline{g_1}-\overline{g_2}\|_r \\
&\leq \tau K_{r,M}\|g_1-g_2\|_r.
\end{aligned}$$

Now, we consider T_2 and again add and substract some terms in order to obtain the following estimate

$$\begin{aligned}
T_2 &= \left\|\tau^2\Psi_2\left(-i\tau\left(c\langle\nabla\rangle_c - \tfrac{1}{2}\Delta\right)\right)\left(\overline{g_1}\left(\Delta g_1\right) - g_1\left(\Delta\overline{g_1}\right) - \overline{g_2}\left(\Delta g_2\right) + g_2\left(\Delta\overline{g_2}\right)\right)\right\|_r \\
&\leq \left\|\tau^2\Psi_2\left(-i\tau\left(c\langle\nabla\rangle_c - \tfrac{1}{2}\Delta\right)\right)\left(\overline{g_1}\left(\Delta g_1\right) - \overline{g_2}\left(\Delta g_1\right)\right)\right\|_r \\
&\quad + \left\|\tau^2\Psi_2\left(-i\tau\left(c\langle\nabla\rangle_c - \tfrac{1}{2}\Delta\right)\right)\left(\overline{g_2}\left(\Delta g_1\right) - \overline{g_2}\left(\Delta g_2\right)\right)\right\|_r \\
&\quad + \left\|\tau^2\Psi_2\left(-i\tau\left(c\langle\nabla\rangle_c - \tfrac{1}{2}\Delta\right)\right)\left(g_2\left(\Delta\overline{g_2}\right) - g_2\left(\Delta\overline{g_1}\right)\right)\right\|_r \\
&\quad + \left\|\tau^2\Psi_2\left(-i\tau\left(c\langle\nabla\rangle_c - \tfrac{1}{2}\Delta\right)\right)\left(g_2\left(\Delta\overline{g_1}\right) - g_1\left(\Delta\overline{g_1}\right)\right)\right\|_r \\
&= \left\|\tau^2\Psi_2\left(-i\tau\left(c\langle\nabla\rangle_c - \tfrac{1}{2}\Delta\right)\right)\left(\Delta g_1\right)\left(\overline{g_1} - \overline{g_2}\right)\right\|_r \\
&\quad + \left\|\tau^2\Psi_2\left(-i\tau\left(c\langle\nabla\rangle_c - \tfrac{1}{2}\Delta\right)\right)\left(\overline{g_2}\right)\Delta\left(g_1 - g_2\right)\right\|_r \\
&\quad + \left\|\tau^2\Psi_2\left(-i\tau\left(c\langle\nabla\rangle_c - \tfrac{1}{2}\Delta\right)\right)g_2\Delta\left(\overline{g_2} - \overline{g_1}\right)\right\|_r \\
&\quad + \left\|\tau^2\Psi_2\left(-i\tau\left(c\langle\nabla\rangle_c - \tfrac{1}{2}\Delta\right)\right)\left(\Delta\overline{g_1}\right)\left(g_2 - g_1\right)\right\|_r .
\end{aligned}$$

With estimate (3.54) and with the bilinear estimate (1.2) we have

$$T_2 \leq \tau K_{r,M}\|g_1 - g_2\|_r.$$

Thus, with the above estimates of T_1 and T_2 we obtain for (3.51) that

$$\|\Phi^\tau_{u_*}(f_1, g_1) - \Phi^\tau_{u_*}(f_2, g_2)\|_r \leq \|f_1 - f_2\|_r + \tau K_{r,M}\|g_1 - g_2\|_r. \tag{3.55}$$

For the remaining equation on $\Phi^\tau_{\mathfrak{n}_*}$ (3.52) we use similar techniques as before and the estimates on φ_1, φ_2, and Ψ_2. Thus, a similar bound holds for $\Phi^\tau_{\mathfrak{n}_*}$, i.e.,

$$\|\Phi^\tau_{\mathfrak{n}_*}(f_1, g_1) - \Phi^\tau_{\mathfrak{n}_*}(f_2, g_2)\|_r \leq \|g_1 - g_2\|_r + \tau K_{r,M}\left(\|f_1 - f_2\|_r + \|g_1 - g_2\|_r\right). \tag{3.56}$$

Replacing $f_1 = u_*(t_n)$, $f_2 = u_*^n$, $g_1 = \mathfrak{n}_*(t_n)$, and $g_2 = \mathfrak{n}_*^n$ yields to the stability estimate for our first-order uniformly accurate method.

Global error: Thanks to the local error bound given in (3.30), as well as the stability bounds (3.55) and (3.56) we have by induction (for more details see the proof of Theorem 3.6), respectively, a *Lady Windermere's fan* argument (see, for example [35, 50]) that

$$\|u_*(t_n) - u_*^n\|_r + \|\mathfrak{n}_*(t_n) - \mathfrak{n}_*^n\|_r \leq \tau^2 k_{r,T,M_4}\mathrm{e}^{TK_{r,M}} \leq \tau^2 K_{r,T,M,M_4},$$

where the constants are uniformly in c. Note again we have by $z = \frac{1}{2}(u + \overline{u})$ and the definition of the twisted variable $u_*(t) = \mathrm{e}^{-ic^2t}u(t)$ that

$$\|z(t_n) - z^n\|_r \leq \|u_*(t_n) - u_*^n\|_r \leq \tau^2 K_{r,T,M,M_4}.$$

This completes the proof. □

The next subsection shows the convergence of the exponential-type integration scheme to the numerical method of the corresponding limit system.

3.3.4 Asymptotic Consistency

In this section we show that our novel class of exponential-type integrators of first- and second-order is indeed asymptotically consistent: In the non-relativistic limit ($c \to \infty$) the schemes converge to the numerical solution of the corresponding non-relativistic limit system (i.e., $c \to \infty$ in (3.1)). The latter can be derived with for instance Modulated Fourier Expansion techniques, see Section 3.2 or [20, 26, 34, 36] and the references therein. In particular, the leading order term z_∞ in the asymptotic expansion of z reads

$$z_\infty(t,x) = \frac{1}{2}\left(\mathrm{e}^{ic^2 t} u_\infty(t,x) + \mathrm{e}^{-ic^2 t}\overline{u_\infty}(t,x)\right),$$

where $(u_\infty, \mathfrak{n}_\infty)$ solve the decoupled free Schrödinger limit system (cf. (3.9))

$$\begin{aligned} i\partial_t u_\infty(t,x) &= \tfrac{1}{2}\Delta u_\infty(t,x), \qquad & u_\infty(0) &= z_0 - iz_1,\\ i\partial_t \mathfrak{n}_\infty(t,x) &= -\Delta \mathfrak{n}_\infty(t,x), \qquad & \mathfrak{n}_\infty(0) &= \mathfrak{n}_0. \end{aligned}$$

For sufficiently smooth solutions (and well prepared initial data) asymptotic convergence of order two holds, i.e.,

$$z(t,x) - z_\infty(t,x) = \mathcal{O}(c^{-2}) \quad \text{and} \quad \mathfrak{n}(t,x) - \mathfrak{n}_\infty(t,x) = \mathcal{O}(c^{-2}).$$

The crucial difference between the limit Schrödinger system (3.9) and the full nonlinear Klein–Gordon–Schrödinger system (3.1) lies in the fact that the limit system is linear. Therefore, it can be solved exactly in Fourier space. Nevertheless, in order to compare its solution with our uniformly accurate schemes we formulate it as a numerical integration scheme as follows

$$\begin{aligned} u_\infty^{n+1} &= \mathrm{e}^{-\frac{i}{2}\Delta\tau} u_\infty^n, \qquad & u_\infty^0 &= z_0 - iz_1,\\ \mathfrak{n}_\infty^{n+1} &= \mathrm{e}^{i\Delta\tau}\mathfrak{n}_\infty^n, \qquad & \mathfrak{n}_\infty^0 &= \mathfrak{n}_0 \end{aligned}$$

with solutions

$$z_\infty^{n+1} = \frac{1}{2}\left(\mathrm{e}^{ic^2 t_{n+1}} u_\infty^{n+1} + \mathrm{e}^{-ic^2 t_{n+1}}\overline{u_\infty^{n+1}}\right) \quad \text{and} \quad \mathfrak{n}_\infty^{n+1}.$$

3.3.4.1 Asymptotic Convergence of the First-Order Method

We motivate the asymptotic convergence of our first-order uniformly accurate exponential-type integrator

$$\begin{aligned} u_*^{n+1} &= \mathrm{e}^{i\tau\mathcal{A}_c} u_*^n - i\tau c\langle\nabla\rangle_c^{-1}\mathrm{e}^{i\tau\mathcal{A}_c}\mathrm{e}^{-ic^2 t_n}\varphi_1(-i\tau c^2)|\mathfrak{n}_*^n|^2, \quad u_*^0 = z(0) - ic^{-1}\langle\nabla\rangle_c^{-1}\partial_t z(0),\\ \mathfrak{n}_*^{n+1} &= \mathrm{e}^{i\tau\Delta}\mathfrak{n}_*^n + \frac{i}{2}\tau\left[\mathrm{e}^{i\tau\Delta}\mathrm{e}^{ic^2 t_n}\varphi_1(ic^2\tau)u_*^n + \mathrm{e}^{i\tau\Delta}\mathrm{e}^{-ic^2 t_n}\varphi_1(-ic^2\tau)\overline{v_*^n}\right]\mathfrak{n}_*^n, \quad \mathfrak{n}_*^0 = \mathfrak{n}_0 \end{aligned} \tag{3.57}$$

(see (3.28)) towards the limit solution (3.10). Thereby, we use (2.27) and (3.19) which yields that

$$\begin{aligned} \left\| \left(\mathcal{A}_c - \tfrac{1}{2}\Delta\right) u_*(t)\right\|_r + \left\| \left(c\langle\nabla\rangle_c^{-1} - 1\right) u_*(t)\right\|_r &\le c^{-2}k_r\|u_*(t)\|_{r+4},\\ \left\|\tau\varphi_1(\pm i\tau c^2)\right\|_r = \left\|\frac{\mathrm{e}^{\pm i\tau c^2} - 1}{\pm ic^2}\right\|_r &\le \frac{2}{c^2}, \end{aligned} \tag{3.58}$$

for some constant $k_r > 0$ independent of c. Applying (3.58) on (3.57) formally yields that

$$\begin{aligned} u_*^{n+1} &= \mathrm{e}^{-\frac{i}{2}\tau\Delta}u_*^n + \mathcal{O}(c^{-2}),\\ \mathfrak{n}_*^{n+1} &= \mathrm{e}^{i\tau\Delta}\mathfrak{n}_*^n + \mathcal{O}(c^{-2}). \end{aligned}$$

Hence, for sufficiently smooth solutions the exponential-type integration scheme (3.57) converges asymptotically to the solution of the corresponding free Schrödinger limit system (3.10).

3.3.4.2 Asymptotic Convergence of the Second-Order Method

Techniques similar to (3.58) allow us to show that formally

$$I^n_{u_*} = \mathcal{O}(c^{-2}) \quad \text{and} \quad I^n_{\mathfrak{n}_*} = \mathcal{O}(c^{-2}).$$

Applying the observation (3.58) in (3.50) formally yields that

$$u_*^{n+1} = \mathrm{e}^{-\frac{i}{2}\tau\Delta} u_*^n + \mathcal{O}(c^{-2}), \quad \mathfrak{n}_*^{n+1} = \mathrm{e}^{i\tau\Delta}\mathfrak{n}_*^n + \mathcal{O}(c^{-2})$$

which implies that also our second-order exponential-type integration scheme (3.50) converges asymptotically to the solution of the corresponding free Schrödinger limit system (3.10).

The uniformly accurate behavior of our novel class of integrators is also underlined with numerical experiments in the next Section 3.4. Also we compare our first-order uniformly accurate scheme with standard time integration schemes in Section 3.4.4.

3.4 Numerical Experiments for the Klein–Gordon–Schrödinger System

In this section we numerically underline first-, respectively, second-order convergence uniformly in c of the exponential-type integration schemes (3.28) and (3.50). We also confirm the convergence of the first- and second-order uniformly accurate scheme to the corresponding limit integrator in the limit $c \to \infty$.

We consider the Klein–Gordon–Schrödinger system on the one dimensional torus, i.e., $x \in \mathbb{T} = [0, 2\pi]$ and on a finite time interval, i.e., $t \in [0, T]$. In all numerical experiments we use a standard Fourier pseudospectral method for the spatial discretization. For more details on pseudospectral methods we refer to [27, 69, 70]. The mesh-size is denoted by $h = \frac{2\pi}{M}$, $M \in \mathbb{N}$ with grid points $x_j = jh$ and time step size $\tau = \frac{T}{N}$ with grid points $t_n = n\tau$, for $j = 0, ..., M$ and $n = 0, ..., N$ respectively. In order to use the Fourier transform efficiently we choose $M = 2^k$, with $k \in \mathbb{N}$. For practical implementation of the Fourier transform in Matlab, we introduce the Fourier grid $K = \left[-\frac{M}{2} : -1, 0, 1 : \frac{M}{2} - 1\right]$.

In the following we choose $M = 2^{10}$, i.e. we have the spatial mesh-size $h = 0.0061$ and integrate up to time $T = 1$ in all numerical simulations.

In all numerical experiments for the Klein–Gordon–Schrödinger system we use the following initial values

$$z(0,x) = \frac{1}{2}\frac{\cos(3x)^2 \sin(2x)}{2-\cos(x)}, \qquad \partial_t z(0,x) = c^2 \frac{1}{2}\frac{\sin(x)\cos(2x)}{2-\cos(x)},$$
$$\mathfrak{n}(0,x) = 1 + i\frac{\sin(x)}{2-\cos(x)}.$$

In Section 3.4.1 we derive a Gautschi-type method following the ansatz of [9] in order to obtain a numerical method to compute the reference solution. Then we recall the numerical method for the limit system in Section 3.4.2 and the uniformly accurate methods in Section 3.4.3. Finally, we compare the different numerical methods in Section 3.4.4.

3.4.1 Numerical Methods for the Reference Solution

In this subsection, based on [4, 39], we state two types of numerical reference methods, namely a second-order Gautschi-type method in Section 3.4.1.1 and a classical first-order exponential integrator in Section 3.4.1.2 for the Klein–Gordon–Schrödinger system.

3.4.1.1 A Gautschi-type Method for the Klein–Gordon Equation

We use the techniques of [9] and construct a two step Gautschi-type method. Therefore, we recall our Klein–Gordon–Schrödinger system

$$\begin{aligned} c^{-2}\partial_{tt}z - \Delta z + c^2 z &= |\mathfrak{n}|^2, \qquad z(0) = z_0, \qquad \partial_t z(0) = c^2 z_1,\\ i\partial_t \mathfrak{n} + \Delta\mathfrak{n} + \mathfrak{n}z &= 0, \qquad \mathfrak{n}(0) = \mathfrak{n}_0. \end{aligned}$$

In a first step we use the variation of constants formula for second-order equations for z and obtain

$$\begin{aligned} z(t_n+\tau) &= \cos(\tau c\langle\nabla\rangle_c)z(t_n) + \tau\frac{\sin(\tau c\langle\nabla\rangle_c)}{\tau\langle\nabla\rangle_0}\dot z(t_n) + c^2\int_0^\tau \frac{\sin\left((\tau-s)c\langle\nabla\rangle_c\right)}{c\langle\nabla\rangle_c}|\mathfrak{n}(t_n+s)|^2\mathrm{d}s,\\ \dot z(t_n+\tau) &= -c\langle\nabla\rangle_c\sin(\tau c\langle\nabla\rangle_c)z(t_n) + \cos(\tau c\langle\nabla\rangle_c)\dot z(t_n) + c^2\int_0^\tau \cos\left((\tau-s)c\langle\nabla\rangle_c\right)|\mathfrak{n}(t_n+s)|^2\mathrm{d}s. \end{aligned} \tag{3.59}$$

For $n=0$ we have

$$\begin{aligned} z(t_1) &= \cos(\tau c\langle\nabla\rangle_c)z(0) + \tau\frac{\sin(\tau c\langle\nabla\rangle_c)}{\tau c\langle\nabla\rangle_c}\dot z(0) + c^2\int_0^\tau \frac{\sin\left((\tau-s)c\langle\nabla\rangle_c\right)}{c\langle\nabla\rangle_c}|\mathfrak{n}(s)|^2\mathrm{d}s,\\ \dot z(t_1) &= -c\langle\nabla\rangle_c\sin(\tau c\langle\nabla\rangle_c)z(0) + \cos(\tau c\langle\nabla\rangle_c)\dot z(0) + c^2\int_0^\tau \cos\left((\tau-s)c\langle\nabla\rangle_c\right)|\mathfrak{n}(s)|^2\mathrm{d}s. \end{aligned} \tag{3.60}$$

For $n\geq 1$ we consider t_{n+1} and t_{n-1} in (3.59) and add the equations, such that we have with

$$\cos(-x) = \cos(x) \qquad \text{and} \qquad \sin(-x) = -\sin(x)$$

that

$$\begin{aligned} z(t_{n+1}) + z(t_{n-1}) &= 2\cos(\tau c\langle\nabla\rangle_c)z(t_n)\\ &\quad + c^2\int_0^\tau \frac{\sin\left((\tau-s)c\langle\nabla\rangle_c\right)}{c\langle\nabla\rangle_c}\Big(|\mathfrak{n}(t_n+s)|^2 + |\mathfrak{n}(t_n-s)|^2\Big)\mathrm{d}s,\\ \dot z(t_{n+1}) + \dot z(t_{n-1}) &= 2\cos(\tau c\langle\nabla\rangle_c)\dot z(0)\\ &\quad + c^2\int_0^\tau \cos\left((\tau-s)c\langle\nabla\rangle_c\right)\Big(|\mathfrak{n}(t_n+s)|^2 + |\mathfrak{n}(t_n-s)|^2\Big)\mathrm{d}s. \end{aligned}$$

We solve the equations for $z(t_{n+1})$, $\dot z(t_{n+1})$ and obtain

$$\begin{aligned} z(t_{n+1}) &= 2\cos(\tau c\langle\nabla\rangle_c)z(t_n) - z(t_{n-1})\\ &\quad + c^2\int_0^\tau \frac{\sin\left((\tau-s)c\langle\nabla\rangle_c\right)}{c\langle\nabla\rangle_c}\Big(|\mathfrak{n}(t_n+s)|^2 + |\mathfrak{n}(t_n-s)|^2\Big)\mathrm{d}s,\\ \dot z(t_{n+1}) &= 2\cos(\tau c\langle\nabla\rangle_c)\dot z(t_n) - \dot z(t_{n-1})\\ &\quad + c^2\int_0^\tau \cos\left((\tau-s)c\langle\nabla\rangle_c\right)\Big(|\mathfrak{n}(t_n+s)|^2 + |\mathfrak{n}(t_n-s)|^2\Big)\mathrm{d}s. \end{aligned} \tag{3.61}$$

We approximate the integrals in (3.61) as follows

$$\begin{aligned}\int_0^\tau \frac{\sin\left((\tau-s)c\langle\nabla\rangle_c\right)}{c\langle\nabla\rangle_c}\Big(|\mathfrak{n}(t_n+s)|^2+|\mathfrak{n}(t_n-s)|^2\Big)\mathrm{d}s &\approx 2\int_0^\tau \frac{\sin\left((\tau-s)c\langle\nabla\rangle_c\right)}{c\langle\nabla\rangle_c}\mathrm{d}s\,|\mathfrak{n}(t_n)|^2\\ &= 2\frac{1-\cos(\tau c\langle\nabla\rangle_c)}{c^2\langle\nabla\rangle_c^2}|\mathfrak{n}(t_n)|^2,\\ \int_0^\tau \cos\left((\tau-s)c\langle\nabla\rangle_c\right)\Big(|\mathfrak{n}(t_n+s)|^2+|\mathfrak{n}(t_n-s)|^2\Big)\mathrm{d}s &\approx 2\int_0^\tau \cos\left((\tau-s)c\langle\nabla\rangle_c\right)\mathrm{d}s\,|\mathfrak{n}(t_n)|^2\\ &= 2\frac{\sin(\tau c\langle\nabla\rangle_c)}{c\langle\nabla\rangle_c}|\mathfrak{n}(t_n)|^2.\end{aligned}\tag{3.62}$$

Now, we compute the integrals in (3.60) with the same approximations as in (3.62) and insert the approximations (3.62) into (3.61). Therefore, we obtain the following two step iteration scheme for $n=0$

$$\begin{aligned}z^1 &= \cos(\tau c\langle\nabla\rangle_c)z^0+\tau\frac{\sin(\tau c\langle\nabla\rangle_c)}{\tau c\langle\nabla\rangle_c}\dot z^0+c^2\frac{1-\cos(\tau c\langle\nabla\rangle_c)}{c^2\langle\nabla\rangle_c^2}|\mathfrak{n}^0|^2,\\ \dot z^1 &= -c\langle\nabla\rangle_c\sin(\tau c\langle\nabla\rangle_c)z^0+\cos(\tau c\langle\nabla\rangle_c)\dot z^0+c^2\frac{\sin(\tau c\langle\nabla\rangle_c)}{c\langle\nabla\rangle_c}|\mathfrak{n}^0|^2,\end{aligned}$$

and for $n\geq 1$

$$\begin{aligned}z^{n+1} &= 2\cos(\tau c\langle\nabla\rangle_c)z^n-z^{n-1}+2c^2\frac{1-\cos(\tau c\langle\nabla\rangle_c)}{c^2\langle\nabla\rangle_c^2}|\mathfrak{n}^n|^2,\\ \dot z^{n+1} &= 2\cos(\tau c\langle\nabla\rangle_c)\dot z^n-\dot z^{n-1}+2c^2\frac{\sin(\tau c\langle\nabla\rangle_c)}{c\langle\nabla\rangle_c}|\mathfrak{n}^n|^2\end{aligned}$$

with initial data

$$z^0=z(0),\qquad \dot z^0=\partial_t z(0).$$

It remains to derive a numerical scheme for $\mathfrak{n}$. Therefore we use the splitting method we introduced in Section 2.4.2. We split the equation for $\mathfrak{n}$ and obtain the following two subproblems

$$\begin{aligned}\partial_t\mathfrak{n} &= i\Delta\mathfrak{n},\\ \partial_t\mathfrak{n} &= iz\mathfrak{n}.\end{aligned}$$

The exact solutions of the subproblems read

$$\begin{aligned}\mathfrak{n}(t_n+\tau) &= \mathrm{e}^{i\tau\Delta}\mathfrak{n}(t_n),\\ \mathfrak{n}(t_n+\tau) &= \mathrm{e}^{i\int_0^\tau z(t_n+s)\mathrm{d}s}\mathfrak{n}(t_n).\end{aligned}\tag{3.63}$$

We use the trapezoidal rule to approximate the integral in the second subproblem of (3.63) and obtain

$$\begin{aligned}\mathfrak{n}(t_n+\tau) &= \mathrm{e}^{i\tau\Delta}\mathfrak{n}(t_n),\\ \mathfrak{n}(t_n+\tau) &= \mathrm{e}^{i\frac{\tau}{2}(z(t_{n+1})+z(t_n))}\mathfrak{n}(t_n).\end{aligned}$$

We apply the Strang splitting scheme, this yields

$$\mathfrak{n}^{n+1}=\mathrm{e}^{i\frac{\tau}{2}\Delta}\mathrm{e}^{i\frac{\tau}{2}\left(z^{n+1}+z^n\right)}\mathrm{e}^{i\frac{\tau}{2}\Delta}\mathfrak{n}^n,\qquad \mathfrak{n}^0=\mathfrak{n}(0).$$

We implement the Gautschi-type method in order to obtain a reference solution for our Klein–Gordon–Schrödinger system. In Figure 3.4 we plot (double logarithmic) the time step size versus the error in z which is measured in a discrete H^1 norm and the error in $\mathfrak{n}$ is measured in a discrete L^2 norm for different values of $c=1,5,10,50,100$. As a reference solution we use the scheme itself with a finer time step size $\tau\approx 10^{-6}$. Figure 3.4 confirms what is shown in Figure 3.1, that Gautschi-type methods suffer from severe time step restriction.

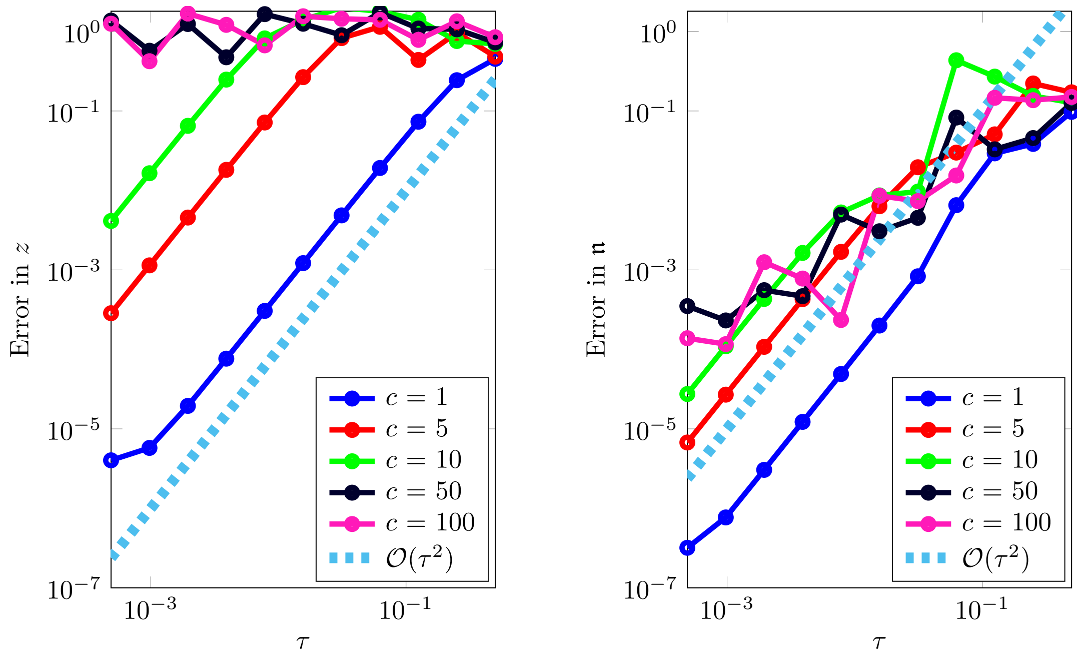

Figure 3.4: Order plot of the Gautschi-type method (double logarithmic scale). Time step size versus error. The slope of the dashed line is two. Left side error in z, right side error in $\mathfrak{n}$. Reference solution computed via the scheme itself with a finer time step size $\tau \approx 10^{-6}$.

3.4.1.2 A Classical Exponential Integrator for the Klein–Gordon–Schrödinger System

Now, we derive a classical exponential integrator for the Klein–Gordon–Schrödinger system. For the details on classical exponential integrators we refer to [39]. For the derivation we recall the first-order system formulation in time (see (3.13))

$$\begin{aligned} i\partial_t u &= -c\langle\nabla\rangle_c u + c\langle\nabla\rangle_c^{-1}|\mathfrak{n}|^2, \quad && u(0) = z_0 - ic\langle\nabla\rangle_c^{-1} z_1,\\ i\partial_t \mathfrak{n} &= -\Delta\mathfrak{n} - \mathfrak{n}\frac{1}{2}(u + \overline{u}), && \mathfrak{n}(0) = \mathfrak{n}_0. \end{aligned}$$

We apply Duhamel's formula

$$\begin{aligned} u(t_n + \tau) &= \mathrm{e}^{i\tau c\langle\nabla\rangle_c} u(t_n) - ic\langle\nabla\rangle_c^{-1} \int_0^\tau \mathrm{e}^{i(\tau-s)c\langle\nabla\rangle_c} |\mathfrak{n}(t_n + s)|^2 \mathrm{d}s,\\ \mathfrak{n}(t_n + \tau) &= \mathrm{e}^{i\tau\Delta}\mathfrak{n}(t_n) + \frac{i}{2}\int_0^\tau \mathrm{e}^{i(\tau-s)\Delta}\mathfrak{n}(t_n+s)\left(u(t_n+s) + \overline{u}(t_n+s)\right)\mathrm{d}s, \end{aligned}$$

and approximate the integrals in the simplest way, i.e., by freezing the nonlinearity at $s = 0$. This yields the following first-order iteration scheme

$$\begin{aligned} u^{n+1} &= \mathrm{e}^{i\tau c\langle\nabla\rangle_c} u^n - \tau ic\langle\nabla\rangle_c^{-1} \mathrm{e}^{i\tau c\langle\nabla\rangle_c}\varphi_1\left(-i\tau c\langle\nabla\rangle_c\right)|\mathfrak{n}^n|^2,\\ \mathfrak{n}^{n+1} &= \mathrm{e}^{i\tau\Delta}\mathfrak{n}^n + \tau\frac{i}{2}c\langle\nabla\rangle_c^{-1}\mathrm{e}^{i\tau\Delta}\varphi_1\left(-i\tau\Delta\right)\mathfrak{n}^n\left(u^n + \overline{u^n}\right). \end{aligned}$$

We implement the first-order exponential integrator in order to obtain a reference solution for the Klein–Gordon–Schrödinger system. In Figure 3.5 we plot (double logarithmic) the time step size versus the error in z and $\mathfrak{n}$ which is measured in a discrete H^1 and L^2 norm, respectively, for different values of $c = 1, 5, 10, 50, 100, 500, 1000, 5000, 10000$. As a reference solution we use the scheme itself with a finer time step size $\tau \approx 10^{-7}$. Figure 3.5 also underlines the time step restrictions for large values of c.

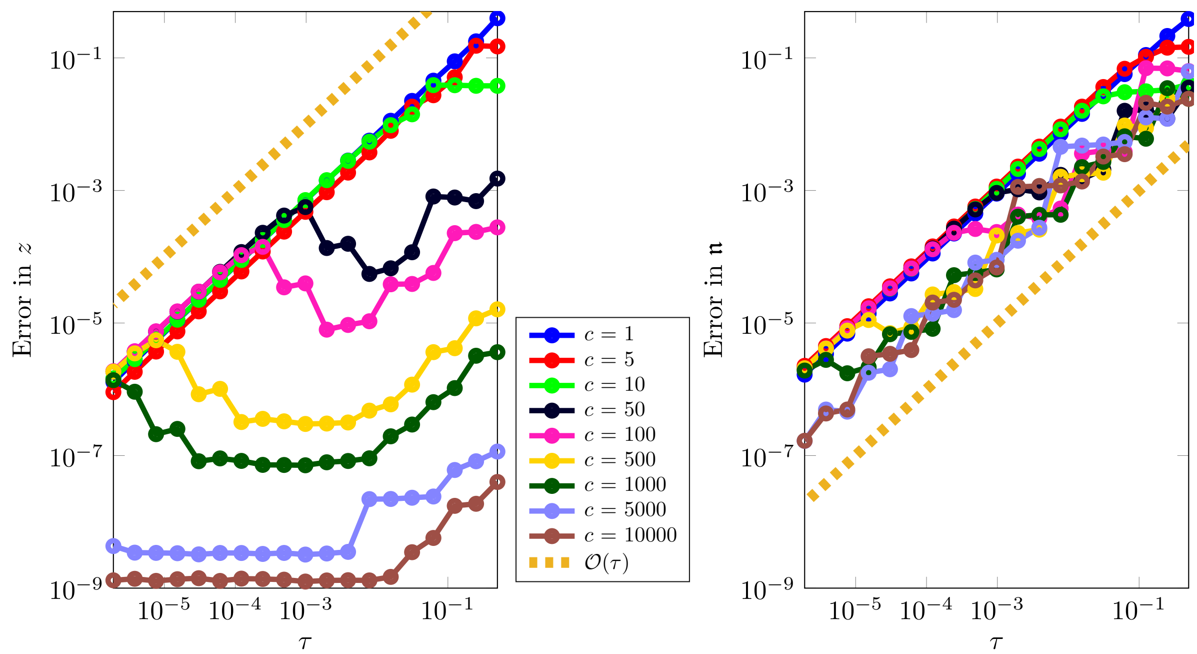

Figure 3.5: Order plot of the first-order exponential integrator (double logarithmic scale). The slope of the dashed line is one. Left side error in z, right side error in $\mathfrak{n}$. Reference solution computed via the scheme itself with a finer time step size $\tau \approx 10^{-7}$.

3.4.2 Numerical Methods for the Limit System

In Section 3.2 we derived a limit system for $c \to \infty$ for the Klein–Gordon–Schrödinger system. The free Schrödinger limit system reads as follows

$$\begin{aligned} \partial_t u_\infty(t,x) &= -\tfrac{i}{2}\Delta u_\infty(t,x), \qquad & u_\infty(0) &= z_0 - iz_1, \\ \partial_t \mathfrak{n}_\infty(t,x) &= i\Delta \mathfrak{n}_\infty(t,x), \qquad & \mathfrak{n}_\infty(0) &= \mathfrak{n}_0. \end{aligned}$$

The benefit is that the free Schrödinger limit system is non-oscillatory and can be solved exactly in Fourier space. Written iteratively we have

$$\begin{aligned} u_\infty^{n+1} &= \mathrm{e}^{-i\frac{\tau}{2}\Delta} u_\infty^n, \qquad & u_\infty^0 &= z_0 - iz_1, \\ \mathfrak{n}_\infty^{n+1} &= \mathrm{e}^{i\tau\Delta}\mathfrak{n}_\infty^n, \qquad & \mathfrak{n}_\infty^0 &= \mathfrak{n}_0. \end{aligned}$$

Here, we do not provide any order plots, since the limit system can be solved exactly.

3.4.3 Uniformly Accurate Methods for the Klein–Gordon–Schrödinger System

We recall the uniformly accurate schemes: the first-order method

$$\begin{aligned} u_*^{n+1} &= \mathrm{e}^{i\tau\mathcal{A}_c} u_*^n - i\tau \mathrm{e}^{-ic^2 t_n}\varphi_1(-i\tau c^2) c\langle\nabla\rangle_c^{-1}\mathrm{e}^{i\tau\mathcal{A}_c}|\mathfrak{n}_*^n|^2, \qquad & u_*^0 &= z_0 - ic\langle\nabla\rangle_c^{-1} z_1, \\ \mathfrak{n}_*^{n+1} &= \mathrm{e}^{i\tau\Delta}\mathfrak{n}_*^n + \frac{i}{2}\tau \mathrm{e}^{i\tau\Delta}\left[\mathrm{e}^{ic^2 t_n}\varphi_1(ic^2\tau) u_*^n \mathfrak{n}_*^n + \mathrm{e}^{-ic^2 t_n}\varphi_1(-ic^2\tau)\overline{u_*^n}\mathfrak{n}_*^n\right], \qquad & \mathfrak{n}_*^0 &= \mathfrak{n}_0, \end{aligned}$$

and the second-order method

$$\begin{aligned}
u_*^{n+1} &= \mathrm{e}^{i\tau\mathcal{A}_c} u_*^n - ic\langle\nabla\rangle_c^{-1}\mathrm{e}^{i\tau\mathcal{A}_c}\mathrm{e}^{-ic^2t_n} I_{u_*}^n(\mathfrak{n}_*^n), &\qquad u_*^0 &= z_0 - ic\langle\nabla\rangle_c^{-1} z_1,\\
\mathfrak{n}_*^{n+1} &= \mathrm{e}^{i\tau\Delta}\mathfrak{n}_*^n + \frac{i}{2}\mathrm{e}^{i\tau\Delta} I_{\mathfrak{n}_*}^n(u_*^n, \mathfrak{n}_*^n), &\qquad \mathfrak{n}_*^0 &= \mathfrak{n}_0
\end{aligned}$$

with

$$I_{u_*}^n(\mathfrak{n}_*^n) = \tau\varphi_1\big(-i\tau c\langle\nabla\rangle_c\big)|\mathfrak{n}_*^n|^2 + i\tau^2\Psi_2\left(-i\tau\big(c\langle\nabla\rangle_c - \tfrac{1}{2}\Delta\big)\right)\Big(\overline{\mathfrak{n}_*^n}\left(\Delta\mathfrak{n}_*^n\right) - \mathfrak{n}_*^n\left(\Delta\overline{\mathfrak{n}_*^n}\right)\Big)$$

and

$$\begin{aligned}
I_{\mathfrak{n}_*}^n &= \mathrm{e}^{ic^2t_n}\tau\varphi_1\left(i\tau(c^2-\Delta)\right)\mathfrak{n}_*^n u_*^n + \tau^2\mathrm{e}^{ic^2t_n}\Psi_2\left(i\tau(c^2-\Delta)\right)\Big[\left(i\Delta\mathfrak{n}_*^n\right)u_*^n + \mathfrak{n}_*^n\left(i\mathcal{A}_c u_*^n\right)\Big]\\
&\quad + \mathrm{e}^{-ic^2t_n}\tau\varphi_1\left(-i\tau(c^2-\Delta)\right)\Big[\mathfrak{n}_*^n\overline{u_*^n}\Big]\\
&\quad + \mathrm{e}^{-ic^2t_n}\tau^2\Psi_2\left(-i\tau(c^2-\Delta)\right)\Big[\left(-2i\Delta\right)\left(\mathfrak{n}_*^n\overline{u_*^n}\right) + \left(i\Delta\mathfrak{n}_*^n\right)\overline{u_*^n} + \mathfrak{n}_*^n\Big(-i\mathcal{A}_c\overline{u_*^n}\Big)\Big]\\
&\quad + \frac{\tau}{2c^2}\mathrm{e}^{2ic^2t_n}\Big(\varphi_1\left(2ic^2\tau\right) - \varphi_1\left(ic^2\tau\right)\Big)\mathfrak{n}_*^n(u_*^n)^2 - \frac{\tau}{2c^2}\mathrm{e}^{-2ic^2t_n}\Big(\varphi_1\left(-2ic^2\tau\right) - \varphi_1\left(-ic^2\tau\right)\Big)\mathfrak{n}_*^n(\overline{u_*^n})^2\\
&\quad + i\tau^2\Big(-\varphi_2\left(ic^2\tau\right) + \varphi_2\left(-ic^2\tau\right)\Big)\mathfrak{n}_*^n\left(c\langle\nabla\rangle_c^{-1}|\mathfrak{n}_*^n|^2\right)\\
&\quad + \frac{i\tau^2}{2}\Big(\varphi_2\left(ic^2\tau\right) + \varphi_2\left(-ic^2\tau\right)\Big)\mathfrak{n}_*^n|u_*^n|^2.
\end{aligned}$$

In Figure 3.6 and 3.7 we numerically confirm the convergence order in time of our first- and second-order uniformly accurate method, respectively. In the figures we plot time step size versus the error of our uniformly accurate schemes for different values of $c = 1, 5, 10, 50, 100, 500, 1000, 5000, 10000$. The error in z is measured in a discrete H^1 norm, the error in $\mathfrak{n}$ is measured in a discrete L^2 norm. As a reference solution we use the scheme itself with a finer time step size $\tau \approx 10^{-7}$.

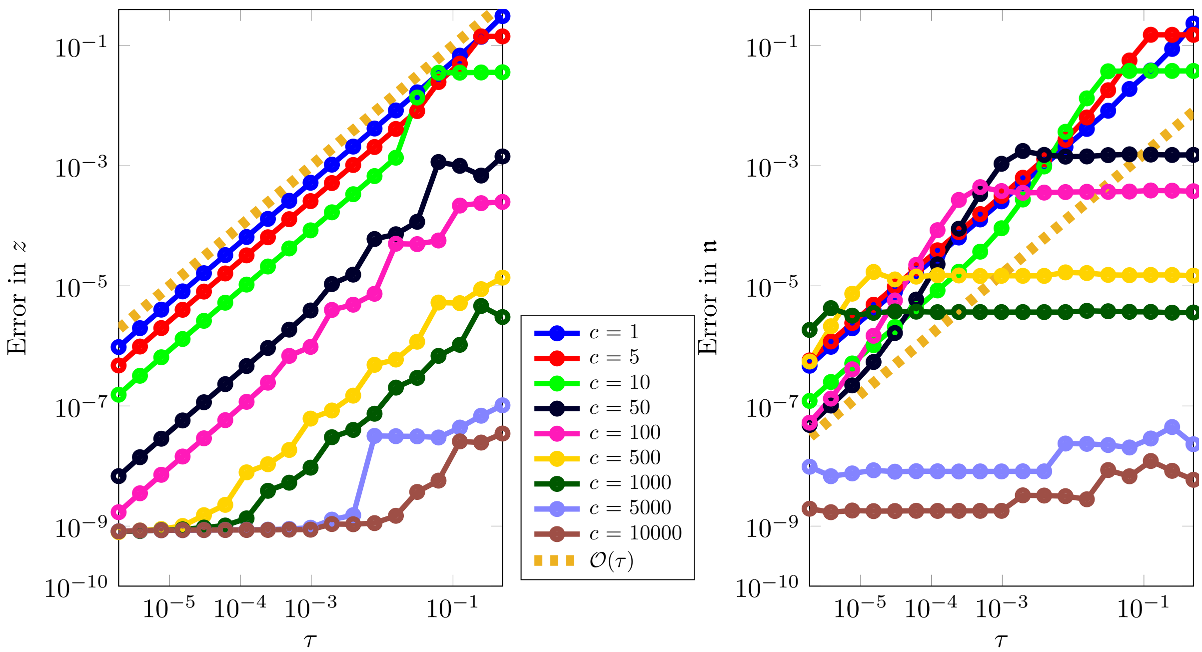

Figure 3.6: Order plot of the first-order uniformly accurate method (double logarithmic scale). The slope of the dashed line is one. Left side error in z, right side error in $\mathfrak{n}$. Reference solution computed via the scheme itself with a finer time step size $\tau \approx 10^{-7}$.

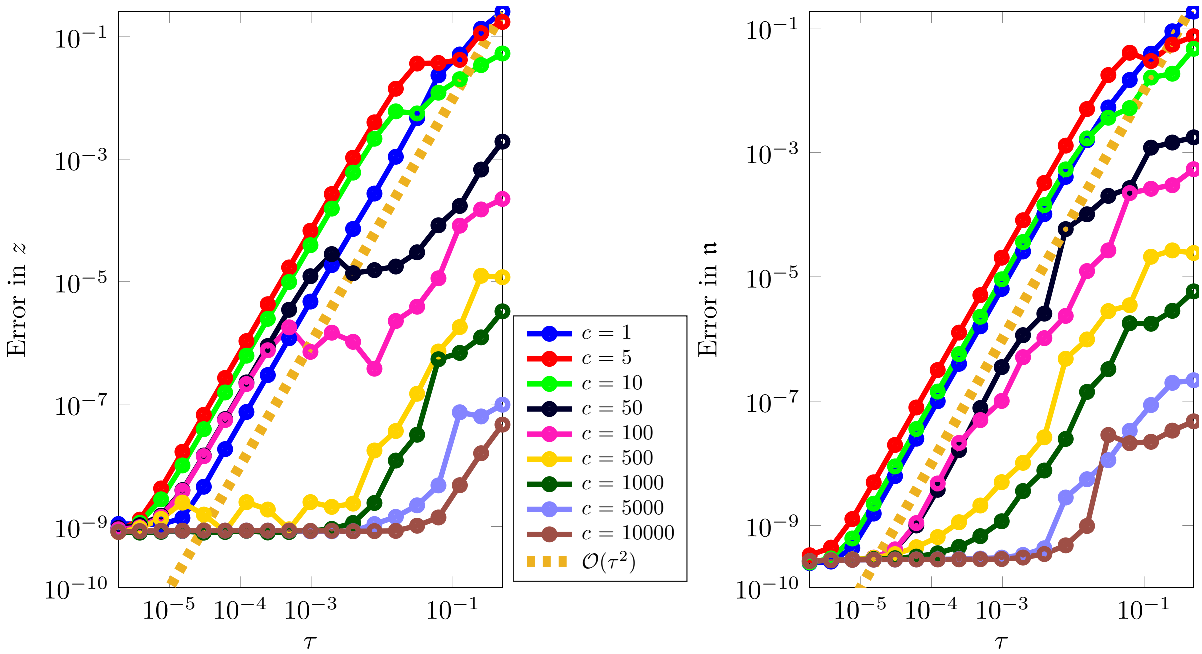

Figure 3.7: Order plot of the second-order uniformly accurate method (double logarithmic scale). The slope of the dashed line is two. Left side error in z, right side error in $\mathfrak{n}$. Reference solution computed via the scheme itself with a finer time step size $\tau \approx 10^{-7}$.

In the numerical experiments (Figure 3.6 and 3.7) we observe that the error does not increase for increasing values of c which is the aim of our novel developed methods. In particular, it is indicated that the error introduced by our schemes reduces with increasing c. This might be due to the fact that our numerical schemes asymptotically converge with order $\mathcal{O}(c^{-2})$ (see also Figure 3.10) to the decoupled free Schrödinger limit system (3.9) which is indeed solved exactly in time.

3.4.4 Comparison of the Numerical Methods

In this subsection we compare our uniformly accurate methods with the established Gautschi-type method, exponential integrator and limit scheme. We confirm that our newly derived uniformly accurate methods are uniformly accurate with respect to c and that they converge asymptotically to the corresponding limit scheme. Finally, we consider work-precision plots and compare the error constants.

We start by comparing our newly derived uniformly accurate first- and second-order method with the first-order exponential integrator. This comparison (see Figure 3.8 and 3.9) confirms that our UA methods are uniformly accurate with respect to c. We use the first-order exponential integrator in order to compute the reference solution with time step size $\tau \approx 10^{-6}$ for different values of $c = 1, 5, 10, 50, 100$. The error between the exponential integrator and our uniformly accurate methods is measured in z in a discrete H^1 norm and in $\mathfrak{n}$ in a discrete L^2 norm.

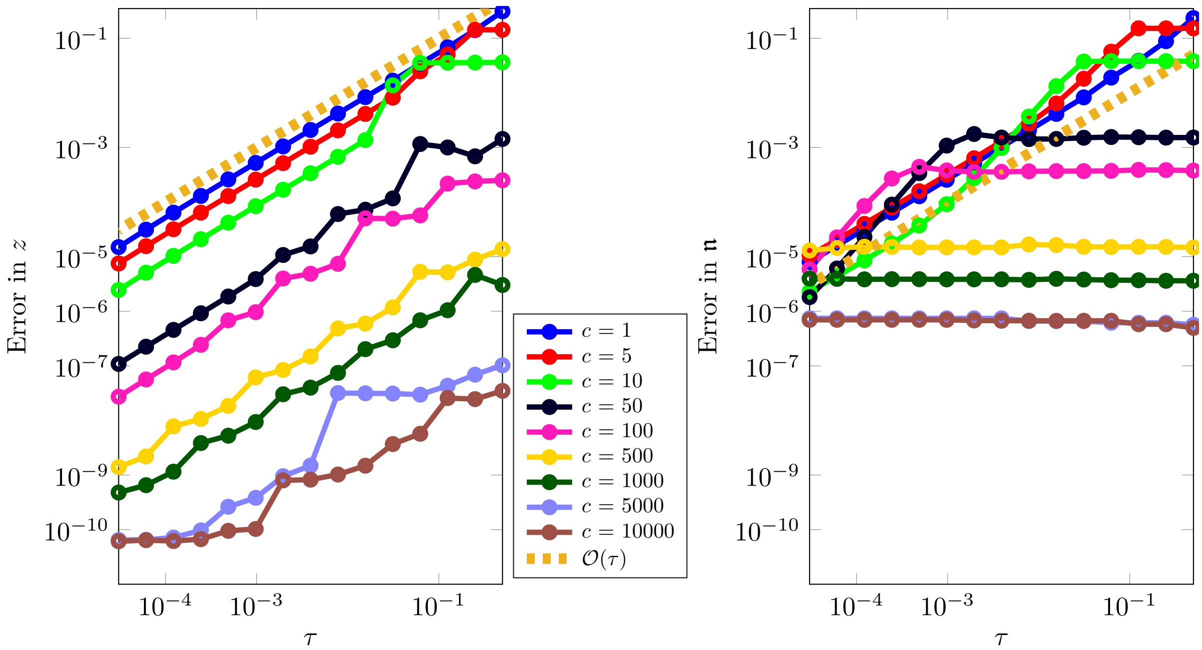

Figure 3.8: Order plot of the first-order uniformly accurate method (double logarithmic scale). Error in z on the left, error in $\mathfrak{n}$ on the right. The slope of the dashed line is one. Reference solution computed via the classical exponential integrator with a finer time step size $\tau \approx 10^{-6}$.

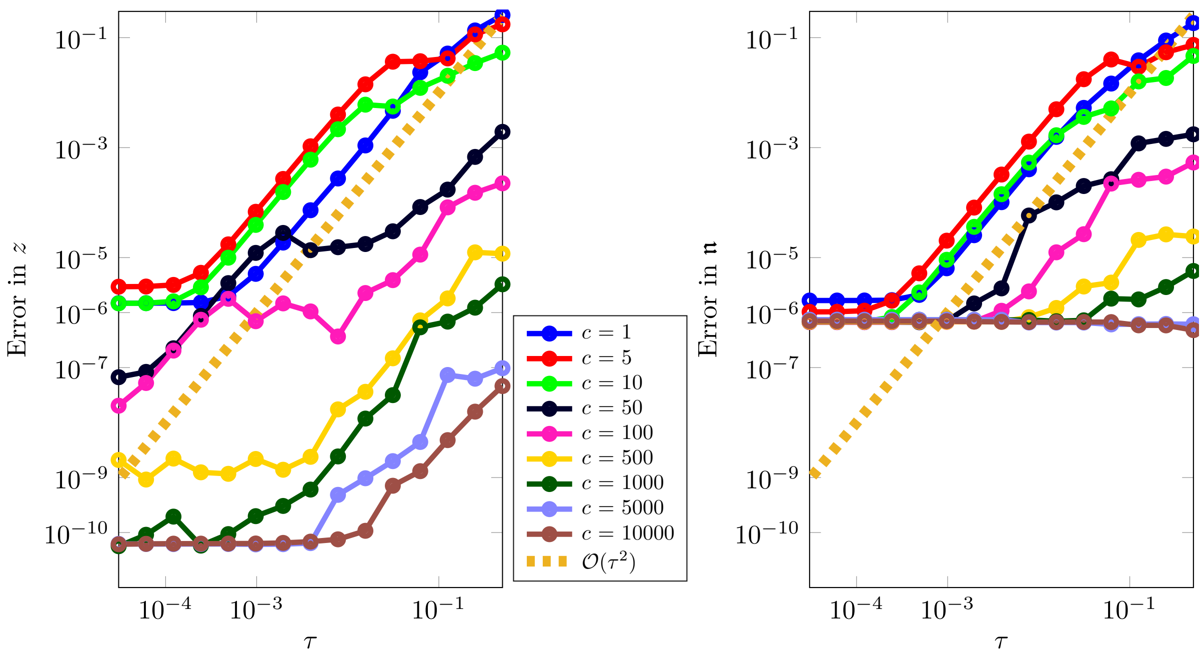

Figure 3.9: Order plot of the second-order uniformly accurate method (double logarithmic scale). The slope of the dashed line is two. Left side error in z, right side error in $\mathfrak{n}$. Reference solution computed via the classical exponential integrator with a finer time step size $\tau \approx 10^{-6}$.

In the next Figure 3.10 we underline the asymptotic convegence to the corresponding numerical methods for the limit system. Therefore, we plot the error of the UA methods and the limit method versus different values of c. This yields the $\mathcal{O}(c^{-2})$ convergence, which is shown in Section 3.3.4. The error in z is measured in a discrete H^1 norm and in $\mathfrak{n}$ in a discrete L^2 norm. Our numerical observations in particular suggest a global error behavior of the type $\min\{\tau, c^{-2}\}$ and $\min\{\tau^2, c^{-2}\}$ for the first-order (3.28) and second-order (3.50) uniformly accurate exponential-type integrator, respectively.

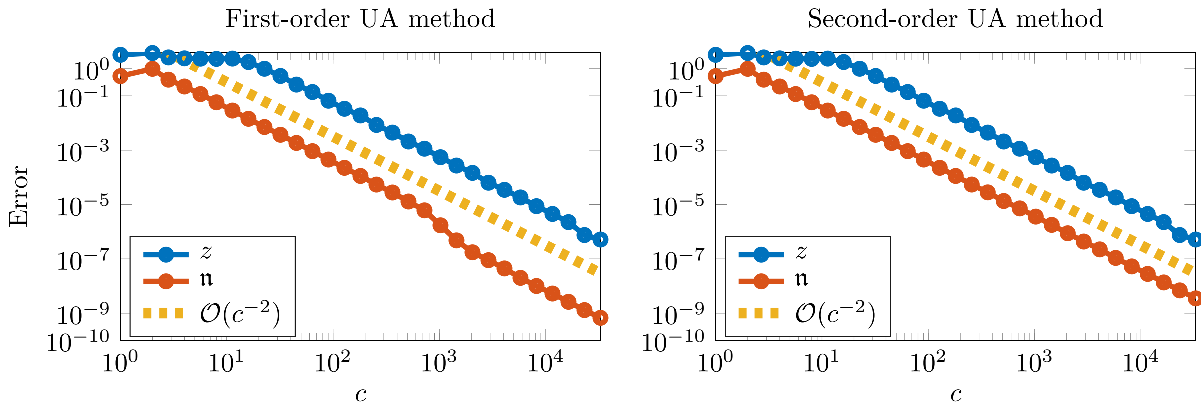

Figure 3.10: Asymptotic consistency plot (double logarithmic scale). Left side error of the first-order UA method, right side error of the second-order UA method. The slope of the dashed line is -2.

Now, we underline the different error constant behaviors of our UA methods. Therefore, we plot the numerical error of the corresponding numerical method against different values of c for different time step sizes τ. In comparison, we also plot the error of the Gautschi-type method against different values of c. For the reference solution we use the exponential integrator with time step size $\tau \approx 10^{-6}$. For our uniformly accurate methods we observe uniform bounds, whereas for the Gautschi-type method we obtain the typical $\mathcal{O}(c^4)$ error (see Figure 3.11).

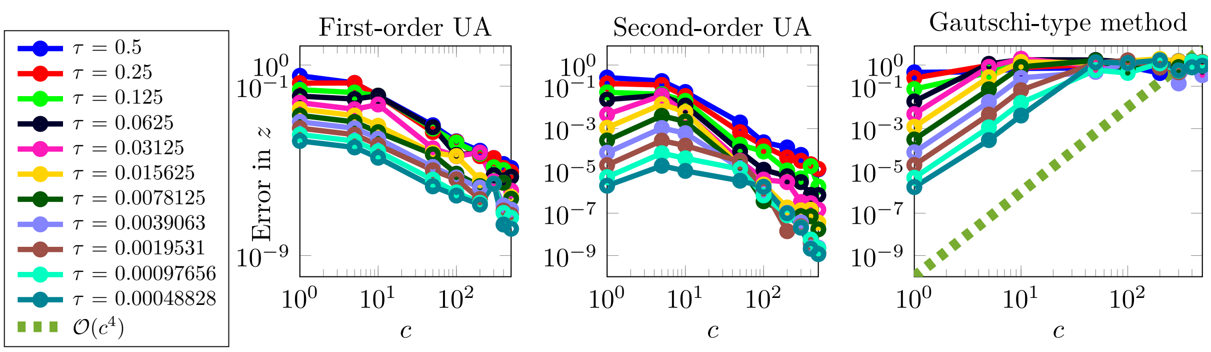

Figure 3.11: Error constant comparison plot (double logarithmic scale). On the left for the first-order uniformly accurate method, in the middle for the second-order uniformly accurate method and on the right for the Gautschi-type method. The slope of the dashed line is four. Reference solution computed via the classical exponential integrator with a finer time step size $\tau \approx 10^{-6}$.

Next, we compare the error of the different methods versus the computation time (see Figure 3.12). The work-precision plots show the efficiency of the numerical methods for different values of c. We plot the corresponding error against the computation time (in seconds) of the corresponding numerical method. We desire values in the lower left corner, i.e., a small error and a short computation time. For the reference solution we use the exponential integrator with time step size $\tau \approx 10^{-6}$. We compare the error of the exponential integrator with the error of the Gautschi-type method, our uniformly accurate methods and the limit scheme. We only show here the plots of z, where the error in z is measured in a discrete H^1 norm. For $\mathfrak{n}$ we obtain similar plots.

We observe that the Gautschi-type method performs well for small c and fails for large c. For the limit scheme we observe this behavior vice versa, i.e., the limit scheme fails for small c but is performing better for increasing values of c. Our uniformly accurate schemes show a good behavior for all values of c. Our uniformly accurate schemes reach smaller errors than both, the Gautschi-type method and the limit scheme for all values of c.

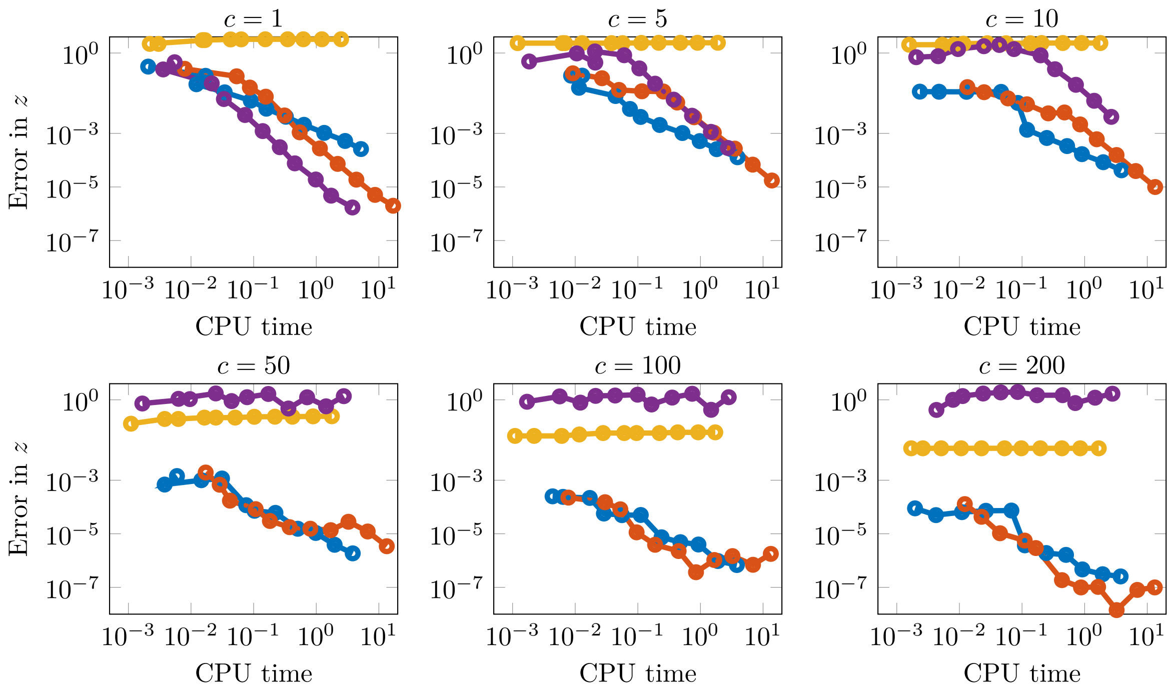

Figure 3.12: Work-precision plot (double logarithmic scale) in z. The yellow line mark the error of the limit scheme. The purple line mark the error of the Gautschi-type method. The blue line mark the error of our first-order uniformly accurate method and the red line mark the error of our second-order uniformly accurate method. The CPU time is measured in seconds. Reference solution computed via the classical exponential integrator with a finer time step size $\tau \approx 10^{-6}$.

In the next chapter we consider the Klein–Gordon–Zakharov system, which is a Klein–Gordon equation coupled with a wave equation. For this system we also derive a limit system and try to derive a uniformly accurate method analogously to the derivation for the KG equation and the KGS system.

CHAPTER 4

The Klein–Gordon–Zakharov System

In this chapter we focus on numerical methods for the Klein–Gordon–Zakharov system. We proceed similarly to the previous chapters. In Section 4.1 we give an overview of the Klein–Gordon–Zakharov system, its high-plasma frequency limit regime and standard numerical methods for solving the Klein–Gordon–Zakharov system. Then we focus in Section 4.2 on the formal derivation of the limit system. We finish this chapter with the derivation of a uniformly accurate method for the Klein–Gordon–Zakharov system (see Section 4.3) in the high-plasma frequency limit regime. The main references for this chapter are [53, 54] for Section 4.1 and Section 4.2. The results of this chapter, in particular Section 4.4, have been published with Katharina Schratz in preprint [12].

4.1 Introduction to Klein–Gordon–Zakharov Systems

The Klein–Gordon–Zakharov (KGZ) system

$$\begin{aligned} c^{-2}\partial_{tt}z(t,x) - \Delta z(t,x) + c^2 z(t,x) &= -\mathfrak{n}(t,x)z(t,x), \\ \partial_{tt}\mathfrak{n}(t,x) - \Delta\mathfrak{n}(t,x) &= \Delta|z(t,x)|^2, \end{aligned} \tag{4.1}$$

with initial conditions

$$\begin{aligned} z(0,x) &= z_0(x), \quad \partial_t z(0,x) = c^2 z_1(x), \\ \mathfrak{n}(0,x) &= \mathfrak{n}_0(x), \quad \partial_t \mathfrak{n}(0,x) = \mathfrak{n}_1(x), \end{aligned}$$

describes the interaction between Langmuir waves, which characterize oscillations of the electron density and ion sound waves in a plasma. Here, z denotes the electric field and $\mathfrak{n}$ denotes the ion density fluctuation. It arises from coupling a Klein–Gordon equation nonlinearly to a wave equation. For existence and uniqueness of global smooth solutions we refer to [53, 54, 60] and the references therein. Numerically the Klein–Gordon–Zakharov system is extensively studied in the *relativistic regime* $c = 1$, see [9, 75]. In contrast, the *non-relativistic regime*, where c tends to infinity, is due to the highly oscillatory behavior of the solution much more challenging numerically.

For a formal overview of the limit system in the high-plasma frequency regime we refer to Section 4.2. Similarly to the previous two chapters, classical numerical methods break down in the high-plasma frequency regime. They fail to resolve the oscillations within the solution. Severe time step size restrictions have to be imposed which leads to huge computational effort and does not permit reasonably accurate simulations.

Analogously to the previous chapters Gautschi-type methods which are especially designed for solving oscillatory second-order differential equations numerically (see [36, 38]), also do not allow a reasonable approximation result as they fail to approximate the highly oscillatory parts properly. We underline this phenomenon in Figure 4.1 for the *high-plasma frequency* regime, i.e., $c \gg 1$. In contrast to the slowly varying relativistic regime $c = 1$ the Gautschi-type method allows a precise approximation of the solution of the Klein–Gordon–Zakharov system. But it fails in the highly oscillatory non-relativistic regime $c \gg 1$. For the classical splitting-type methods we observe a similar error behavior as for the Gautschi-type methods.

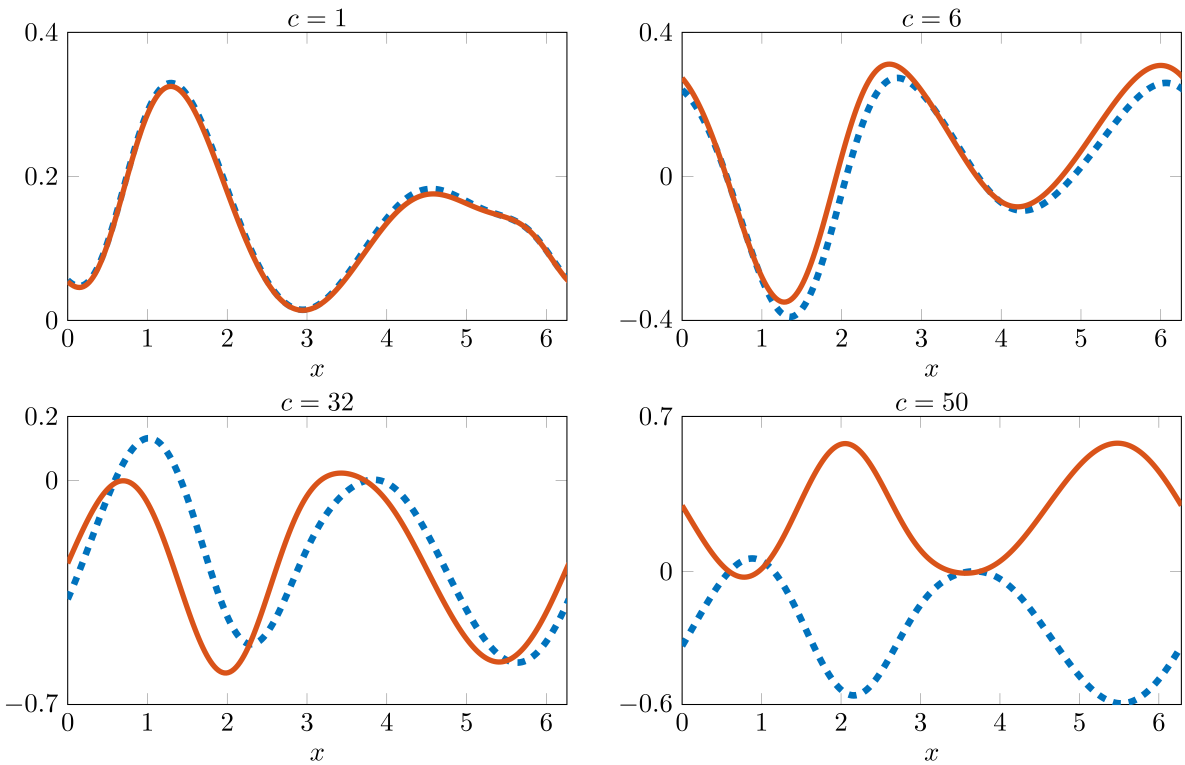

Figure 4.1: Numerical solution of the Klein–Gordon–Zakharov system for z. Exponential Gautschi-type scheme (red solid line) for different c with time step size $\tau \approx 10^{-2}$ at time $t = 0.6$. The blue dashed line represents the reference solution at time $t = 0.6$, computed via the same exponential Gautschi-type scheme with a small time step size $\tau \approx 10^{-6}$. The spatial discretization is done via a Fourier pseudospectral method with mesh-size $h = 0.0245$.

Analogously to the previous chapters numerical limit schemes for the Klein–Gordon–Zakharov system in the strongly non-relativistic limit regime $c \gg 1$ are introduced in Section 4.2. This limit ansatz allows us to reduce the highly oscillatory problem (4.1) to the integration of the corresponding *non-oscillatory* limit equation. Due to the non-oscillatory behavior of the limit system it can be carried out very efficiently without imposing any c-dependent step size restriction.

However, this approach only allows error bounds of order

$$\mathcal{O}(c^{-2}).$$

Henceforth, the limit integration method only yields an accurate approximation of the exact solution for sufficiently large values of c (see Figure 4.2). For more details on the formal derivation of the limit system we refer to Section 4.2.

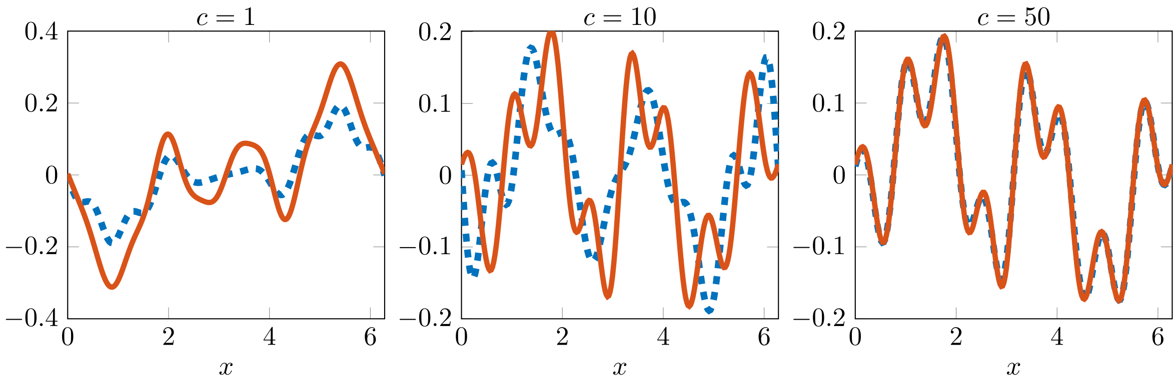

Figure 4.2: Numerical solution of the Klein–Gordon–Zakharov for z for different c, i.e., in the high-plasma frequency case. Limit integration scheme (red solid line) for different c with time step size $\tau \approx 10^{-2}$ at time $t = 1$. The blue dashed line represents the reference solution at time $t = 1$, computed via an exponential Gautschi-type scheme with a small time step size $\tau \approx 10^{-5}$. The spatial discretization is done via a Fourier pseudospectral method with mesh-size $h = 0.0245$.

Here, we want to establish the same novel type of exponential-type integrators as for the Klein–Gordon and Klein–Gordon–Schrödinger which allow convergence with first- and second-order accuracy in time uniformly for all $c \geq 1$. Our first ansatz lies in considering the so-called *twisted variables*. For more details on *twisted variables* and their appearance in physics and numerical analysis we refer to Section 2.1 and Section 3.1. But we see in Section 4.3 that the ansatz of *twisted variables* causes a loss of derivative. Therefore, in Section 4.4 we introduce a novel concept of uniformly accurate *oscillatory integrators* for the Klein–Gordon–Zakharov system which converge uniformly with respect to c. This ansatz allows us to overcome the loss of derivative and to establish rigorous error estimates in the low-plasma as well as in the high-plasma frequency regime. The idea is inspired by the recent work of Herr and Schratz (see [37]). Our novel *oscillatory integrator* is in particular asymptotic consistent and converges in the limit $c \to \infty$ to the solution of the corresponding Zakharov limit system.
In the next section we formally derive and introduce the limit system of the KGZ system.

4.2 Formal Derivation of the High-Plasma Frequency Limit System

We consider formally the *high-plasma frequency* limit regime. For a rigorous analysis, see [15, 21, 54, 55].

In a first step, analogously to the previous chapters, we rewrite the Klein–Gordon–Zakharov system as a first-order system in time. Therefore, we recall the definition of the $\langle\nabla\rangle_c$ operator

$$\langle\nabla\rangle_c = \sqrt{-\Delta + c^2}.$$

Similar to the previous chapters we rewrite (4.1) as a first-order system in time via the following ansatz

$$\begin{aligned} u &= z - ic^{-1}\langle\nabla\rangle_c^{-1}\partial_t z, \\ v &= \overline{z} - ic^{-1}\langle\nabla\rangle_c^{-1}\partial_t \overline{z}, \\ \mathfrak{h} &= \mathfrak{n} - i\langle\nabla\rangle_0^{-1}\partial_t \mathfrak{n}, \end{aligned} \tag{4.2}$$

such that we have

$$\begin{aligned} z &= \tfrac{1}{2}\left(u + \overline{v}\right), \\ \mathfrak{n} &= \Re(\mathfrak{h}). \end{aligned}$$

In order to obtain a first-order system we differentiate u with respect to t and obtain

$$\partial_t u = \partial_t z - ic^{-1}\langle\nabla\rangle_c^{-1}\partial_{tt} z. \tag{4.3}$$

We solve the original equation (4.1) with respect to $\partial_{tt} z$ and equation (4.2) with respect to $\partial_t z$ and plug the two equations into (4.3) which yields

$$\begin{aligned} \partial_t u &= ic\langle\nabla\rangle_c(u - z) - ic^{-1}\langle\nabla\rangle_c^{-1}\partial_{tt} z \\ &= ic\langle\nabla\rangle_c u - ic\langle\nabla\rangle_c z - ic^{-1}\langle\nabla\rangle_c^{-1}(-c^2\mathfrak{n}z) - ic^{-1}\langle\nabla\rangle_c^{-1}(-c^2\langle\nabla\rangle_c^2 z) \\ &= ic\langle\nabla\rangle_c u - ic\langle\nabla\rangle_c z + ic\langle\nabla\rangle_c^{-1}\mathfrak{n}z + ic\langle\nabla\rangle_c z \\ &= ic\langle\nabla\rangle_c u + ic\langle\nabla\rangle_c^{-1}\mathfrak{n}z. \end{aligned} \tag{4.4}$$

Now, we multiply the equation (4.4) by i and obtain

$$i\partial_t u = -c\langle\nabla\rangle_c u - c\langle\nabla\rangle_c^{-1}\mathfrak{n}z.$$

After completing this procedure analogously for v and h, we obtain the first-order formulation of the KGZ system

$$\begin{aligned} i\partial_t u &= -c\langle\nabla\rangle_c u - c\langle\nabla\rangle_c^{-1}\mathfrak{n}z, \\ i\partial_t v &= -c\langle\nabla\rangle_c v - c\langle\nabla\rangle_c^{-1}\mathfrak{n}\overline{z}, \\ i\partial_t \mathfrak{h} &= -\langle\nabla\rangle_0\mathfrak{h} - \langle\nabla\rangle_0|z|^2, \end{aligned}$$

equipped with the initial conditions

$$\begin{aligned} u(0,x) &= z(0,x) - ic^{-1}\langle\nabla\rangle_c^{-1}\partial_t z(0,x) = z_0 - ic\langle\nabla\rangle_c^{-1}z_1, \\ v(0,x) &= \overline{z}(0,x) - ic^{-1}\langle\nabla\rangle_c^{-1}\partial_t \overline{z}(0,x) = \overline{z_0} - ic\langle\nabla\rangle_c^{-1}\overline{z_1}, \\ \mathfrak{h}(0,x) &= \mathfrak{n}(0,x) - i\langle\nabla\rangle_0^{-1}\partial_t \mathfrak{n}(0,x) = \mathfrak{n}_0 - i\langle\nabla\rangle_0^{-1}\mathfrak{n}_1. \end{aligned} \tag{4.5}$$

This yields the following first-order system with initial conditions

$$\begin{aligned} i\partial_t u &= -c\langle\nabla\rangle_c u - c\langle\nabla\rangle_c^{-1}\mathfrak{n}z, & u(0) &= z_0 - ic\langle\nabla\rangle_c^{-1}z_1, \\ i\partial_t v &= -c\langle\nabla\rangle_c v - c\langle\nabla\rangle_c^{-1}\mathfrak{n}\overline{z}, & v(0) &= \overline{z_0} - ic\langle\nabla\rangle_c^{-1}\overline{z_1}, \\ i\partial_t \mathfrak{h} &= -\langle\nabla\rangle_0\mathfrak{h} - \langle\nabla\rangle_0|z|^2, & \mathfrak{h}(0) &= \mathfrak{n}_0 - i\langle\nabla\rangle_0^{-1}\mathfrak{n}_1. \end{aligned} \tag{4.6}$$

We have to be careful with the initial value of $\mathfrak{h}$ (see (4.5) or (4.6)), due to the fact that in Fourier space for the zeroth Fourier mode the term $\langle\nabla\rangle_0^{-1}$ is not well-posed. Therefore, we have to make the assumption that the zeroth Fourier mode of $\partial_t\mathfrak{n}(0)$ has to be equal to zero.

Assumption 4.1. *We assume that the zeroth Fourier mode of $\partial_t\mathfrak{n}(0)$ denoted by $(\widehat{\partial_t\mathfrak{n}(0)})_0$ is zero, i.e., we have*

$$(\widehat{\partial_t\mathfrak{n}(0)})_0 = 0.$$

For notational simplicity we assume $z(t,x) \in \mathbb{R}$, such that we have $z = \frac{1}{2}(u+\overline{u})$. Now, we firstly apply the twisted variable ansatz $u_* := \mathrm{e}^{-ic^2t}u$. Therefore, we have

$$\begin{aligned} i\partial_t u_* &= c^2 u_* + \mathrm{e}^{-ic^2t} i\partial_t u \\ &= -\left(c\langle\nabla\rangle_c - c^2\right) u_* - \frac{1}{2} c\langle\nabla\rangle_c^{-1}\mathfrak{n}\left(u_* + \mathrm{e}^{-2ic^2t}\overline{u_*}\right). \end{aligned}$$

Together with the following approximations (see also (3.18) and (3.19))

$$\begin{aligned} c\langle\nabla\rangle_c - c^2 &\to -\tfrac{1}{2}\Delta + \mathcal{O}\left(c^{-2}\Delta^2\right), \\ c\langle\nabla\rangle_c^{-1} &\to 1 + \mathcal{O}\left(c^{-2}\Delta\right) \end{aligned}$$

we formally obtain

$$2i\partial_t u_* = \Delta u_* - \mathfrak{n}u_* - \mathrm{e}^{-2ic^2t}\,\mathfrak{n}\overline{u_*} + \mathcal{O}(c^{-2}).$$

The equation in $\mathfrak{n}$ in terms of u_* is given by

$$\partial_{tt}\mathfrak{n} = \Delta\mathfrak{n} + \frac{1}{4}\Delta\left(2|u_*|^2 + \mathrm{e}^{2ic^2t}(u_*)^2 + \mathrm{e}^{-2ic^2t}(\overline{u_*})^2\right) + \mathcal{O}(c^{-2}).$$

For a smooth function f we furthermore have (by integration by parts) that

$$\begin{aligned} \int_0^t \mathrm{e}^{\pm 2ic^2\xi}\, f\left(u_*(\xi), n(\xi)\right) \mathrm{d}\xi = {} & \frac{1}{\pm 2ic^2}\left(\mathrm{e}^{\pm 2ic^2t}\, f\left(u_*(t), n(t)\right) - \, f\left(u_*(0), n(0)\right)\right) \\ & + \frac{1}{\mp 2ic^2}\int_0^t \mathrm{e}^{\pm 2ic^2\xi}\partial_\xi\, f\left(u_*(\xi), n(\xi)\right) \mathrm{d}\xi. \end{aligned}$$

Thus, as $c^{-2} \xrightarrow{c\to\infty} 0$ the KGZ system formally turns to the classical Zakharov system

$$\begin{aligned} 2i\partial_t u_\infty - \Delta u_\infty &= -\mathfrak{n}_\infty u_\infty, \\ \partial_{tt}\mathfrak{n}_\infty - \Delta\mathfrak{n}_\infty &= \frac{1}{2}\Delta|u_\infty|^2. \end{aligned} \tag{4.7}$$

4.3 Uniformly Accurate Methods for the Klein–Gordon–Zakharov System: Standard Approach

The aim of this section is to show that we cannot construct uniformly accurate methods with our standard twisted variable ansatz we used in the previous chapters. In this section we show that in the error analysis, the estimate amounts a *loss of derivative*.

We introduce analogously to the previous chapters a *twisted variable* ansatz and iterate Duhamel's formula in the new variables. Thereby, we integrate the highly oscillatory phases exactly. We recall the first-order system of the KGZ system (4.6)

$$
\begin{aligned}
i\partial_t u &= -c\langle\nabla\rangle_c u - \tfrac{1}{2}c\langle\nabla\rangle_c^{-1}\Re(\mathfrak{h})\big(u+\overline{v}\big),\\
i\partial_t v &= -c\langle\nabla\rangle_c v - \tfrac{1}{2}c\langle\nabla\rangle_c^{-1}\Re(\mathfrak{h})\big(v+\overline{u}\big),\\
i\partial_t \mathfrak{h} &= -\langle\nabla\rangle_0\mathfrak{h} - \tfrac{1}{4}\langle\nabla\rangle_0|u+\overline{v}|^2
\end{aligned}
$$

with initial values

$$
\begin{aligned}
u(0) &= z_0 - ic\langle\nabla\rangle_c^{-1}z_1,\\
v(0) &= \overline{z_0} - ic\langle\nabla\rangle_c^{-1}\overline{z_1},\\
\mathfrak{h}(0) &= \mathfrak{n}_0 - i\langle\nabla\rangle_0^{-1}\mathfrak{n}_1.
\end{aligned}
$$

Analogously to the previous chapters we use the *twisted variable* ansatz and set

$$
u_*(t) = \mathrm{e}^{-ic^2t}u(t), \qquad v_*(t) = \mathrm{e}^{-ic^2t}v(t).
$$

Note that for the wave equation part $\mathfrak{h}$ of the KGZ system (4.1) we do not need to apply the twisting, since there are no highly oscillatory actions in the variable. However, for notational reason we write $\mathfrak{h}_*$ instead of $\mathfrak{h}$. After a simple calculation we obtain

$$
\begin{aligned}
i\partial_t u_* = i\partial_t\left(\mathrm{e}^{-ic^2t}u\right) &= -i^2c^2\mathrm{e}^{-ic^2t}u + \mathrm{e}^{-ic^2t}i\partial_t u\\
&= c^2\mathrm{e}^{-ic^2t}u + \mathrm{e}^{-ic^2t}\Big(-c\langle\nabla\rangle_c u - \frac{1}{2}c\langle\nabla\rangle_c^{-1}\Re(\mathfrak{h}_*)\big(u+\overline{v}\big)\Big)\\
&= c^2u_* - c\langle\nabla\rangle_c u_* - \frac{1}{2}c\langle\nabla\rangle_c^{-1}\Re(\mathfrak{h}_*)\Big(u_* + \mathrm{e}^{-2ic^2t}\overline{v_*}\Big)\\
&= -\mathcal{A}_c u_* - \frac{1}{2}c\langle\nabla\rangle_c^{-1}\Re(\mathfrak{h}_*)\Big(u_* + \mathrm{e}^{-2ic^2t}\overline{v_*}\Big)
\end{aligned}
$$

with leading operator $\mathcal{A}_c = c\langle\nabla\rangle_c - c^2$. A similar equation holds for v_*

$$
i\partial_t v_* = -\mathcal{A}_c v_* - \frac{1}{2}c\langle\nabla\rangle_c^{-1}\Re(\mathfrak{h}_*)\Big(v_* + \mathrm{e}^{-2ic^2t}\overline{u_*}\Big).
$$

As it is mentioned in the previous chapters the advantage of looking at the twisted system in (u_*, v_*), instead of (u, v), lies in the fact that the leading operator formally satisfies $\mathcal{A}_c = \mathcal{O}(1)$ in c. The twisted KGZ system now reads

$$
\begin{aligned}
i\partial_t u_* &= -\mathcal{A}_c u_* - \frac{1}{2}c\langle\nabla\rangle_c^{-1}\Re(\mathfrak{h}_*)\Big(u_* + \mathrm{e}^{-2ic^2t}\overline{v_*}\Big),\\
i\partial_t v_* &= -\mathcal{A}_c v_* - \frac{1}{2}c\langle\nabla\rangle_c^{-1}\Re(\mathfrak{h}_*)\Big(v_* + \mathrm{e}^{-2ic^2t}\overline{u_*}\Big),\\
i\partial_t \mathfrak{h}_* &= -\langle\nabla\rangle_0\mathfrak{h}_* - \frac{1}{4}\langle\nabla\rangle_0\Big|\mathrm{e}^{ic^2t}u_* + \mathrm{e}^{-ic^2t}\overline{v_*}\Big|^2
\end{aligned}
$$

with Duhamel's formula we have

$$
\begin{aligned}
u_*(t_n+\tau) &= \mathrm{e}^{i\tau\mathcal{A}_c}u_*(t_n) + \frac{i}{2}c\langle\nabla\rangle_c^{-1}\int_0^\tau \mathrm{e}^{i(\tau-s)\mathcal{A}_c}\Re\big(\mathfrak{h}_*(t_n+s)\big)\Big(u_*(t_n+s) + \mathrm{e}^{-2ic^2(t_n+s)}\overline{v_*}(t_n+s)\Big)\mathrm{d}s,\\
v_*(t_n+\tau) &= \mathrm{e}^{i\tau\mathcal{A}_c}v_*(t_n) + \frac{i}{2}c\langle\nabla\rangle_c^{-1}\int_0^\tau \mathrm{e}^{i(\tau-s)\mathcal{A}_c}\Re\big(\mathfrak{h}_*(t_n+s)\big)\Big(v_*(t_n+s) + \mathrm{e}^{-2ic^2(t_n+s)}\overline{u_*}(t_n+s)\Big)\mathrm{d}s,\\
\mathfrak{h}_*(t_n+\tau) &= \mathrm{e}^{i\tau\langle\nabla\rangle_0}\mathfrak{h}_*(t_n) + \frac{i}{4}\langle\nabla\rangle_0\int_0^\tau \mathrm{e}^{i(\tau-s)\langle\nabla\rangle_0}\Big|\mathrm{e}^{ic^2(t_n+s)}u_*(t_n+s) + \mathrm{e}^{-ic^2(t_n+s)}\overline{v_*}(t_n+s)\Big|^2\mathrm{d}s.
\end{aligned}
\tag{4.8}
$$

For details on the local well-posedness of highly oscillatory Klein–Gordon equations we refer to [53, 73] and for the full Klein–Gordon–Zakharov system to [61] and the references therein. Analogously to the previous chapters we again employ the concept of the φ- and Ψ-functions which are defined as in Section 2.3. We recall the definitions of the φ- and Ψ-functions in the following remark.

Remark 4.2. For a $\xi \in \mathbb{C}$ we set

$$\varphi_0(\xi) = \mathrm{e}^{\xi}, \qquad \varphi_1(\xi) = \frac{\varphi_0(\xi) - 1}{\xi}, \qquad \varphi_2(\xi) = \frac{\varphi_1(\xi) - 1}{\xi}, \qquad \Psi_2(\xi) = \frac{\varphi_0(\xi) - \varphi_1(\xi)}{\xi}.$$

In the next section we formally show that an exponential integrator applied on the twisted system is not an appropriate method to obtain a uniformly accurate method for the KGZ system in the high-plasma frequency regime.

4.3.1 A Classical Exponential Integrator for the Twisted Klein–Gordon–Zakharov System

In this section we derive a classical exponential integrator for the twisted KGZ system based on [39]. Therefore, we go on analogously to the previous chapters and use Duhamel's formulas given in (4.8). We recall Duhamel's formulas

$$\begin{aligned}
u_*(t_n+\tau) &= \mathrm{e}^{i\tau\mathcal{A}_c}u_*(t_n) + \frac{i}{2}c\langle\nabla\rangle_c^{-1}\int_0^\tau \mathrm{e}^{i(\tau-s)\mathcal{A}_c}\Re\big(\mathfrak{h}_*(t_n+s)\big)\Big(u_*(t_n+s)+\mathrm{e}^{-2ic^2(t_n+s)}\overline{v_*}(t_n+s)\Big)\mathrm{d}s,\\
v_*(t_n+\tau) &= \mathrm{e}^{i\tau\mathcal{A}_c}v_*(t_n) + \frac{i}{2}c\langle\nabla\rangle_c^{-1}\int_0^\tau \mathrm{e}^{i(\tau-s)\mathcal{A}_c}\Re\big(\mathfrak{h}_*(t_n+s)\big)\Big(v_*(t_n+s)+\mathrm{e}^{-2ic^2(t_n+s)}\overline{u_*}(t_n+s)\Big)\mathrm{d}s,\\
\mathfrak{h}_*(t_n+\tau) &= \mathrm{e}^{i\tau\langle\nabla\rangle_0}\mathfrak{h}_*(t_n) + \frac{i}{4}\langle\nabla\rangle_0\int_0^\tau \mathrm{e}^{i(\tau-s)\langle\nabla\rangle_0}\Big|\mathrm{e}^{ic^2(t_n+s)}u_*(t_n+s)+\mathrm{e}^{-ic^2(t_n+s)}\overline{v_*}(t_n+s)\Big|^2\mathrm{d}s
\end{aligned}$$

and freeze the following terms at $s=0$

$$\begin{aligned}
\Re\big(\mathfrak{h}(t_n+s)\big)\Big(u_*(t_n+s)+\mathrm{e}^{-2ic^2(t_n+s)}\overline{v_*}(t_n+s)\Big) &\approx \Re\big(\mathfrak{h}_*(t_n)\big)\Big(u_*(t_n)+\mathrm{e}^{-2ic^2t_n}\overline{v_*}(t_n)\Big),\\
\Re\big(\mathfrak{h}(t_n+s)\big)\Big(v_*(t_n+s)+\mathrm{e}^{-2ic^2(t_n+s)}\overline{u_*}(t_n+s)\Big) &\approx \Re\big(\mathfrak{h}_*(t_n)\big)\Big(v_*(t_n)+\mathrm{e}^{-2ic^2t_n}\overline{u_*}(t_n)\Big),\\
\Big|\mathrm{e}^{ic^2(t_n+s)}u_*(t_n+s)+\mathrm{e}^{-ic^2(t_n+s)}\overline{v_*}(t_n+s)\Big|^2 &\approx \Big|\mathrm{e}^{ic^2t_n}u_*(t_n)+\mathrm{e}^{-ic^2t_n}\overline{v_*}(t_n)\Big|^2.
\end{aligned}$$

So we obtain

$$\begin{aligned}
u_*(t_n+\tau) &\approx \mathrm{e}^{i\tau\mathcal{A}_c}u_*(t_n) + \frac{i}{2}c\langle\nabla\rangle_c^{-1}\int_0^\tau \mathrm{e}^{i(\tau-s)\mathcal{A}_c}\Re\big(\mathfrak{h}_*(t_n)\big)\Big(u_*(t_n)+\mathrm{e}^{-2ic^2t_n}\overline{v_*}(t_n)\Big)\mathrm{d}s,\\
v_*(t_n+\tau) &\approx \mathrm{e}^{i\tau\mathcal{A}_c}v_*(t_n) + \frac{i}{2}c\langle\nabla\rangle_c^{-1}\int_0^\tau \mathrm{e}^{i(\tau-s)\mathcal{A}_c}\Re\big(\mathfrak{h}_*(t_n)\big)\Big(v_*(t_n)+\mathrm{e}^{-2ic^2t_n}\overline{u_*}(t_n)\Big)\mathrm{d}s,\\
\mathfrak{h}_*(t_n+\tau) &\approx \mathrm{e}^{i\tau\langle\nabla\rangle_0}\mathfrak{h}_*(t_n) + \frac{i}{4}\langle\nabla\rangle_0\int_0^\tau \mathrm{e}^{i(\tau-s)\langle\nabla\rangle_0}\Big|\mathrm{e}^{ic^2t_n}u_*(t_n)+\mathrm{e}^{-ic^2t_n}\overline{v_*}(t_n)\Big|^2\mathrm{d}s.
\end{aligned}$$

We integrate the remaining terms $\mathrm{e}^{i(\tau-s)\mathcal{A}_c}$ and $\mathrm{e}^{i(\tau-s)\langle\nabla\rangle_0}$ exactly. Thus, with the definition of the φ_1-functions we have

$$\begin{aligned}
u_*(t_n+\tau) &\approx \mathrm{e}^{i\tau\mathcal{A}_c}u_*(t_n) + \frac{i}{2}c\langle\nabla\rangle_c^{-1}\tau\varphi_1\left(i\tau\mathcal{A}_c\right)\Re\big(\mathfrak{h}_*(t_n)\big)\Big(u_*(t_n)+\mathrm{e}^{-2ic^2t_n}\overline{v_*}(t_n)\Big),\\
v_*(t_n+\tau) &\approx \mathrm{e}^{i\tau\mathcal{A}_c}v_*(t_n) + \frac{i}{2}c\langle\nabla\rangle_c^{-1}\tau\varphi_1\left(i\tau\mathcal{A}_c\right)\Re\big(\mathfrak{h}_*(t_n)\big)\Big(v_*(t_n)+\mathrm{e}^{-2ic^2t_n}\overline{u_*}(t_n)\Big),\\
\mathfrak{h}_*(t_n+\tau) &\approx \mathrm{e}^{i\tau\langle\nabla\rangle_0}\mathfrak{h}_*(t_n) + \frac{i}{4}\langle\nabla\rangle_0\tau\varphi_1\left(i\tau\langle\nabla\rangle_0\right)\Big|\mathrm{e}^{ic^2t_n}u_*(t_n)+\mathrm{e}^{-ic^2t_n}\overline{v_*}(t_n)\Big|^2.
\end{aligned}$$

With

$$i\langle\nabla\rangle_0\tau\varphi_1(i\tau\langle\nabla\rangle_0) = \mathrm{e}^{i\tau\langle\nabla\rangle_0} - 1$$

we obtain the following exponential integration scheme

$$\begin{aligned}
u_*^{n+1} &= \mathrm{e}^{i\tau\mathcal{A}_c}u_*^n + \frac{i}{2}c\langle\nabla\rangle_c^{-1}\tau\varphi_1\left(i\tau\mathcal{A}_c\right)\Re\big(\mathfrak{h}_*^n\big)\left(u_*^n + \mathrm{e}^{-2ic^2t_n}\overline{v_*^n}\right),\\
v_*^{n+1} &= \mathrm{e}^{i\tau\mathcal{A}_c}v_*^n + \frac{i}{2}c\langle\nabla\rangle_c^{-1}\tau\varphi_1\left(i\tau\mathcal{A}_c\right)\Re\big(\mathfrak{h}_*^n\big)\left(v_*^n + \mathrm{e}^{-2ic^2t_n}\overline{u_*^n}\right),\\
\mathfrak{h}_*^{n+1} &= \mathrm{e}^{i\tau\langle\nabla\rangle_0}\mathfrak{h}_*^n + \frac{1}{4}\left(\mathrm{e}^{i\tau\langle\nabla\rangle_0} - 1\right)\left|\mathrm{e}^{ic^2t_n}u_*^n + \mathrm{e}^{-ic^2t_n}\overline{v_*}^n\right|^2
\end{aligned}$$

with initial values

$$\begin{aligned}
u_*^0 &= z_0 - ic\langle\nabla\rangle_c^{-1}z_1,\\
v_*^0 &= \overline{z_0} - ic\langle\nabla\rangle_c^{-1}\overline{z_1},\\
\mathfrak{n}_*^0 &= \mathfrak{n}_0 - i\langle\nabla\rangle_0^{-1}\mathfrak{n}_1,
\end{aligned}$$

where we have to take in account Assumption 4.1.

Figure 4.3 underlines that the exponential integrator schemes is not uniformly accurate with respect to c. More precisely for large values of c the exponential integrator fails to approximate numerically the solution of the Klein–Gordon–Zakharov system, which can be explained by the following approximation of the highly oscillatory terms

$$\mathrm{e}^{ic^2(t_n+s)} = \mathrm{e}^{ic^2t_n} + \mathcal{O}(sc^2).$$

Thus, the exponential integrator also suffers from severe time step restrictions, similarly to the Gautschi-type methods shown in Figure 4.1.

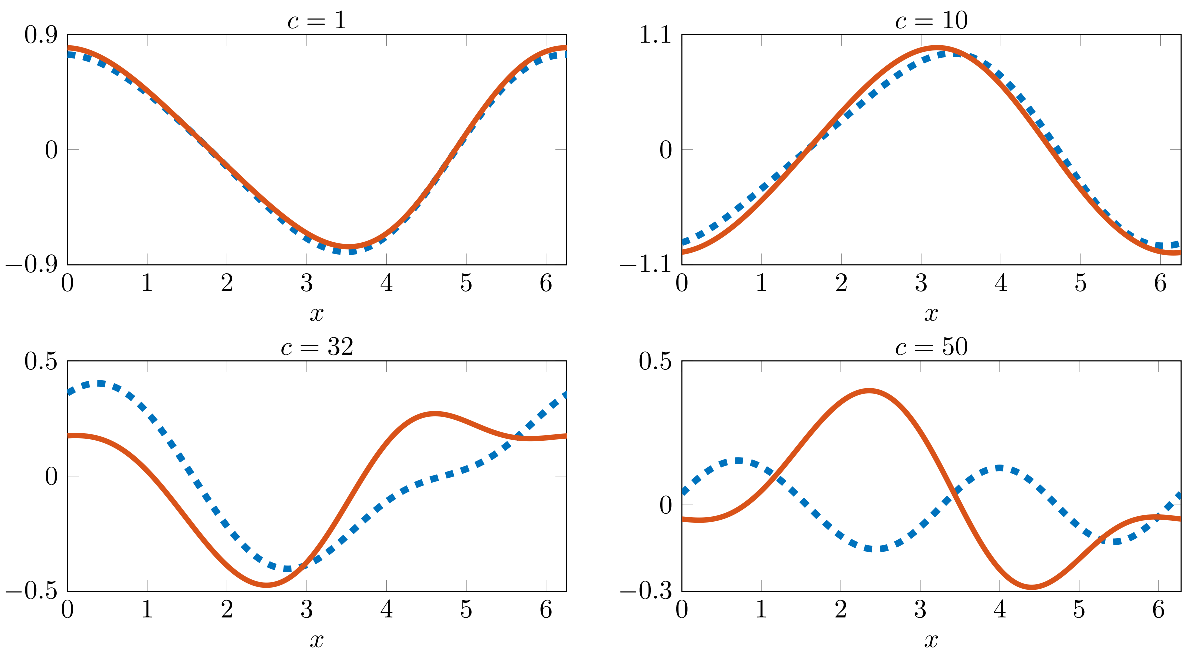

Figure 4.3: Numerical solution of the Klein–Gordon–Zakharov system for z. Exponential integrator (red solid line) for different c with time step size $\tau \approx 10^{-2}$ at time $t = 0.6$. The blue dashed line represents the reference solution at time $t = 0.6$, computed via an exponential Gautschi-type scheme with a small time step size $\tau \approx 10^{-6}$. The spatial discretization is done via a Fourier pseudospectral method with mesh-size $h = 0.0245$.

In the next section we construct our exponential-type integrator. Therefore, we also integrate the highly oscillatory phases terms $\mathrm{e}^{\pm \ell i c^2 (t_n+s)}$, for $\ell \in \mathbb{N}$ in the Duhamel's formulas exactly.

4.3.2 Construction of a First-Order Exponential-type Integrator

In this section, we formally derive a fist-order exponential-type integrator for the solution $(u_*, v_*, \mathfrak{h}_*)$ based on Duhamel's formula (4.8). In order to construct a scheme of first-order, we proceed analogously to the previous chapters. However, integrating the oscillatory phases as before does not yield to a uniformly accurate method.

Below we derive the numerical scheme for u_*^{n+1} approximating $u_*(t_{n+1})$, with $t_{n+1} = t_n + \tau$. We recall Duhamel's formula for u_* (see (4.8))

$$u_*(t_n+\tau) = \mathrm{e}^{i\tau\mathcal{A}_c} u_*(t_n) + \frac{i}{2} c\langle\nabla\rangle_c^{-1} \int_0^\tau \mathrm{e}^{i(\tau-s)\mathcal{A}_c} \Re\big(\mathfrak{h}_*(t_n+s)\big)\Big(u_*(t_n+s) + \mathrm{e}^{-2ic^2(t_n+s)}\overline{v_*}(t_n+s)\Big)\mathrm{d}s.$$

Analogously to the previous chapters we use Taylor series expansions of

$$\begin{aligned} \mathfrak{h}_*(t_n+s) &= \mathfrak{h}_*(t_n) + \mathcal{O}(s\mathfrak{h}_*'), \qquad & u_*(t_n+s) &= u_*(t_n) + \mathcal{O}(su_*'), \\ \overline{v_*}(t_n+s) &= \overline{v_*}(t_n) + \mathcal{O}(s\overline{v_*}'), & \mathrm{e}^{-is\mathcal{A}_c} &= 1 + \mathcal{O}(s\mathcal{A}_c). \end{aligned}$$

We plug the Taylor series expansions into Duhamel's formula of u_*, integrate the highly oscillatory phase $\mathrm{e}^{-ic^2 s}$ exactly, and obtain

$$\begin{aligned} u_*(t_n+\tau) &= \mathrm{e}^{i\tau\mathcal{A}_c} u_*(t_n) + \frac{i}{2} c\langle\nabla\rangle_c^{-1} \mathrm{e}^{i\tau\mathcal{A}_c} \int_0^\tau \Re\big(\mathfrak{h}_*(t_n)\big)\Big(u_*(t_n) + \mathrm{e}^{-2ic^2(t_n+s)}\overline{v_*}(t_n)\Big)\mathrm{d}s \\ &\quad + R_1(\tau, t_n, u_*, v_*, \mathfrak{h}_*) \\ &= \mathrm{e}^{i\tau\mathcal{A}_c} u_*(t_n) + \frac{i}{2}\tau c\langle\nabla\rangle_c^{-1} \mathrm{e}^{i\tau\mathcal{A}_c}\Big[\Re\big(\mathfrak{h}_*(t_n)\big)u_*(t_n) + \mathrm{e}^{-2ic^2 t_n}\varphi_1(-2ic^2\tau)\Re\big(\mathfrak{h}_*(t_n)\big)\overline{v_*}(t_n)\Big] \\ &\quad + R_1(\tau, t_n, u_*, v_*, \mathfrak{h}_*), \end{aligned}$$

where the remainder R_1 satisfies

$$\|R_1(\tau, t_n, u_*, v_*, \mathfrak{h}_*)\|_r \leq \tau^2 k_{r,M_3},$$

for a constant k_{r,M_3} independent of c.

Thus, we obtain the following exponential-type integration scheme

$$u_*^{n+1} = \mathrm{e}^{i\tau\mathcal{A}_c} u_*^n + \frac{i}{2}\tau c\langle\nabla\rangle_c^{-1}\mathrm{e}^{i\tau\mathcal{A}_c}\Big[\Re\big(\mathfrak{h}_*^n\big)u_*^n + \mathrm{e}^{-2ic^2 t_n}\varphi_1(-2ic^2\tau)\Re\big(\mathfrak{h}_*^n\big)\overline{v_*^n}\Big].$$

For v_* we can derive analogously to u_* the following scheme

$$v_*^{n+1} = \mathrm{e}^{i\tau\mathcal{A}_c} v_*^n + \frac{i}{2}\tau c\langle\nabla\rangle_c^{-1}\mathrm{e}^{i\tau\mathcal{A}_c}\Big[\Re\big(\mathfrak{h}_*^n\big)v_*^n + \mathrm{e}^{-2ic^2 t_n}\varphi_1(-2ic^2\tau)\Re\big(\mathfrak{h}_*^n\big)\overline{u_*^n}\Big].$$

Given the numerical schemes for u_*^{n+1} and v_*^{n+1} we can easily compute z^{n+1} as follows

$$z^{n+1} = \frac{1}{2}\left(\mathrm{e}^{ic^2 t_{n+1}} u_*^{n+1} + \mathrm{e}^{-ic^2 t_{n+1}}\overline{v_*^{n+1}}\right).$$

For $\mathfrak{h}_*$ we use also Duhamel's formula (see (4.8))

$$\mathfrak{h}_*(t_n+\tau) = \mathrm{e}^{i\tau\langle\nabla\rangle_0}\mathfrak{h}_*(t_n) + \frac{i}{4}\langle\nabla\rangle_0\int_0^\tau \mathrm{e}^{i(\tau-s)\langle\nabla\rangle_0}\Big|\mathrm{e}^{ic^2(t_n+s)}u_*(t_n+s) + \mathrm{e}^{-ic^2(t_n+s)}\overline{v_*}(t_n+s)\Big|^2\mathrm{d}s$$

and plug in the following Taylor series expansions

$$u_*(t_n+s)=u_*(t_n)+\mathcal{O}(su_*'),\qquad \overline{v_*}(t_n+s)=\overline{v_*}(t_n)+\mathcal{O}(s\overline{v_*}'),$$

such that we obtain

$$\begin{aligned}\mathfrak{h}_*(t_n+\tau)=\mathrm{e}^{i\tau\langle\nabla\rangle_0}\mathfrak{h}_*(t_n)+\frac{i}{4}\langle\nabla\rangle_0\mathrm{e}^{i\tau\langle\nabla\rangle_0}\int_0^\tau \mathrm{e}^{-is\langle\nabla\rangle_0}\Big[&|u_*(t_n)|^2+\mathrm{e}^{2ic^2(t_n+s)}u_*(t_n)v_*(t_n)\\&+|v_*(t_n)|^2+\mathrm{e}^{-2ic^2(t_n+s)}\overline{u_*}(t_n)\overline{v_*}(t_n)\Big]\mathrm{d}s\\+R_1(\tau,t_n,u_*,v_*,\mathfrak{h}_*),&\end{aligned}$$

where the remainder R_1 satisfies

$$\|R_1(\tau,t_n,u_*,v_*,\mathfrak{h}_*)\|_r\leq\tau^2k_r(M_3)$$

for a constant k_r independent of c. Now we integrate the highly oscillatory phases exactly and obtain

$$\begin{aligned}\mathfrak{h}_*(t_n+\tau)=\mathrm{e}^{i\tau\langle\nabla\rangle_0}\mathfrak{h}_*(t_n)+\frac{i}{4}\tau\langle\nabla\rangle_0\mathrm{e}^{i\tau\langle\nabla\rangle_0}\Big[&\varphi_1(-i\tau\langle\nabla\rangle_0)|u_*(t_n)|^2+\varphi_1(-i\tau\langle\nabla\rangle_0)|v_*(t_n)|^2\\&+\mathrm{e}^{2ic^2t_n}\varphi_1\big(i(2c^2-\langle\nabla\rangle_0)\tau\big)u_*(t_n)v_*(t_n)\\&+\mathrm{e}^{-2ic^2t_n}\varphi_1\big(-i(2c^2+\langle\nabla\rangle_0)\tau\big)\overline{u_*}(t_n)\overline{v_*}(t_n)\Big]\\+R_1(\tau,t_n,u_*,v_*,\mathfrak{h}_*).&\end{aligned}$$

This motivates the following numerical scheme for $\mathfrak{h}_*$

$$\begin{aligned}\mathfrak{h}_*^{n+1}=\mathrm{e}^{i\tau\langle\nabla\rangle_0}\mathfrak{h}_*^n+\frac{i}{4}\tau\langle\nabla\rangle_0\mathrm{e}^{i\tau\langle\nabla\rangle_0}\Big[&\varphi_1(-i\tau\langle\nabla\rangle_0)\big(|u_*^n|^2+|v_*^n|^2\big)+\mathrm{e}^{2ic^2t_n}\varphi_1\big(i(2c^2-\langle\nabla\rangle_0)\tau\big)u_*^nv_*^n\\&+\mathrm{e}^{-2ic^2t_n}\varphi_1\big(-i(2c^2+\langle\nabla\rangle_0)\tau\big)\overline{u_*^nv_*^n}\Big].\end{aligned}$$

Collecting the results, yields the following full numerical scheme in u_*, v_*, and $\mathfrak{h}_*$

$$\begin{aligned}u_*^{n+1}&=\mathrm{e}^{i\tau\mathcal{A}_c}u_*^n+\frac{i}{2}\tau c\langle\nabla\rangle_c^{-1}\mathrm{e}^{i\tau\mathcal{A}_c}\Big[\Re\big(\mathfrak{h}_*^n\big)u_*^n+\mathrm{e}^{-2ic^2t_n}\varphi_1(-2ic^2\tau)\Re\big(\mathfrak{h}_*^n\big)\overline{v_*^n}\Big],\\v_*^{n+1}&=\mathrm{e}^{i\tau\mathcal{A}_c}v_*^n+\frac{i}{2}\tau c\langle\nabla\rangle_c^{-1}\mathrm{e}^{i\tau\mathcal{A}_c}\Big[\Re\big(\mathfrak{h}_*^n\big)v_*^n+\mathrm{e}^{-2ic^2t_n}\varphi_1(-2ic^2\tau)\Re\big(\mathfrak{h}_*^n\big)\overline{u_*^n}\Big],\\\mathfrak{h}_*^{n+1}&=\mathrm{e}^{i\tau\langle\nabla\rangle_0}\mathfrak{h}_*^n+\frac{i}{4}\tau\langle\nabla\rangle_0\mathrm{e}^{i\tau\langle\nabla\rangle_0}\Big[\varphi_1(-i\tau\langle\nabla\rangle_0)\big(|u_*^n|^2+|v_*^n|^2\big)+\mathrm{e}^{2ic^2t_n}\varphi_1\big(i(2c^2-\langle\nabla\rangle_0)\tau\big)u_*^nv_*^n\\&\qquad+\mathrm{e}^{-2ic^2t_n}\varphi_1\big(-i(2c^2+\langle\nabla\rangle_0)\tau\big)\overline{u_*^nv_*^n}\Big]\end{aligned}$$

with initial values

$$\begin{aligned}u_*^0&=z_0-ic\langle\nabla\rangle_c^{-1}z_1,\\v_*^0&=\overline{z_0}-ic\langle\nabla\rangle_c^{-1}\overline{z_1},\\\mathfrak{h}_*^0&=\mathfrak{n}_0-i\langle\nabla\rangle_0^{-1}\mathfrak{n}_1,\end{aligned}$$

where we have to take into account Assumption 4.1.

However, if we want to do a rigorous convergence analysis of the derived first-order exponential-type uniformly accurate integration scheme we have to estimate the nonlinearity of $\mathfrak{h}_*$. Since φ_1 is bounded and $\mathrm{e}^{it\langle\nabla\rangle_0}$ is a linear isometry, formally we have for $\mathfrak{h}_*$

$$\|\mathfrak{h}_*(t_{n+1})-\mathfrak{h}_*^{n+1}\|_r\leq\|\mathfrak{h}_*(t_n)-\mathfrak{h}_*^n\|_r+\tau K_{r,M}\Big(\|u_*(t_n)-u_*^n\|_{r+1}+\|v_*(t_n)-v_*^n\|_{r+1}\Big),$$

where $K_{r,M}$ is independent of c, but the estimate amounts to a *loss of derivative*. In order to avoid this we follow in the next section the strategy given in [37, 59]. Thus, in a first step we have to reformulate the KGZ system as it is shown in [37] in a suitable way and then derive a uniformly accurate oscillatory integrator.

4.4 Uniformly Accurate Methods for the Klein–Gordon–Zakharov System: Refined Approach

As we have seen before, due to the loss of derivative, the twisted variable ansatz is not appropriate for the Klein–Gordon–Zakharov system. In this section we derive a uniformly accurate oscillatory integrator by following the strategy given in [37, 59]. This section is a detailed version of [12, chapter 2-4].
For practical implementation issues, we consider z and $\mathfrak{n}$, as functions defined on $(t,x) \in \mathbb{R} \times \mathbb{T}^d$ with values in $\mathbb{R}$ and smooth initial values. All the results in this section can be extended to complex valued solution $z \in \mathbb{C}$, but, for clarity of presentation we restrict ourselves to the real setting.
We recall the KGZ system rewritten as a first-order system in time in z (see also (4.6))

$$\begin{aligned} &i\partial_t u = -c\langle\nabla\rangle_c u - \frac{1}{2}c\langle\nabla\rangle_c^{-1}\ \mathfrak{n}(u+\overline{u}), && u(0) = z_0 - ic\langle\nabla\rangle_c^{-1} z_1,\\ &\partial_{tt}\mathfrak{n} = \Delta\mathfrak{n} + \frac{1}{4}\Delta|u+\overline{u}|^2, && \mathfrak{n}(0) = \mathfrak{n}_0, \quad \partial_t\mathfrak{n}(0) = \mathfrak{n}_1, \end{aligned} \tag{4.9}$$

where we have $z = \frac{1}{2}(u+\overline{u})$.

Remark 4.3 (Nonlinear coupling)**.** Note that the coupling in the Klein–Gordon and wave part is driven by the operator $c\langle\nabla\rangle_c^{-1}$ and $\langle\nabla\rangle_0$, respectively. With the aid of the Fourier expansion we easily see that the coupling operator $c\langle\nabla\rangle_c^{-1}\ \times \langle\nabla\rangle_0$ satisfies

$$\left\|c\langle\nabla\rangle_c^{-1}\ \langle\nabla\rangle_0 f\right\|_r^2 = \sum_{k\in\mathbb{Z}} \left|\frac{ck}{\sqrt{c^2+k^2}}\right|^2 |\hat{f}_k|^2$$

which implies

$$\left\|c\langle\nabla\rangle_c^{-1}\ \langle\nabla\rangle_0 f\right\|_r^2 \le c\|f\|_r \qquad \text{as well as} \qquad \left\|c\langle\nabla\rangle_c^{-1}\ \langle\nabla\rangle_0 f\right\|_r^2 \le \|f\|_{r+1}.$$

From the first bound we can easily deduce that no loss of derivative occurs if $c = \mathcal{O}(1)$, and hence the KGZ system (4.1) can be solved much more easily in the low-plasma frequency regime $c = 1$. However, standard techniques fail in the high-plasma frequency regime $c \gg 1$ due to the loss of derivative highlighted through the second bound.

To overcome this *loss of derivative* in the high-plasma frequency regime we pursue the following strategy: Inspired by the numerical analysis of the Zakharov system given in [37], see also [59] for the original idea in context of the local wellposedness analysis of the Zakharov system, we introduce the new variable

$$F = \partial_t u$$

and will further look at (4.9) as a system in $(u, \partial_t u, \mathfrak{n}, \partial_t\mathfrak{n}) = (u, F, \mathfrak{n}, \dot{\mathfrak{n}})$. With this notation the equation in u given in (4.9) can be expressed as follows

$$c\langle\nabla\rangle_c u = -iF - \frac{1}{2}c\langle\nabla\rangle_c^{-1}\ \mathfrak{n}(u+\overline{u}). \tag{4.10}$$

Furthermore, taking the time derivative in the first line of (4.9) yields by the product formula

$$i\partial_t F = -c\langle\nabla\rangle_c F - \frac{1}{2}c\langle\nabla\rangle_c^{-1}\Big[\partial_t \mathfrak{n}(u+\overline{u}) + \mathfrak{n}\partial_t(u+\overline{u})\Big]. \tag{4.11}$$

As $\mathfrak{n}$ is real valued we have

$$\begin{aligned}
\partial_t u &= ic\langle\nabla\rangle_c u + \frac{i}{2}c\langle\nabla\rangle_c^{-1}\ \mathfrak{n}(u+\overline{u}),\\
\partial_t \overline{u} &= -ic\langle\nabla\rangle_c \overline{u} - \frac{i}{2}c\langle\nabla\rangle_c^{-1}\ \mathfrak{n}(u+\overline{u})
\end{aligned}$$

which implies

$$\partial_t(u+\overline{u}) = ic\langle\nabla\rangle_c(u-\overline{u}). \tag{4.12}$$

Plugging (4.12) into (4.11) yields

$$i\partial_t F = -c\langle\nabla\rangle_c F - \frac{1}{2}c\langle\nabla\rangle_c^{-1}\Big[\dot{\mathfrak{n}}(u+\overline{u}) + i\mathfrak{n}c\langle\nabla\rangle_c(u-\overline{u})\Big]. \tag{4.13}$$

System (4.9) together with equation (4.10) and (4.13) thus takes the form

$$\begin{aligned}
i\partial_t F &= -c\langle\nabla\rangle_c F - \frac{1}{2}c\langle\nabla\rangle_c^{-1}\Big[\dot{\mathfrak{n}}(u+\overline{u}) + i\mathfrak{n}c\langle\nabla\rangle_c(u-\overline{u})\Big],\\
\partial_{tt}\mathfrak{n} &= \Delta\mathfrak{n} + \frac{1}{4}\Delta|u+\overline{u}|^2,\\
u &= (c\langle\nabla\rangle_c)^{-1}\left\{-iF - \frac{1}{2}c\langle\nabla\rangle_c^{-1}\mathfrak{n}\left(u(0) + \int_0^t F(s)\mathrm{d}s + \overline{u(0) + \int_0^t F(s)\mathrm{d}s}\right)\right\}.
\end{aligned} \tag{4.14}$$

Thereby, we use that $c\langle\nabla\rangle_c$ is invertible for all $c \neq 0$ as well as the representation

$$u(t) = u(0) + \int_0^t F(s)\mathrm{d}s.$$

4.4.1 Construction of the Uniformly Accurate Oscillatory Integrator

In this section we develop a *uniformly accurate numerical scheme* which allows us to approximate solutions of the system (4.9) uniformly in the parameter c. Our approach is thereby based on looking at the reformulated system (4.14) and approximating the corresponding Duhamel's formula in $(F, \mathfrak{n}, \dot{\mathfrak{n}})$. However, and in great difference to classical exponential and trigonometric integration techniques (see, e.g., [31, 36, 37, 39]), we will carefully treat the highly oscillatory phases triggered by the plasma frequency c in an exact way.
Duhamel's formula in $(F, \mathfrak{n}, \dot{\mathfrak{n}})$ reads (see (4.14))

$$\begin{aligned}
F(t_n+\tau) &= \mathrm{e}^{i\tau c\langle\nabla\rangle_c}F(t_n) + \frac{i}{2}c\langle\nabla\rangle_c^{-1}\int_0^\tau \mathrm{e}^{i(\tau-s)c\langle\nabla\rangle_c}\Big\{\dot{\mathfrak{n}}(t_n+s)\big(u(t_n+s)+\overline{u}(t_n+s)\big)\\
&\qquad\qquad + i\mathfrak{n}(t_n+s)c\langle\nabla\rangle_c\big(u(t_n+s)-\overline{u}(t_n+s)\big)\Big\}\mathrm{d}s,\\
\mathfrak{n}(t_n+\tau) &= \cos\left(\tau\langle\nabla\rangle_0\right)\mathfrak{n}(t_n) + \langle\nabla\rangle_0^{-1}\sin\left(\tau\langle\nabla\rangle_0\right)\dot{\mathfrak{n}}(t_n)\\
&\quad + \frac{1}{4}\langle\nabla\rangle_0^{-1}\int_0^\tau \sin((\tau-s)\langle\nabla\rangle_0)\Delta\big|u(t_n+s)+\overline{u}(t_n+s)\big|^2\mathrm{d}s,\\
\dot{\mathfrak{n}}(t_n+\tau) &= -\langle\nabla\rangle_0\sin\left(\tau\langle\nabla\rangle_0\right)\mathfrak{n}(t_n) + \cos\left(\tau\langle\nabla\rangle_0\right)\dot{\mathfrak{n}}(t_n)\\
&\quad + \frac{1}{4}\int_0^\tau \cos((\tau-s)\langle\nabla\rangle_0)\Delta\big|u(t_n+s)+\overline{u}(t_n+s)\big|^2\mathrm{d}s.
\end{aligned} \tag{4.15}$$

Furthermore, observe that for u we have (see (4.9))

$$u(t_n+\tau) = \mathrm{e}^{i\tau c\langle\nabla\rangle_c} u(t_n) + \frac{i}{2} c\langle\nabla\rangle_c^{-1} \int_0^\tau \mathrm{e}^{i(\tau-s)c\langle\nabla\rangle_c} \mathfrak{n}(t_n+s)\big(u(t_n+s)+\overline{u}(t_n+s)\big)\mathrm{d}s. \tag{4.16}$$

Remark 4.4. Note that $\partial_t u = F = \mathcal{O}(c\langle\nabla\rangle_c)$. Thus, if we would approximate the integrals in (4.15) by employing the classical Taylor series expansion

$$u(t_n+s) = u(t_n) + \mathcal{O}(s\partial_t u) = u(t_n) + \mathcal{O}(sc\langle\nabla\rangle_c)$$

(or a classical quadrature formula) this yields a local error of order $\mathcal{O}(\tau^2 c^2)$ and, in particular, not the aimed uniform approximation property. Henceforth, standard exponential integrator techniques (cf. [39]) fail, and a more careful approximation technique has to be applied.

4.4.1.1 Collection of Essential Lemma and Notation

We start off by collecting some useful lemma which will be essential in the derivation of uniform approximations with respect to c. Thereby, we will in particular exploit the following refined bilinear estimates: For $\sigma_1+\sigma_2 \geq 0$ (and as we assume that $1 \leq d \leq 3$) it holds that

$$\begin{aligned} &\|fg\|_\sigma \leq K_{r,d}\|f\|_{\sigma_1}\|g\|_{\sigma_2} \quad \text{for all } \sigma \leq \sigma_1+\sigma_2-\tfrac{d}{2} \quad \text{with } \sigma_1,\sigma_2 \text{ and } \; -\sigma \neq \tfrac{d}{2},\\ &\|fg\|_\sigma \leq K_{r,d}\|f\|_{\sigma_1}\|g\|_{\sigma_2} \quad \text{for all } \sigma < \sigma_1+\sigma_2-\tfrac{d}{2} \quad \text{with } \sigma_1,\sigma_2 \text{ or } \; -\sigma = \tfrac{d}{2}. \end{aligned}$$

In particular, by setting $\sigma = \sigma_1 = r-1$ and $\sigma_2 = r$ we can thus conclude

$$\|fg\|_{r-1} \leq K_{r,d}\|f\|_{r-1}\|g\|_r, \tag{4.17}$$

where we use that $\sigma_2 = r > d/2$ as well as $\sigma_1+\sigma_2 = 2r-1 > 0$.

Lemma 4.5 (cf. Lemma 3 in [12])**.** *For all $t \in \mathbb{R}$ and $c \neq 0$ we have*

$$\begin{aligned} &\big\|c\langle\nabla\rangle_c^{-1} f\big\|_r \leq \|f\|_r, \quad \|\mathrm{e}^{itc\langle\nabla\rangle_c} f\|_r = \|f\|_r, \quad \big\|(c\langle\nabla\rangle_c - c^2)f\big\|_r \leq \frac{1}{2}\|f\|_{r+2},\\ &\|(\mathrm{e}^{-i\xi c\langle\nabla\rangle_c} - \mathrm{e}^{-i\xi c^2})f\|_r \leq \frac{1}{2}\xi\|f\|_{r+2},\\ &\|\langle\nabla\rangle_c^{-2} f\|_r \leq \min\left(\frac{1}{c}\|f\|_{r-1}, \|f\|_{r-2}, \frac{1}{c^2}\ \|f\|_r\right), \quad \|\langle\nabla\rangle_c^{-2}\left(fc\langle\nabla\rangle_c g\right)\|_{r-1} \leq K\|f\|_{r-1}\|g\|_{r+1}. \end{aligned} \tag{4.18}$$

Proof. The estimates in the first and second row follow from (2.27), (2.28) and (2.30) (see also [13]). Furthermore, observe that $\langle\nabla\rangle_c^{-2}$ and $c^{-1}\langle\nabla\rangle_c$ in Fourier space can be estimated as follows

$$\frac{1}{c^2+k^2} \leq \min\left(\frac{1}{c|k|}, \frac{1}{k^2}, \frac{1}{c^2}\right) \qquad \text{and} \qquad \frac{\sqrt{c^2+k^2}}{c} \leq \frac{c+|k|}{c} \leq 1 + c^{-1}|k|.$$

The second inequality together with the bilinear estimate (4.17) and the definition of $\langle\nabla\rangle_c$ in Fourier space (see (2.12)) in particular implies

$$\big\|\langle\nabla\rangle_c^{-2}\left(fc\langle\nabla\rangle_c g\right)\big\|_{r-1} \leq \left\|f\frac{c\langle\nabla\rangle_c}{c^2} g\right\|_{r-1} \leq K\|f\ \|_{r-1}\left\|\frac{\langle\nabla\rangle_c}{c} g\right\|_r \leq K\|f\|_{r-1}\|g\|_{r+1},$$

for some constant $K > 0$ independent of c. This concludes the estimates in the last row of (4.18). □

In the following we set

$$M_{T,r} \;= \max\left(\sup_{0\leq t\leq T}\left\{\|u(t)\|_{r+1} + \left\|(c\langle\nabla\rangle_c^{-1})F(t)\right\|_{r+1} + \|\mathfrak{n}(t)\|_r + \|\dot{\mathfrak{n}}(t)\|_{r-1}\right\}, 1\right) \tag{4.19}$$

and introduce a suitable definition for the occuring remainders.

Definition 4.6 (Remainder)**.** *We will denote all constants which can be chosen independently of c by K. Furthermore, we write*

$$f = g + \mathcal{R}_{r+s} \qquad \textit{if} \qquad \|f-g\|_r \leq KM^p_{T,r+s} \tag{4.20}$$

for some $p \in \mathbb{N}$ and $K > 0$ independent of c.

We will also make use of the φ functions defined in (2.8).
The following lemma will allow us to carry out a classical Taylor series expansions in $\mathfrak{n}(t_n+s)$ and $\dot{\mathfrak{n}}(t_n+s)$ in the construction of our numerical scheme without producing remainders which depend on c.

Lemma 4.7 (cf. Lemma 6 in [12])**.** *For all $s \in \mathbb{R}$ it holds that*

$$\|\mathfrak{n}(t_n+s) - \mathfrak{n}(t_n)\|_r + \|\dot{\mathfrak{n}}(t_n+s) - \dot{\mathfrak{n}}(t_n)\|_{r-1} \leq |s|KM^2_{r+1},$$

for some constant $K > 0$ which can be chosen independently of c such that in particular

$$\mathfrak{n}(t_n+s) = \mathfrak{n}(t_n) + s\,\mathcal{R}_{r+1}, \qquad \dot{\mathfrak{n}}(t_n+s) = \dot{\mathfrak{n}}(t_n) + s\,\mathcal{R}_{r+2}. \tag{4.21}$$

Proof. Duhamel's formula (4.15) in $(\mathfrak{n}, \dot{\mathfrak{n}})$ yields

$$\begin{aligned}
\mathfrak{n}(t_n+s) - \mathfrak{n}(t_n) &= \big(\cos(s\langle\nabla\rangle_0) - 1\big)\mathfrak{n}(t_n) + s\,\mathrm{sinc}(s\langle\nabla\rangle_0)\dot{\mathfrak{n}}(t_n) + s\,\mathcal{R}_{r+1},\\
\dot{\mathfrak{n}}(t_n+s) - \dot{\mathfrak{n}}(t_n) &= \big(\cos(s\langle\nabla\rangle_0) - 1\big)\dot{\mathfrak{n}}(t_n) - s\,\mathrm{sinc}(s\langle\nabla\rangle_0)\langle\nabla\rangle_0^2\mathfrak{n}(t_n) + s\,\mathcal{R}_{r+2}.
\end{aligned}$$

The assertion thus follows by the estimate

$$\|(\cos(s\langle\nabla\rangle_0) - 1)f\|_r + \|(\mathrm{sinc}(s\langle\nabla\rangle_0) - 1)f\|_r \leq 3s^2\|f\|_{r+2}$$

together with the bilinear estimate (1.2). □

In the approximation of u, however, we need to be much more careful as a classical Taylor series expansion would lead to

$$u(t_n+s) = u(t_n) + sc\langle\nabla\rangle_c\mathcal{R}_r$$

and trigger an error at order $\mathcal{O}(sc^2)$ (see also Remark 4.4).

Lemma 4.8 (cf. Lemma 7 in [12])**.** *For all $s \in \mathbb{R}$ it holds*

$$\|u(t_n+s) - \mathrm{e}^{ic^2s}\,u(t_n)\|_r + \|u(t_n+s) - \mathrm{e}^{isc\langle\nabla\rangle_c}\,u(t_n)\|_r \leq |s|K\left(M_{r+2} + M_r^2\right),$$

for some constant $K > 0$ which can be chosen independently of c such that in particular

$$u(t_n+s) = \mathrm{e}^{isc\langle\nabla\rangle_c}u(t_n) + s\mathcal{R}_r \quad \textit{and} \quad u(t_n+s) = \mathrm{e}^{ic^2s}u(t_n) + s\mathcal{R}_{r+2}. \tag{4.22}$$

Proof. Duhamel's formula in u (see (4.16)) implies

$$u(t_n+s) = \mathrm{e}^{isc\langle\nabla\rangle_c} u(t_n) + s\mathcal{R}_r$$

which yields the first assertion. Furthermore, we can write

$$u(t_n+s) - \mathrm{e}^{ic^2 s} u(t_n) = \left(\mathrm{e}^{isc\langle\nabla\rangle_c} - \mathrm{e}^{ic^2 s}\right) u(t_n) + s\mathcal{R}_r.$$

Together with Lemma 4.5 this concludes the second assertion. □

Now, we derive our uniformly accurate oscillatory integrator. Therefore, we approximate the different terms F, u and $(\mathfrak{n}, \dot{\mathfrak{n}})$ separately.

a) Approximation in F:
Recall Duhamel's formula in F (see (4.15))

$$\begin{aligned} F(t_n+\tau) = \mathrm{e}^{i\tau c\langle\nabla\rangle_c} F(t_n) + \frac{i}{2} c\langle\nabla\rangle_c^{-1} \int_0^\tau \mathrm{e}^{i(\tau-s)c\langle\nabla\rangle_c} \Big\{ &\dot{\mathfrak{n}}(t_n+s)\big(u(t_n+s) + \overline{u}(t_n+s)\big) \\ &+ i\mathfrak{n}(t_n+s) c\langle\nabla\rangle_c \big(u(t_n+s) - \overline{u}(t_n+s)\big)\Big\} \mathrm{d}s. \end{aligned}$$

Multiplying the above formula with the operator $(c\langle\nabla\rangle_c)^{-1}$ and employing the expansions for $(\mathfrak{n}, \dot{\mathfrak{n}})(t_n+s)$ given in (4.21) and for $u(t_n+s)$ given in (4.22) we obtain by Lemma 4.5 together with the approximation

$$\|\mathrm{e}^{is(c^2 - c\langle\nabla\rangle_c)} f - \mathrm{e}^{is\frac{1}{2}\Delta} f\|_r \le K s c^{-2} \|f\|_{r+4}$$

that

$$\begin{aligned} (c\langle\nabla\rangle_c)^{-1} F(t_n+\tau) = \mathrm{e}^{i\tau c\langle\nabla\rangle_c} (c\langle\nabla\rangle_c)^{-1} F(t_n) + \frac{i}{2} \langle\nabla\rangle_c^{-2} \int_0^\tau \mathrm{e}^{i(\tau-s)c\langle\nabla\rangle_c} \Big\{ &\dot{\mathfrak{n}}(t_n)\big(\mathrm{e}^{ic^2 s} u(t_n) + \mathrm{e}^{-ic^2 s}\overline{u}(t_n)\big) \\ &+ i\mathfrak{n}(t_n) c\langle\nabla\rangle_c \big(\mathrm{e}^{ic^2 s}\ u(t_n) - \mathrm{e}^{-ic^2 s}\overline{u}(t_n)\big)\Big\} \mathrm{d}s \\ + \tau^2 \mathcal{R}_{r+2} \qquad\qquad\qquad\qquad & \\ = \mathrm{e}^{i\tau c\langle\nabla\rangle_c} (c\langle\nabla\rangle_c)^{-1} F(t_n) \qquad\qquad & \\ + \frac{i}{2} \langle\nabla\rangle_c^{-2} \mathrm{e}^{i\tau c\langle\nabla\rangle_c} \int_0^\tau \Big\{ \mathrm{e}^{is\frac{1}{2}\Delta} \big(\dot{\mathfrak{n}}(t_n) u(t_n)\big) &+ \mathrm{e}^{-is(c\langle\nabla\rangle_c + c^2)} \big(\dot{\mathfrak{n}}(t_n)\overline{u}(t_n)\big) \\ + i\mathrm{e}^{is\frac{1}{2}\Delta} \big(\mathfrak{n}(t_n) c\langle\nabla\rangle_c u(t_n)\big) &- i\mathrm{e}^{-is(c\langle\nabla\rangle_c + c^2)} \big(\mathfrak{n}(t_n) c\langle\nabla\rangle_c \overline{u}(t_n)\big)\Big\} \mathrm{d}s \\ + \tau^2 \mathcal{R}_{r+2}. \qquad\qquad\qquad\qquad & \end{aligned}$$

Now, we integrate the remaining exponential terms exactly. With the definition of the φ_1-function in (2.8) we furthermore obtain

$$\begin{aligned}(c\langle\nabla\rangle_c)^{-1}F(t_n+\tau) &= \mathrm{e}^{i\tau c\langle\nabla\rangle_c}(c\langle\nabla\rangle_c)^{-1}F(t_n) + i\frac{\tau}{2}\langle\nabla\rangle_c^{-2}\mathrm{e}^{i\tau c\langle\nabla\rangle_c}\varphi_1\left(\tfrac{i}{2}\tau\Delta\right)\Big(\dot{\mathfrak{n}}(t_n)u(t_n)\Big)\\ &\quad + i\frac{\tau}{2}\langle\nabla\rangle_c^{-2}\mathrm{e}^{i\tau c\langle\nabla\rangle_c}\varphi_1\left(-i\tau(c\langle\nabla\rangle_c+c^2)\right)\Big(\dot{\mathfrak{n}}(t_n)\overline{u}(t_n)\Big)\\ &\quad - \frac{\tau}{2}\langle\nabla\rangle_c^{-2}\mathrm{e}^{i\tau c\langle\nabla\rangle_c}\varphi_1\left(\tfrac{i}{2}\tau\Delta\right)\Big(\mathfrak{n}(t_n)c\langle\nabla\rangle_c u(t_n)\Big)\\ &\quad + \frac{\tau}{2}\langle\nabla\rangle_c^{-2}\mathrm{e}^{i\tau c\langle\nabla\rangle_c}\varphi_1\left(-i\tau(c\langle\nabla\rangle_c+c^2)\right)\Big(\mathfrak{n}(t_n)c\langle\nabla\rangle_c\overline{u}(t_n)\Big) + \tau^2\mathcal{R}_{r+2}\\ &= \mathrm{e}^{i\tau c\langle\nabla\rangle_c}(c\langle\nabla\rangle_c)^{-1}F(t_n)\\ &\quad + i\frac{\tau}{2}\langle\nabla\rangle_c^{-2}\mathrm{e}^{i\tau c\langle\nabla\rangle_c}\varphi_1\left(\tfrac{i}{2}\tau\Delta\right)\Big(\dot{\mathfrak{n}}(t_n)u(t_n) + i\mathfrak{n}(t_n)c\langle\nabla\rangle_c u(t_n)\Big)\\ &\quad + i\frac{\tau}{2}\langle\nabla\rangle_c^{-2}\mathrm{e}^{i\tau c\langle\nabla\rangle_c}\varphi_1\left(-i\tau(c\langle\nabla\rangle_c+c^2)\right)\Big(\dot{\mathfrak{n}}(t_n)\overline{u}(t_n) - i\mathfrak{n}(t_n)c\langle\nabla\rangle_c\overline{u}(t_n)\Big)\\ &\quad + \tau^2\mathcal{R}_{r+2}.\end{aligned} \tag{4.23}$$

b) Approximation in u:

Recall that at time $t = t_n$ we have (see (4.14))

$$u(t_n) = (c\langle\nabla\rangle_c)^{-1}\left\{-iF(t_n) - \frac{1}{2}c\langle\nabla\rangle_c^{-1}\mathfrak{n}(t_n)\Big(I_F(t_n) + \overline{I_F(t_n)}\Big)\right\}, \tag{4.24}$$

where we have set

$$I_F(t_n) := u(0) + \int_0^{t_n} F(s)\mathrm{d}s = u(0) + \sum_{k=0}^{n-1}\int_0^\tau F(t_k+s)\mathrm{d}s.$$

To obtain an approximation of $I_F(t_n)$ we will use the approximation (4.23) which yields

$$\begin{aligned}I_F(t_n) &= u(0) + \sum_{k=0}^{n-1}\int_0^\tau \Big(\mathrm{e}^{isc\langle\nabla\rangle_c}\ F(t_k) + c^2 s\left(\mathcal{R}_{r+2}\right)_k\Big)\,\mathrm{d}s\\ &= u(0) + \left(\tau\sum_{k=0}^{n-1}\varphi_1(i\tau c\langle\nabla\rangle_c)F(t_k)\right) + \tau c^2 t_n\mathcal{R}_{r+2}.\end{aligned} \tag{4.25}$$

In the following we approximate $I_F(t_n)$ by $S_F(t_n)$, therefore we set

$$S_F(t_n) = u(0) + \tau\sum_{k=0}^{n-1}\varphi_1(i\tau c\langle\nabla\rangle_c)F(t_k). \tag{4.26}$$

Then, plugging the approximation (4.25) into (4.24) yields thanks to the estimate $\|\langle\nabla\rangle_c^{-2}c^2\|_r \leq 1$ (see Lemma 4.5) that

$$\begin{aligned}u(t_n) &= (c\langle\nabla\rangle_c)^{-1}\left\{-iF(t_n) - \frac{1}{2}c\langle\nabla\rangle_c^{-1}\mathfrak{n}(t_n)\Big(S_F(t_n) + \overline{S_F(t_n)}\Big)\right\} + \frac{1}{2}\langle\nabla\rangle_c^{-2}\left\{\mathfrak{n}(t_n)\tau c^2\mathcal{R}_{r+2}\right\}\\ &= (c\langle\nabla\rangle_c)^{-1}\left\{-iF(t_n) - \frac{1}{2}c\langle\nabla\rangle_c^{-1}\mathfrak{n}(t_n)\Big(S_F(t_n) + \overline{S_F(t_n)}\Big)\right\} + \tau\mathcal{R}_{r+2}.\end{aligned} \tag{4.27}$$

c) Approximation in $(\mathfrak{n}, \dot{\mathfrak{n}})$**:**
Recall Duhamel's formula in $(\mathfrak{n}, \dot{\mathfrak{n}})$ (cf. (4.15))

$$\begin{aligned}
\mathfrak{n}(t_n+\tau) &= \cos\left(\tau\langle\nabla\rangle_0\right)\mathfrak{n}(t_n) + \langle\nabla\rangle_0^{-1}\sin\left(\tau\langle\nabla\rangle_0\right)\dot{\mathfrak{n}}(t_n)\\
&\quad + \frac{1}{4}\langle\nabla\rangle_0^{-1}\int_0^\tau \sin((\tau-s)\langle\nabla\rangle_0)\Delta\big|u(t_n+s)+\overline{u}(t_n+s)\big|^2\mathrm{d}s,\\
\dot{\mathfrak{n}}(t_n+\tau) &= -\langle\nabla\rangle_0\sin\left(\tau\langle\nabla\rangle_0\right)\mathfrak{n}(t_n) + \cos\left(\tau\langle\nabla\rangle_0\right)\dot{\mathfrak{n}}(t_n)\\
&\quad + \frac{1}{4}\int_0^\tau \cos((\tau-s)\langle\nabla\rangle_0)\Delta\big|u(t_n+s)+\overline{u}(t_n+s)\big|^2\mathrm{d}s.
\end{aligned}$$

Employing the approximation of $u(t_n+s)$ given in (4.22) together with the trigonometric approximations

$$\|(\sin(s\langle\nabla\rangle_0) - s\langle\nabla\rangle_0)f\|_r + \|(\cos(s\langle\nabla\rangle_0)-1)f\|_r + \|(\mathrm{sinc}(s\langle\nabla\rangle_0)-1)f\|_r \leq 3s^2\|f\|_{r+2}$$

we obtain

$$\begin{aligned}
\mathfrak{n}(t_n+\tau) &= \cos\left(\tau\langle\nabla\rangle_0\right)\mathfrak{n}(t_n) + \langle\nabla\rangle_0^{-1}\sin\left(\tau\langle\nabla\rangle_0\right)\dot{\mathfrak{n}}(t_n)\\
&\quad + \frac{1}{4}\langle\nabla\rangle_0^{-1}\mathrm{sinc}\left(\tau\langle\nabla\rangle_0\right)\int_0^\tau \left((\tau-s)\langle\nabla\rangle_0\right)\Delta\left\{2|u(t_n)|^2 + \mathrm{e}^{2ic^2s}u(t_n)^2 + \mathrm{e}^{-2ic^2s}\left(\overline{u}(t_n)\right)^2\right\}\mathrm{d}s\\
&\quad + \tau^3\mathcal{R}_{r+4},\\
\dot{\mathfrak{n}}(t_n+\tau) &= -\langle\nabla\rangle_0\sin\left(\tau\langle\nabla\rangle_0\right)\mathfrak{n}(t_n) + \cos\left(\tau\langle\nabla\rangle_0\right)\dot{\mathfrak{n}}(t_n)\\
&\quad + \frac{1}{4}\cos\left(\tau\langle\nabla\rangle_0\right)\int_0^\tau \Delta\left\{2|u(t_n)|^2 + \mathrm{e}^{2ic^2s}u(t_n)^2 + \mathrm{e}^{-2ic^2s}\left(\overline{u}(t_n)\right)^2\right\}\mathrm{d}s + \tau^2\mathcal{R}_{r+4}.
\end{aligned}$$

Again integrating the remaining exponential terms exactly, together with the definition of the φ_1- and φ_2-function (see Definition (2.8)) we thus derive

$$\begin{aligned}
\mathfrak{n}(t_n+\tau) &= \cos\left(\tau\langle\nabla\rangle_0\right)\mathfrak{n}(t_n) + \langle\nabla\rangle_0^{-1}\sin\left(\tau\langle\nabla\rangle_0\right)\dot{\mathfrak{n}}(t_n)\\
&\quad + \frac{\tau^2}{4}\mathrm{sinc}\left(\tau\langle\nabla\rangle_0\right)\Delta\left\{|u(t_n)|^2 + \varphi_2(2ic^2\tau)u(t_n)^2 + \varphi_2(-2ic^2\tau)\left(\overline{u}(t_n)\right)^2\right\} + \tau^3\mathcal{R}_{r+4},\\
\dot{\mathfrak{n}}(t_n+\tau) &= -\langle\nabla\rangle_0\sin\left(\tau\langle\nabla\rangle_0\right)\mathfrak{n}(t_n) + \cos\left(\tau\langle\nabla\rangle_0\right)\dot{\mathfrak{n}}(t_n)\\
&\quad + \frac{\tau}{4}\cos\left(\tau\langle\nabla\rangle_0\right)\Delta\left\{2|u(t_n)|^2 + \varphi_1(2ic^2\tau)u(t_n)^2 + \varphi_1(-2ic^2\tau)\left(\overline{u}(t_n)\right)^2\right\} + \tau^2\mathcal{R}_{r+4}.
\end{aligned} \tag{4.28}$$

4.4.1.2 A Uniformly Accurate Oscillatory Integrator

Collecting the approximations in (4.23), (4.27) (together with (4.26)) and (4.28) motivate us to define our numerical scheme as follows.

For $n \geq 1$ we set

$$
\begin{aligned}
(c\langle\nabla\rangle_c)^{-1}F^{n+1} &= \mathrm{e}^{i\tau c\langle\nabla\rangle_c}(c\langle\nabla\rangle_c)^{-1}F^n + i\frac{\tau}{2}\langle\nabla\rangle_c^{-2}\mathrm{e}^{i\tau c\langle\nabla\rangle_c}\varphi_1\left(\tfrac{i}{2}\tau\Delta\right)\left(\dot{\mathfrak{n}}^n u^n + i\mathfrak{n}^n c\langle\nabla\rangle_c u^n\right)\\
&\quad + i\frac{\tau}{2}\langle\nabla\rangle_c^{-2}\mathrm{e}^{i\tau c\langle\nabla\rangle_c}\varphi_1\left(-i\tau(c\langle\nabla\rangle_c + c^2)\right)\left(\dot{\mathfrak{n}}^n \overline{u}^n - i\mathfrak{n}^n c\langle\nabla\rangle_c \overline{u}^n\right),\\
\mathfrak{n}^{n+1} &= \cos\left(\tau\langle\nabla\rangle_0\right)\mathfrak{n}^n + \langle\nabla\rangle_0^{-1}\sin\left(\tau\langle\nabla\rangle_0\right)\dot{\mathfrak{n}}^n\\
&\quad + \frac{\tau^2}{4}\operatorname{sinc}\left(\tau\langle\nabla\rangle_0\right)\Delta\left\{|u^n|^2 + \varphi_2(2ic^2\tau)(u^n)^2 + \varphi_2(-2ic^2\tau)\overline{u^n}^2\right\},\\
\dot{\mathfrak{n}}^{n+1} &= -\langle\nabla\rangle_0\sin\left(\tau\langle\nabla\rangle_0\right)\mathfrak{n}^n + \cos\left(\tau\langle\nabla\rangle_0\right)\dot{\mathfrak{n}}^n\\
&\quad + \frac{\tau}{4}\cos\left(\tau\langle\nabla\rangle_0\right)\Delta\left\{2|u^n|^2 + \varphi_1(2ic^2\tau)(u^n)^2 + \varphi_1(-2ic^2\tau)\overline{u^n}^2\right\},\\
S_F^{n+1} &= S_F^n + \tau\varphi_1(i\tau c\langle\nabla\rangle_c)F^{n+1},\\
u^{n+1} &= c^{-1}\langle\nabla\rangle_c^{-1}\left\{-iF^{n+1} - \frac{1}{2}c\langle\nabla\rangle_c^{-1}\mathfrak{n}^{n+1}\left(S_F^{n+1} + \overline{S_F^{n+1}}\right)\right\}
\end{aligned}
\tag{4.29}
$$

and choose the following initial values (cf. (4.10))

$$
\begin{aligned}
u^0 &:= u(0), \qquad \mathfrak{n}^0 := \mathfrak{n}(0), \qquad \dot{\mathfrak{n}}^0 := \partial_t\mathfrak{n}(0),\\
F^0 &:= ic\langle\nabla\rangle_c u^0 + \frac{i}{2}c\langle\nabla\rangle_c^{-1}\,\mathfrak{n}^0(u^0 + \overline{u^0}),\\
S_F^0 &:= u^0 + \tau\varphi_1(i\tau c\langle\nabla\rangle_c)F^0.
\end{aligned}
\tag{4.30}
$$

Remark 4.9. Note that for practical implementation issues we write

$$
\begin{aligned}
S_F^{n+1} &= S_F^n + \tau\varphi_1(i\tau c\langle\nabla\rangle_c)F^{n+1}\\
&= S_F^n - i\left(\mathrm{e}^{i\tau c\langle\nabla\rangle_c} - 1\right)(c\langle\nabla\rangle_c)^{-1}\,F^{n+1}
\end{aligned}
$$

thanks to the definition of the φ_1-function given in (2.8).

In the next section we carry out the convergence analysis of the scheme (4.29).

4.4.2 Convergence Analysis

Before we state our convergence result, we derive the different error bounds for F, u and $(\mathfrak{n}, \dot{\mathfrak{n}})$ to shorten the proof. In the following we set (see (4.19))

$$
B_{t_n,r} = \max\left(\sup_{0\leq k\leq n}\left\{\|u^k\|_{r+1} + \|(c\langle\nabla\rangle_c)^{-1}F^k\|_{r+1} + \|\mathfrak{n}^k\|_r + \|\dot{\mathfrak{n}}^k\|_{r-1}\right\}, 1\right). \tag{4.31}
$$

a) Error in F

Taking the difference of $F(t_n+\tau)$ given in (4.23) and F^{n+1} defined in (4.29) we readily obtain thanks to the error bounds on the remainders (4.20) (see Definition 4.6), the bilinear estimate (1.2) and the isometric property $\|e^{i\tau c\langle\nabla\rangle_c} f\|_r = \|f\|_r$ (see Lemma 4.5) that

$$\begin{aligned}
&\left\|(c\langle\nabla\rangle_c)^{-1}\left(F(t_n+\tau)-F^{n+1}\right)\right\|_{r+1}\\
&\qquad\le \left\|(c\langle\nabla\rangle_c)^{-1}\left(F(t_n)-F^{n}\right)\right\|_{r+1}\\
&\qquad\quad+\tau\left\|\langle\nabla\rangle_c^{-2}(\dot{\mathfrak{n}}(t_n)u(t_n)-\dot{\mathfrak{n}}^n u^n)\right\|_{r+1}\\
&\qquad\quad+\tau\left\|\langle\nabla\rangle_c^{-2}\varphi_1\left(\tfrac{i}{2}\tau\Delta\right)\Big(\mathfrak{n}(t_n)c\langle\nabla\rangle_c u(t_n)-\mathfrak{n}^n c\langle\nabla\rangle_c u^n\Big)\right\|_{r+1}\\
&\qquad\quad+\tau\left\|\langle\nabla\rangle_c^{-2}\varphi_1\left(-i\tau(c\langle\nabla\rangle_c+c^2)\right)\Big(\mathfrak{n}(t_n)c\langle\nabla\rangle_c\overline{u}(t_n)-\mathfrak{n}^n c\langle\nabla\rangle_c\overline{u}^n\Big)\right\|_{r+1}\\
&\qquad\quad+\tau^2 K M^p_{t_{n+1},r+3}\\
&\qquad=: \left\|(c\langle\nabla\rangle_c)^{-1}\left(F(t_n)-F^{n}\right)\right\|_{r+1}+T_1^F+T_2^F+T_3^F+\tau^2 K M^p_{t_{n+1},r+3}.
\end{aligned}\tag{4.32}$$

We have used that the definition of the φ_1 function (see (2.8)) implies

$$\left\|\varphi_1\left(\tfrac{i}{2}\tau\Delta\right)\right\|_r\le 1 \quad\text{and}\quad \left\|\varphi_1\left(-i\tau(c\langle\nabla\rangle_c+c^2)\right)\right\|_r\le 1.$$

We will estimate the terms on the right hand side T_j^F separately.

Bound on the first term T_1^F: Note that

$$\begin{aligned}
\dot{\mathfrak{n}}(t_n)u(t_n)-\dot{\mathfrak{n}}^n u^n &= \dot{\mathfrak{n}}(t_n)u(t_n)-\left(\dot{\mathfrak{n}}^n-\dot{\mathfrak{n}}(t_n)+\dot{\mathfrak{n}}(t_n)\right)u^n\\
&= \dot{\mathfrak{n}}(t_n)u(t_n)-\dot{\mathfrak{n}}^n u^n+\dot{\mathfrak{n}}(t_n)u^n-\dot{\mathfrak{n}}(t_n)u^n\\
&= \left(\dot{\mathfrak{n}}(t_n)-\dot{\mathfrak{n}}^n\right)u^n+\dot{\mathfrak{n}}(t_n)\left(u(t_n)-u^n\right).
\end{aligned}$$

Thanks to Lemma 4.5 and the bilinear estimate (4.17) we have

$$\|\langle\nabla\rangle_c^{-2}(fg)\|_{r+1}\ \le \|fg\|_{r-1}\ \le K\|f\|_{r-1}\|g\|_{r+1}$$

which thus implies that

$$\begin{aligned}
T_1^F &:= \tau\left\|\langle\nabla\rangle_c^{-2}(\dot{\mathfrak{n}}(t_n)u(t_n)-\dot{\mathfrak{n}}^n u^n)\right\|_{r+1}\\
&\le \tau K\left(\|\dot{\mathfrak{n}}(t_n)-\dot{\mathfrak{n}}^n\|_{r-1}\|u^n\|_{r+1}+\|\dot{\mathfrak{n}}(t_n)\|_{r-1}\|u(t_n)-u^n\|_{r+1}\right)\\
&\le \tau K M_{t_n,r}B_{t_n,r}\left(\|\dot{\mathfrak{n}}(t_n)-\dot{\mathfrak{n}}^n\|_{r-1}+\|u(t_n)-u^n\|_{r+1}\right),
\end{aligned}\tag{4.33}$$

where $M_{t_n,r}$ and $B_{t_n,r}$ are defined in (4.19) and (4.31), respectively.
The second and third term have to be bounded more carefully.

Bound on the second term T_2^F: Note that for $\zeta\in\mathbb{R}$ with $\zeta\neq 0$ we have

$$\|\tau\varphi_1(i\tau\zeta)f\|_{r+1}=\left\|\tau\frac{e^{i\tau\zeta}-1}{i\tau\zeta}f\right\|_{r+1}\le\|(\zeta)^{-1}f\|_{r+1}.\tag{4.34}$$

Thanks to the relation

$$\begin{aligned}
\mathfrak{n}(t_n)c\langle\nabla\rangle_c u(t_n)-\mathfrak{n}^n c\langle\nabla\rangle_c u^n &= \mathfrak{n}(t_n)c\langle\nabla\rangle_c u(t_n)-(\mathfrak{n}^n-\mathfrak{n}(t_n)+\mathfrak{n}(t_n))c\langle\nabla\rangle_c u^n\\
&= (\mathfrak{n}(t_n)-\mathfrak{n}^n)c\langle\nabla\rangle_c u^n+\mathfrak{n}(t_n)c\langle\nabla\rangle_c(u(t_n)-u^n)
\end{aligned}\tag{4.35}$$

we thus obtain that

$$\begin{aligned}
T_2^F &:= \tau \, \| \, \langle\nabla\rangle_c^{-2}\varphi_1\left(\tfrac{i}{2}\tau\Delta\right)\Big(\mathfrak{n}(t_n)c\langle\nabla\rangle_c u(t_n) - \mathfrak{n}^n c\langle\nabla\rangle_c u^n\Big) \, \|_{r+1} \\
&\le \Big\| \langle\nabla\rangle_c^{-2}\left(\tau\varphi_1\left(\tfrac{i}{2}\tau\Delta\right)\right)\Big((\mathfrak{n}(t_n)-\mathfrak{n}^n)c\langle\nabla\rangle_c u^n\Big)\Big\|_{r+1} \\
&\quad + \tau\Big\|\langle\nabla\rangle_c^{-2}\varphi_1\left(\tfrac{i}{2}\tau\Delta\right)\Big(\mathfrak{n}(t_n)c\langle\nabla\rangle_c(u(t_n)-u^n)\Big)\Big\|_{r+1} \\
&\le \Big\|\langle\nabla\rangle_c^{-2}\Big((\mathfrak{n}(t_n)-\mathfrak{n}^n)c\langle\nabla\rangle_c u^n\Big)\Big\|_{r-1} + \tau\Big\|\langle\nabla\rangle_c^{-2}\Big(\mathfrak{n}(t_n)c\langle\nabla\rangle_c(u(t_n)-u^n)\Big)\Big\|_{r+1} \\
&=: T_{2,a}^F + T_{2,b}^F.
\end{aligned} \tag{4.36}$$

We consider $T_{2,a}^F$ and $T_{2,b}^F$ separately. Thanks to the last estimate in Lemma 4.5 we have

$$T_{2,a}^F = \Big\|\langle\nabla\rangle_c^{-2}\Big((\mathfrak{n}(t_n)-\mathfrak{n}^n)c\langle\nabla\rangle_c u^n\Big)\Big\|_{r-1} \le K\|\mathfrak{n}(t_n)-\mathfrak{n}^n\|_{r-1}\,\|u^n\|_{r+1}. \tag{4.37}$$

Furthermore, the estimate $\frac{c|k|}{c(c+|k|)} \le 1$ together with the definition of the operator $\langle\nabla\rangle_c$ in Fourier space (see equation (2.12)) yields that

$$\left\|\frac{c\langle\nabla\rangle_c}{c(c+\langle\nabla\rangle_0)}f\right\|_r \le \|f\|_r. \tag{4.38}$$

With the aid of Lemma 4.5 we can estimate $T_{2,b}^F$ as follows

$$\begin{aligned}
T_{2,b}^F &= \tau\Big\|\langle\nabla\rangle_c^{-2}\Big(\mathfrak{n}(t_n)c\langle\nabla\rangle_c(u(t_n)-u^n)\Big)\Big\|_{r+1} \\
&= \tau\left\|\langle\nabla\rangle_c^{-2}\left(\mathfrak{n}(t_n)\frac{c\langle\nabla\rangle_c}{c(c+\langle\nabla\rangle_0)}c(c+\langle\nabla\rangle_0)(u(t_n)-u^n)\right)\right\|_{r+1} \\
&\le \tau\left\|\langle\nabla\rangle_c^{-2}\left(\mathfrak{n}(t_n)\frac{c\langle\nabla\rangle_c}{c(c+\langle\nabla\rangle_0)}c^2(u(t_n)-u^n)\right)\right\|_{r+1} \\
&\quad + \tau\left\|\langle\nabla\rangle_c^{-2}\left(\mathfrak{n}(t_n)\frac{c\langle\nabla\rangle_c}{c(c+\langle\nabla\rangle_0)}c\langle\nabla\rangle_0(u(t_n)-u^n)\right)\right\|_{r+1} \\
&\le \tau\frac{1}{c^2}\left\|\mathfrak{n}(t_n)\frac{c\langle\nabla\rangle_c}{c(c+\langle\nabla\rangle_0)}c^2(u(t_n)-u^n)\right\|_{r+1} + \tau\frac{1}{c}\left\|\mathfrak{n}(t_n)\frac{c\langle\nabla\rangle_c}{c(c+\langle\nabla\rangle_0)}c\langle\nabla\rangle_0(u(t_n)-u^n)\right\|_r .
\end{aligned}$$

Now, we use the above bound (4.38), which implies

$$T_{2,b}^F \le \tau K\|\mathfrak{n}(t_n)\|_{r+1}\|u(t_n)-u^n\|_{r+1}. \tag{4.39}$$

Plugging (4.37) and (4.39) into (4.36) we can thus conclude

$$\begin{aligned}
T_2^F &\le K\Big(\|\mathfrak{n}(t_n)-\mathfrak{n}^n\|_{r-1}\|u^n\|_{r+1} + \tau\|\mathfrak{n}(t_n)\|_{r+1}\,\|u(t_n)-u^n\|_{r+1}\Big) \\
&\le \tau K M_{t_n,r+1}B_{t_n,r}\Big(\frac{1}{\tau}\,\|\mathfrak{n}(t_n)-\mathfrak{n}^n\|_{r-1} + \|u(t_n)-u^n\|_{r+1}\Big).
\end{aligned} \tag{4.40}$$

Bound on the third term T_3^F: Similarly to the bound on T_2^F we obtain by the relation (4.35) using (4.34) together with the estimate

$$\left\|\frac{1}{c\langle\nabla\rangle_c + c^2}f\right\|_r \le \frac{1}{c^2}\,\|f\|_r$$

that

$$\begin{aligned}
T_3^F &:= \Big\|\langle\nabla\rangle_c^{-2}\varphi_1\left(-i\tau(c\langle\nabla\rangle_c+c^2)\right)\Big(\mathfrak{n}(t_n)c\langle\nabla\rangle_c\overline{u}(t_n) - \mathfrak{n}^n c\langle\nabla\rangle_c\overline{u}^n\Big)\Big\|_{r+1} \\
&\le \left\|\langle\nabla\rangle_c^{-2}\frac{1}{c\langle\nabla\rangle_c+c^2}\Big((\mathfrak{n}(t_n)-\mathfrak{n}^n)c\langle\nabla\rangle_c\overline{u}^n\Big)\right\|_{r+1} + \tau\Big\|\langle\nabla\rangle_c^{-2}\Big(\mathfrak{n}(t_n)c\langle\nabla\rangle_c\overline{(u(t_n)-u^n)}\Big)\Big\|_{r+1} \\
&\le \left\|(\mathfrak{n}(t_n)-\mathfrak{n}^n)\frac{c\langle\nabla\rangle_c}{c^2}\overline{u}^n\right\|_{r-1} + \tau\Big\|\langle\nabla\rangle_c^{-2}\Big(\mathfrak{n}(t_n)c\langle\nabla\rangle_c\overline{(u(t_n)-u^n)}\Big)\Big\|_{r+1} .
\end{aligned}$$

With similar arguments (see (1.2), (4.18), (4.39)) as above we can thus conclude

$$\begin{aligned} T_3^F &\leq K\Big(\|\mathfrak{n}(t_n) - \mathfrak{n}^n\|_{r-1}\|u^n\|_{r+1} + \tau\|\mathfrak{n}(t_n)\|_{r+1}\,\|u(t_n) - u^n\|_{r+1}\Big) \\ &\leq \tau K M_{t_n,r+1} B_{t_n,r}\Big(\frac{1}{\tau}\,\|\mathfrak{n}(t_n) - \mathfrak{n}^n\|_{r-1} + \|u(t_n) - u^n\|_{r+1}\Big). \end{aligned} \tag{4.41}$$

Bound on error in F: Plugging the bounds (4.33), (4.40) and (4.41) into (4.32) yields that

$$\begin{aligned} &\left\|(c\langle\nabla\rangle_c)^{-1}\left(F(t_n+\tau) - F^{n+1}\right)\right\|_{r+1} \\ &\quad\leq \left\|(c\langle\nabla\rangle_c)^{-1}\left(F(t_n) - F^n\right)\right\|_{r+1} \\ &\quad\quad + \tau K M_{t_n,r+1} B_{t_n,r}\Big(\|u(t_n) - u^n\|_{r+1} + \tfrac{1}{\tau}\|\mathfrak{n}(t_n) - \mathfrak{n}^n\|_{r-1} + \|\dot{\mathfrak{n}}(t_n) - \dot{\mathfrak{n}}^n\|_{r-1}\Big) \\ &\quad\quad + \tau^2 K M^p_{t_{n+1},r+3}. \end{aligned} \tag{4.42}$$

b) Error in u

Taking the difference of the approximation of $u(t_n)$ given in (4.27) and the numerical solution u^n defined in (4.29) we readily obtain by the definition of the remainder $\mathcal{R}_{r+3}$ (see Definition 4.6) together with the relation

$$\begin{aligned} \mathfrak{n}(t_n)S_F(t_n) - \mathfrak{n}^n S_F^n &= \mathfrak{n}(t_n)S_F(t_n) - (\mathfrak{n}^n - \mathfrak{n}(t_n) + \mathfrak{n}(t_n))S_F^n \\ &= (\mathfrak{n}(t_n) - \mathfrak{n}^n)S_F^n + \mathfrak{n}(t_n)(S_F(t_n) - S_F^n) \end{aligned}$$

that

$$\begin{aligned} \|u(t_n) - u^n\|_{r+1} \;&\leq \left\|c^{-1}\langle\nabla\rangle_c^{-1}\left(F^n - F(t_n)\right)\right\|_{r+1} + \left\|\langle\nabla\rangle_c^{-2}\left((\mathfrak{n}(t_n) - \mathfrak{n}^n)S_F^n\right)\right\|_{r+1} \\ &\quad + \left\|\langle\nabla\rangle_c^{-2}\Big(\mathfrak{n}(t_n)\Big(S_F(t_n) - S_F^n\Big)\Big)\right\|_{r+1} + \tau\mathcal{R}_{r+3}. \end{aligned} \tag{4.43}$$

Thanks to Lemma 4.5 we have

$$\left\|\langle\nabla\rangle_c^{-2}\left((\mathfrak{n}(t_n) - \mathfrak{n}^n)S_F^n\right)\right\|_{r+1} \leq K\|(\mathfrak{n}(t_n) - \mathfrak{n}^n)S_F^n\|_{r-1} \leq K\left(\frac{1}{\tau}\|\mathfrak{n}(t_n) - \mathfrak{n}^n\|_{r-1}\right)\left(\tau\|S_F^n\|_{r+1}\right). \tag{4.44}$$

Furthermore, the bound (4.39) with $u(t_n) - u^n$ replaced by $(c\langle\nabla\rangle_c^{-1})(S_F(t_n) - S_F^n)$ implies with the aid of (4.39) that

$$\begin{aligned} \left\|\langle\nabla\rangle_c^{-2}\Big(\mathfrak{n}(t_n)\Big(S_F(t_n) - S_F^n\Big)\Big)\right\|_{r+1} &\leq \left\|\langle\nabla\rangle_c^{-2}\Big(\mathfrak{n}(t_n)(c\langle\nabla\rangle_c)\left[(c\langle\nabla\rangle_c)^{-1}\Big(S_F(t_n) - S_F^n\Big)\right]\Big)\right\|_{r+1} \\ &\leq K\|\mathfrak{n}(t_n)\|_{r+1}\left\|(c\langle\nabla\rangle_c)^{-1}\,\Big(S_F(t_n) - S_F^n\Big)\right\|_{r+1}. \end{aligned} \tag{4.45}$$

Plugging (4.44) and (4.45) into (4.43) yields

$$\begin{aligned} \|u(t_n) - u^n\|_{r+1} \;&\leq \left\|c^{-1}\langle\nabla\rangle_c^{-1}\left(F^n - F(t_n)\right)\right\|_{r+1} \\ &\quad + K\left(\frac{1}{\tau}\|\mathfrak{n}(t_n) - \mathfrak{n}^n\|_{r-1}\right)\left(\tau\|S_F^n\|_{r+1}\right) \\ &\quad + K\|\mathfrak{n}(t_n)\|_{r+1}\left\|(c\langle\nabla\rangle_c)^{-1}\,\Big(S_F(t_n) - S_F^n\Big)\right\|_{r+1} \\ &\quad + \tau\mathcal{R}_{r+3}. \end{aligned} \tag{4.46}$$

Taking the difference of $S_F(t_n)$ defined in (4.26) and S_F^n given through (4.29) we obtain

$$\begin{aligned} \left\|(c\langle\nabla\rangle_c)^{-1}\,\Big(S_F(t_n) - S_F^n\Big)\right\|_{r+1} &= \tau\sum_{k=0}^{n}\left\|(c\langle\nabla\rangle_c)^{-1}\varphi_1(i\tau c\langle\nabla\rangle_c)\Big(F(t_k) - F^k\Big)\right\|_{r+1} \\ &\leq \tau\sum_{k=0}^{n}\left\|(c\langle\nabla\rangle_c)^{-1}\Big(F(t_k) - F^k\Big)\right\|_{r+1}, \end{aligned} \tag{4.47}$$

where we have used that $\|\varphi_1(i\tau c\langle\nabla\rangle_c)\|_r \leq 1$.
The definition of S_F^n (see (4.29) with initial value (4.30)) also yields

$$\|S_F^n\|_{r+1} \leq \|u(0)\|_{r+1} + \tau \sum_{k=0}^{n} \left\|\varphi_1(i\tau c\langle\nabla\rangle_c)F^k\right\|_{r+1}.$$

From the estimate (4.34) we can furthermore conclude that

$$\begin{aligned} \tau\,\|S_F^n\|_{r+1} &\leq \tau\|u(0)\|_{r+1} + \tau \sum_{k=0}^{n} \left\|\tau\varphi_1(i\tau c\langle\nabla\rangle_c)F^k\right\|_{r+1} \\ &\leq \tau\|u(0)\|_{r+1} + \tau \sum_{k=0}^{n} \left\|(c\langle\nabla\rangle_c)^{-1}F^k\right\|_{r+1} \\ &\leq \tau\|u(0)\|_{r+1} + t_{n+1} \sup_{0\leq k\leq n} \left\|(c\langle\nabla\rangle_c)^{-1}F^k\right\|_{r+1}. \end{aligned} \tag{4.48}$$

Plugging (4.47) and (4.48) into (4.46) we thus obtain by the definition of $B_{t_n,r}$ in (4.31) that

$$\begin{aligned} \|u(t_n) - u^n\|_{r+1} &\leq \left\|c^{-1}\langle\nabla\rangle_c^{-1}\left(F^n - F(t_n)\right)\right\|_{r+1} + KB_{t_n,r}t_n\left(\frac{1}{\tau}\|\mathfrak{n}(t_n) - \mathfrak{n}^n\|_{r-1}\right) \\ &\quad + KM_{t_n,r+1}\left(\tau\sum_{k=0}^{n}\left\|c^{-1}\langle\nabla\rangle_c^{-1}\left(F(t_k) - F^k\right)\right\|_{r+1}\right). \end{aligned} \tag{4.49}$$

c) Error in $(n, \dot{\mathfrak{n}})$

In the following we define the rotation matrix

$$\mathcal{D}(\tau\langle\nabla\rangle_0) = \begin{pmatrix} \cos(\tau\langle\nabla\rangle_0) & \sin(\tau\langle\nabla\rangle_0) \\ -\sin(\tau\langle\nabla\rangle_0) & \cos(\tau\langle\nabla\rangle_0) \end{pmatrix}. \tag{4.50}$$

Taking the difference of the approximation to the exact solution $(\mathfrak{n}(t_{n+1}), \dot{\mathfrak{n}}(t_{n+1}))$ given in (4.28) and the numerical solution $(n^{n+1}, \dot{\mathfrak{n}}^{n+1})$ defined in (4.29) we readily obtain by the definition of the remainder $\mathcal{R}_{r+2}$ (see Definition 4.6), the rotation matrix (4.50) and the relation

$$\begin{aligned} |u(t_n)| - |(u^n)^2| &= (u(t_n) - u^n)\overline{u(t_n)} + u^n\overline{(u(t_n) - u^n)}, \\ u(t_n)^2 - (u^n)^2 &= (u(t_n) - u^n)(u(t_n) + u^n) \end{aligned} \tag{4.51}$$

(with the corresponding complex conjugate version) that

$$\begin{aligned} \begin{pmatrix} \mathfrak{n}(t_{n+1}) - \mathfrak{n}^{n+1} \\ \langle\nabla\rangle_0^{-1}(\,\dot{\mathfrak{n}}(t_n) - \dot{\mathfrak{n}}^n) \end{pmatrix} &= \mathcal{D}(\tau\langle\nabla\rangle_0)\begin{pmatrix} \mathfrak{n}(t_n) - \mathfrak{n}^n \\ \langle\nabla\rangle_0^{-1}(\,\dot{\mathfrak{n}}(t_n) - \dot{\mathfrak{n}}^n) \end{pmatrix} \\ &\quad + \frac{\tau}{4}\begin{pmatrix} \tau\frac{\sin(\tau\langle\nabla\rangle_0)}{\tau\langle\nabla\rangle_0}\langle\nabla\rangle_0^2\Big(p_1(u(t_n), u^n)(u(t_n) - u^n)\Big) \\ \cos(\tau\langle\nabla\rangle_0)\,\langle\nabla\rangle_0\Big(p_2(u(t_n), u^n)(u(t_n) - u^n)\Big) \end{pmatrix} + \begin{pmatrix} \tau^3\mathrm{sinc}(\tau\langle\nabla\rangle_0)\mathcal{R}_{r+4} \\ \tau^2\mathcal{R}_{r+3} \end{pmatrix}. \end{aligned}$$

Thereby, p_1 and p_2 simply denote polynomials in $u(t_n), u^n$ (according to (4.51)) due to the bounds (see (2.8))

$$\left|\varphi_1(\pm 2ic^2)\right| \leq 1, \qquad \left|\varphi_2(\pm 2ic^2)\right| \leq 1.$$

Solving the above recursion we obtain

$$\begin{pmatrix} \mathfrak{n}(t_{n+1}) - \mathfrak{n}^{n+1} \\ \langle\nabla\rangle_0^{-1}(\ \dot{\mathfrak{n}}(t_n) - \dot{\mathfrak{n}}^n) \end{pmatrix} = \frac{\tau}{4}\sum_{k=0}^{n} \mathcal{D}(\tau\langle\nabla\rangle_0)^k \begin{pmatrix} \tau\frac{\sin(\tau\langle\nabla\rangle_0)}{\tau\langle\nabla\rangle_0}\langle\nabla\rangle_0^2\Big(p_1\left(u(t_{n-k}), u^{n-k}\right)\left(u(t_{n-k}) - u^{n-k}\right)\Big) \\ \cos\left(\tau\langle\nabla\rangle_0\right)\langle\nabla\rangle_0\Big(p_2\left(u(t_{n-k}), u^{n-k}\right)\left(u(t_{n-k}) - u^{n-k}\right)\Big) \end{pmatrix}$$

$$+ n\tau \begin{pmatrix} \tau^2 \mathrm{sinc}(\tau\langle\nabla\rangle_0)\mathcal{R}_{r+4} \\ \tau\mathcal{R}_{r+3} \end{pmatrix}$$

$$= \frac{\tau}{4}\sum_{k=1}^{n} \mathcal{D}(\tau\langle\nabla\rangle_0)^{k-1}\left\{\mathcal{N}(u(t_{n-k}), u^{n-k})\right\}$$

$$+ \frac{\tau}{4}\begin{pmatrix} \tau\frac{\sin(\tau\langle\nabla\rangle_0)}{\tau\langle\nabla\rangle_0}\langle\nabla\rangle_0^2\Big(p_1\left(u(t_n), u^n\right)\left(u(t_n) - u^n\right)\Big) \\ \cos\left(\tau\langle\nabla\rangle_0\right)\langle\nabla\rangle_0\Big(p_2\left(u(t_n), u^n\right)\left(u(t_n) - u^n\right)\Big) \end{pmatrix}$$

$$+ t_n \begin{pmatrix} \tau^2 \mathrm{sinc}(\tau\langle\nabla\rangle_0)\mathcal{R}_{r+4} \\ \tau\mathcal{R}_{r+3} \end{pmatrix},$$

where we have set

$$\mathcal{N}(u(t_{n-k}), u^{n-k}) = \begin{pmatrix} \mathcal{N}_1(u(t_{n-k}), u^{n-k}) \\ \mathcal{N}_2(u(t_{n-k}), u^{n-k}) \end{pmatrix}$$

$$:= \mathcal{D}(\tau\langle\nabla\rangle_0)\begin{pmatrix} \tau\frac{\sin(\tau\langle\nabla\rangle_0)}{\tau\langle\nabla\rangle_0}\langle\nabla\rangle_0^2\Big(p_1\left(u(t_{n-k}), u^{n-k}\right)\left(u(t_{n-k}) - u^{n-k}\right)\Big) \\ \cos\left(\tau\langle\nabla\rangle_0\right)\langle\nabla\rangle_0\Big(p_2\left(u(t_{n-k}), u^{n-k}\right)\left(u(t_{n-k}) - u^{n-k}\right)\Big) \end{pmatrix}.$$

Note that for all $k \geq 1$ it holds

$$\left\|\mathcal{D}(\tau\langle\nabla\rangle_0)^{k-1}\right\|_r \leq 1.$$

Together with the observation

$$\begin{aligned}\mathcal{N}_1(u(t_{n-k}), u^{n-k}) &= \cos\left(\tau\langle\nabla\rangle_0\right)\tau\frac{\sin\left(\tau\langle\nabla\rangle_0\right)}{\tau\langle\nabla\rangle_0}\langle\nabla\rangle_0^2\Big(p_1\left(u(t_{n-k}), u^{n-k}\right)\left(u(t_{n-k}) - u^{n-k}\right)\Big) \\ &\quad + \sin\left(\tau\langle\nabla\rangle_0\right)\cos\left(\tau\langle\nabla\rangle_0\right)\langle\nabla\rangle_0\Big(p_2\left(u(t_{n-k}), u^{n-k}\right)\left(u(t_{n-k}) - u^{n-k}\right)\Big) \\ &= \tau\cos\left(\tau\langle\nabla\rangle_0\right)\frac{\sin\left(\tau\langle\nabla\rangle_0\right)}{\tau\langle\nabla\rangle_0}\langle\nabla\rangle_0^2\Big\{\Big(p_1\left(u(t_{n-k}), u^{n-k}\right)\left(u(t_{n-k}) - u^{n-k}\right)\Big) \\ &\qquad + \Big(p_2\left(u(t_{n-k}), u^{n-k}\right)\left(u(t_{n-k}) - u^{n-k}\right)\Big)\Big\}\end{aligned}$$

we thus obtain

$$\|\mathfrak{n}(t_{n+1}) - \mathfrak{n}^{n+1}\|_{r-1} \leq \tau K M_{t_n,r} B_{t_n,r}\left(\tau\sum_{k=0}^{n}\|u(t_k) - u^k\|_{r+1}\right) + \tau^2 M^p_{t_{n+1},r+3}$$

as well as the (classical) bound

$$\|\mathfrak{n}(t_{n+1}) - \mathfrak{n}^{n+1}\|_r + \|\langle\nabla\rangle_0^{-1}(\ \dot{\mathfrak{n}}(t_n) - \dot{\mathfrak{n}}^n)\|_r \leq K M_{t_n,r} B_{t_n,r}\left(\tau\sum_{k=0}^{n}\|u(t_k) - u^k\|_{r+1}\right) + \tau M^p_{t_{n+1},r+3}.$$

Hence, we can conclude

$$\begin{aligned}&\frac{1}{\tau}\|\mathfrak{n}(t_{n+1}) - \mathfrak{n}^{n+1}\|_{r-1} + \|\mathfrak{n}(t_{n+1}) - \mathfrak{n}^{n+1}\|_r + \|\dot{\mathfrak{n}}(t_n) - \dot{\mathfrak{n}}^n\|_{r-1} \\ &\qquad \leq K M_{t_n,r} B_{t_n,r}\left(\tau\sum_{k=0}^{n}\|u(t_k) - u^k\|_{r+1}\right) + \tau M^p_{t_{n+1},r+3}.\end{aligned} \tag{4.52}$$

4.4.2.1 The Convergence Theorem

The numerical solutions $(u^n, F^n, \mathfrak{n}^n, \dot{\mathfrak{n}}^n)$ defined by the oscillatory integration scheme (4.29) allows a first-order approximation to the exact solution $(u(t_n), F(t_n), \mathfrak{n}(t_n), \dot{\mathfrak{n}}(t_n))$ of the Klein–Gordon–Zakharov system (4.14) uniformly in c. More precisely, with

$$z_n := \tfrac{1}{2}\left(u^n + \overline{u^n}\right)$$

the following convergence result holds.

Theorem 4.10 (Convergence bound for the first-order scheme, cf. Theorem 9 in [12]). *Fix $r > d/2$. Assume that $(u(0), \mathfrak{n}(0), \dot{\mathfrak{n}}(0)) \in H^{r+4} \times H^{r+3} \times H^{r+2}$. Then there exists constants $T > 0, \tau_0 > 0, K > 0$ such that for all $t_n \leq T, \tau \leq \tau_0$ and all $c \geq 1$ we have*

$$\|z(t_n) - z^n\|_{r+1} + \|\mathfrak{n}(t_n) - \mathfrak{n}^n\|_r \ + \|\dot{\mathfrak{n}}(t_n) - \dot{\mathfrak{n}}^n\|_{r-1} \leq K\tau,$$

where the constant K depends on T, on $M_{T,r+3}$ defined in (4.19), and on r, but can be chosen independently of c.

Proof. Due to the local wellposedness of the Klein–Gordon–Zakharov system (4.14) (see, e.g., [54, 55, 61]) we know that there exists a $T > 0$ such that $M_{T,r+3}$ defined in (4.19) is finite. Thereby, observe that by the definition of $F = \partial_t u$ we have (see (4.9))

$$iF = -c\langle\nabla\rangle_c u - \frac{1}{2}c\langle\nabla\rangle_c^{-1}\, \mathfrak{n}(u + \overline{u})$$

such that by Lemma 4.5 and the bilinear estimate (4.17) we obtain

$$\|(c\langle\nabla\rangle_c)^{-1}F\|_{r+1} \leq \|u\|_{r+1} + \|\mathfrak{n}u\|_{r-1} \leq \|u\|_{r+1} + K\|\mathfrak{n}\|_{r-1}\|u\|_{r+1}.$$

Collecting the error bounds (4.42), (4.49) and (4.52) yields

$$\begin{aligned}
&\left\|(c\langle\nabla\rangle_c)^{-1}\left(F(t_n+\tau) - F^{n+1}\right)\right\|_{r+1} \\
&\qquad \leq \left\|(c\langle\nabla\rangle_c)^{-1}\left(F(t_n) - F^n\right)\right\|_{r+1} \\
&\qquad\quad + \tau K M_{t_n,r+1} B_{t_n,r}\Big(\|u(t_n) - u^n\|_{r+1} + \tfrac{1}{\tau}\|\mathfrak{n}(t_n) - \mathfrak{n}^n\|_{r-1} + \|\dot{\mathfrak{n}}(t_n) - \dot{\mathfrak{n}}^n\|_{r-1}\Big) \\
&\qquad\quad + \tau^2 K M^p_{t_{n+1},r+3}, \\
&\|u(t_{n+1}) - u^{n+1}\|_{r+1} \\
&\qquad \leq \left\|c^{-1}\langle\nabla\rangle_c^{-1}\left(F(t_{n+1}) - F^{n+1}\right)\right\|_{r+1} + K B_{t_n,r} t_n\left(\frac{1}{\tau}\|\mathfrak{n}(t_{n+1}) - \mathfrak{n}^{n+1}\|_{r-1}\right) \\
&\qquad\quad + K M_{t_n,r+1}\left(\tau\sum_{k=0}^{n+1}\left\|c^{-1}\langle\nabla\rangle_c^{-1}\left(F(t_k) - F^k\right)\right\|_{r+1}\right), \\
&\frac{1}{\tau}\|\mathfrak{n}(t_{n+1}) - \mathfrak{n}^{n+1}\|_{r-1} + \|\mathfrak{n}(t_{n+1}) - \mathfrak{n}^{n+1}\|_r + \|\dot{\mathfrak{n}}(t_{n+1}) - \dot{\mathfrak{n}}^{n+1}\|_{r-1} \\
&\qquad \leq K M_{t_n,r} B_{t_n,r}\left(\tau\sum_{k=0}^{n}\|u(t_k) - u^k\|_{r+1}\right) + \tau M^p_{t_{n+1},r+3}.
\end{aligned} \tag{4.53}$$

In the following we assume

$$\text{for all } k \leq n \quad : \quad B_{t_n,r} \leq M_1, \quad M_{t_{n+1},r+1} \leq M_2, \quad M_{t_{n+1},r+3} \leq M_3.$$

Plugging the estimates on the error in $\mathfrak{n}$ and $\dot{\mathfrak{n}}$ into the error recursions in u and F yields together with

$$\tau \sum_{k=0}^{n} \|f_k\|_r \leq t_{n+1} \sup_{0\leq k\leq n} \|f_k\|_r$$

by (4.53) that

$$\begin{aligned}\left\|(c\langle\nabla\rangle_c)^{-1}\left(F(t_n+\tau)-F^{n+1}\right)\right\|_{r+1} \leq \left\|(c\langle\nabla\rangle_c)^{-1}\left(F(t_n)-F^n\right)\right\|_{r+1} \\ + \tau t_n \mathcal{K}_1(M_1,M_2,M_3) \sup_{0\leq k\leq n} \|u(t_n)-u^n\|_{r+1} \\ + \tau^2 K M^p_{t_{n+1},r+3}\end{aligned} \tag{4.54}$$

as well as

$$\begin{aligned}\|u(t_{n+1})-u^{n+1}\|_{r+1} \leq t_n \mathcal{K}_2(M_1,M_2,M_3) \sup_{0\leq k\leq n} \left\|c^{-1}\langle\nabla\rangle_c^{-1}\left(F(t_{k+1})-F^{k+1}\right)\right\|_{r+1} \\ + \tau K B_{t_n,r} t_n M^p_{t_{n+1},r+3},\end{aligned} \tag{4.55}$$

where the constants $\mathcal{K}_1$ and $\mathcal{K}_2$ depend on t_n, M_1, M_2 and M_3, but can be chosen independently of c.

Plugging (4.55) into (4.54) finally yields with the inductive assumption that the error in F is growing as

$$\begin{aligned}\left\|(c\langle\nabla\rangle_c)^{-1}\left(F(t_n+\tau)-F^{n+1}\right)\right\|_{r+1} \leq \left(1+\widetilde{\mathcal{K}}_1(t_n,M_1,M_2,M_3)\tau\right)\left\|(c\langle\nabla\rangle_c)^{-1}\left(F(t_n)-F^n\right)\right\|_{r+1} \\ + \tau^2 \widetilde{\mathcal{K}}_2(t_n,M_1,M_2,M_3),\end{aligned} \tag{4.56}$$

where $\widetilde{\mathcal{K}}_1$ and $\widetilde{\mathcal{K}}_2$ depend on t_n, M_1, M_2 and M_3, but can be chosen independently of c.

Collecting the estimates in (4.56), (4.55) and (4.52) the assertion then follows by $z = \frac{1}{2}(u+\overline{u})$ together with an inductive, respectively, *Lady Windermere's fan* argument (see, for example [35, 50]). □

The uniform convergence rate in c stated in Theorem 4.10 is numerically confirmed in Figure 4.7.

Remark 4.11 (Higher-order methods)**.** Our novel technique allows us to develop (in a similar way) higher-order uniformly accurate schemes (with order $p \in \mathbb{N}$) for the Klein–Gordon–Zakharov system (4.1) with convergence rate $\mathcal{O}(\tau^p)$ uniformly in c. This can be achived by iterating the Duhamel's formulas.

For instance, a second-order uniformly accurate integrator can be obtained by plugging the *locally second-order uniform approximations* of $u(t_n+s), \mathfrak{n}(t_n+s)$ and $\dot{\mathfrak{n}}(t_n+s)$ given in Lemma 4.12 below into Duhamel's formula (4.15) and integrating the remaining highly oscillatory phases of type

$$\mathrm{e}^{ikc^2t} \quad \text{with} \quad k \in \mathbb{Z}$$

exactly.

Lemma 4.12 (cf. Lemma 11 in [12]). *Locally second-order uniform approximations to* $(u, \mathfrak{n}, \dot{\mathfrak{n}})(t_n + s)$ *are given by*

$$
\begin{aligned}
u(t_n+s) &= \mathrm{e}^{isc\langle\nabla\rangle_c}u(t_n)\\
&\quad + is\frac{1}{2}c\langle\nabla\rangle_c^{-1}\mathrm{e}^{isc\langle\nabla\rangle_c}\Big(\varphi_1\left(is\tfrac{1}{2}\Delta\right)\left(\mathfrak{n}(t_n)u(t_n)\right) + \varphi_1\left(-is(c\langle\nabla\rangle_c + c^2)\right)\left(\mathfrak{n}(t_n)\overline{u}(t_n)\right)\Big)\\
&\quad + s^2\mathcal{R}_{r+4},\\
\mathfrak{n}(t_n+s) &= \cos(s\langle\nabla\rangle_0)\mathfrak{n}(t_n) + \langle\nabla\rangle_0^{-1}\sin(s\langle\nabla\rangle_0)\dot{\mathfrak{n}}(t_n)\\
&\quad + \frac{s^2}{4}\mathrm{sinc}(s\langle\nabla\rangle_0)\Delta\left\{|u(t_n)|^2 + \varphi_2(2ic^2s)u(t_n)^2 + \varphi_2(-2ic^2s)\left(\overline{u}(t_n)\right)^2\right\} + s^3\mathcal{R}_{r+4},\\
\dot{\mathfrak{n}}(t_n+s) &= -\langle\nabla\rangle_0\sin(s\langle\nabla\rangle_0)\mathfrak{n}(t_n) + \cos(s\langle\nabla\rangle_0)\dot{\mathfrak{n}}(t_n)\\
&\quad + \frac{s}{4}\cos(s\langle\nabla\rangle_0)\mathfrak{n}\Delta\left\{2|u(t_n)|^2 + \varphi_1(2ic^2s)u(t_n)^2 + \varphi_1(-2ic^2s)\left(\overline{u}(t_n)\right)^2\right\} + s^2\mathcal{R}_{r+4}.
\end{aligned}
$$

Proof. Duhamel's formula in u (see (4.16)) together with the approximations (see Lemma 4.5)

$$
u(t_n+\xi) = \mathrm{e}^{ic^2\xi}\, u(t_n) + \xi\mathcal{R}_{r+2}, \qquad \mathrm{e}^{i\xi(c^2-c\langle\nabla\rangle_c)} = \mathrm{e}^{i\xi\frac{1}{2}\Delta} + \xi\mathcal{R}_{r+4}
$$

(cf. (4.22)) implies by the definition of the φ_1 function (see (2.8)) the following

$$
\begin{aligned}
u(t_n+s) &= \mathrm{e}^{isc\langle\nabla\rangle_c}u(t_n) + \frac{i}{2}c\langle\nabla\rangle_c^{-1}\int_0^s \mathrm{e}^{i(s-\xi)c\langle\nabla\rangle_c}\mathfrak{n}(t_n+\xi)\big(u(t_n+\xi) + \overline{u}(t_n+\xi)\big)\mathrm{d}\xi\\
&= \mathrm{e}^{isc\langle\nabla\rangle_c}u(t_n) + \frac{i}{2}c\langle\nabla\rangle_c^{-1}\int_0^s \mathrm{e}^{i(s-\xi)c\langle\nabla\rangle_c}\mathfrak{n}(t_n)\big(\mathrm{e}^{i\xi c^2}u(t_n) + \mathrm{e}^{-i\xi c^2}\overline{u}(t_n)\big)\mathrm{d}\xi + s\mathcal{R}_{r+2}\\
&= \mathrm{e}^{isc\langle\nabla\rangle_c}u(t_n) + \frac{i}{2}c\langle\nabla\rangle_c^{-1}\mathrm{e}^{isc\langle\nabla\rangle_c}\int_0^s \Big(\mathrm{e}^{i\xi\frac{1}{2}\Delta}\big(\mathfrak{n}(t_n)u(t_n)\big) + \mathrm{e}^{-i\xi(c\langle\nabla\rangle_c + c^2)}\big(\mathfrak{n}(t_n)\overline{u}(t_n)\big)\Big)\,\mathrm{d}\xi\\
&\quad + s\mathcal{R}_{r+4}\\
&= \mathrm{e}^{isc\langle\nabla\rangle_c}u(t_n) + \frac{i}{2}sc\langle\nabla\rangle_c^{-1}\mathrm{e}^{isc\langle\nabla\rangle_c}\Big(\varphi_1\left(is\tfrac{1}{2}\Delta\right)\left(\mathfrak{n}(t_n)u(t_n)\right)\\
&\quad + \varphi_1\left(-is(c\langle\nabla\rangle_c + c^2)\right)\left(\mathfrak{n}(t_n)\overline{u}(t_n)\right)\Big) + s^2\mathcal{R}_{r+4}.
\end{aligned}
$$

The assertion for $(\mathfrak{n}, \dot{\mathfrak{n}})$ directly follows from (4.28) by replacing τ with s. □

4.4.3 Asymptotic Consistency

The oscillatory integrator (4.29) is *asymptotic consistent* in the sense that it converges asymptotically (i.e., for $c \to \infty$) to the solution of the corresponding Zakharov limit system (4.7) (for sufficiently smooth solutions).

Remark 4.13 (The Zakharov limit). Note that exact solutions $(z, \mathfrak{n})$ of the Klein–Gordon–Zakharov system (4.1) converge asymptotically to the Zakharov system (4.7) in the following sense: For sufficiently smooth solutions we have (see, e.g., [15, 54, 55, 74])

$$
\begin{aligned}
z(t,x) &= \frac{1}{2}\left(\mathrm{e}^{ic^2t}\, u_\infty(t,x) + \mathrm{e}^{-ic^2t}\,\overline{u_\infty}(t,x)\right) + c^{-2}\mathcal{R}_{r+4},\\
\mathfrak{n}(t,x) &= \mathfrak{n}_\infty(t,x) + c^{-2}\mathcal{R}_{r+5},
\end{aligned}
\tag{4.57}
$$

where (u_∞, n_∞) solve the Zakharov system (cf. (4.7))

$$
\begin{aligned}
2i\partial_t u_\infty - \Delta u_\infty &= -\mathfrak{n}_\infty u_\infty,\\
\partial_{tt}\mathfrak{n}_\infty - \Delta\mathfrak{n}_\infty &= \tfrac{1}{2}\Delta\left|u_\infty\right|^2
\end{aligned}
\tag{4.58}
$$

equipped with the initial values

$$u_\infty(0) = z(0) - ic^{-2}\partial_t z(0), \quad \mathfrak{n}_\infty(0) = \mathfrak{n}(0) \quad \text{and} \quad \dot{\mathfrak{n}}_\infty(0) = \dot{\mathfrak{n}}(0).$$

Theorem 4.10 together with the approximation in (4.57) implies that the oscillatory integrator (4.29) converges at order $\tau + c^{-2}$ towards the limit solutions of the Zakharov system. More precisely, for sufficiently smooth solutions the scheme (4.29) allows an approximation towards the solutions (u_∞, n_∞) of the Zakharov limit system (4.58) with the convergence rate

$$\|u_\infty(t_n) - \mathrm{e}^{-ic^2 t_n} u^n\|_{r+1} + \|\mathfrak{n}_\infty(t_n) - \mathfrak{n}^n\|_r \ + \|\dot{\mathfrak{n}}_\infty(t_n) - \dot{\mathfrak{n}}^n\|_{r-1} \leq K\left(\tau + c^{-2}\right),$$

for some constant $K > 0$ which is independent of τ and c. With $z = \frac{1}{2}(u + \overline{u})$ we can in particular deduce for

$$z_\infty := \frac{1}{2}\left(\mathrm{e}^{ic^2 t}\, u_\infty(t, x) + \mathrm{e}^{-ic^2 t}\, \overline{u_\infty}(t, x)\right) \quad \text{and} \quad z^n := \frac{1}{2}(u^n + \overline{u}^n)$$

that

$$\|z_\infty(t_n) - z^n\|_{r+1} + \|\mathfrak{n}_\infty(t_n) - \mathfrak{n}^n\|_r \ + \|\dot{\mathfrak{n}}_\infty(t_n) - \dot{\mathfrak{n}}^n\|_{r-1} \leq K\left(\tau + c^{-2}\right). \tag{4.59}$$

The asymptotic convergence (4.59) of our scheme (4.29) towards the solutions of the Zakharov limit system (4.58) is numerically confirmed in Figure 4.9.

4.5 Numerical Experiments for the Klein–Gordon–Zakharov System

In this section we numerically underline the first-order convergence uniformly in c of the uniformly accurate oscillatory integration scheme (4.29). We also confirm that the first-order uniformly accurate scheme converge in the limit to the corresponding limit integrator for $c \to \infty$.

We consider the Klein–Gordon–Zakharov system on the one dimensional torus, i.e., $x \in \mathbb{T} = [0, 2\pi]$ and on a finite time interval, i.e., $t \in [0, T]$. In all numerical experiments we use a standard Fourier pseudospectral method for the spatial discretization. For more details on pseudospectral methods we refer to [27, 69, 70]. The mesh-size is denoted by $h = \frac{2\pi}{M}$ with grid points $x_j = jh$ and time step size $\tau = \frac{T}{N}$ with grid points $t_n = n\tau$, for $j = 0, ..., M$ and $n = 0, ..., N$ respectively. In order to use the Fourier transform efficiently we choose $M = 2^k$, with $k \in \mathbb{N}$. For practical implementation of the Fourier transform in Matlab, we introduce the Fourier grid $K = \left[-\frac{M}{2} : -1, 0, 1 : \frac{M}{2} - 1\right]$.

In the following we choose $M = 2^{10}$, i.e., we have the spatial mesh-size $h = 0.0061$ and integrate up to $T = 1$ in all numerical simulations.

In all numerical methods for the Klein–Gordon–Zakharov system we use the following initial values

$$\begin{aligned} z(0, x) &= \frac{1}{2}\frac{\cos(3x)^2 \sin(2x)}{2 - \cos(x)}, & \partial_t z(0, x) &= c^2 \frac{1}{2}\frac{\sin(x)\cos(2x)}{2 - \cos(x)}, \\ \mathfrak{n}(0, x) &= \frac{\sin(x)\cos(2x)}{2 - \sin(2x)^2}, & \partial_t \mathfrak{n}(0, x) &= \frac{\sin(x)}{2 - \cos(2x)^2}. \end{aligned}$$

In Section 4.5.1 we derive a Gautschi-type method following the ansatz of [9] and a classical exponential integrator (see [39]) in order to obtain a numerical method to compute the reference solution. Then we recall the numerical method for the limit system in Section 4.5.2 and the uniformly accurate methods in Section 4.5.3. Finally, we compare the different numerical methods in Section 4.5.4.

4.5.1 Numerical Methods for the Reference Solution

In this subsection we derive a second-order Gautschi-type method and a first-order exponential integrator for the Klein–Gordon–Zakharov system.

4.5.1.1 A Gautschi-type Method for the Klein–Gordon–Zakharov System

We use the techniques of [9] and construct a two step Gautschi-type method. Therefore, we recall our Klein–Gordon–Zakharov system

$$\begin{aligned} \partial_{tt} z + c^2 \langle\nabla\rangle_c^2 z &= -c^2 \mathfrak{n} z, \qquad && z(0) = z_0, \qquad && \partial_t z(0) = c^2 z_1, \\ \partial_{tt}\mathfrak{n} + \langle\nabla\rangle_0^2 \mathfrak{n} &= \Delta |z|^2, && \mathfrak{n}(0) = \mathfrak{n}_0, && \partial_t \mathfrak{n}(0) = \mathfrak{n}_1. \end{aligned}$$

In a first step we use the variation of constants formula for second-order equations for z and $\mathfrak{n}$ and obtain

$$\begin{aligned} z(t_n+\tau) &= \cos(\tau c\langle\nabla\rangle_c) z(t_n) + \tau \frac{\sin(\tau c\langle\nabla\rangle_c)}{\tau\langle\nabla\rangle_c}\dot{z}(t_n) - c^2 \int_0^\tau \frac{\sin\left((\tau-s)c\langle\nabla\rangle_c\right)}{c\langle\nabla\rangle_c}\mathfrak{n}(t_n+s)z(t_n+s)\mathrm{d}s, \\ \dot{z}(t_n+\tau) &= -c\langle\nabla\rangle_c \sin(\tau c\langle\nabla\rangle_c)z(t_n) + \cos(\tau c\langle\nabla\rangle_c)\dot{z}(t_n) - c^2\int_0^\tau \cos\left((\tau-s)c\langle\nabla\rangle_c\right)\mathfrak{n}(t_n+s)z(t_n+s)\mathrm{d}s, \\ \mathfrak{n}(t_n+\tau) &= \cos(\tau\langle\nabla\rangle_0)\mathfrak{n}(t_n) + \tau\frac{\sin(\tau c\langle\nabla\rangle_0)}{\tau\langle\nabla\rangle_0}\dot{\mathfrak{n}}(t_n) - \langle\nabla\rangle_0 \int_0^\tau \sin\left((\tau-s)\langle\nabla\rangle_0\right)|z(t_n+s)|^2\mathrm{d}s, \\ \dot{\mathfrak{n}}(t_n+\tau) &= -\langle\nabla\rangle_0\sin(\tau\langle\nabla\rangle_0)\mathfrak{n}(t_n) + \cos(\tau\langle\nabla\rangle_0)\dot{\mathfrak{n}}(t_n) - \langle\nabla\rangle_0^2\int_0^\tau\cos\left((\tau-s)\langle\nabla\rangle_0\right)|z(t_n+s)|^2\mathrm{d}s. \end{aligned} \tag{4.60}$$

For $n = 0$ we have

$$\begin{aligned} z(t_1) &= \cos(\tau c\langle\nabla\rangle_c) z(0) + \tau \frac{\sin(\tau c\langle\nabla\rangle_c)}{\tau\langle\nabla\rangle_c}\dot{z}(0) - c^2 \int_0^\tau \frac{\sin\left((\tau-s)c\langle\nabla\rangle_c\right)}{c\langle\nabla\rangle_c}\mathfrak{n}(s)z(s)\mathrm{d}s, \\ \dot{z}(t_1) &= -c\langle\nabla\rangle_c \sin(\tau c\langle\nabla\rangle_c)z(0) + \cos(\tau c\langle\nabla\rangle_c)\dot{z}(0) - c^2\int_0^\tau \cos\left((\tau-s)c\langle\nabla\rangle_c\right)\mathfrak{n}(s)z(s)\mathrm{d}s, \\ \mathfrak{n}(t_1) &= \cos(\tau\langle\nabla\rangle_0)\mathfrak{n}(0) + \tau\frac{\sin(\tau c\langle\nabla\rangle_0)}{\tau\langle\nabla\rangle_0}\dot{\mathfrak{n}}(0) - \langle\nabla\rangle_0 \int_0^\tau \sin\left((\tau-s)\langle\nabla\rangle_0\right)|z(s)|^2\mathrm{d}s, \\ \dot{\mathfrak{n}}(t_1) &= -\langle\nabla\rangle_0\sin(\tau\langle\nabla\rangle_0)\mathfrak{n}(0) + \cos(\tau\langle\nabla\rangle_0)\dot{\mathfrak{n}}(0) - \langle\nabla\rangle_0^2\int_0^\tau\cos\left((\tau-s)\langle\nabla\rangle_0\right)|z(s)|^2\mathrm{d}s. \end{aligned} \tag{4.61}$$

For $n \geq 1$ we consider t_{n+1} and t_{n-1} in (4.60) and add the equations, such that we have with $\cos(-x) = \cos(x)$ and $\sin(-x) = -\sin(x)$ that

$$\begin{aligned} z(t_{n+1}) &= -z(t_{n-1}) + 2\cos(\tau c\langle\nabla\rangle_c)z(t_n) \\ &\qquad - c^2\int_0^\tau \frac{\sin\left((\tau-s)c\langle\nabla\rangle_c\right)}{c\langle\nabla\rangle_c}\left(\mathfrak{n}(t_n+s)z(t_n+s) + \mathfrak{n}(t_n-s)z(t_n-s)\right)\mathrm{d}s, \\ \dot{z}(t_{n+1}) &= \dot{z}(t_{n-1}) - 2c\langle\nabla\rangle_c\sin(\tau c\langle\nabla\rangle_c)z(t_n) \\ &\qquad - c^2\int_0^\tau \cos\left((\tau-s)c\langle\nabla\rangle_c\right)\left(\mathfrak{n}(t_n+s)z(t_n+s) + \mathfrak{n}(t_n-s)z(t_n-s)\right)\mathrm{d}s, \\ \mathfrak{n}(t_{n+1}) &= -\mathfrak{n}(t_{n-1}) + 2\cos(\tau\langle\nabla\rangle_0)\mathfrak{n}(t_n) - \langle\nabla\rangle_0\int_0^\tau \sin\left((\tau-s)\langle\nabla\rangle_0\right)\left(|z(t_n+s)|^2 + |z(t_n-s)|^2\right)\mathrm{d}s, \\ \dot{\mathfrak{n}}(t_{n+1}) &= \dot{\mathfrak{n}}(t_{n-1}) - 2\langle\nabla\rangle_0\sin(\tau\langle\nabla\rangle_0)\mathfrak{n}(t_n) - \langle\nabla\rangle_0^2\int_0^\tau\cos\left((\tau-s)\langle\nabla\rangle_0\right)\left(|z(t_n+s)|^2 + |z(t_n-s)|^2\right)\mathrm{d}s. \end{aligned} \tag{4.62}$$

We approximate the integrals in (4.62) and (4.61) as in the previous chapter, so it follows

$$\begin{aligned}
&\int_0^\tau \frac{\sin\left((\tau-s)c\langle\nabla\rangle_c\right)}{c\langle\nabla\rangle_c}\Big(\mathfrak{n}(t_n+s)z(t_n+s)+\mathfrak{n}(t_n-s)z(t_n-s)\Big)\mathrm{d}s \approx 2\frac{1-\cos(\tau c\langle\nabla\rangle_c)}{c^2\langle\nabla\rangle_c^2}\mathfrak{n}(t_n)z(t_n),\\
&\int_0^\tau \cos\left((\tau-s)c\langle\nabla\rangle_c\right)\Big(\mathfrak{n}(t_n+s)z(t_n+s)+\mathfrak{n}(t_n-s)z(t_n-s)\Big)\mathrm{d}s \approx 2\frac{\sin(\tau c\langle\nabla\rangle_c)}{c\langle\nabla\rangle_c}\mathfrak{n}(t_n)z(t_n),\\
&\int_0^\tau \sin\left((\tau-s)\langle\nabla\rangle_0\right)\left(|z(t_n+s)|^2+|z(t_n-s)|^2\right)\mathrm{d}s \approx 2\frac{1-\cos\left(\tau\langle\nabla\rangle_0\right)}{\langle\nabla\rangle_0}|z(t_n)|^2,\\
&\int_0^\tau \cos\left((\tau-s)\langle\nabla\rangle_0\right)\left(|z(t_n+s)|^2+|z(t_n-s)|^2\right)\mathrm{d}s \approx 2\frac{\sin(\tau\langle\nabla\rangle_0)}{\langle\nabla\rangle_0}|z(t_n)|^2.
\end{aligned} \tag{4.63}$$

With the aid of (4.63) we also approximate the integral terms in (4.61). Therefore, as shown in the previous chapters we obtain the following two step iteration scheme for $n=0$

$$\begin{aligned}
z^1 &= \cos(\tau c\langle\nabla\rangle_c)z^0+\tau\frac{\sin(\tau c\langle\nabla\rangle_c)}{\tau\langle\nabla\rangle_c}\dot z^0+c^2\frac{\cos\left(\tau c\langle\nabla\rangle_c\right)-1}{c^2\langle\nabla\rangle_c^2}\mathfrak{n}^0z^0,\\
\dot z^1 &= -c\langle\nabla\rangle_c\sin(\tau c\langle\nabla\rangle_c)z^0+\cos(\tau c\langle\nabla\rangle_c)\dot z^0-c^2\frac{\sin(\tau c\langle\nabla\rangle_c)}{c\langle\nabla\rangle_c}\mathfrak{n}^0z^0,\\
\mathfrak{n}^1 &= \cos(\tau\langle\nabla\rangle_0)\mathfrak{n}^0+\tau\frac{\sin(\tau c\langle\nabla\rangle_0)}{\tau\langle\nabla\rangle_0}\dot{\mathfrak{n}}^0+\left[\cos(\tau\langle\nabla\rangle_0)-1\right]|z^0|^2,\\
\dot{\mathfrak{n}}^1 &= -\langle\nabla\rangle_0\sin(\tau\langle\nabla\rangle_0)\mathfrak{n}^0+\cos(\tau\langle\nabla\rangle_0)\dot{\mathfrak{n}}^0-\langle\nabla\rangle_0\sin(\tau\langle\nabla\rangle_0)|z^0|^2,
\end{aligned}$$

and for $n\ge 1$

$$\begin{aligned}
z^{n+1} &= -z^{n-1}+2\cos(\tau c\langle\nabla\rangle_c)z^n+2c^2\frac{\cos(\tau c\langle\nabla\rangle_c)-1}{c^2\langle\nabla\rangle_c^2}\mathfrak{n}^nz^n,\\
\dot z^{n+1} &= \dot z^{n-1}-2c\langle\nabla\rangle_c\sin(\tau c\langle\nabla\rangle_c)z^n-2c^2\frac{\sin(\tau c\langle\nabla\rangle_c)}{c\langle\nabla\rangle_c}\mathfrak{n}^nz^n,\\
\mathfrak{n}^{n+1} &= -\mathfrak{n}^{n-1}+2\cos(\tau\langle\nabla\rangle_0)\mathfrak{n}^n-2\left[\cos(\tau\langle\nabla\rangle_0)-1\right]|z^n|^2,\\
\dot{\mathfrak{n}}^{n+1} &= \dot{\mathfrak{n}}^{n-1}-2\langle\nabla\rangle_0\sin(\tau\langle\nabla\rangle_0)\mathfrak{n}^n-2\langle\nabla\rangle_0\sin(\tau\langle\nabla\rangle_0)|z^n|^2
\end{aligned}$$

with initial data

$$z^0=z(0),\qquad \dot z^0=\partial_t z(0),\qquad \mathfrak{n}^0=\mathfrak{n}(0),\qquad \dot{\mathfrak{n}}^0=\partial_t\mathfrak{n}(0).$$

We implement the Gautschi-type method in order to obtain a reference solution for our Klein–Gordon–Zakharov system. In Figure 4.4 we plot (double logarithmic) the time step size versus the error in z is measured in a discrete H^1 norm and the error in $\mathfrak{n}$ is measured in a discrete L^2 norm for different values of $c=1,5,10,50,100$. As a reference solution we use the scheme itself with a finer time step size $\tau\approx 10^{-6}$. Figure 4.4 confirms what is shown in Figure 4.1, that Gautschi-type methods suffer from severe time step restriction.

4.5.1.2 A Classical Exponential Integrator for the Klein–Gordon-Zakharov System

Now, we derive a classical exponential integrator for the Klein–Gordon–Zakharov system. For more details on classical exponential integrators we refer to [39]. We recall the first-order system in time in z (cf. (4.6))

$$i\partial_t u=-c\langle\nabla\rangle_c u-\frac{1}{2}c\langle\nabla\rangle_c^{-1}\mathfrak{n}\left(u+\overline{u}\right),\qquad u(0)=z_0-ic\langle\nabla\rangle_c^{-1}z_1$$

with $z=\frac{1}{2}\left(u+\overline{u}\right)$. We apply Duhamel's formula

$$u(t_n+\tau)=\mathrm{e}^{i\tau c\langle\nabla\rangle_c}u(t_n)+\frac{i}{2}c\langle\nabla\rangle_c^{-1}\int_0^\tau \mathrm{e}^{i(\tau-s)c\langle\nabla\rangle_c}\mathfrak{n}(t_n+s)\left(u(t_n+s)+\overline{u}(t_n+s)\right)\mathrm{d}s,$$

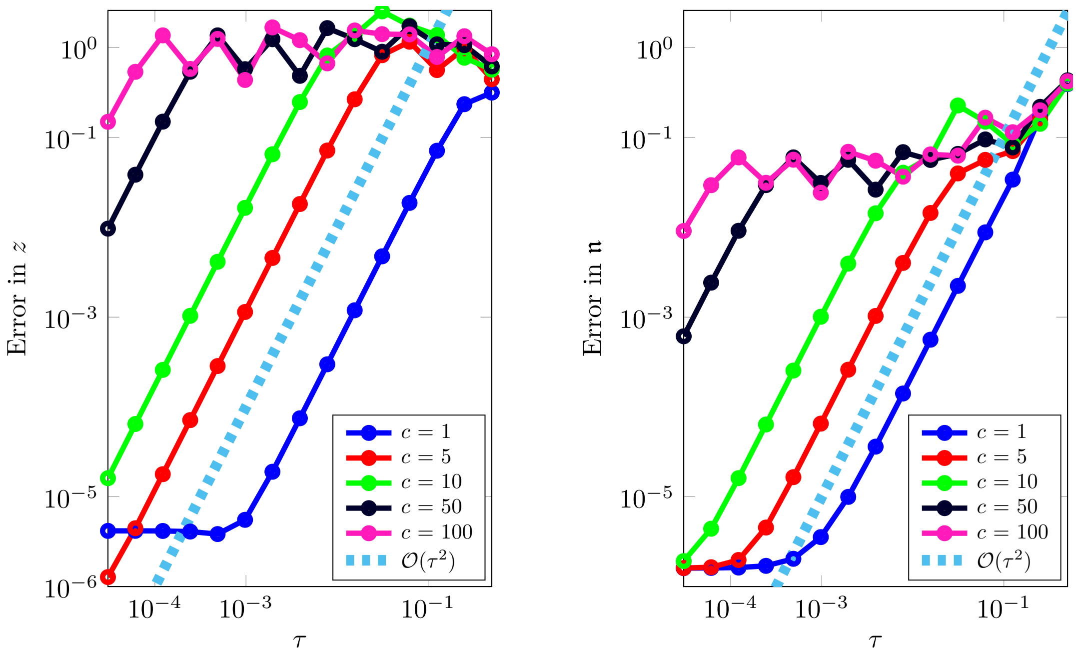

Figure 4.4: Order plot of the Gautschi-type method (double logarithmic scale). Time step size versus the error. The slope of the dashed line is two. Left side error in z, right side error in $\mathfrak{n}$. Reference solution computed via the scheme itself with a finer time step size $\tau \approx 10^{-6}$.

and approximate the integrals in the simplest way, by freezing the values of n and u at $s = 0$

$$u(t_n + \tau) \approx \mathrm{e}^{i\tau c\langle\nabla\rangle_c} u(t_n) + \frac{i}{2} c\langle\nabla\rangle_c^{-1} \mathrm{e}^{i\tau c\langle\nabla\rangle_c} \int_0^\tau \mathrm{e}^{-isc\langle\nabla\rangle_c} \mathrm{d}s\, \mathfrak{n}(t_n)\left(u(t_n) + \overline{u}(t_n)\right).$$

Now, we integrate the remaining exponential function exactly. This yields the following first-order iteration scheme

$$u^{n+1} = \mathrm{e}^{i\tau c\langle\nabla\rangle_c} u^n + \tau \frac{i}{2} c\langle\nabla\rangle_c^{-1} \mathrm{e}^{i\tau c\langle\nabla\rangle_c} \varphi_1\left(-i\tau c\langle\nabla\rangle_c\right) \mathfrak{n}^n \left(u^n + \overline{u^n}\right).$$

For n we use the variation of constants formula for second-order differential equations (see also (4.60)), this yields the following iteration scheme

$$\begin{aligned}
\mathfrak{n}^{n+1} &= \cos(\tau\langle\nabla\rangle_0)\mathfrak{n}^n + \tau \frac{\sin(\tau c\langle\nabla\rangle_0)}{\tau\langle\nabla\rangle_0} \dot{\mathfrak{n}}^n + \frac{1}{4}\left[\cos(\tau\langle\nabla\rangle_0) - 1\right] |u^n + \overline{u^n}|^2, \\
\dot{\mathfrak{n}}^{n+1} &= -\langle\nabla\rangle_0 \sin(\tau\langle\nabla\rangle_0)\mathfrak{n}^n + \cos(\tau\langle\nabla\rangle_0)\dot{\mathfrak{n}}^n - \frac{1}{4}\langle\nabla\rangle_0 \sin(\tau\langle\nabla\rangle_0) |u^n + \overline{u^n}|^2.
\end{aligned}$$

The full integration scheme reads

$$\begin{aligned}
u^{n+1} &= \mathrm{e}^{i\tau c\langle\nabla\rangle_c} u^n + \tau \frac{i}{2} c\langle\nabla\rangle_c^{-1} \mathrm{e}^{i\tau c\langle\nabla\rangle_c} \varphi_1\left(-i\tau c\langle\nabla\rangle_c\right) \mathfrak{n}^n \left(u^n + \overline{u^n}\right), \\
\mathfrak{n}^{n+1} &= \cos(\tau\langle\nabla\rangle_0)\mathfrak{n}^n + \tau \frac{\sin(\tau c\langle\nabla\rangle_0)}{\tau\langle\nabla\rangle_0} \dot{\mathfrak{n}}^n + \frac{1}{4}\left[\cos(\tau\langle\nabla\rangle_0) - 1\right] |u^n + \overline{u^n}|^2, \\
\dot{\mathfrak{n}}^{n+1} &= -\langle\nabla\rangle_0 \sin(\tau\langle\nabla\rangle_0)\mathfrak{n}^n + \cos(\tau\langle\nabla\rangle_0)\dot{\mathfrak{n}}^n - \frac{1}{4}\langle\nabla\rangle_0 \sin(\tau\langle\nabla\rangle_0) |u^n + \overline{u^n}|^2
\end{aligned}$$

with $z = \frac{1}{2}(u + \overline{u})$ and initial values

$$u^0 = z_0 - ic\langle\nabla\rangle_c^{-1}, \qquad \mathfrak{n}^0 = \mathfrak{n}_0, \qquad \dot{\mathfrak{n}}^0 = \mathfrak{n}_1.$$

We implement the first-order exponential integrator in order to obtain a reference solution for our Klein–Gordon–Zakharov system. In Figure 4.5 we plot (double logarithmic) the time step size versus the error in z and $\mathfrak{n}$ is measured in a discrete H^1 and L^2 norm, respectively, for different values of $c = 1, 5, 10, 50, 100, 500$. As a reference solution we use the scheme itself with a finer time step size $\tau \approx 10^{-7}$. In Figure 4.5 we also see the time step restrictions for large values of c.

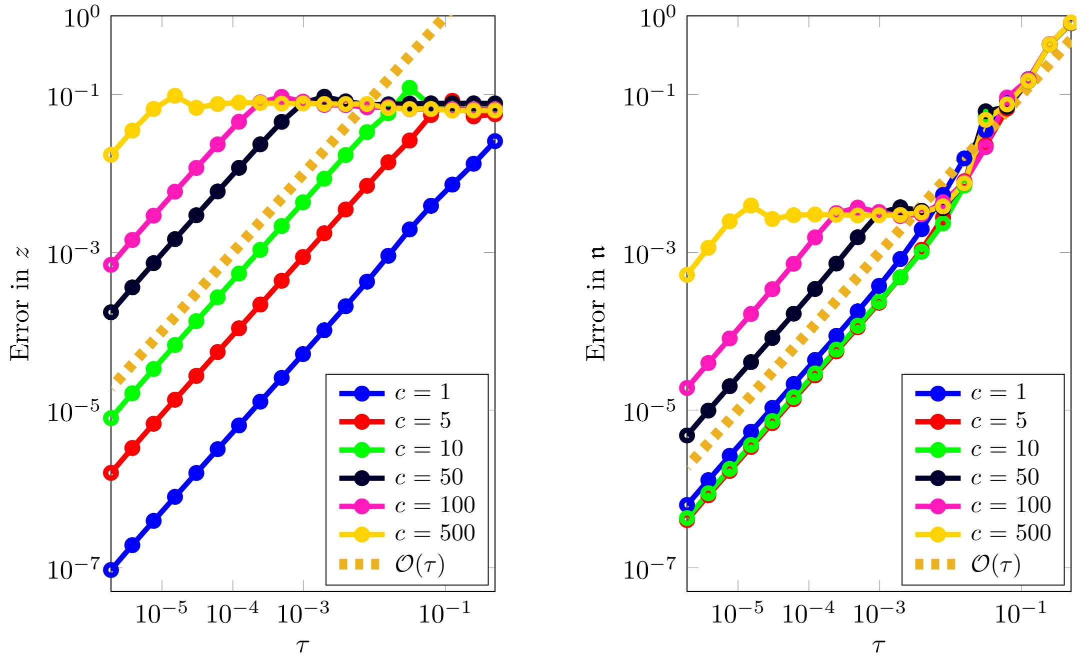

Figure 4.5: Order plot of the first-order exponential integrator (double logarithmic scale). The slope of the dashed line is one. Left side error in z, right side error in $\mathfrak{n}$. Reference solution computed via the scheme itself with a finer time step size $\tau \approx 10^{-7}$.

4.5.2 Numerical Methods for the Limit System

As it is formally shown in Section 4.2 the limit system in the high-plasma frequency case is the classical Zakharov system which reads as follows

$$\begin{aligned} i\partial_t u_\infty(t,x) &= \frac{1}{2}\Delta u_\infty(t,x) - \frac{1}{2}\mathfrak{n}_\infty(t,x)u_\infty(t,x), \\ \partial_{tt}\mathfrak{n}_\infty(t,x) &= \Delta\mathfrak{n}_\infty(t,x) + \frac{1}{2}\Delta|u_\infty(t,x)|^2, \end{aligned} \tag{4.64}$$

where

$$z(t,x) = \frac{1}{2}\left(\mathrm{e}^{ic^2t}u_\infty(t,x) + \mathrm{e}^{-ic^2t}\overline{u_\infty}(t,x)\right) + \mathcal{O}(c^{-2})$$

and the initial values are given by

$$u_\infty(0) = z_0 - iz_1, \qquad \mathfrak{n}_\infty = \mathfrak{n}_0, \qquad \dot{\mathfrak{n}}_\infty = \mathfrak{n}_1.$$

We solve this equation numerically with the ansatz in [37]. Therefore, we rewrite (4.64) with $F_\infty = \partial_t u_\infty$

as follows

$$\begin{aligned} iF_\infty &= \frac{1}{2}\Delta u_\infty - \frac{1}{2}\mathfrak{n}_\infty u_\infty, \\ \partial_{tt}\mathfrak{n}_\infty &= \Delta\mathfrak{n}_\infty + \frac{1}{2}\Delta|u_\infty|^2, \\ (1-\tfrac{1}{2}\Delta)u_\infty &= -iF_\infty - (\tfrac{1}{2}\mathfrak{n}_\infty - 1)I_{F_\infty}, \end{aligned} \tag{4.65}$$

where

$$I_{F_\infty}(t) = u_\infty(0) + \int_0^t F_\infty(s)\mathrm{d}s.$$

We differentiate the first equation of (4.65) with respect to t and obtain

$$\partial_t F_\infty = -\frac{i}{2}\Delta F_\infty + \frac{i}{2}\left(u_\infty\partial_t\mathfrak{n}_\infty + \mathfrak{n}_\infty F_\infty\right).$$

With Duhamel's formula we have for F_∞

$$\begin{aligned} F_\infty(t_n+\tau) &= \mathrm{e}^{-\frac{i}{2}\tau\Delta}F_\infty(t_n) + \frac{i}{2}\int_0^\tau \mathrm{e}^{-\frac{i}{2}(\tau-s)\Delta}\left(u_\infty(t_n+s)\dot{\mathfrak{n}}_\infty(t_n+s) + \mathfrak{n}_\infty(t_n+s)F_\infty(t_n+s)\right)\mathrm{d}s \\ &= \mathrm{e}^{-\frac{i}{2}\tau\Delta}F_\infty(t_n) + \tau\frac{i}{2}\mathrm{e}^{-\frac{i}{2}\tau\Delta}\varphi_1\left(\frac{i}{2}\tau\Delta\right)\left(u_\infty(t_n)\dot{\mathfrak{n}}_\infty(t_n) + \mathfrak{n}_\infty(t_n)F_\infty(t_n)\right) + R(\tau,t_n), \end{aligned}$$

where the remainder is of order $\mathcal{O}(\tau^2)$. For $\mathfrak{n}_\infty$ we have

$$\begin{aligned} \mathfrak{n}_\infty(t_n+\tau) &= \cos(\tau\langle\nabla\rangle_0)\mathfrak{n}_\infty(t_n) + \tau\mathrm{sinc}(\tau\langle\nabla\rangle_0)\dot{\mathfrak{n}}_\infty(t_n) + \frac{\tau}{2}\frac{1-\cos(\tau\langle\nabla\rangle_0)}{\tau\langle\nabla\rangle_0}\Delta|u_\infty(t_n)|^2 + R(\tau,t_n) \\ &= \cos(\tau\langle\nabla\rangle_0)\mathfrak{n}_\infty(t_n) + \tau\mathrm{sinc}(\tau\langle\nabla\rangle_0)\dot{\mathfrak{n}}_\infty(t_n) + \frac{1}{2}(\cos(\tau\langle\nabla\rangle_0)-1)|u_\infty(t_n)|^2 + R(\tau,t_n), \\ \dot{\mathfrak{n}}_\infty(t_n+\tau) &= -\langle\nabla\rangle_0\sin(\tau\langle\nabla\rangle_0)\mathfrak{n}_\infty(t_n) + \cos(\tau\langle\nabla\rangle_0)\dot{\mathfrak{n}}_\infty(t_n) + \frac{\tau}{2}\mathrm{sinc}(\tau\langle\nabla\rangle_0)\Delta|u_\infty(t_n)|^2 + R(\tau,t_n). \end{aligned}$$

We approximate I_{F_∞} as follows

$$I_{F_\infty}(t_n+\tau) \approx S_{F_\infty}(t_n+\tau) = u_\infty(0) + \tau\sum_{k=0}^n F_\infty(t_k).$$

With S_{F_∞} we have for u_∞

$$u_\infty(t_n+\tau) = \left(1-\tfrac{1}{2}\Delta\right)^{-1}\left[-iF_\infty(t_n+\tau) - \left(\tfrac{1}{2}\mathfrak{n}_\infty(t_n+\tau)-1\right)S_{F_\infty}(t_n+\tau)\right].$$

Thus, we obtain the following iteration scheme

$$\begin{aligned} F_\infty^{n+1} &= \mathrm{e}^{-\frac{i}{2}\tau\Delta}F_\infty^n + \tau\frac{i}{2}\mathrm{e}^{-\frac{i}{2}\tau\Delta}\varphi_1\left(\frac{i}{2}\tau\Delta\right)\left(u_\infty^n\dot{\mathfrak{n}}_\infty^n + \mathfrak{n}_\infty^n F_\infty^n\right), \\ \mathfrak{n}_\infty^{n+1} &= \cos(\tau\langle\nabla\rangle_0)\mathfrak{n}_\infty^n + \tau\mathrm{sinc}(\tau\langle\nabla\rangle_0)\dot{\mathfrak{n}}_\infty^n + \frac{1}{2}(\cos(\tau\langle\nabla\rangle_0)-1)|u_\infty^n|^2, \\ \dot{\mathfrak{n}}_\infty^{n+1} &= -\langle\nabla\rangle_0\sin(\tau\langle\nabla\rangle_0)\mathfrak{n}_\infty^n + \cos(\tau\langle\nabla\rangle_0)\dot{\mathfrak{n}}_\infty^n + \frac{\tau}{2}\mathrm{sinc}(\tau\langle\nabla\rangle_0)\Delta|u_\infty^n|^2, \\ S_{F_\infty}^{n+1} &= S_{F_\infty}^n + \tau F_\infty^{n+1}, \\ u_\infty^{n+1} &= \left(1-\tfrac{1}{2}\Delta\right)^{-1}\left[-iF_\infty^{n+1} - \left(\tfrac{1}{2}\mathfrak{n}_\infty^{n+1}-1\right)S_{F_\infty}^{n+1}\right], \\ z^{n+1} &= \frac{1}{2}\left(\mathrm{e}^{ic^2t_{n+1}}u^{n+1} + \mathrm{e}^{-ic^2t_{n+1}}\overline{u^{n+1}}\right) \end{aligned}$$

with initial values

$$u_\infty(0) = z_0 - iz_1, \qquad \mathfrak{n}_\infty(0) = \mathfrak{n}_0, \qquad \dot{\mathfrak{n}}_\infty(0) = \mathfrak{n}_1,$$
$$F_\infty(0) = -\frac{i}{2}\Delta u_\infty(0) + \frac{i}{2}\mathfrak{n}_\infty(0)u_\infty(0),$$
$$S_{F_\infty}(0) = u_\infty(0) + \tau F_\infty(0).$$

In Figure 4.6 we numerically confirm the convergence order in time of our first-order integration method for our Zakharov limit system. In the figure we plot time step size versus the error of the limit method. The error in z_∞ is measured in a discrete H^1 norm and in $\mathfrak{n}_\infty$ in a discrete L^2 norm. As a reference solution we use the scheme itself with a finer time step size $\tau \approx 10^{-7}$.

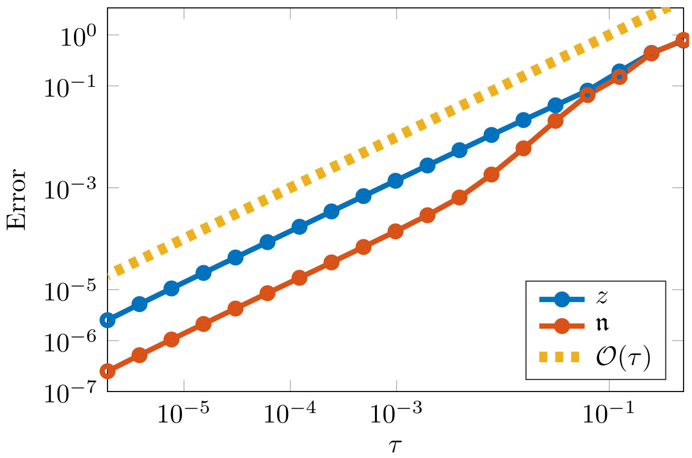

Figure 4.6: Order plot of the first-order limit method (double logarithmic scale). The slope of the yellow dashed line is one. Reference solution computed via the scheme itself with a finer time step size $\tau \approx 10^{-7}$.

4.5.3 Uniformly Accurate Method for the Klein–Gordon–Zakharov System

We recall the uniformly accurate oscialltory integrator (4.29)

$$\begin{aligned}
(c\langle\nabla\rangle_c)^{-1}F^{n+1} &= \mathrm{e}^{i\tau c\langle\nabla\rangle_c}(c\langle\nabla\rangle_c)^{-1}F^n + i\frac{\tau}{2}\langle\nabla\rangle_c^{-2}\mathrm{e}^{i\tau c\langle\nabla\rangle_c}\varphi_1\left(\tfrac{i}{2}\tau\Delta\right)\left(\dot{\mathfrak{n}}^n u^n + i\mathfrak{n}^n c\langle\nabla\rangle_c u^n\right)\\
&\quad + i\frac{\tau}{2}\langle\nabla\rangle_c^{-2}\mathrm{e}^{i\tau c\langle\nabla\rangle_c}\varphi_1\left(-i\tau(c\langle\nabla\rangle_c + c^2)\right)\left(\dot{\mathfrak{n}}^n\overline{u}^n - i\mathfrak{n}^n c\langle\nabla\rangle_c\overline{u}^n\right),\\
\mathfrak{n}^{n+1} &= \cos\left(\tau\langle\nabla\rangle_0\right)\mathfrak{n}^n + \langle\nabla\rangle_0^{-1}\sin\left(\tau\langle\nabla\rangle_0\right)\dot{\mathfrak{n}}^n\\
&\quad + \frac{\tau^2}{4}\mathrm{sinc}\left(\tau\langle\nabla\rangle_0\right)\Delta\left\{|u^n|^2 + \varphi_2(2ic^2\tau)(u^n)^2 + \varphi_2(-2ic^2\tau)\overline{u^n}^2\right\},\\
\dot{\mathfrak{n}}^{n+1} &= -\langle\nabla\rangle_0\sin\left(\tau\langle\nabla\rangle_0\right)\mathfrak{n}^n + \cos\left(\tau\langle\nabla\rangle_0\right)\dot{\mathfrak{n}}^n\\
&\quad + \frac{\tau}{4}\cos\left(\tau\langle\nabla\rangle_0\right)\Delta\left\{2|u^n|^2 + \varphi_1(2ic^2\tau)(u^n)^2 + \varphi_1(-2ic^2\tau)\overline{u^n}^2\right\},\\
S_F^{n+1} &= S_F^n + \tau\varphi_1(i\tau c\langle\nabla\rangle_c)F^{n+1},\\
u^{n+1} &= c^{-1}\langle\nabla\rangle_c^{-1}\left\{-iF^{n+1} - \frac{1}{2}c\langle\nabla\rangle_c^{-1}\mathfrak{n}^{n+1}\left(S_F^{n+1} + \overline{S_F^{n+1}}\right)\right\}
\end{aligned}$$

with $z^{n+1} = \frac{1}{2}(u^{n+1} + \overline{u^{n+1}})$ and initial values

$$u^0 = z_0 - ic\langle\nabla\rangle_c^{-1} z_1, \qquad \mathfrak{n}^0 = \mathfrak{n}_0, \qquad \dot{\mathfrak{n}}^0 = \mathfrak{n}_1,$$
$$F^0 = ic\langle\nabla\rangle_c u^0 + \frac{i}{2} c\langle\nabla\rangle_c^{-1}\, \mathfrak{n}^0(u^0 + \overline{u^0}),$$
$$S_F^0 = u^0 + \tau\varphi_1(i\tau c\langle\nabla\rangle_c)F^0.$$

In Figure 4.7 we numerically confirm the convergence order in time of our first-order uniformly accurate method. In the figure we plot time step size versus the error of our uniformly accurate schemes for different values of $c = 1, 5, 10, 50, 100, 500, 1000, 5000, 10000$. The error in z is measured in a discrete H^1 norm, the error in $\mathfrak{n}$ is measured in a discrete L^2 norm. As a reference solution we use the scheme itself with a finer time step size $\tau \approx 10^{-7}$.

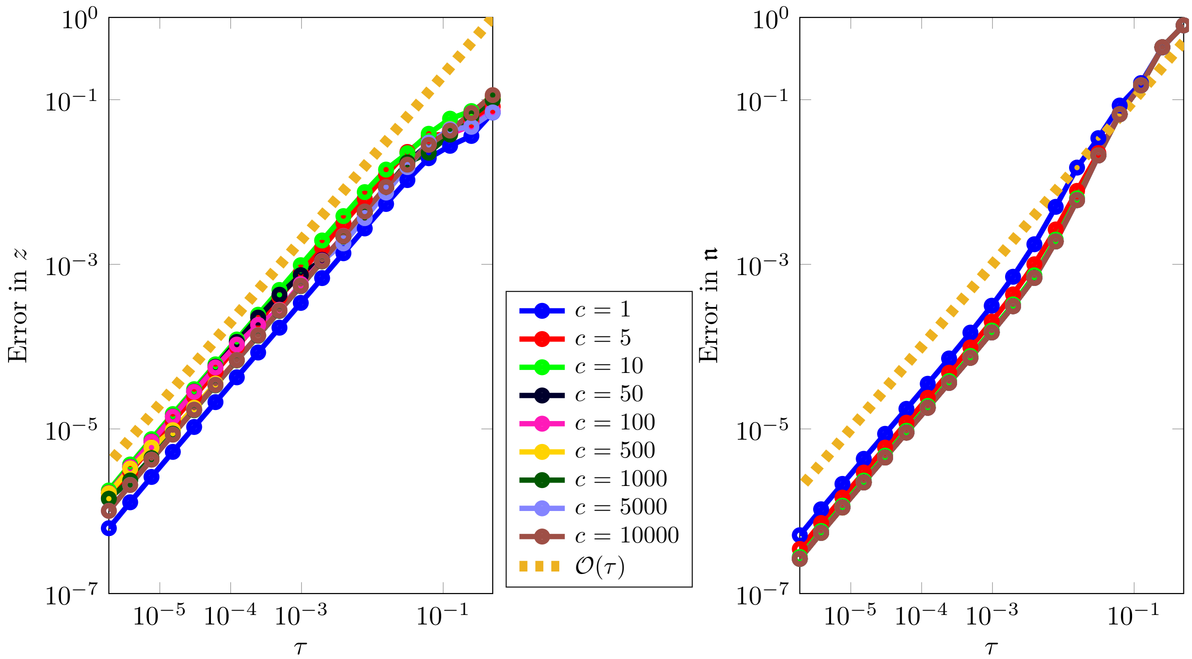

Figure 4.7: Order plot of the first-order uniformly accurate method (double logarithmic scale). The slope of the dashed line is one. Left side error in z, right side error in $\mathfrak{n}$. Reference solution computed via the scheme itself with a finer time step size $\tau \approx 10^{-7}$.

4.5.4 Comparison of the Numerical Methods

In this subsection we compare our uniformly accurate methods with the established Gautschi-type method, exponential integrator and limit scheme. We confirm that our newly derived uniformly accurate methods are uniformly accurate with respect to c and that they converge asymptotically to the corresponding limit scheme. Finally, we consider work-precision plots and compare the error constants.

We start by comparing our newly derived uniformly accurate first-order method with the first-order exponential integrator. This comparison (see Figure 4.8) confirms that our UA methods are uniformly accurate with respect to c. We use the first-order exponential integrator in order to compute the reference solution with time step size $\tau \approx 10^{-7}$ for different values of $c = 1, 5, 10, 50, 100$. The error between the

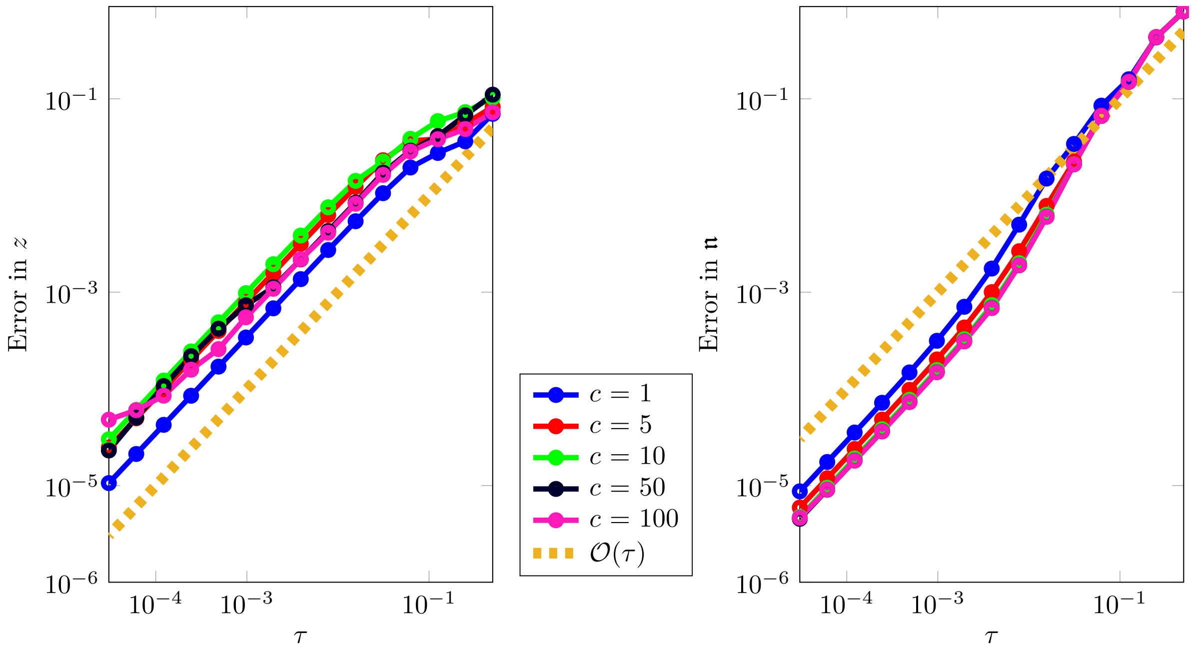

Figure 4.8: Order plot of the first-order uniformly accurate method (double logarithmic scale). Error in z on the left, error in $\mathfrak{n}$ on the right. The slope of the dashed line is one. The reference solution is computed via the classical exponential integrator with a finer time step size. Reference solution computed via the classical exponential integrator with a finer time step size $\tau \approx 10^{-7}$.

exponential integrator and our uniformly accurate methods is measured in z in a discrete H^1 norm and in $\mathfrak{n}$ in a discrete L^2 norm.

In the next Figure 4.9 we confirm the asymptotic convergence to the corresponding numerical methods for the limit system. We plot the error of the UA method and the limit method versus different values of c. This yields the $\mathcal{O}(c^{-2})$ convergence, which is shown in Section 4.4.3. The error in z is measured in a discrete H^1 norm and in $\mathfrak{n}$ in a discrete L^2 norm.

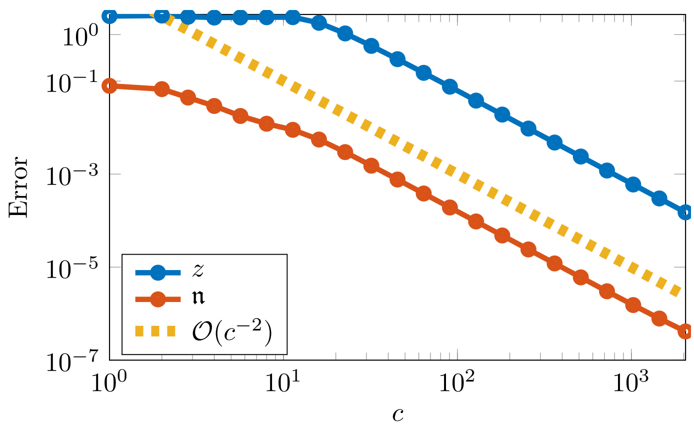

Figure 4.9: Asymptotic consistency plot (double logarithmic scale). Left side error of the first-order UA method, right side error of the second-order UA method. The slope of the dashed line is -2.

Now, we use the following initial values

$$z(0) = \frac{\cos(x)\sin(x)}{2-\cos(x)}, \qquad \partial_t z(0) = c^2 \frac{\sin(x)^2}{2-\cos(x)},$$
$$\mathfrak{n}(0) = \frac{\sin(x)\cos(2x)}{2-\sin(2x)^2}, \qquad \partial_t \mathfrak{n}(0) = \frac{\sin(x)}{2-\cos(2x)^2}.$$

Next, we compare the error of the different methods versus the computation time (see Figure 4.10). The work-precision plots show the efficiency of the numerical methods for different values of c. We plot the corresponding error against the computation time (in seconds) of the corresponding numerical method. We desire values in the lower left corner, i.e., a small error and a short computation time. For the reference solution we use the exponential integrator with time step size $\tau \approx 10^{-7}$. We compare the solution of the exponential integrator with the Gautschi-type method, our uniformly accurate methods and with the limit scheme. We only show here the plots of z, where the error in z is measured in a discrete H^1 norm. For $\mathfrak{n}$ we obtain similar plots.

We observe that the Gautschi-type method performs well for small c and fails for large c. For the limit scheme we observe this behavior vice versa, i.e., the limit scheme fails for small c and performs good for large c. Our uniformly accurate schemes show a good behavior for all values of c. For $c = 1$ the Gautschi-type method performs better than the UA methods and for the largest value of c the limit scheme performs best. But our uniformly accurate schemes obtain smaller errors than both, the Gautschi-type method and the limit scheme.

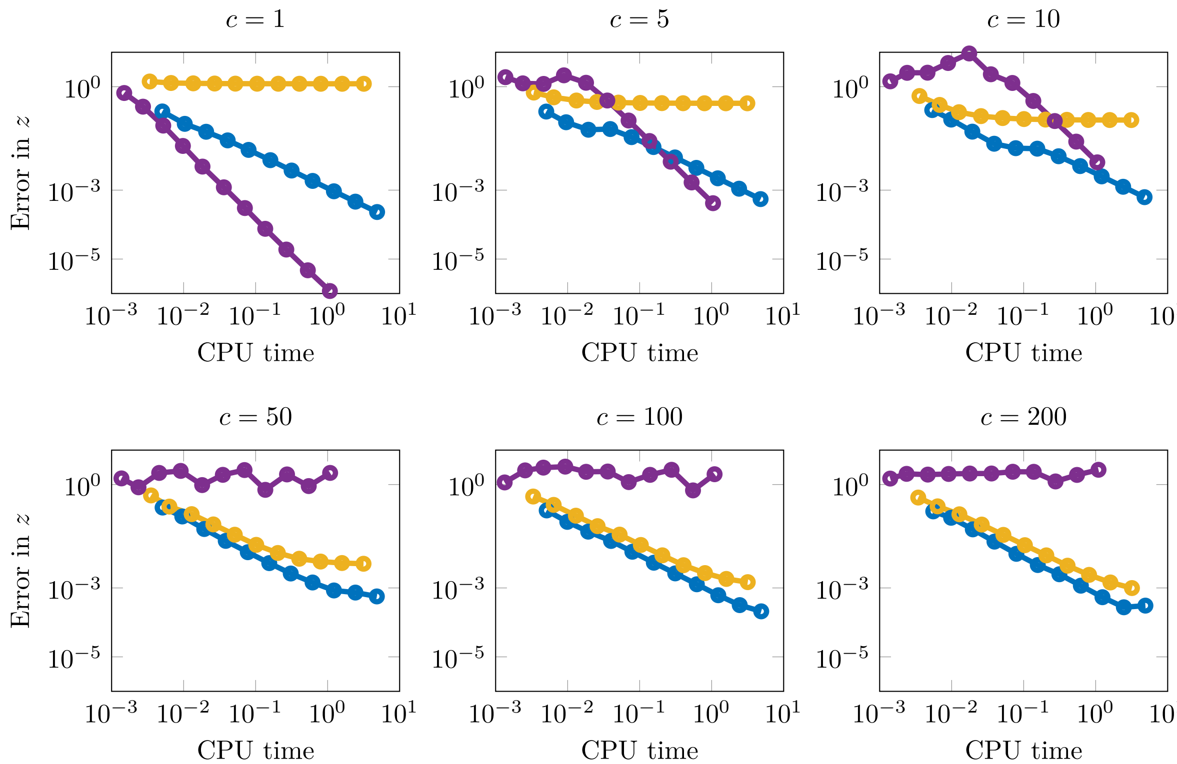

Figure 4.10: Work-precision plot (double logarithmic scale). The purple lines mark the error of the Gautschi-type method. The yellow lines mark the error of the limit method. The blue lines mark the error of our first-order uniformly accurate method. The CPU time is measured in seconds. Reference solution computed via the classical exponential integrator with a finer time step size $\tau \approx 10^{-7}$.

We underline the different error constant behaviors of our UA methods in z. Therefore, we plot the numerical error of the corresponding numerical method against different values of c for different time step sizes τ. In comparison, we also plot the error of the Gautschi-type method against different values of c. For the reference solution we use the exponential integrator with time step size $\tau \approx 10^{-6}$.
For our uniformly accurate methods we observe uniformly bounds, whereas for the Gautschi-type method we obtain the typical $\mathcal{O}(c^4)$ error (see Figure 4.11). In the plots of the uniformly accurate methods the error of the exponential integrator of order $\mathcal{O}(c^2)$ is obtained for large values of c.

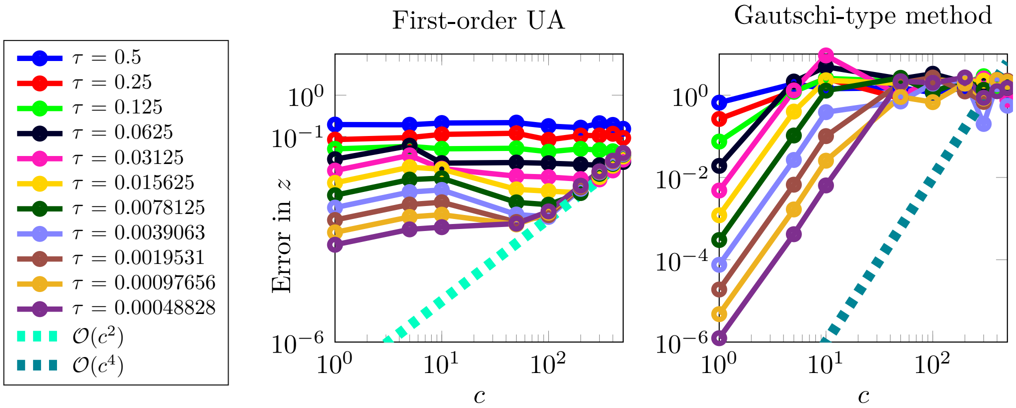

Figure 4.11: Error constant comparison plot (double logarithmic scale). On the left for the first-order uniformly accurate method and on the right for the Gautschi-type method. The slope of the dashed line is two on the left and four on the right. Reference solution computed via the classical exponential integrator with a finer time step size $\tau \approx 10^{-6}$.

CHAPTER 5

Conclusion and Outlook

This thesis presents a new class of uniformly accurate time integration schemes for Klein–Gordon type equations, which are efficient and unconditionally stable in the slowly varying relativistic as well as in the highly oscillatory non-relativistic limit regime. The theory of this work covers the construction of these schemes for the Klein–Gordon equation, the Klein–Gordon–Schrödinger system and the Klein–Gordon–Zakharov system and can be extended to related Klein–Gordon type equations (see [45]).

The non-relativistic limit regime of Klein–Gordon type equations is numerically challenging due to the highly oscillatory behavior of the solution. In order to resolve the oscillations numerically standard methods suffer from severe time step restrictions and so they only work well for small values of c and fail for large values of c. In order to underline the failure of classical schemes we derived a Gautschi-type method for several Klein–Gordon type equations (based on [9]) and numerically observed its failure to resolve the highly oscillatory behavior of the solution for $c \gg 1$. Furthermore, we constructed a classical exponential integrator based on [39] for which we also observed its failure for large $c \gg 1$.

Recently, a new approach was invented based on an asymptotic expansion ansatz (see [26]). Following this approach we formally derived the limit systems of different Klein–Gordon type equations and determined efficient and stable numerical methods to approximate the limit solution. This ansatz allows us to reduce the highly oscillatory equation to a non-oscillatory limit system. Unfortunately, this ansatz only works for large values of c, but fails for small c. We also observed this behavior in our numerical experiments.

The main contribution of this thesis is the development of a novel class of uniformly accurate methods for Klein–Gordon type equations. For the derivation and analysis of the different uniformly accurate schemes we followed the ansatz and procedure of [13] for the Klein–Gordon equation and Klein–Gordon–Schrödinger system. For the derivation of a uniformly accurate method for the Klein–Gordon–Zakharov system in the high-plasma frequency case we followed the ansatz of [37]. For all uniformly accurate methods we obtained error bounds of order $\mathcal{O}(\tau)$ and $\mathcal{O}(\tau^2)$ independent of c, for the first- and second-order schemes, respectively. We received good numerical results for the solution of Klein–Gordon type equations for all $c \geq 1$.

In this thesis we focused on the time discretization of the numerical schemes. In combination with Fourier pseudospectral methods for the space discretization we observed that due to the very accurate approximation behavior of the Fourier pseudospectral method, the numerical space approximation error is negligible compared to the error of the time integration (see Figure 5.1 for the Klein–Gordon equation).

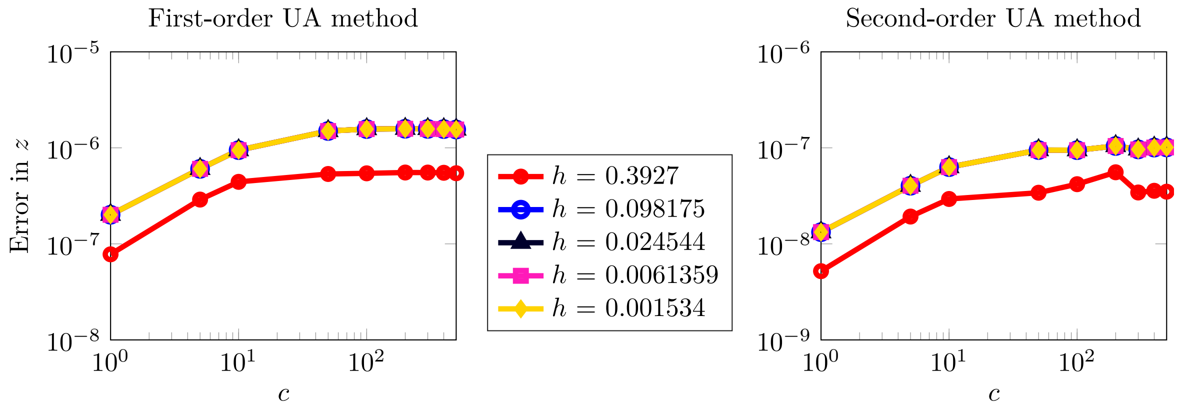

Figure 5.1: Error constant comparison plot for different values of the spatial discretization mesh-size h (double logarithmic scale). Klein–Gordon equation solved via the first- and second-order UA method. Left side first-order, right side second-order method. Reference solution computed via the scheme itself with a finer time step size $\tau \approx 10^{-6}$.

In the previous chapters we focus on Klein–Gordon type equations where the oscillatory behavior arises from the Klein–Gordon part of the differential equation. In the following we underline the challenge for the Klein–Gordon–Zakharov system in the case when the wave part becomes oscillatory.

Uniformly accurate methods for the Klein–Gordon–Zakharov system in the subsonic limit regime and also in the simultaneous limit regimes remain an open problem. For more details on the subsonic limit regime see [5, 6, 56] and on the simultaneous limit regimes we refer to [9, 54, 56]. The Klein–Gordon–Zakharov system with a parameter $\alpha \geq 1$ in the wave part reads

$$\begin{aligned} c^{-2}\partial_{tt}z(t,x) - \Delta z(t,x) + c^2 z(t,x) &= -\mathfrak{n}(t,x)z(t,x), \\ \alpha^{-2}\partial_{tt}\mathfrak{n}(t,x) - \Delta\mathfrak{n}(t,x) &= \Delta|z(t,x)|^2 \end{aligned}$$

with initial values

$$\begin{aligned} z(0,x) &= z_0(x), \quad \partial_t z(0,x) = c^2 z_1(x), \\ \mathfrak{n}(0,x) &= \mathfrak{n}_0(x), \quad \partial_t \mathfrak{n}(0,x) = \alpha\mathfrak{n}_1(x). \end{aligned}$$

Similarly to the previous chapters classical numerical methods break down in the subsonic ($\alpha \gg 1$) and simultaneous limit regimes ($c \gg 1$ and $\alpha \gg 1$) as they fail to resolve the oscillations within the solution. We underline this phenomenon in Figure 5.2 for the subsonic regime. We obtain similar plots for the simultaneous limit regimes.

In the following we explain why our presented technique in this thesis does not apply to the Klein–Gordon–Zakharov system in the subsonic limit regime.

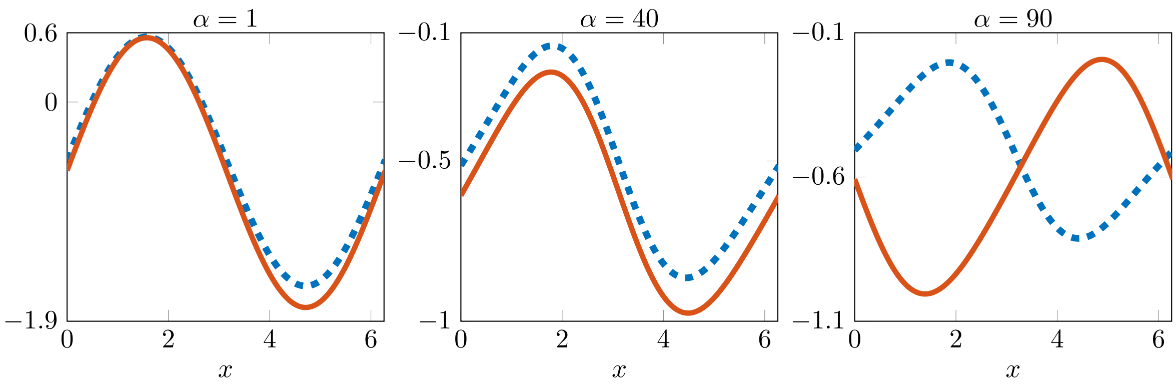

Figure 5.2: Numerical solution of the Klein–Gordon–Zakharov system for $\mathfrak{n}$. Exponential Gautschi-type scheme (red solid line) for different α with time step size $\tau \approx 10^{-2}$ at time $t = 0.2$ and with fixed $c = 1$. The blue dashed line represents the reference solution at time $t = 0.2$, computed via the same exponential Gautschi-type scheme with a smaller time step size $\tau \approx 10^{-6}$. The spatial discretization is done via a Fourier pseudospectral method with mesh-size $h = 0.0245$.

Setting $c = 1$, the first-order system in time of the corresponding Klein–Gordon–Zakharov system (4.6) reads

$$
\begin{aligned}
i\partial_t u &= -\langle\nabla\rangle_1 u - \tfrac{1}{2}\langle\nabla\rangle_1^{-1}\Re\left(\mathfrak{h}\right)\left(u+\overline{v}\right),\\
i\partial_t v &= -\langle\nabla\rangle_1 v - \tfrac{1}{2}\langle\nabla\rangle_1^{-1}\Re\left(\mathfrak{h}\right)\left(v+\overline{u}\right),\\
i\partial_t \mathfrak{h} &= -\alpha\langle\nabla\rangle_0\mathfrak{h} - \tfrac{1}{4}\alpha\langle\nabla\rangle_0|u+\overline{v}|^2
\end{aligned}
$$

with $z = \frac{1}{2}\left(u+\overline{v}\right)$ and $\mathfrak{n} = \Re(\mathfrak{h})$. The *twisted variable* ansatz in $\mathfrak{h}$ reads

$$
\mathfrak{h}_*(t) = \mathrm{e}^{-i\alpha\langle\nabla\rangle_0 t}\mathfrak{h}(t).
$$

We differentiate $\mathfrak{h}_*$ with respect to t and obtain

$$
\begin{aligned}
i\partial_t\mathfrak{h}_* = i\partial_t\left(\mathrm{e}^{-i\alpha\langle\nabla\rangle_0 t}\mathfrak{h}\right) &= -i^2\alpha\langle\nabla\rangle_0\mathrm{e}^{-i\alpha\langle\nabla\rangle_0 t}\mathfrak{h} + \mathrm{e}^{-i\alpha\langle\nabla\rangle_0 t} i\partial_t\mathfrak{h}\\
&= \alpha\langle\nabla\rangle_0\mathrm{e}^{-i\alpha\langle\nabla\rangle_0 t}\mathfrak{h} + \mathrm{e}^{-i\alpha\langle\nabla\rangle_0 t}\Big(-\alpha\langle\nabla\rangle_0\mathfrak{h} - \tfrac{1}{4}\alpha\langle\nabla\rangle_0|u_* + \overline{v_*}|^2\Big)\\
&= -\frac{1}{4}\alpha\langle\nabla\rangle_0\left|u_* + \overline{v_*}\right|^2.
\end{aligned}
$$

In the previous chapters the advantage of considering the twisted system in (u_*, v_*) in the case of the Klein–Gordon equation and Klein–Gordon–Schrödinger system was the fact that the leading operator formally is of order $\mathcal{O}(1)$ in c. But here the leading operator reads $\alpha\langle\nabla\rangle_0$, which is not independent of α nor of order $\mathcal{O}(1)$ in α. The same problem occurs if we consider the simultaneous limit regimes, i.e., $c \gg 1$ and $\alpha \gg 1$. Uniformly accurate methods for all highly oscillatory regimes hence remain an interesting future research problem.

Bibliography

[1] R. A. Adams and J. J. F. Fournier. *Sobolev Spaces*. Elsevier/Academic Press, second edition, 2003.

[2] V. M. Alekseev. An estimate for the perturbations of the solutions of ordinary differential equations. *Vestnik Moskov. Univ. Ser. I Mat. Meh.*, 2:28–36, 1961.

[3] T. Arens, F. Hettlich, C. Karpfinger, U. Kockelkorn, K. Lichtenegger, and H. Stachel. *Mathematik*. Springer-Verlag, third edition, 2015.

[4] W. Bao and X. Dong. Analysis and comparison of numerical methods for the Klein–Gordon equation in the non-relativistic limit regime. *Numer. Math.*, 120:189–229, 2012.

[5] W. Bao and C. Su. Uniform error bounds of a finite difference method for the Klein–Gordon–Zakharov system in the subsonic limit regime. *Math. Comp.*, to appear, 2018. URL `https://arxiv.org/pdf/1612.09404.pdf`.

[6] W. Bao and C. Su. Uniformly and optimally accurate methods for the Zakharov system in the subsonic limit regime. *SIAM J. Sci. Comput.*, 40:A929–A953, 2018.

[7] W. Bao and L. Yang. Efficient and accurate numerical methods for the Klein–Gordon–Schrödinger equations. *J. Comput. Phys.*, 225:1863–1893, 2007.

[8] W. Bao and X. Zhao. A uniformly accurate (UA) multiscale time integrator Fourier pseoduspectral method for the Klein–Gordon–Schrödinger equations in the nonrelativistic limit regime. *Numer. Math.*, 135:833–873, 2017.

[9] W. Bao, X. Dong, and X. Zhao. An exponential wave integrator pseudospectral method for the Klein–Gordon–Zakharov system. *SIAM J. Sci. Comput.*, 35:A2903–A2927, 2013.

[10] W. Bao, Y. Cai, and X. Zhao. A uniformly accurate multiscale time integrator pseudospectral method for the Klein–Gordon equation in the nonrelativistic limit regime. *SIAM J. Numer. Anal.*, 52:2488–2511, 2014.

[11] W. Bao, X. Dong, and X. Zhao. Uniformly accurate multiscale time integrators for highly oscillatory second order differential equations. *J. Math. Study*, 47:111–150, 2014.

[12] S. Baumstark and K. Schratz. Uniformly accurate oscillatory integrators for the klein-gordon-zakharov system from low- to high-plasma frequency regimes. submitted, 2018. URL `https://arxiv.org/abs/1803.09126`.

[13] S. Baumstark, E. Faou, and K. Schratz. Uniformyl accurate exponential–type integrators for Klein–Gordon equations with asymptotic convergence to the classical NLS splitting. *Math. Comp.*, 87:1227–1254, 2018.

[14] S. Baumstark, G. Kokkala, and K. Schratz. Asymptotic consistent exponential–type integrators for Klein–Gordon–Schrödinger systems from relativistic to non–relativistic regimes. *ETNA*, 48:63–80, 2018.

[15] L. Berge, B. Bidegaray, and T. Colin. A perturbative analysis of the time–envelope approximation in strong Langmuir turbulence. *Physica D*, 95:351–379, 1996.

[16] J. Bourgain. Fourier transform restriction phenomena for certain lattice subsets and applications to nonlinear evolution equations. Part i: Schrödinger equations. *Geom. Funct. Anal.*, 3:107–156, 1993.

[17] J. Bourgain. Fourier transform restriction phenomena for certain lattice subsets and applications to nonlinear evolution equations. Part ii: The KdV-equation. *Geom. Funct. Anal.*, 3:209–262, 1993.

[18] P. Chartier, N. Crouseilles, M. Lemou, and F. Méhats. Uniformly accurate numerical schemes for highly oscillatory Klein–Gordon and nonlinear Schrödingier equations. *Numer. Math.*, 129:211–250, 2015.

[19] D. Cohen, E. Hairer, and C. Lubich. Modulated fourier expansions of highly oscillatory differential equations. *Foundations of Comput. Math.*, 3:327–345, 2003.

[20] D. Cohen, E. Hairer, and C. Lubich. Long-time analysis of nonlinearly perturbed wave equations via modulated Fourier expansions. *Arch. Ration. Mech. Anal.*, 187:341–368, 2008.

[21] T. Colin, G. Ebrard, G. Gallice, and B. Texier. Justification of the Zakharov model from Klein–Gordon–wave systems. *Comm. Partial Differential Equations*, 29(9-10):1365–1401, 2004.

[22] J. Crank and Nicolson. A practical method for numerical evaluation of solutions of partial differential equations of the heat–conduction type. *Advances in Computational Mathematics*, 6:207–226, 1996.

[23] M. Daub, G. Schneider, and K. Schratz. From the Klein–Gordon–Zakharov system to the Klein–Gordon equation. *Math. Methods Appl. Sci.*, 39:5371–5380, 2016.

[24] B. Engquist, A. Fokas, E. Hairer, and A. Iserles. *Highly Oscillatory Problems.* Cambridge University Press, 2009.

[25] E. Faou. *Geometric numerical integration and Schrödinger equations.* European Math. Soc., 2012.

[26] E. Faou and K. Schratz. Asymptotic preserving schemes for the Klein–Gordon equation in the non–relativistic limit regime. *Numer. Math.*, 126:441–469, 2014.

[27] B. Fornberg. *A practical guide o pseudospectral methods.* Cambridge University Press, 1996.

[28] I. Fukuda and M. Tsutsumi. On the Yukawa–coupled Klein–Gordon–Schrödinger equations in three space dimensions. *Prof. Jpn. Acad.*, 51:402–405, 1975.

[29] I. Fukuda and M. Tsutsumi. On coupled Klein–Gordon–Schrödinger equations II. *J. Math. Anal. Appl.*, 66:358–378, 1978.

[30] I. Fukuda and M. Tsutsumi. On coupled Klein–Gordon–Schrödinger equations III. *Math. Jpn.*, 24:358–378, 1979.

[31] L. Gauckler. Error analysis of trigonometric integrators for seimilinear wave equations. *SIAM J. Numer. Anal.*, 53: 1082–1106, 2015.

[32] W. Gautschi. Numerical integration of ordinary differential equations based on trigonometric polynomials. *Numer. Math.*, 3:381–397, 1961.

[33] M. Gubinelli. Rough solutions for the periodic Korteweg–de Vries equation. *Comm. Pure Appl. Anal.*, 11:709–733, 2012.

[34] E. Hairer and C. Lubich. *Modulated Fourier expansions for continuous and discrete oscillatory systems.* Cambridge University Press, 2012.

[35] E. Hairer, S. P. Norsett, and G. Wanner. *Solving Ordinary Differential Equations I.* Springer, Second edition, 1993.

[36] E. Hairer, C. Lubich, and G. Wanner. *Geometric Numerical Integration. Structure–Preserving Algorithms for Ordinary Differential Equations.* Springer, Second edition, 2006.

[37] S. Herr and K. Schratz. Trigonometric time integrators for the zakharov system. *IMA J. Numer. Anal.*, 37:2042–2066, 2017.

[38] M. Hochbruck and C. Lubich. A Gautschi–type method for oscillatory second–order differential equations. *Numer. Math.*, 83:403–426, 1999.

[39] M. Hochbruck and A. Ostermann. Exponential integrators. *Acta Numer.*, 19:209–286, 2010.

[40] M. Hofmanová and K. Schratz. An exponential–type integrator for the KdV equation. *Numer. Math.*, 136:1117–1137, 2017.

[41] J. Hong, S. Jiang, and C. Li. Explicit mulit–symplectic methods for Klein–Gordon–Schrödinger equations. *J. Comput. Phys.*, 228:3517–3532, 2009.

[42] L. Hörmander. *Lectures on nonlinear hyperbolic differential equations.* Springer-Verlag, 1997.

[43] F. John. *Partial differential equations.* Springer-Verlag, 1982.

[44] L. Kong, R. Liu, and Z. Xu. Numerical simulation of interaction between Schrödinger field and Klein–Gordon field by multisymplectic method. *Appl. Math. Comput.*, 181:342–350, 2006.

[45] P. Krämer. Numerical integrators for Maxwell–Klein–Gordon and Maxwell–Dirac systems in highly to slowly oscillatory regimes. *PhD thesis (KIT)*, 2017. URL `https://publikationen.bibliothek.kit.edu/1000076449`.

[46] P. Krämer and K. Schratz. Efficient time integration of the Maxwell–Klein–Gordon equation in the non-relativistic limit regime. *J. Comput. Appl. Math.*, 316:247–259, 2017.

[47] H. P. Langtangen. *Computational Partial Differential Equations*. Springer-Verlag, 2003.

[48] J. D. Lawson. Generalized Runge–Kutta processes for stable systems with large Lipschitz constants. *SIAM J. Numer. Anal.*, 4:372–380, 1967.

[49] K. Lorenz, T. Jahnke, and C. Lubich. Adiabatic integrators for highly–oscillatory second-order linear differential equations with time–varying eigendecomposition. *BIT*, 45:91–115, 2005.

[50] C. Lubich. On splitting methods for Schrödinger–Poisson and cubic nonlinear Schrödinger equations. *Math. Comp.*, 77:2141–2153, 2008.

[51] M. Luskin, R. Rannacher, and W. Wendland. On the smoothing property of the Crank–Nicolson scheme. *Applicable Analysis*, 14:117–135, 1982.

[52] S. Machihara, K. Nakanishi, and T. Ozawa. Nonrelativistic limit in the energy space for nonlinear Klein–Gordon equations. *Math. Ann.*, 322:603–621, 2002.

[53] N. Masmoudi and K. Nakanishi. From nonlinear Klein–Gordon equation to a system of coupled nonlinear Schrödinger equations. *Math. Ann.*, 324:359–389, 2002.

[54] N. Masmoudi and K. Nakanishi. From the Klein–Gordon–Zakharov system to the nonlinear Schrödinger equation. *J. Hyperbolic Differ. Equ.*, 2:975–1008, 2005.

[55] N. Masmoudi and K. Nakanishi. Energy convergence for singular limits of Zakharov type systems. *Invent. Math.*, 172: 535–583, 2008.

[56] N. Masmoudi and K. Nakanishi. From the Klein–Gordon–Zakharov system to a singular nonlinear Schrödinger system. *Ann. Inst. Henri Poincare, Anal. Non Lineaire*, 27:1073–1096, 2010.

[57] V. G. Maz'ya. *Sobolev spaces*. Springer-Verlag, 1985.

[58] A. Ostermann and K. Schratz. Low regularity exponential–type integrators for semilinear Schrödinger equations. *Found. Comput. Math.*, Open access publication, 2017. URL `https://link.springer.com/article/10.1007/s10208-017-9352-1`.

[59] T. Ozawa and Y. Tsutsumi. Existence and smoothing effect of solutions for the Zakharov equations. *Publ. Res. Inst. Math. Sci.*, 28:329–361, 1992.

[60] T. Ozawa, K. Tsutaya, and Y. Tsutsumi. Normal form and global solutions for the Klein–Gordon–Zakharov equations. *Ann. Inst. Henri Poincare, Anal. Non Lineaire*, 12:459–503, 1995.

[61] T. Ozawa, K. Tsutaya, and Y. Tsutsumi. Well-posedness in energy space for the Cauchy problem of Klein–Gordon–Zakharov equations with different propagation speeds in three space dimensions. *Math. Ann.*, 313:127–140, 1999.

[62] H. J. Roessel and J. C. Bowman. Math 538: Asymptotic methods. pages University pf Alberta, Edmonton, Canada, 2012. URL `http://www.math.ualberta.ca/~bowman/m538/m538.pdf`.

[63] T. Schlick, M. Mandziuk, R. D. Skeel, and K. Srinivas. Nonlinear resonances artifacts in molecular dynamics simulations. *J. Comput. Phys.*, 139:1–29, 1998.

[64] G. Schneider. Validity and limitation of the Newell–Whitehead equation. *Math. Nachr.*, 176:249–263, 1995.

[65] G. Schneider. Justification of modulation equations for hyperbolic systems via normal forms. *NoDEA, Nonlinear Differ. Equ. Appl.*, 5:69–82, 1998.

[66] G. Schneider. Approximation of the Korteweg–de Vries equation by the nonlinear Schrödinger equation. *J. Differ. Equations*, 147:333–354, 1998.

[67] G. Schneider. *Validity and non-validity of the nonlinear Schrödinger equation as a model for water waves*. Cambridge University Press, 2014.

[68] K. Schratz and X. Zhao. On the comparison of asymptotic expansion techniques in the numerical analysis of Klein–Gordon equations in the nonrelativistic limit regime. *preprint*, 2017.

[69] J. Shen and W. L. Tang, T. *Spectral methods*. Springer-Verlag, 2011.

[70] B. Shizgal. *Spectral methods in chemistry and physics*. Springer-Verlag, 2015.

[71] R. D. Skeel, G. Zhang, and T. Schlick. A family of symplectic integrators: Stability, accuracy, and molecular dynamics applications. *SIAM J. Sci. Comput.*, 18:203–222, 1997.

[72] W. Strauss and L. Vazqez. Numerical solution of a nonlinear Klein–Gordon equation. *J. Comput. Phys.*, 28:271–278, 1978.

[73] T. Tao. *Nonlinear Dispersive Equations: Local and Global Analysis*. Amer. Math. Soc., 2006.

[74] B. Texier. Derivation of the Zakharov equations. *Arch. Ration. Mech. Anal.*, 185:121–183, 2007.

[75] T. Wang, J. Chen, and L. Zhang. Conservative difference methods for the Klein–Gordon–Zakharov equations. *J. Comput. Appl. Math.*, 205:430–452, 2007.